

**The role of the CXCL12 – CXCR4
chemokine ligand – receptor
interaction in the metastasis of
prostate cancer**

by

Manit Arya

**A thesis submitted in fulfilment of the
requirements for the degree of MD(Res),
Division of Surgery and Interventional Science,
University College London.**

DECLARATION

This work has not previously been accepted in substance for any degree and is not being concurrently submitted in candidature for any degree.

This thesis is the result of my own investigations, except where otherwise stated.

I hereby give consent for my thesis, if accepted, to be available for photocopying and for inter-library loan, and for the title and summary to be made available to outside organisations.

Signed...Manit ARYA..... (candidate)

Date...10TH Sept 2010.....

ABSTRACT

The aim was to investigate whether chemokine ligand – receptor interactions are involved in the chemotaxis of prostate cancer to favoured metastatic sites.

Initially, chemokine receptor mRNA expression, CXCR and CCR groups, was determined using conventional RT-PCR in cell lines derived from prostate cancer metastases, DU145, LNCaP and PC3, the primary prostate cancer cell line 1542 CPT3X and the normal prostate epithelial/ stromal cell lines 1542 NPTX, Pre 2.8 and S2.13. It was observed that in the cell lines derived from prostate cancer metastases, CXCR4 mRNA expression was relatively high. Using real-time quantitative PCR it was subsequently established that in DU145, LNCaP and PC3 cells, CXCR4 mRNA expression was 1287, 407 and 21 times respectively that of 1542 CPT3X. 1542 NPTX and 1542 CPT3X had similar levels of CXCR4 mRNA (the former had only twice that of the latter) and Pre 2.8 had no detectable CXCR4 mRNA expression. In laser microdissected patient primary tumour samples and patient benign tissue specimens CXCR4 mRNA expression was higher than that of the metastatic cell lines. Flow cytometry analysis showed that significantly higher levels of the CXCR4 protein were present on the cell membrane of the three metastatic cell lines. Cell migration assays revealed that chemotaxis of the metastatic cell lines PC3 and DU145 was enhanced by CXCL12 ligand and inhibited anti-CXCR4 antibody.

We have demonstrated that human prostate cell lines derived from metastases express functional CXCR4 receptor and that CXCL12 ligand enhances their migratory capabilities. Also, primary patient tumours and patient benign tissue specimens express CXCR4 mRNA at high levels (it is suggested that in vivo post-transcriptional modification and/ or regulation of CXCR4 receptor at the protein stage may significantly affect cellular protein levels). These results suggest that the CXCL12-CXCR4 axis may be involved in the metastasis of prostate cancer to preferred organs.

ACKNOWLEDGEMENTS

I would like to thank Professor John Masters and Dr Magali Williamson for their scientific guidance and support and also for the great patience they have shown in supervising me during this thesis.

Additionally, I would like to thank Helmut Klocker for providing patient derived RNA samples, Claire McGurk for advice regarding real time quantitative polymerase chain reaction and Roger Tatoud for advice as regards flow cytometry.

ABBREVIATIONS

A – adenosine
Ab – antibody
AIDS – acquired immune deficiency syndrome
AC – adenylyl cyclase
ADC – analog to digital converter
AR – androgen receptor
ATCC – The American Type Culture Collection

BLAST – basic local alignment search tool
BMP – bone morphogenetic protein
bp – base pairs
BPE – bovine pituitary extract
BPH – benign prostatic hyperplasia
BSA – bovine serum albumin
BSA-PBS – bovine serum albumin in phosphate buffered saline

⁰C – degrees Celsius
cAMP – adenosine 3', 5'-cyclic-monophosphate
CAMs – cell adhesion molecules
CCD – charge-coupled device
CD – cluster of differentiation
cDNA – complementary (to RNA) deoxyribonucleic acid
c-Met – Met tyrosine kinase
CSC – cancer stem cells
Ct – threshold cycle

DAG – diacyl-glycerol
dATP – deoxyadenosine triphosphate
dCTP – deoxycytidine triphosphate
ddNTPs – di-deoxynucleoside triphosphates
DEPC – diethylpyrocarbonate
dGTP – deoxyguanosine triphosphate
DNA – deoxyribonucleic acid
dNTPs – deoxynucleoside triphosphates
dsDNA – double stranded deoxyribonucleic acid
DTT – dithiothreitol
dTTP – deoxythymidine triphosphate
dUTP – deoxyuridine triphosphate

e value – expectation value
EB buffer – elution buffer
ECL – extracellular loop

ECM – extra-cellular matrix
EDTA – ethylenediaminetetraacetic acid
EGF – epidermal growth factor
EGFR – epidermal growth factor receptor
ELR – glutamic acid-leucine-arginine
EPC – endothelial progenitor cells
ERK – extracellular signal-regulated kinase
ET-1 – endothelin-1
ETV4 – Ets variant 4 (part of Ets family of transcription factors)
Ets – E twenty-six family of transcription factors

FACS – Fluorescence Activated Cell Sorter
FAM – 6-carboxyfluorescein
FBS – foetal bovine serum
FDA – Food and Drug Administration
FGF – fibroblast growth factor
FITC – fluorescein isothiocyanate
FRET – fluorescence resonance energy transfer
FS – fluorescent sequencing

GA1000 – gentamicin, amphotericin B
GAPDH – glyceraldehyde-3-phosphate dehydrogenase
GDF-9 – growth differentiation factor 9
GDP – guanosine diphosphate
GI number – GenInfo Identifier sequence identification number
GITC – guanidine isothiocyanate
GMFI – geometric mean fluorescent intensity
GTP – guanosine triphosphate

HAEC-I – immortalised human aortic endothelial cells
hASCs – human adipose tissue derived stem cells
HBME – human bone marrow endothelial cells
HDMVEC – human dermal microvascular endothelial cells
hEGF – human epidermal growth factor
HEX – hexachloro-6- carboxyfluorescein
HGF – hepatocyte growth factor/ scatter factor
HIF-1 – hypoxia-inducible factor-1
HIV - human immunodeficiency virus
HPF – high power field
HSC – haematopoietic stem cell
HUVEC – human umbilical vein endothelial cells

IGF – insulin-like growth factor
IL – interleukin
IP3 – inositol-1,4,5-triphosphate
IUIS – International Union of Immunological Societies

JOE – 6-carboxy-4,5-dichloro-2,7-dimethoxyfluorescein

kb – kilobase pairs

kDa – kilodalton

Keratinocyte-SFM – keratinocyte serum free medium

KSHV-GPCR – Kaposi's sarcoma herpesvirus-G protein-coupled receptor

M – molar

MAP kinase – mitogen-activated protein kinase

mg – milligrams

ml – millilitres

mM – millimolar

MMP – matrix metalloproteinase

mRNA – messenger ribonucleic acid

NCBI – National Centre for Biotechnology Information

ng – nanograms

NK cells – natural killer cells

nM – nanomolar

nmol – nanomoles

NSCLC – non-small cell lung cancer

NTC – no template control

OD – optical density

oligodT – oligodeoxythymidine

OPG – osteoprotegerin

p – probability

³²P – radioactive isotope of phosphorus

PBS – phosphate buffered saline

PCR – polymerase chain reaction

PDGF – platelet derived growth factor

PE – phycoerythrin

PE buffer – wash buffer

PE-CY5 – phycoerythrin and cyanine-5 conjugate

PGE2 – prostaglandin E2

PI – propidium iodide

PI3K – phosphatidylinositol-3-OH-kinase

PIP2 – phosphatidylinositol-4,5-biphosphate

PKB – protein kinase B

PKC – protein kinase C

PLA2 – phospholipase A2

PLC – phospholipase C

pmol – picomoles

PMT – photomultiplier tube

PrEGM – prostate epithelial specific growth medium

PSA – prostate specific antigen
PTHrP – parathyroid hormone-related peptide
PYK – proline-rich tyrosine kinase

QG buffer – solubilisation buffer

R110 – rhodamine 110
R6G – rhodamine 6G
RANKL – receptor activator of NF-kappaB ligand
RCC – renal cell cancer
RLT buffer – guanidine isothiocyanate containing lysis buffer
Rn – normalised reporter signal
RNA – ribonucleic acid
Rnb – fluorescence emission of the baseline
Rnp – fluorescence emission of the product
ROX – passive reference dye
RPMI – Roswell Park Memorial Institute Medium
rRNA – ribosomal ribonucleic acid
RT – reverse transcriptase
RT-PCR – reverse transcriptase polymerase chain reaction

SCID – severe combined immune deficiency
SCLC – small cell lung cancer
SD – standard deviation
SDF – 1 - stromal cell derived factor 1
SE – standard error
SEER – Surveillance Epidemiology and End Results
Ser – serine
STR – short tandem repeat
SYBR Green – Synergy Brands, Inc Green

T – thymidine
TAE – tris acetate EDTA buffer
Taq – Thermus aquaticus
TAMRA – tetramethyl-6-carboxyrhodamine
TAMs – tumour associated macrophages
TET – tetrachloro-6 carboxyfluorescein
TGF – transforming growth factor
Thr – threonine
Tm – melting temperature of primers
TNF – tumour necrosis factor
TCSC – tissue-committed stem cell
TRIS – tris – (hydroxymethyl) – aminoethane
Tween 20 – polyoxyethylene-sorbitan monolaurate

µg – micrograms

μl – microlitres

μm – micrometre

μM – micromolar

UNG – uracil DNA glycosylase (uracil N-glycosylase)

uPA – urokinase type plasminogen activator

uPAR – urokinase type plasminogen activator receptor

UV – ultraviolet radiation

V – volts

VEGF – vascular endothelial growth factor

VCAM – vascular cell adhesion molecule

VIC – fluorescent reporter dye (composition not released by Applied Biosystems)

VHL – von Hippel-Lindau

WHO – World Health Organisation

TABLE OF CONTENTS

	<u>Page</u>
<u>CHAPTER 1: INTRODUCTION</u>	19
<u>Section 1.1:</u> The epidemiology and the spread of prostate cancer	20
<u>Section 1.2:</u> The theory of metastasis and prostate cancer	22
<u>Section 1.3:</u> Chemokines and their structure	37
<u>Section 1.4:</u> The role of chemokines and their receptors in cancer	56
<u>Section 1.5:</u> Hypothesis and aims	78
<u>CHAPTER 2: THEORY OF TECHNIQUES</u>	80
<u>Section 2.1:</u> Polymerase chain reaction and reverse transcriptase-polymerase chain reaction	81
<u>Section 2.2:</u> Real-time quantitative PCR	82
<u>Section 2.3:</u> Flow cytometry	103
<u>Section 2.4:</u> Cell migration assays	118
<u>CHAPTER 3: MATERIALS AND METHODS</u>	120
<u>Section 3.1:</u> Materials and methods used in chapter 4: Elucidation of chemokine receptor mRNA expression (CXCR and CCR groups) in prostate cell lines	121

<u>Section 3.2:</u> Materials and methods used in chapter 5: Quantitation of CXCR4 mRNA expression in cell lines and patient prostate tissue samples	138
<u>Section 3.3:</u> Materials and methods used in chapter 6: Elucidation of cell membrane CXCR4 chemokine receptor (protein) expression in prostate cell lines	145
<u>Section 3.4:</u> Materials and methods used in chapter 7: Establishing that the CXCR4 receptor is functional in cell lines derived from prostate cancer metastases	151
<u>CHAPTER 4: ELUCIDATION OF CHEMOKINE RECEPTOR mRNA EXPRESSION (CXCR AND CCR GROUPS) IN PROSTATE CELL LINES</u>	154
<u>Section 4.1:</u> Introduction and Aims	155
<u>Section 4.2:</u> Results	156
<u>Section 4.3:</u> Discussion	168
<u>CHAPTER 5: QUANTITATION OF CXCR4 mRNA EXPRESSION IN CELL LINES AND PATIENT PROSTATE TISSUE SAMPLES</u>	173
<u>Section 5.1:</u> Introduction and Aims	174
<u>Section 5.2:</u> Results	176
<u>Section 5.3:</u> Discussion	189

<u>CHAPTER 6: ELUCIDATION OF CELL MEMBRANE CXCR4 CHEMOKINE RECEPTOR (PROTEIN) EXPRESSION IN PROSTATE CELL LINES</u>	192
<u>Section 6.1:</u> Introduction and Aims	193
<u>Section 6.2:</u> Results	195
<u>Section 6.3:</u> Discussion	217
<u>CHAPTER 7: ESTABLISHING THAT THE CXCR4 RECEPTOR IS FUNCTIONAL IN CELL LINES DERIVED FROM PROSTATE CANCER METASTASES</u>	223
<u>Section 7.1:</u> Introduction and Aims	224
<u>Section 7.2:</u> Results	226
<u>Section 7.3:</u> Discussion	233
<u>CHAPTER 8: FURTHER DISCUSSION</u>	235
<u>Section 8.1:</u> Results summary and evaluation	236
<u>Section 8.2:</u> Confirmatory studies of CXCL12 – CXCR4 interaction in the migration and dissemination of prostate cancer	242
<u>Section 8.3:</u> The importance of the CXCL12 – CXCR4 axis in tumour cell migration	246

<u>Section 8.4:</u> Therapeutic implications	256
<u>Section 8.5:</u> Concluding remarks	264
<u>REFERENCES</u>	265
<u>APPENDIX: ABSTRACTS OF ARTICLES PUBLISHED FROM THESIS</u>	308

LIST OF FIGURES

	<u>Page</u>
<u>CHAPTER 1</u>	
<u>Figure 1.1:</u> The metastatic cascade	24
<u>Figure 1.2:</u> Structural classification of the chemokine family	40
<u>Figure 1.3:</u> Diagrammatic representation of the chemokine receptor CXCR4 (Fusin)	46
<u>Figure 1.4:</u> The chemokine receptor signal transduction pathway in leucocytes	49
<u>CHAPTER 2</u>	
<u>Figure 2.1:</u> The polymerase chain reaction	81
<u>Figure 2.2:</u> The Taqman real time quantitative PCR assay (hydrolysis probes)	85
<u>Figure 2.3:</u> The ABI PRISM® 7700	88
<u>Figure 2.4:</u> Model of a single amplification plot illustrating the nomenclature commonly used in real-time quantitative PCR	91
<u>Figure 2.5:</u> Emission spectra for 3 common fluorochromes	107
<u>Figure 2.6:</u> The coaxial stream	109
<u>Figure 2.7:</u> Basic optics of a flow cytometer	110
<u>CHAPTER 3</u>	
<u>Figure 3.1:</u> Optimisation of GAPDH PCR cycles	132
<u>Figure 3.2:</u> Costar Transwell® culture chamber	151

CHAPTER 4

- Figures 4.1a – n:** The expression of CXCR and CCR chemokine receptors and CXCL12 ligand in cell lines using standard RT-PCR performed at 35 cycles **158**
- Figure 4.2:** Nucleotide sequence electropherogram obtained by extracting the CXCR4 PCR product from an agarose gel using the DU145 cell line **167**

CHAPTER 5

- Figure 5.1:** Optimisation of CXCR4 primer concentrations **177**
- Figure 5.2:** Optimisation of starting RNA quantity **178**
- Figure 5.3:** Relative amplification efficiency scatter plot **180**
- Figure 5.4a and b:** Relative CXCR4 mRNA expression in cell lines and patient samples using real-time (Taqman) quantitative RT-PCR **186-87**

CHAPTER 6

- Figures 6.1a – e:** Representative flow cytometry histograms and dot plots for the results of differential primary anti-CXCR4 antibody binding to DU145 cells using five different primary antibodies **198-202**
- Figures 6.2a – e:** Dot plots demonstrating autofluorescence and non-specific binding of secondary antibody **205**
- Figures 6.3a – h:** Representative flow cytometry histograms and dot plots are shown for cell membrane CXCR4 receptor expression in each cell line **207-14**

CHAPTER 7

- Figure 7.1:** Photograph of migrating cells in one high power field in a Transwell® well at x200 magnification **227**

Figure 7.2a-c: Effect of CXCL12 α on chemotaxis of prostate cell lines **229-31**

CHAPTER 8

Figure 8.1: A summary of the pathophysiological role of CXCL12 – CXCR4 interaction in cellular migration/ chemotaxis **247**

Figure 8.2: The hypoxic control of CXCR4 expression in renal carcinoma cells **251**

LIST OF TABLES

	<u>Page</u>
<u>Chapter 1</u>	
<u>Table 1.1:</u> Chemokine nomenclature	42
<u>Table 1.2:</u> The four classes of chemokine receptors and their ligands	44
<u>Chapter 2</u>	
<u>Table 2.1:</u> A summary of the primer and probe design guidelines used by the primer/probe design program, Primer Express®, for real-time quantitative Taqman PCR	101
<u>Table 2.2:</u> Universal Thermal Cycling Parameters for real-time quantitative TaqMan PCR	102
<u>Table 2.3:</u> Photomultiplier detection of light emission produced by common fluorochromes/ dyes in the Becton Dickinson FACScan	112
<u>Chapter 3</u>	
<u>Table 3.1:</u> Details of continuous human cell lines used	123
<u>Table 3.2:</u> Details of chemokine receptor primers used in PCR	126
<u>Table 3.3:</u> Constituents of a 20µl reverse transcriptase reaction	130
<u>Table 3.4:</u> PCR master mix for 1x 50µl reaction	131
<u>Table 3.5:</u> CXCR4 Primers, Probe and Amplicon Details (designed using Primer Express® software and supplied by Applied Biosystems)	139
<u>Table 3.6:</u> Clinically localized patient primary prostate tumour and benign prostate samples - summary of available information (all tissue derived from frozen fresh radical prostatectomy specimens)	141
<u>Tables 3.7a and b:</u> Details of primary and secondary antibodies used	147-48

Chapter 4

<u>Table 4.1:</u> Summary of CXCR and CCR receptor and CXCL12 ligand expression observed in cell lines	165
---	------------

Chapter 5

<u>Table 5.1:</u> Combination of CXCR4 forward and reverse primer concentrations for optimisation (all primer concentrations are nM solutions)	176
---	------------

<u>Table 5.2a:</u> Calculation of relative CXCR4 mRNA quantitation, using the comparative threshold ($2^{-\Delta\Delta C_t}$) method, for one experiment consisting of three samples for each cell line	183
--	------------

<u>Table 5.2b:</u> Mean relative CXCR4 mRNA expression in cell lines (with standard deviation) for the three samples run in experiments 1, 2 and 3	184
---	------------

<u>Table 5.2c:</u> Represented here are the results of the mean relative CXCR4 mRNA expression for the laser microdissected patient samples, numbered 1 to 18	185
--	------------

Chapter 6

<u>Table 6.1:</u> The results of differential primary antibody binding to the cell membrane CXCR4 receptor in the DU145 cell line using each of five different primary anti-CXCR4 antibodies	197
---	------------

<u>Table 6.2:</u> This table summarises the results data from figure 6.3 and shows the results from one experiment elucidating cell membrane CXCR4 receptor expression in cell lines	206
--	------------

<u>Table 6.3:</u> The overall mean GMFI +/- standard deviation has been calculated from 3 separate flow cytometry experiments investigating CXCR4 receptor expression in each cell line	216
--	------------

Chapter 7

<u>Table 7.1:</u> Results of cell migration assays	228
---	------------

CHAPTER 1

INTRODUCTION and HYPOTHESIS

SECTION 1.1

The epidemiology and the spread of prostate cancer

The burden of prostate cancer in the community

Prostate cancer is one of the most frequently diagnosed cancers in Western men, with the incidence rate increasing in most countries since the 1980s. The highest incidence rates are reported in the USA, where in 2003 - 2007 the annual age adjusted incidence rate was 150.4 per 100,000 caucasian men and 234.6 per 100,000 men of Afro-Caribbean descent, using the Surveillance Epidemiology and End Results (SEER) data [www.seer.cancer.gov/statfacts/ accessed June 2010]. In 2000, prostate cancer became the most frequently diagnosed cancer in men in the UK, surpassing both lung and colorectal cancer. This trend has continued and in England alone in 2007 there were 30,201 newly diagnosed patients registered with prostate cancer [www.statistics.gov.uk accessed June 2010]. The overall age standardised incidence rate of prostate cancer in England in 2007 was 97.2 per 100,000 men. The incidence rates increase with age; the rate is 10.0 per 100,000 in men aged 45–49 years, rising to 737.4 per 100,000 in men aged ≥ 85 years [www.statistics.gov.uk accessed June 2010]. Additionally, similarly to the USA, prostate cancer is the second leading cause of cancer associated death, and in the latest figures provided for England, by the Office for National Statistics, there were 9,157 deaths from prostate cancer in 2008 with an age standardised mortality rate of 240 per 1 million population [www.statistics.gov.uk accessed June 2010]. It has been estimated that the lifetime risk of a man developing clinically significant prostatic cancer is 10% and the risk of dying from prostate cancer is 3% [Melia J 2005].

The spread of prostate cancer

a) Local invasion - in prostate adenocarcinomas, extraprostatic extension preferentially occurs posteriorly and posterolaterally, which parallels the location of most neoplasms. Further local spread of tumour can result in invasion of the muscular wall of the seminal vesicle and also the rectum.

b) Metastasis - the most frequent sites of metastatic prostate carcinoma are lymph node and bone. As regards the lymphatic dissemination, prostate cancer initially spreads to the obturator, external iliac, internal iliac, presacral, and lateral sacral (presciatic) lymph nodes [Breyer BN et al 2008, Brossner C et al 2001, Heidenreich A et al 2002, Wawroschek F et al 2001].

Prostate cancer metastasizes to bone more frequently than does any other solid tumour [Arya M et al 2006, Coleman RE 2001]. In a comprehensive autopsy study of 358 patients who died from cancer between 1927 and 1941, Walther HE 1948 found that bone was the most common site of metastases for prostate cancer. In this series, the frequency of bone metastasis in prostate cancer was about 60% although several other autopsy series have since put the frequency closer to 80–90% [Cumming J et al 1990, Shah RB et al 2004, Rana A et al 1993]. Metastasis to bone usually occurs as a result of the haematogenous dissemination of cancer cells and this represents the major cause of morbidity (including impaired mobility, pathological fracture, spinal cord compression) and mortality in this disease. In fact, after diagnosis of bone metastasis, median survival is approximately 2 to 3 years [Coleman RE 1997, Nørgaard M et al 2010], depending on the hormone responsiveness of the disease. However, in spite of the severe complications

of prostate cancer skeletal metastasis, there have not been many therapeutic advances to prevent or diminish these lesions.

The development of efficacious therapies to decrease or prevent lymph node and particularly skeletal metastasis in prostate malignancy has been hampered up till now by the lack of an adequate understanding of the mechanisms of organ specific metastasis in cancer. The molecular genetics and pathophysiology of these processes are now being elucidated and this will help to provide the basis for creating strategies to prevent or diminish their occurrence and associated complications.

SECTION 1.2

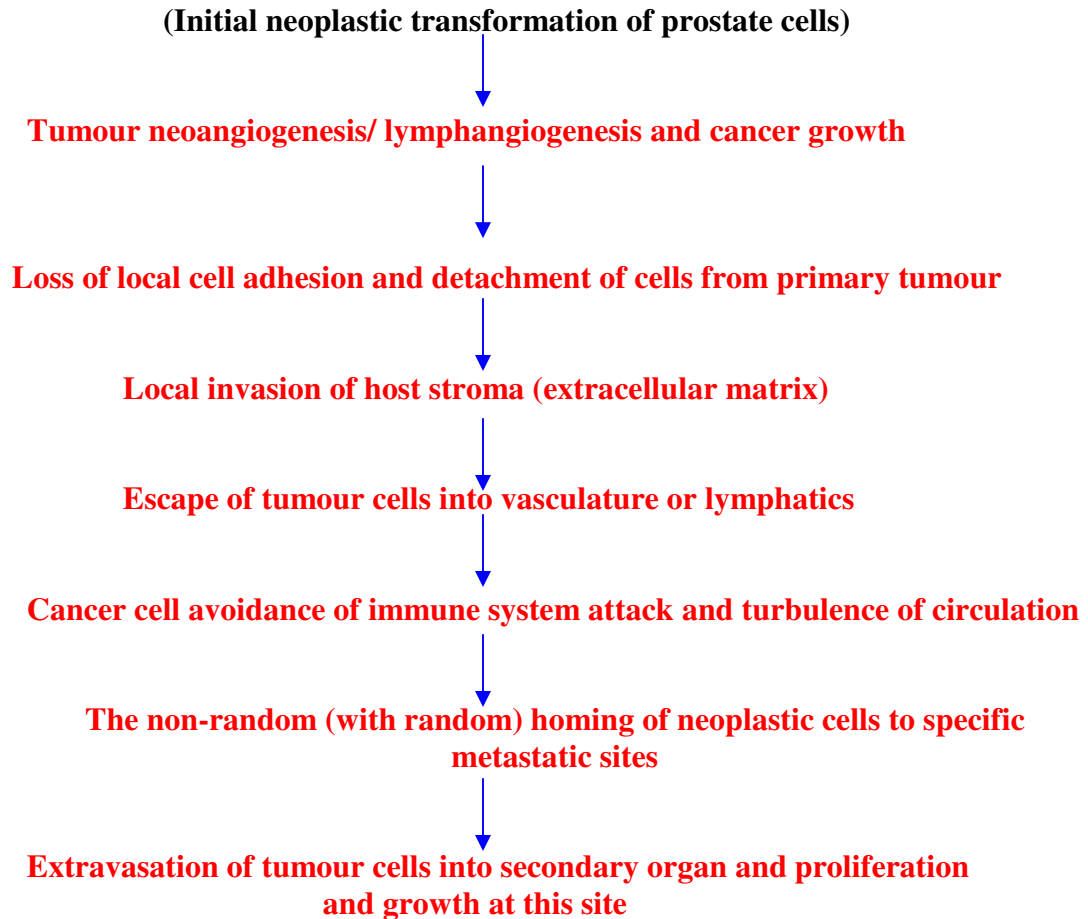
The theory of metastasis and prostate cancer

The leading cause of death from cancer is tumour metastasis. Metastasis is defined as the process by which a malignant cell leaves the primary tumour, travels to a distant site via the circulatory system, and establishes a secondary tumour. This is a multi-step process, which consists of a series of sequential events involving complex interactions between the cancer cell and its surroundings in the host [Mundy GR 2002, Geiger TR and Peeper DS 2009]. Not all cancer cells have the ability to metastasise due to the great difficulties involved in the process. Additionally, it has been shown that metastasis is an inefficient process with only a minority of the cells leaving the primary organ (such as the prostate) having the potential to establish colonies in secondary sites (such as lymph nodes and bone marrow) and eventually proliferating into clinically detectable metastatic neoplasms. This was demonstrated in the study by Rosol TJ et al

2003, who performed intracardiac injection of luciferase-labelled PC3 prostate cancer cell line cells into immunocompromised mice. Neoplastic cells were localised, using non-invasive imaging, in the lungs, kidneys and long bones 15 minutes after injection. However, 24 hours later, no viable cells were detected signifying that most of the injected cells were either dead or metabolically inactive. In another study Luzzi KJ et al 1998 used videomicroscopy of various types of cancer, and showed that only 2% of cancer cells formed micrometastases. Other groups have demonstrated that only 1% of these micrometastatic deposits eventually develop into larger established tumours, despite a significant number of undivided solitary cells remaining in tissues several months after injection [Naumov GN et al 2001 and 2002, Macdonald IC et al 2002, Townson JL and Chambers AF 2006]. In renal cancer radical nephrectomy patients, Glaves D et al 1988 estimated the rates at which cancer cells were released directly into the renal vein. They found that cancer cells were released as single cells and multi-cell emboli in 8 of 10 patients, in numbers varying between 14 and 7,509 emboli per millilitre of blood. Despite a calculated median input into the circulation of 3.7×10^7 cancer cells per day for ≥ 180 days, only 3 of 10 patients had metastases before surgery, and only 1 of the remaining disease-free patients subsequently developed distant metastases over a maximum 35 month period.

After the initial transformation of the cells, metastasis is thought to involve the following steps shown in figure 1.1. Completion of all steps in sequential order is required for successful metastasis [Chambers AF et al 2002, Fidler IJ 2003, Geiger TR and Peeper DS 2009].

Figure 1.1: The metastatic cascade



Of particular interest to this thesis is the non-random homing of cancer cells to specific metastatic sites and their survival in specific organs. This is due to:

- Directional migration of cancer cells down a chemotactic gradient to organs exhibiting peak levels of the chemoattractant.
- Capillary bed arrest of tumour cells in receptive organs/ cancer cell endothelial interactions.

- Extravasation from the capillaries into the surrounding host tissue, proliferation within the host organ microenvironment resulting in the establishment of micrometastases.

These final steps of the metastatic cascade have been grouped together, as collectively, they play a key role in the appreciation of metastasis as an organ-specific, non-random process. Factors that affect the directional migration of cancer cells, the capillary bed arrest of tumour cells in target organs, extravasation from the capillaries into the surrounding tissue, proliferation within specific host organs, or formation of new blood vessels to support growth in host organs could all result in potentiation of site specific metastasis.

It is well established that different cancer types have preferred metastatic sites. Breast cancer favours regional lymph nodes, bone marrow, lung and liver. Malignant melanoma has a similar pattern but also has a high incidence of skin metastasis. Prostate cancer particularly favours the bone marrow as well as lymph nodes. Several explanations for these metastatic patterns have been proposed.

In 1889, Stephen Paget, an English surgeon, studied autopsy records of 735 women who died of breast cancer [Paget S 1889]. He noticed that the majority of metastatic deposits were in the liver and that metastasis to the spleen was extremely uncommon. In contrast to this, autopsy cases of patients who died of sepsis demonstrated that abscesses occurred in similar frequency in both the liver and spleen. Paget suggested that the difference in the number of metastases could not be explained simply by circulatory patterns because the liver and spleen received approximately the same volume of blood. Paget's findings were published in a seminal article in the "Lancet" [Paget S

1889]. Based on these observations, Paget proposed the “seed and soil” hypothesis, stating that certain tumours, the “seeds”, have specific metastatic affinity for particular organs, the “soil”. He hypothesised that it was the compatibility between the “seed” and the “soil” that determined whether tumours could survive and grow at a distant site.

Forty years later, in 1928, an American pathologist, James Ewing, proposed an alternative theory to the “seed and soil” hypothesis. He postulated that neoplastic cells grew specific sites because they were directed to these sites by the direction of blood flow and lymphatics [Ewing J 1928]. He stated that “the mechanisms of circulation will doubtless explain most of peculiarities, for there is as yet no evidence that any one parenchymatous organ is more adaptable than others to the growth of embolic tumour cells.” However, Ewing also noted there was an exception in that “the spleen seems to escape with peculiar frequency.”

It is likely that these two theories are not mutually exclusive. Fidler IJ 2002 combined the two theories and defined the modern seed-and-soil hypothesis consisting of three principles. First, cancerous tissues contain heterogeneous subpopulations of cells with different angiogenic, invasive, and metastatic properties. Second, the metastatic process is selective for the small subpopulation of cells that have survived the long journey to a distal organ. Third, the success of the metastatic cells depends on their ability to interact and utilize the “soil” provided in their new microenvironment [Fidler IJ 2002]. These heterogeneous subpopulations of cells within a tumour can be seen on co-culture of an isolated mouse femur with PC-3 human prostate cancer cells. On a scanning electron micrograph after 3 days of culture, cells exhibiting diverse phenotypes are attached to the bone. It has been hypothesized that these variable morphologies may

represent the heterogeneous population of prostate cancer cells that differentially respond to growth on bone [Tantivejkul K et al 2004].

However, Fidler's modern seed-and-soil hypothesis does not entirely incorporate the growing evidence for the 'homing' theory, which states that different organs have special abilities to attract, through chemotactic factors, specific types of cancer cells [Moore MA 2001, Muller A 2001, Ben-Baruch A et al 2008]. It is likely that a combination of all these factors is likely to be involved and there is evidence supporting all these theories in the organ-specific metastasis of prostate cancer. This evidence is now presented:

i) Vascular flow patterns - there is some supporting evidence for Ewing's theory that cancer cell delivery to the bone is related to only the volume of blood flow [Ewing J 1928], but this explanation is not widely acknowledged in the metastasis of prostate cancer. Batson first confirmed the existence of a portal-like venous system between the prostate and the lower lumbar vertebrae [Batson OV 1940]. Early researchers suggested that prostate cancer cells migrated to the bone because of venous drainage through the so called Batson's Plexus. However, this hypothesis did not explain the high occurrence of prostate cancer metastases outside the vertebral column and bony pelvis nor did it account for the low incidence of prostate cancer metastases to the lungs. More recently there has been further support of this theory. In a review of bone scans from 27 patients with limited skeletal involvement, the distribution pattern of early prostate cancer metastases was similar to the distribution of normal adult bone marrow [Imbriaco M et al 1998]. More importantly, Bubendorf L et al 2000 studied more than 19,000 male autopsies, of which 1589 had prostate cancer. The group observed that there was an

increased incidence of bone metastases in prostate cancer patients in comparison with those who had kidney or bladder neoplasms. Additionally, in prostate cancer patients, there was also a high prevalence of expected peri-aortic and pelvic lymph node metastases, and there was a strong association between the presence of lymphatic metastasis and haematogenous (skeletal and visceral) metastases. Greater than 90% of the patients with haematogenous metastasis had skeletal metastases. The highest frequency of metastases was noted in the lower lumbar spine followed by higher vertebral levels, and then ribs, long bones, and skull suggesting an upward metastatic spread along spinal veins after initial lumbar deposits. More detailed scrutiny confirmed that involvement of these levels almost certainly proceeded in a step-wise fashion as it was very rare for the less frequently affected bones to be involved without simultaneous disease in the more regularly affected bones. Interestingly, patients with lung metastases were noted to have a statistically reduced chance of skeletal metastasis. It was concluded that these results supported the theory that a portal venous circulatory system existed between the prostate and lower lumbar vertebrae leading to a higher delivery of circulating prostate cancer cells flowing to these vertebrae. Another method of haematogenous spread would be the flow of prostatic venous blood directly into the inferior vena cava: this would account for the investigators' finding of an inverse correlation between lung and skeletal metastasis because caval blood has to circulate through the lungs before systemic dissemination.

Cancer cells in the lymphatic system can also move directly into Batson's plexus due to the presence of potential lymphatic-blood vessel shunts present at this site (these shunts are also present at the primary tumour site). Alternatively, the lymphatic system converges with the bloodstream via the thoracic duct.

ii) Chemotactic gradients and homing of cancer cells - there is increasing support for the “homing” theory to explain the directional cell migration of malignant cells to specific organs which exhibit peak expression of chemoattractant molecules. When prostate carcinoma cells are injected adjacent to adult human bone implanted in SCID mice, the prostate carcinoma cells migrate towards the adult human bone [Tsingotjidou AS et al 2001]. This observation provides evidence that bone provides chemotactic factors for prostate carcinoma cells. Using in-vitro assays, Jacob K et al 1999 found that extracts from bone promoted an increase in chemotaxis and invasion by PC-3 cells compared with brain and other tissue extracts, thus demonstrating that bone contains significant migration and chemoinvasion promoting factors for prostate cancer cells. The purified active chemoattractant factor was found to be the minor bone matrix protein osteonectin (also known as SPARC or BM-40). Osteonectin also enhanced matrix metalloproteinase activity in the prostate cancer cells. It has also been shown that the cytokine TGF β 1, which is secreted by osteoblasts, stimulated the chemotaxis (as well as invasion and integrin expression) of PC3 cells [Festuccia C et al 1999, Ding Q et al 2010].

Furthermore, epidermal growth factor (EGF) was noted to be expressed at favoured sites of prostate cancer metastasis in the stroma of both lymph nodes and medullary bone [Rajan R et al 1996]. EGF resulted in increased motility and enhanced the chemomigration of PC3 prostate cancer cells in Boyden chambers [Festuccia C et al 2005, Jarrard DF et al 1994] and increased their invasion through Matrigel [Festuccia C et al 2005, Unlü A and Leake RE 2003]. Also, it was demonstrated that inhibition of the EGF receptor decreased the chemotaxis and invasion of PC3 cells [Festuccia C et al

2005, Unlü A and Leake RE 2003]. These results support the hypothesis that bone and lymph nodes are the preferred site for prostate cancer metastasis due to a chemoattractant mechanism involving EGF [Lu X and Kang Y 2010]. Additionally, these observations have implications for therapeutic intervention as does the finding that the Rho-kinase inhibitor, Y-27632, inhibited in vitro PC3 cell chemotactic migration to bone marrow fibroblast conditioned media and their metastatic growth in immune compromised mice [Somlyo AV et al 2000].

Increased chemotaxis has also been shown to occur in DU145, PC3 and LNCaP cells in migration assays, in response to insulin-like growth factors 1 and 2 (IGF1 and 2), which are known to be produced by bone cells [Marelli MM et al 2006, Ritchie CK et al 1997]. Gmyrek GA et al 2001 observed that HGF (scatter factor) acting via its receptor, Met tyrosine kinase (c-Met), induced the migration of DU145 cells in-vitro. Recently these results have been consolidated by Dai Y and Siemann DW 2010, who demonstrated BMS-777607, a small-molecule met kinase inhibitor, suppressed HGF-stimulated cell migration in c-Met-expressing PC-3 and DU145 prostate cancer cells. Other bone factors, which may be involved in the chemomigration of prostate cancer include type 1 collagen peptides (which are bone stromal factors); these have been revealed to be chemoattractants for bone derived metastatic prostate cancer cell lines VCaP and PC3 [Cooper CR et al 2003].

Recently, an exciting body of evidence has emerged that has implicated chemokines and their receptors as having a pivotal role in the chemotaxis of cancer cells to specific organs such as bone and lymph nodes. This will be discussed in the later section titled “Chemokines and their role in cancer”.

iii) Interaction with the endothelium - tumour cells, in order to develop a cancer at secondary sites, must arrest in the capillary beds of distant organs, and extravasate through the vessel wall. Evidence suggests that only endothelium-attached cancer cells can give rise to metastases [Al-Mehdi AB et al 2000, Bussard KM et al 2008]. In prostate cancer it has been hypothesised that prostate carcinoma metastasis to bone is mediated, at least in part, by the cancer cells' preferential adhesion to bone marrow endothelium as opposed to endothelium from other sites. This was observed in studies showing that PC3 prostate carcinoma cells adhered preferentially to immortalized human bone marrow endothelial (HBME) cells as compared to human umbilical vein endothelial cells (HUVEC), immortalized human aortic endothelial cells (HAEC-I), and immortalized human dermal microvascular endothelial cells (HDMVEC) [Cooper CR et al 2000, Lehr JE and Pienta KJ 1998]. This adhesion was promoted when HBME cells were cultured on bone extracellular matrix components [Cooper CR et al 2000]. Romanov VI et al 2004 indicated that this preferential binding of prostate cancer C4-2B cells to bone marrow endothelium is related to PSA expressed as secreted and surface-associated molecules in the C4-2B cells. The interaction of the cancer cells with the endothelium may occur via the "dock and lock" mechanism [Honn KV and Tang 1992, Miles FL et al 2008], which is comparable to leucocyte trafficking and extravasation at areas of inflammation. Both of these processes involve the arrest of circulating cells on the endothelium by low-affinity binding, induction of a firmer cell adhesion, extravasation, and subsequent invasion of the surrounding matrix. The cell adhesion molecules (CAMs) involved in the "docking" phase may include P-selectin, which can be found on activated endothelial cells and which binds to its ligand sialyl Lewis^X carbohydrate antigen located on the cell surface of

cancer cells or platelets. Expression of sialyl Lewis^X by prostate cancer cells is associated with a poor prognosis [Martensson S et al 1995].

Kierszenbaum AL et al 2000 identified a potential cell membrane receptor in prostate cancer cells that mediated the binding of the tumour cells to bone marrow endothelium. The galactosyl receptor, a C-type lectin that binds to specific sugar moieties via a specific carbohydrate recognition domain, was demonstrated to be present on both normal and PC3 cells. Blocking this receptor with antibodies that bind to the carbohydrate recognition domain prevented the adhesion of the malignant PC3 cells to the endothelium [Kierszenbaum AL et al 2000]. Also, prostate cancer cells express Thomsen-Friedenreich glycoantigen (Galb1-3GalNAc), which has been discovered to bind with β -galactoside binding lectin, galectin-3, expressed on microvascular endothelium of metastatic tissues [Ellerhorst J et al 1999, Glinsky VV et al 2001, Glinsky VV et al 2003, Nangia-Makker P et al 2002]. Najy AJ et al 2008 have suggested, using an SCID mouse model of human prostate cancer metastasis, that the disintegrin ADAM15, supports prostate cancer metastasis by modulating tumour cell-endothelial cell interaction. Other CAMs thought to be involved in prostate cancer cell “docking” on the endothelium include vascular cell adhesion molecule (VCAM), CD11a (alpha-L), CD18 (beta-2), and leucocyte functional antigen – 1 pectin [Morrissey C and Vessella RL 2007, Pienta KJ et al 1995].

In a similar manner to the inflammatory response of leucocytes, the “locking” of prostate cancer cells to endothelial cells is attained via the complex collaboration of integrins. This is illustrated by the finding that antibodies to the β 1 integrin subunit inhibited adhesion of PC-3 cells to bone marrow endothelial cells [Scott LJ et al 2001]

and cooperativity between $\alpha v\beta 3$, $\alpha 5\beta 1$ and $\alpha 3\beta 1$ integrins is necessary for PC-3 and DU145 cell adhesion to interleukin-1-stimulated HUVEC [Romanov VI and Goligorsky MS 1999]. Prostate cancer cell binding to the endothelium may aid extravasation as it can result in retraction of endothelial cells in preclinical models [Sikes RA et al 2004].

iv) Interaction between tumour cells and tumour microenvironment at the metastatic site - as recognised originally by Paget S 1889 and then reinforced more recently by Fidler IJ 2002 the establishment of successful cancer metastasis depends on a “fertile soil” at the metastatic site. In the case of prostate cancer many factors potentially contribute to cancer cell growth, particularly in the bone. It has been hypothesized that prostate cancer cells are “osteomimetic” [Josson S et al 2010, Koeneman KS et al 1999, Rucci N and Teti A et al 2010]. In other words they develop properties similar to bone cells upon entering the bone marrow. This is also known as epithelial-mesenchymal transition and refers to epithelial cells losing their epithelial features and acquiring mesenchymal characteristics. This process occurs mainly during embryogenesis and allows the epithelial cells to migrate to a new environment and differentiate into a distinct cell type by the reverse process of mesenchymal-epithelial transition. However, in cancer cells, epithelial mesenchymal transition confers the invasive phenotype. The process is partly illustrated by LNCaP cell derivatives, which like osteoblasts, synthesize and deposit bone matrix proteins such as osteopontin, osteocalcin, osteonectin, and bone sialoprotein when in the bone [Gardner TA et al 2009, Zhau HE et al 2000]. Typically, external stimuli are needed to initiate epithelial-mesenchymal transition and in the bone microenvironment these include extracellular matrix components, and soluble factors including members of the TGF β superfamily, FGF family, EGF, HGF, IGF-2 and

proteins of the Wnt and Hedgehog families. Additionally, many of the growth factors, which may be secreted by a variety of cells including osteoblasts, stromal cells and the cancer cells themselves, have been demonstrated to stimulate prostate carcinoma growth in vitro. For example, prostate carcinoma cells have IGF receptors [Cohen P et al 1991, Hellowell GO et al 2002] and proliferate in response to IGF [Gennigens C et al 2006, Ritchie CK et al 1997]. Transfection of LNCaP cells with FGF-8 expression vector induced an increased growth rate, higher soft agar clonogenic efficiency, enhanced in vitro invasion, and increased in vivo tumourigenesis [Song Z et al 2000].

The interactions between tumour cells and host microenvironment contribute greatly to the formation of osteoblastic lesions. Bone morphogenetic proteins (BMPs) are known to contribute to bone formation. Bentley H et al 1992 first reported that the expression of BMP-6, a member of the TGF- β superfamily, was detected in prostate tissue samples of over 50% of patients with clinically defined metastatic prostate cancer, but not non-metastatic or benign prostate samples. Subsequent studies have confirmed the increased expression of BMP-6 in metastatic prostate cancer cells [Autzen P et al 1998, Dai J et al 2005, Thomas BG and Hamdy FC 2000]. It is believed that secretion of BMP-6 by prostate cancer cells contributes to osteoblastic lesions because BMP-6 stimulates osteoblastic differentiation of pluripotent mesenchymal cells [Ebisawa T et al 1999]. Another BMP, GDF-9, has been shown to promote the growth rate of both PC-3 and DU-145 cells by protecting them from apoptosis [Bokobza SM et al 2010].

Endothelin-1 (ET-1), a potent vasoconstrictor, is produced by tumour cells and is also a direct mitogen for osteoblast progenitors in vitro [Takuwa Y et al 1990] and in vivo [Nelson JB et al 1999, Tsukahara H et al 1998]. Patients with osteoblastic prostatic

metastasis have high serum levels of ET-1 [Nelson JB et al 1995]. Administration of an ET-1 receptor antagonist in vivo resulted in both decreased tumour burden and osteosclerotic features of the metastatic bone lesions [Yin JJ et al 2003].

There is evidence that the presence of prostate cancer cells in bone stimulates bone matrix formation (osteoblastic activity; apparent as osteosclerotic lesions on imaging) as well as bone matrix degradation (osteolytic activity). The majority of bone matrix degradation caused by prostate cancer cells is thought to be due to enhanced osteoclast activity, but there is increasing evidence that prostate cancer cells directly participate in the process by producing and secreting matrix degrading enzymes. Sanchez-Sweatman OH et al 1998 observed that PC3 cells and their conditioned medium are able to degrade non-mineralized bone matrix. Furthermore, the cells themselves degraded mineralized bone matrix directly. This activity was correlated with production and secretion of matrix metalloproteinases (MMPs) because it was found that the matrix degrading activity could be reduced by inhibition of metalloproteinase activity. It is thought that bone matrix degradation can in fact release embedded growth factors and cytokines that may in turn stimulate the proliferation of prostate cancer cells. Thus, if prostate cancer cells participate in bone degradation, a vicious cycle is set up whereby the cancer cells stimulate bone turnover and bone turnover stimulates the cancer cell proliferation [Chung LW 2003].

Parathyroid hormone-related peptide (PTHrP) is secreted by the majority of solid osteotropic cancers and plays a significant role in the development of osteolytic features of metastatic bone lesions. PTHrP, produced by tumour cells in the bone microenvironment, stimulates osteoclast generation and recruitment (osteoclastogenesis)

by inducing the secretion of receptor activator of NF-kappaB ligand (RANKL), which binds to the RANK receptor present on osteoclast precursors [Guise TA et al 1996]. Additionally, PTHrP simultaneously decreases secretion of the molecule osteoprotegerin (OPG) by osteoblastic cells, which also results in osteoclast differentiation as OPG normally binds to RANK and thus prevents RANKL/RANK interaction on osteoclast progenitors [Guise TA et al 1996]. Studies in prostate cancer patients have reported data suggesting a positive association between the presence of metastatic disease and raised OPG levels [Brown JM et al 2001] and in one study, serum OPG levels showed the best discriminatory power to differentiate between patients with and without bone metastases [Jung K et al 2004]. This association provides an attractive explanation for the osteosclerotic nature of prostatic cancer metastases.

Another factor contributing to the “fertile soil” in bone is collagen type 1, the main component of bone, which has been reported to increase the proliferation rate of prostate cancer cells compared with cells cultured on plastic or fibronectin [Kiefer J et al 2004]. A component of the non-collagenous extracellular matrix of bone is osteopontin, which has been shown to stimulate proliferation and anchorage-independent growth of human prostate cancer cell lines [Elgavish A et al 1998, Thalmann GN et al 1999]. Castellano G et al 2008 have correlated activation of the osteopontin/ MMP-9 pathway (osteopontin activates MMPs) with prostate cancer progression using patient samples.

The factors involved in the interaction of the lymph node microenvironment in relation to prostate cancer (or other neoplasms) have not been extensively studied. However, Chu JH et al 2006 orthotopically implanted prostate cancer PC-3 cells into nude mice and subsequently compared the gene expression patterns of cells harvested

from the primary site versus those from spontaneous lymph node metastasis. A complementary DNA array platform containing 96 human tumour metastasis-related genes was used. Among them, 10 were upregulated in lymph node metastasis. These could be divided into 4 categories: extracellular matrix degrading enzymes (cathepsin B, D, and L, and MMP16), adhesion molecules (integrins $\alpha 5$ and $\alpha 6$), transcription factors (Ets1, Ets2, and ETV4), and cell surface receptors (uPA receptor). These genes and their products may well be involved in enhancing the metastasis of prostate cancer to lymph nodes, perhaps by regulating the host microenvironment at this site.

There is evidence supporting all the above-mentioned theories in the organ-specific metastasis of prostate cancer and it is likely that the process involves a combination of all the hypotheses discussed. However, there is increasing evidence for the “homing” theory of metastasis. Importantly, it is now postulated that chemokines and their receptors are involved in all aspects of tumour development, progression and migration with an essential and exciting role in the homing and organ-specific metastasis of cancer cells. Prior to discussing this, we must address the issue of chemokine / chemokine receptor nomenclature, structure and their physiological role.

SECTION 1.3

Chemokines and their structure

What are chemokines?

Cytokines are a category of signaling molecules which are important in intercellular communication. More than 200 of these polypeptides regulate cell proliferation, differentiation, maturation and death. The cytokine network includes

several cytokine families (lymphokines, interleukins, chemokines) that can be classified in terms of ligand and receptor structure, although most cytokines have little homology in their DNA or amino acid sequence [Baird PN et al 1995, Cohen MC and Cohen S 1996, Germano G et al 2008]. One exception to this is the family of chemoattractant cytokines or chemokines. With approximately 50 closely related members and at least 19 receptors, chemokines are now the largest known cytokine family.

The history of chemokines began over two decades ago when investigators discovered a factor produced by lipopolysaccharide-stimulated monocytes, later named interleukin-8 (IL-8; the only chemokine originally named an interleukin), that showed chemotactic activity for neutrophils [Yoshimura et al 1987, Walz et al 1987]. Since this discovery, interest in chemokines and their receptors has greatly increased and in the Third International Symposium on Chemotactic Cytokines in 1992, the term “chemokines” was introduced for this large and growing family of structurally related proteins, which were recognized mainly for their ability to act as chemoattractants (as well as activators) of specific types of leucocytes in a variety of immune and inflammatory responses. Similar to other cytokines, the chemokines are secretory proteins produced by leucocytes and tissue cells either constitutively or after induction, and many of their effects are exerted locally in a paracrine or autocrine fashion. However, chemokines are much smaller than other cytokines (8-14kDa) and act via heptahelical G-protein coupled receptors.

Chemokines can be made by virtually every nucleated cell type under appropriate conditions [Gale LM and McColl SR 1999, Hippe A et al 2010]. Most chemokines are expressed in response to a stimulus, but some are constitutively expressed in a tissue-

specific manner. Therefore, the distinction between inducible and constitutive expression might depend only on the origin of the cells under study. For example, the chemokine CXCL14 (originally named BRAK because of its expression in breast and kidney) is constitutively expressed at high levels in normal squamous epithelium, but might require a stimulus to be expressed by inflammatory cells (and certain cancers) [Frederick MJ et al 2000].

The main function of chemokines is in leucocyte chemotaxis or migration, in addition to leucocyte activation, in both physiological and pathological conditions. They control leucocyte circulation, homing, extravasation and recirculation between the blood vessels, lymphatic vessels and lymphoid organs and tissues [Baggiolini M et al 1997, Hippe A et al 2010, Mantovani A 1999, Murphy PM et al 2000, Rollins JB 1997]. In addition to their traditional chemotactic effects in the immune system, chemokines have been implicated in the modulation of cell adhesion, phagocytosis, apoptosis, angiogenesis, proliferation and viral pathogenesis [Baggiolini M et al 1997, Hippe A et al 2010, Murphy PM et al 2000, Rollins JB 1997]. Additionally, chemokines and their receptors are essential for normal embryological development because based on knock-out studies of mice, lack of the chemokine ligand CXCL12 (SDF-1) or its receptor, CXCR4, resulted in impaired foetal development of the cerebellum, the cardiac septum, gastric vasculature, and B-cell lymphopoiesis. These mice died either in utero or at birth [Raz E and Mahabaleshwar H 2009, Tachibana K et al 1998, Zou YR et al 1998].

Chemokine structure and nomenclature

Chemokines consist of approximately 70-130 amino acids and are divided into four subfamilies defined by the arrangement of the conserved N-terminal cysteine (C) residues of the mature proteins. The first three classes all have 4 conserved cysteines whereas the fourth has only two (Figure 1.2) [Bajetto A et al 2001]:

the CXC or α chemokines have one amino acid residue separating the first two conserved cysteine residues near the amino or N-terminus;

the CX₃C or δ chemokines have three amino acid residues between the first and second cysteines near the N-terminus;

the CC or β chemokines in which the first two conserved cysteine residues near the N-terminus are adjacent;

the C or γ chemokines which lack two (the first and third) of the four conserved cysteine residues

Figure 1.2. Structural classification of the chemokine family

Fig. 1.2: Structural classification of the chemokine family

CHEMOKINE GROUP	STRUCTURE
C:C.....C.....
CC:C----C.....C.....C.....
CXC:CX---C.....C.....C.....
CX ₃ C:CXXXC.....C.....C.....

Footnote: C – cysteine; X - an amino acid other than cysteine

The conserved cysteines are important in creating the tertiary structure of chemokines as they form disulphide bonds between themselves (C1 to C3 and C2 to C4), which subsequently results in the characteristic three-dimensional folding of the chemokines. The disulphide bonds keep two amino-terminal regions together that are essential for receptor recognition and biological activity.

As new chemokines were discovered, they were named by the individual laboratories that identified and/or characterized them. Therefore a single chemokine often had many names, which resulted in much confusion. As a result of this a new nomenclature system was developed several years ago, in which the chemokine structural code (CXC, CC, CX3C, or C) is followed by the letter 'L' (ligand) for each chemokine (as in CXCL1) or by the letter 'R' (receptor) for each receptor (as in CXCR1) [Zlotnik A and Yoshie O 2000]. Table 1.1 is an extensive list of the chemokines identified to date together with their synonyms and official names.

It is important to note that within the CXC subfamily, the chemokines are further divided structurally (and functionally) into two groups. One group of the CXC chemokines have the characteristic three amino acid sequence, glutamic acid-leucine-arginine (ELR) motif, immediately before the first cysteine residue of the CXC motif near the amino terminus. A second group of CXC chemokines lack such an ELR domain. The CXC chemokines with the ELR domain (including CXCL1, CXCL2, CXCL3, CXCL5, CXCL6, CXCL8) act mainly as chemoattractants of neutrophils (and promote angiogenesis in wound healing and tumours). The CXC chemokines without the ELR domain (including CXCL4, CXCL9, CXCL10), are chemoattractants primarily for T-lymphocytes and monocytes (and are non or antiangiogenic). However, one exception is

Table 1.1: Chemokine nomenclature

<u>New official name</u>	<u>Alternative/original name (other names may exist)</u>
CXCL1	GRO α – growth related oncogene α
CXCL2	GRO β – growth related oncogene β
CXCL3	GRO γ – growth related oncogene γ
CXCL4	PF-4 – platelet derived factor 4
CXCL5	ENA-78 – epithelial cell derived neutrophil activating factor 78
CXCL6	GCP-2 – granulocyte chemoattractant protein 2
CXCL7	NAP-2 – neutrophil activating protein 2
CXCL8	IL-8 – interleukin 8
CXCL9	MIG – monokine induced by γ -interferon
CXCL10	IP-10 – γ -interferon inducible protein 10
CXCL11	I-TAC – interferon inducible T cell α -chemoattractant
CXCL12	SDF-1 – stromal cell derived factor 1
CXCL13	BCA-1 – B cell activating chemokine 1
CXCL14	BRAK – breast and kidney chemokine
CXCL15	Lungkine
CXCL16	SR-PSOX – scavenger receptor that binds phosphatidylserine and oxidized lipoprotein
CXCL17	VCC-1 – vascular endothelial growth factor correlated chemokine - 1
CCL1	I-309
CCL2	MCP-1 – monocyte chemoattractant protein 1
CCL3	MIP-1 α – macrophage inflammatory protein 1 α
CCL4	MIP-1 β – macrophage inflammatory protein 1 β
CCL5	RANTES – regulated on activation, normally T cell expressed and secreted
CCL6	Unknown
CCL7	MCP-3 – monocyte chemoattractant protein 3
CCL8	MCP-2 – monocyte chemoattractant protein 2
*CCL9/ CCL10	MIP - 1 γ – macrophage inflammatory protein 1 γ
CCL11	Eotaxin
CCL12	MCP-5 – monocyte chemoattractant protein 5
CCL13	MCP-4 – monocyte chemoattractant protein 4
CCL14	HCC-1 – haemofiltrate CC chemokine
CCL15	Lkn-1 – leukotactin 1
CCL16	LEC – liver expressed chemokine
CCL17	TARC – thymus and activation regulated chemokine
CCL18	PARC – pulmonary and activation regulated chemokine
CCL19	ELC – Epstein–Barr virus induced receptor ligand chemokines
CCL20	LARC – liver and activation regulated chemokine
CCL21	SLC – secondary lymphoid tissue chemokine
CCL22	MDC – macrophage derived chemokine
CCL23	MPIF-1 – myeloid progenitor inhibitory factor 1
CCL24	MPIF-2 – myeloid progenitor inhibitory factor 2
CCL25	TECK – thymus expressed chemokine
CCL26	Eotaxin-3
CCL27	ESkine
CCL28	MEC – mucosa-associated epithelial chemokine
XCL1	Lymphotactin- α
XCL2	Lymphotactin- β
CX3CL1	Fractalkine

*CCL9 has also been designated CCL10 but the latter term is no longer in use

CXCL12 (stromal cell derived factor 1; SDF-1), which lacks the ELR domain but induces neovascularisation in vivo (discussed in next section).

The CC chemokines induce the migration of various cell types including monocytes, dendritic cells, basophils, eosinophils, natural killer (NK) cells and T lymphocytes [Baggiolini M et al 1997, Hippe A et al 2010]. The C chemokine subfamily is represented by only two members, XCL1 and 2 (lymphotactin- α and β respectively), which specifically promote the chemotaxis of T-lymphocytes [Kelner GS et al 1994, Kennedy J et al 1995, Hippe A et al 2010].

Additionally, CX3CL1 (fractalkine), is the only member of the CX3C chemokine group. Unlike other chemokines it exists as a membrane bound glycoprotein with the chemokine atop an extended mucin-like stalk. It promotes the chemotaxis and adhesion of monocytes, NK cells and T-lymphocytes to endothelial, epithelial and dendritic cells [Bazan JF et al 1997].

Chemokine Receptors

The specific effects of chemokines on their target cells are mediated by members of a family of 7-transmembrane-domain, G-protein-coupled receptors (also known as serpentine receptors). These chemokine receptors are part of a much bigger superfamily of G-protein-coupled receptors that include receptors for hormones, neurotransmitters, paracrine substances and inflammatory mediators [Murphy PM et al 2000]. To date 19 human chemokine receptors have been identified (table 1.2). Among the 7 receptors that selectively bind certain CXC chemokines are chemokine receptors CXCR1 to CXCR7, whereas the CC receptor family consists of 10 receptors, CCR1 to CCR10. The

Table 1.2 The four classes of chemokine receptors and their ligands* (some chemokines may bind other receptors)

<u>Chemokine receptor</u>	<u>Chemokine ligand</u>
CXCR1	CXCL6, CXCL8
CXCR2	CXCL1, CXCL2, CXCL3, CXCL5, CXCL6, CXCL7, CXCL8
CXCR3	CXCL4, CXCL9, CXCL10, CXCL11
CXCR4	CXCL12
CXCR5	CXCL13
CXCR6	CXCL16
CXCR7	CXCL11, CXCL12, ?non-signaling scavenger receptor
CCR1	CCL3, CCL4, CCL5, CCL7, CCL8, CCL9/CCL10, CCL14, CCL15, CCL16, CCL23
CCR2	CCL2, CCL6, CCL7, CCL8, CCL12, CCL13, CCL16
CCR3	CCL7, CCL8, CCL11, CCL13, CCL15, CCL24, CCL26, CCL28
CCR4	CCL3, CCL5, CCL17, CCL22
CCR5	CCL3, CCL4, CCL5, CCL8, CCL13, CCL16
CCR6	CCL20
CCR7	CCL19, CCL21
CCR8	CCL1, CCL16
CCR9	CCL25
CCR10	CCL27, CCL28
XCR1	XCL1, XCL2
CX3CR1	CX3CL1

*Chemokines also interact with another receptor having seven transmembrane regions, the Duffy receptor – this is a non-signalling receptor and therefore is not included in this table

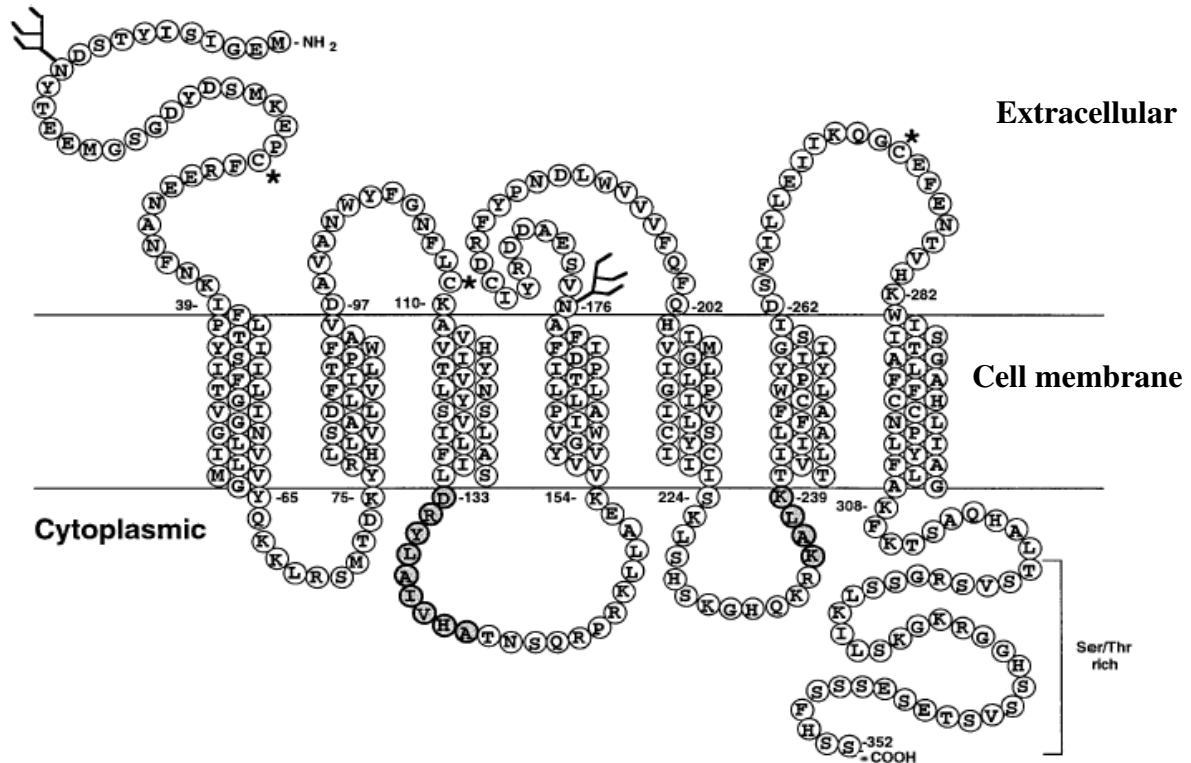
receptor for CX3CL1 (fractalkine) is CX3CR1, and XCR1 is the receptor for XCL1 and 2 (lymphotactin). Another chemokine receptor, known as the Duffy antigen receptor for chemokines (DARC) has been shown to bind to both CXC and CC chemokines. However, this is a non-signalling receptor as no function has been observed on chemokine ligand binding. The relationship between chemokines and their receptors is termed promiscuous, with each receptor being able to bind to more than one chemokine and each chemokine being able to use more than one receptor. However, monogamous chemokine ligand – receptor interactions have been thought to exist eg. CXCL12 –

CXCR4, CCL25 – CCR9, CXCL13 – CXCR5, but this is being disputed as more chemokines and chemokine receptors are being discovered.

Chemokine receptors have been exploited by intracellular pathogens as cell entry and disease transmission factors. The most striking examples of this are the promiscuous chemokine binding protein DARC which is used as a portal of entry into human erythrocytes by the malarial parasite *Plasmodium vivax* [Horuk R 1994], and the chemokine receptors CCR5 and CXCR4 which are used as co-receptors by the HIV-1 virus to promote cellular fusion and infection which results in the disease AIDS [D'Souza MP and Harden VA 1996].

Figure 1.3 shows a diagrammatic representation of CXCR4 and exemplifies the basic structure of chemokine receptors [Lodowski DT and Palczewski K et al 2009]. Characteristic features of chemokine receptors include: they measure approximately 350 amino acids in length and require the introduction of few gaps in the primary sequence to be aligned to other chemokine receptors; a short N-terminus sequence, which is extracellular and is acidic overall and which may be sulfated on tyrosine residues and contain N-linked glycosylation sites; an intracellular C-terminus contains serine and threonine residues that act as phosphorylation sites for receptor regulation; 7 hydrophobic α -helical transmembrane domains - with 3 intracellular and 3 extracellular connecting loops composed of hydrophilic amino acids - are oriented perpendicularly to the plasma membrane; a disulfide bond links highly conserved cysteines in extracellular loops 1 and 2; G-proteins are coupled through the C-terminus segment and possibly through the third intracellular loop.

Figure 1.3: Diagrammatic representation of the chemokine receptor CXCR4 (Fusin). CXCR4 is a 352 amino acid protein. Extracellular cysteine residues are indicated by an asterisk. The two potential N-linked glycosylation sites are shown. By analogy with other chemokine receptors, the cysteine residues in extracellular loops 1 and 2 form a disulfide bond. Ser - serine. Thr - threonine
Diagram modified from Berson JF et al 1996.



Signal Transduction (figure 1.4)

The first study on chemokine signaling was performed in human neutrophils stimulated by CXCL8 (IL-8; the only chemokine originally named as an interleukin). It showed that functional responses were prevented by pretreatment of the cells with Bordetella pertussis toxin, indicating that the receptor was coupled to GTP-binding proteins of the Gi-type, which eventually turned out to be the rule for all chemokine receptors [Thelen M et al 1988]. These G-proteins are inactive when GDP is bound to the G-protein subunit. However, on chemokine ligand binding, the chemokine receptors

associate with the Bordetella pertussis toxin-sensitive heterotrimeric (i.e. consists of three subunits) G-protein, which facilitates the exchange of guanosine diphosphate (GDP) for guanosine triphosphate (GTP), resulting in G-protein activation. On activation, the G-proteins dissociate into the GTP-bound $G\alpha$ and $G\beta\gamma$ subunits. This results in the following effects:

a) $G\alpha$ subunit dependent effects: this results in the direct inhibition of adenylyl cyclase activity leading to decreased intracellular cAMP levels [Bajetto A et al 1999, Zheng J et al 1999]. Evidence also suggests that the $G\alpha$ subunit may activate tyrosine kinases [Thelen M 2001].

b) $G\beta\gamma$ subunit dependent effects:

i) activation of the cell membrane associated enzyme phospholipase C (PLC), which cleaves phosphatidylinositol-4,5-bisphosphate (PIP₂) yielding the two second messengers, inositol-1,4,5-trisphosphate (IP₃) and diacyl-glycerol (DAG).

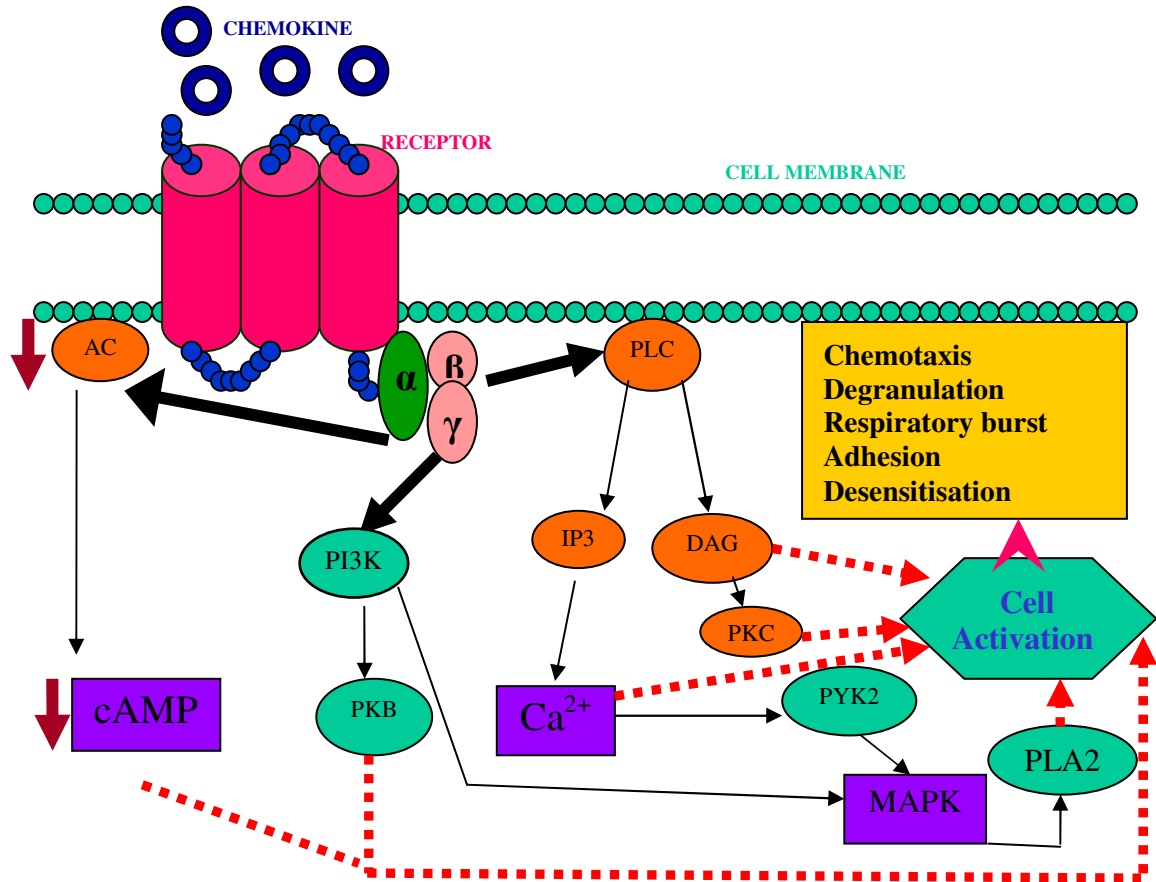
IP₃ triggers the release of calcium from intracellular stores, resulting in a transient rise in free intracellular calcium, whereas DAG, acting in conjunction with calcium, activates the enzyme protein kinase C (PKC). The former has been used widely to test the responsiveness of chemokine receptors to different chemokines [Baggiolini M et al 1997] and the latter is stimulated by almost any surface receptor and is therefore not a characteristic event in chemokine-induced signal transduction. The rise in intracellular calcium activates proline-rich tyrosine kinases (PYK2) which activate MAP kinases. The MAP kinases in turn activate phospholipase A₂ (PLA₂).

DAG, intracellular calcium, PKC, PLA2 and decreased cAMP all interact with specific cell activation mechanisms leading to cell motility, degranulation, release of superoxide anions and modification of integrin avidity (latter are part of family of CAMs).

ii) another well established effector of $G\beta\gamma$ subunits is phosphatidylinositol-3-OH-kinase (PI3K) which activates protein kinase B (PKB). This results in a chemotactic cell response.

After GTP hydrolysis, the GDP-bound $G\alpha$ subunit re-associates with the $G\beta\gamma$ subunit; this then terminates signaling. Additionally, after activation, chemokine receptors become either partially or totally desensitized to repeated stimulation with the same or other agonists. This process is thought to involve both phosphorylation of serine and threonine residues in the C-tail of the chemokine receptor by G-protein-coupled receptor kinases (eg. PYK2 activated by the rise in intracellular calcium), and also receptor sequestration by internalization. Desensitization is thought to be important in maintaining the capacity of the cell to sense a chemoattractant gradient [Thelen M 2001].

Figure 1.4: The chemokine receptor signal transduction pathway in leucocytes. AC – adeny cyclase, cAMP – cyclic AMP, PI3K – phosphatidylinositol-3-OH-kinase, PKB – protein kinase B, PLC – phospholipase C, DAG – diacylglycerol, PKC – protein kinase C, IP3 – inositol triphosphate, PYK2 – proline-rich tyrosine kinase, MAPK – mitogen-activated protein kinase, PLA2 – phospholipase A2



CXCR Receptors – history, location and physiological role in leucocytes

CXCR1 and CXCR2 - receptors for CXCL8 (IL-8; the only chemokine originally named as an interleukin) were first shown to be present on the surface of neutrophils by Peveri P et al 1988. However, two types of CXCL8 binding sites were elucidated, one of which bound CXCL7 and CXCL1, 2, and 3 with high affinity and one of which bound these ligands with low affinity [Besemer J et al 1989]. Both, however, had high affinity for CXCL8 [Lee J et al 1992, Moser B et al 1991]. Eventually, 2 receptors for CXCL8 i.e. CXCR1 and CXCR2 were cloned.

CXCR1 was originally cloned by Holmes et al 1991. CXCR2 was simultaneously cloned by Murphy PM and Tiffany HL 1991. *CXCR1 and CXCR2 bind all known N-terminal Glu-Leu-Arg (ELR) positive, CXC chemokines. They do not bind other types of chemokines.* CXCR1 and CXCR2 are expressed on all granulocytes, monocytes, and mast cells and on some T-cells and NK cells [Chuntharapai A et al 1994].

CXCR3 - CXCR3 binds the non-ELR-containing CXC chemokines, CXCL9 and CXCL10 [Loetscher M et al 1996], CXCL11 [Cole KE et al 1998] and CXCL4 [Lasagni L et al 2003]. The receptor is expressed by IL-2-activated T-lymphocytes [Loetscher M et al 1996]. Two isoforms have been established [Lasagni L et al 2003].

CXCR4 - CXCR4 (Fusin) was first cloned by Loetscher M et al 1994 as an orphan chemokine receptor (that is, a receptor whose ligand has not yet been discovered) and was given the acronym LESTR. It was found to be expressed on neutrophils, myeloid cells, and T lymphocytes [Loetscher M et al 1994]. LESTR was subsequently discovered to be a necessary co-receptor for the entry of T-tropic HIV-1 and HIV-2 into CD4⁺-expressing cells [Feng Y et al 1996]. When CXCL12 (SDF-1) was identified as the ligand for LESTR, the receptor was renamed CXCR4 [Bleul CC et al 1996, Oberlin E et al 1996]. CXCR4 gene deletion in mice results in impaired B lymphopoiesis, myelopoiesis, hematopoiesis, impaired cerebellar neurone migration, cardiac defects and defective formation of large vessels supplying the gastrointestinal tract [Ma Q et al 1998, Nagasawa T et al 1996, Tachibana K et al 1998, Zou YR et al 1998] suggesting that CXCL12 and CXCR4 have significantly different functions from those of other chemokines and their receptors.

CXCR5 - BLR1, an orphan receptor expressed in Burkitt's lymphoma cells and B lymphocytes, was noted to have significant homology with other CXC receptors [Dobner T et al 1992]. Subsequently, CXCL13, a chemokine with strong B-cell-attracting/activating functions, was found to bind BLR1 [Legler DF et al 1998], and thus BLR1 was reclassified as CXCR5.

CXCR6 - this was originally identified as an orphan receptor in 1997 until it was demonstrated that it bound CXCL16, at which time it was renamed CXCR6 [Matloubian M et al 2000, Murphy PM 2002, Wilbanks et al 2001]. CXCR6 is expressed mainly on T lymphocytes [Kim CH et al 2001, Tabata S et al 2005, Unutmaz D et al 2000] and binding of the ligand, CXCL16, results in chemotaxis of these cells in the inflammatory process [Tabata S et al 2005].

CXCR7 - the orphan receptor, RDC-1, was demonstrated by Balabanian K et al 2005, to result in the chemotaxis of T lymphocytes by binding CXCL12 (thought previously to be the only ligand for CXCR4). Therefore the group proposed naming this orphan receptor, CXCR7. There is no information publicly available at this time to confirm whether this designation has been accepted by the International Union of Immunological Societies (IUIS) / World Health Organisation (WHO) Subcommittee on Chemokine Nomenclature. This receptor also has high affinity for CXCL11. The function of this receptor is currently controversial as some studies suggest it is a non-signaling scavenger receptor for CXCL11 and CXCL12 [Naumann U et al 2010].

CCR Receptors – history, location and physiological role in leucocytes

CCR1 - CCR1 was the first CC chemokine receptor to be identified [Neote K et al 1993]. Ligands for CCR1 include CCL3, CCL5, CCL7 and CCL8 [Ben-Baruch A et al 1995, Combadiere C et al 1995, Gong X et al 1997]. Subsequently, CCL14, CCL15 and CCL23 were shown to bind to this receptor [Tsou CL et al 1998, Youn BS et al 1998]. CCR1 is expressed by monocytes [Sica A et al 1997], neutrophils [Bonecchi R et al 1999] and activated T cells [Loetscher P et al 1996, Perera LP et al 1999].

CCR2 - two groups simultaneously discovered CCR2. Yamagami S et al 1994 identified CCR2B but Charo IF et al 1994 discovered two isoforms of CCR2 - CCR2A and CCR2B. CCR2 binds the the monocyte chemotactic proteins (MCPs) [Baggiolini M et al 1994] and thus ligands for CCR2 include CCL2, CCL7, CCL8, CCL13 and CCL16 [Combadiere C et al 1995, Gong X et al 1997, Nomiya H et al 2001].

CCR3 – Daugherty BL et al 1996 and Kitaura M et al 1996 both initially identified CCR3, which is found predominantly on eosinophils but also on basophils and T cells [Gerber BO et al 1997, Ugucioni M et al 1997]. Ligands include CCL11, CCL24, CCL5, CCL7, CCL13, CCL15 and CCL28 [Daugherty BL et al 1996, Forssmann U et al 1997, Ugucioni M et al 1997, Pan J et al 2000].

CCR4 - Power et al 1995 identified CCR4. CCR4 binds CCL3, CCL5, CCL17 and CCL22 [Imai T et al 1997, Imai T et al 1998]. The latter two ligands both activate T lymphocytes.

CCR5 – this was discovered by Samson M et al 1996. Ligands include CCL3, CCL4, CCL5, CCL8 [Ruffing N et al 1998] and also CCL13 and CCL16 [Blanpain C et al 1999]. CCR5 is found in peripheral T lymphocytes and macrophages [Raport CJ et al 1996]. Importantly, CCR5 (and also CXCR4) has been shown to be the major co-receptor, in association with CD4, for HIV-1 entry into permissive cells [Doranz BJ et al 1996].

CCR6 – this was initially cloned as an orphan receptor by a few laboratories. When Baba M et al 1997 discovered that CCL20 specifically bound to this receptor, it was renamed CCR6. The receptor is expressed by memory T cells, B lymphocytes, and dendritic cells [Liao F et al 1999].

CCR7 – initially cloned as an orphan receptor, this was named CCR7 when it was found that it specifically bound CCL19 [Yoshida R et al 1997]. It also binds CCL21 [Campbell JJ et al 1998]. CCR7 is known to be expressed on activated T and B lymphocytes and dendritic cells [Yoshida R et al 1997, Yanagihara S et al 1998].

CCR8 – when Roos RS et al 1997 and Tiffany HL et al 1997 established that several orphan receptors specifically bound CCL1, they were all renamed CCR8. The receptor also binds CCL16 [Howard OM et al 2000]. CCR8 is significantly expressed in thymus T lymphocytes and monocytes [Tiffany HL et al 1997]. Similarly to CXCR4 and CCR5, CCR8 is a cofactor in the infection of permissive cells with the HIV-1 virus [Horuk R et al 1998].

CCR9 – when Zaballos A et al 1999 found that CCL25 bound a known orphan receptor, this was reclassified as CCR9. This receptor is expressed on both immature and mature T cells [Zaballos A et al 1999].

CCR10 – this receptor was first cloned by Marchese A et al 1995. It binds the ligands CCL27 [Baird JW et al. 1999, Homey B et al. 2000] and CCL28 [Wang W et al 2000].

CCR11 – this has been disqualified as a chemokine receptor [Murphy PM 2002].

SECTION 1.4

The role of chemokines and their receptors in cancer

Over the past decade it has become clear that chemokines are not only involved in foetal development, mobilization of haematopoietic stem cells and inflammatory processes by trafficking of naive lymphocytes, but they may be pivotal at all stages of malignant development, including initiation of neoplasia, growth of tumour and progression to invasion and metastasis.

Chemokines in cellular transformation

There is increasing evidence that chemokines are implicated in the neoplastic transformation of cells. The chemokine receptor CXCR2 shares a high degree of homology to the G-protein-coupled receptor ORF74 or Kaposi's sarcoma herpesvirus-G protein-coupled receptor (KSHV-GPCR), encoded by Kaposi's sarcoma-associated herpes virus-8 [Bais C et al 1998]. This is an agonist-independent receptor whose signalling is further upregulated by binding of CXC chemokines CXCL8 and CXCL1 (GRO α). Yang TY et al 2000 showed that over-expression of this receptor within haematopoietic cells of transgenic mice led to the development of angioproliferative lesions resembling Kaposi's sarcoma. Furthermore, Burger M et al 1999 demonstrated that a point mutation of CXCR2 leads to constitutive signalling of the receptor and cellular transformation of transfected NIH 3T3 cells (a fibroblast cell line derived from mouse embryo) comparable to results seen with KSHV-GPCR. This work with others

suggests that CXC chemokines (CXCL8 and CXCL1) continually stimulate certain cells expressing the CXCR2 receptor by autocrine and paracrine mechanisms, ultimately leading to promotion of oncogenic cellular transformation.

Using ovarian cancer cell lines, it has been shown that the presence of the receptor CXCR2 promoted cell cycle progression by modulating cell cycle regulatory proteins and inhibited cellular apoptosis, thus implicating this receptor in the carcinogenesis of ovarian neoplasms [Yang G et al 2010].

Wang D et al 2000 have established that over-expression of human CXCL1, CXCL2 and CXCL3 (GRO α , β , γ) in immortalised murine melanocytes enables these cells to form tumours in SCID and nude mice and additionally they have established that the malignant transformation of the melanocytes by these chemokines requires Ras activation.

Other chemokines might play similar role in neoplastic transformation. CXCL13, the only chemokine known to specifically chemoattract B lymphocytes, has been shown to be highly expressed in *Helicobacter pylori*-induced gastric lymphoma [Mazzucchelli L et al 1999], suggesting a role for CXCL13 in the localization of the tumor as well as possibly in the oncogenic event itself. More recently, using a mouse model, Popivanova BK et al 2009, identified CCL2 as a crucial mediator of the initiation and progression of chronic colitis-associated colon carcinogenesis.

Chemokines and leucocyte recruitment in tumours

The production of inflammatory chemokines by tumour cells (or stromal cells) results in the presence of various types of leucocytes in the tumour tissue. The leucocytes secrete a variety of molecules including cytokines, chemokines and proteases, which affect tumour growth and invasion. However, there is great debate as regards to the role of infiltrating leucocytes in the cancer microenvironment and their relevance to cancer growth and progression [Allavena P et al 2008, Whiteside TL 2006, Yang L and Carbone DP 2004].

Many tumours and metastatic deposits contain numerous macrophages as the major leucocyte component of the cancer stroma. These macrophages are referred to as tumour associated macrophages (TAMs) and most are derived from peripheral blood monocytes recruited into the neoplastic mass [Mantovani A et al 1992]. The role of TAMs in tumours is contentious but they are mostly associated with tumour progression and metastasis although in a significant number they result in cancer regression [Allavena P et al 2008, Bingle L et al 2002, Whiteside TL 2006, Yang L and Carbone DP 2004]. This effect of TAMs is thought to be regulated by modulation of the host immune system. TAMs demonstrate tumour cell growth-promoting effects through release of various cytokines (including chemokines), growth factors, inflammatory mediators and proteolytic enzymes. Once within the tumour, the tumouricidal activity of the macrophages seems not to be activated. Also, macrophages have been shown to suppress many T cell and NK cell anti-tumour responses and also lead to generalised immunosuppression in the host (eg. by secretion of IL-10 and prostaglandin-E2 by TAMs) [Balkwill F 2004a, Elgert KD et al 1998]. On the other hand, tumour growth

reduction by TAMs can be mediated by non-specific anti-tumour cytotoxic mechanisms or induction of specific cell lytic effects. Thus some studies suggest the presence of tumour-associated macrophages is associated with a worse prognosis whereas others show a better or no prognostic significance [Allavena P et al 2008, Bingle L et al 2002, Whiteside TL 2006]. The determinants of the role of TAMs in each tumour are, as yet, poorly understood.

In the seminal work by Mantovani's group they described a tumour-derived chemotactic factor for monocytes produced by human and mouse cancer cell lines [Bottazzi B et al 1983], that was later identified as the chemokine CCL2 (MCP-1), which binds to the CCR2 receptor [Bottazzi B et al 1990]. The chemokine CCL2 has since been shown to induce recruitment of macrophages in many malignancies and furthermore, the levels of this chemokine are further amplified by its secretion by the TAMs. In cancer of the oesophagus, CCL2 expression correlates positively with the level of macrophage infiltration, tumour angiogenesis, and invasion indicating that tumour associated macrophages may promote tumour progression. However, Monti P et al 2003 observed that CCL2 is secreted by pancreatic carcinoma cells and is released into the patient circulation. Serum CCL2 levels were found to be positively correlated with intratumoural macrophage infiltration but inversely correlated with tumour cell proliferative activity. Also, patients with high circulating levels of CCL2 had significantly longer survival than those with low levels. Gene transfer of CCL2 into cancers has also demonstrated confusing results with some studies showing reduced tumorigenicity whilst others have shown increased rates of neoplastic growth and metastases [Conti I et al 2004].

Examples of other tumour secreted chemokines associated with an increased infiltration of macrophages in the neoplasm include CCL5 (RANTES), which is secreted by breast cancer cells and whose level of expression correlates with the extent of macrophage infiltration and progression and lymph node metastasis [Azenshtein, E et al. 2002]. More recently it has been shown that co-culture with macrophages increased the expression of CXCL8 (IL-8) in a glioma cell line and that in 43 human glioma specimens IL-8 mRNA expression and microvessel count in glioma surgical specimens correlated positively with the density of TAMs [Hong TM et al 2009]. It was suggested that macrophages could play a role in promoting glioma growth and angiogenesis by inducing IL-8 expression in glioma cells via inflammatory stimuli or the nuclear factor kappa B pathway.

CCL2, with a number of other chemokines, also aids in the recruitment of dendritic cells into neoplasms [Sozzani S et al 2000]. Dendritic cells play a vital role of antigen-presentation and stimulation of naive T cells that function in the adaptive arm of the immune system; thus it follows that CCL2 recruitment of these antigen presenting cells could promote tumour immunity. However, once again, the role of dendritic cells is not as straightforward as it seems and it is not clear whether their presence is associated with a beneficial or adverse outcome. Data indicate that if dendritic cells were to be recruited into tumours in an immature form they may actually prime the immune system to be tolerant of the tumour antigens rather than immunogenic. There is clear data on the infiltration of cancers by dendritic cells [Chaput N et al 2008, Lespagnard L et al 1999, Vicari AP and Caux C 2002, Whiteside TL 2006] but further work is required to clarify these contradictory findings and understand the intricate balance between immunogenic

induction and toleration of tumours, which occurs within this population of cells [Bennaceur K et al 2008, Hackstein H et al 2001]

Chemokines as tumour growth factors

It is widely known that cells respond to growth factors in an autocrine and paracrine manner, which in turn can induce cells to enter and proceed through the G1 phase of cell cycle. This growth regulation has been observed in a number of tumour systems and highlights the important role for chemokines.

CXCL8 has been established as an essential autocrine growth factor for some human melanoma cell lines and acts via CXCR1 or CXCR2 receptors, which have also been shown to be present in melanoma cell lines [Payne AS and Cornelius LA 2002, Satyamoorthy K et al 2003, Schadendorf D et al 1993, Varney ML et al 2003]. These findings have been more recently confirmed by Gabellini C et al 2009, who also demonstrated that CXCL8 was as an autocrine/ paracrine growth factor in melanoma cell lines acting via CXCR1 and CXCR2 (CXCL8 also induced angiogenesis via this route). However, this group also observed that only CXCR2 receptor plays an important role in regulating the CXCL8-mediated invasive and migratory behaviour of human melanoma cells.

Zhu YM et al 2004 demonstrated that in the non-small cell lung cancer (NSCLC) cell lines, H460 and MOR/P, cell proliferation could be induced by CXCL8 and constitutive proliferation could be inhibited by neutralizing antibodies against CXCL8 ligand or CXCR1 receptor. This indicated that constitutive CXCL8 and CXCR1 protein expression enabled an autocrine growth mechanism in these cells. Using similar

methodology, it has been observed that an autocrine mitogenic effect due to CXCL8 occurs in human epidermoid carcinoma cell lines A431 and KB, but this is via the CXCR2 receptor [Metzner B et al 1999]. Interestingly, Luppi F et al 2007, discovered that CXCL8 stimulates cell proliferation in NSCLC cell lines through epidermal growth factor receptor (EGFR) transactivation.

In vitro studies on androgen-independent PC3 cells have confirmed the mitogenic activity of CXCL8, increasing the rate of cell proliferation through activation of both CXCR1 and CXCR2 receptors [Murphy C et al 2005]. Using CXCL8 LNCaP transfectants Araki S et al 2007 showed that CXCL8 induced cell proliferation was mediated through CXCR1 and was independent of androgen receptor (AR) i.e. CXCL8 is a molecular determinant of androgen-independent prostate cancer growth and progression.

Other tumour cell lines in which CXCL8 acts as an autocrine growth factor are those obtained from human cancers of the colon, stomach, liver, pancreas, and Kaposi's sarcoma [Brew R et al 2000, Fujisawa N et al 2000, Kamohara H et al 2007, Kitadai Y et al 2000, Li A et al 2001, Miyamoto M et al 1998, Takamori H et al 2000, Masood R et al 2001]. CXCL8 has additionally been found to inhibit TNF-related apoptosis in the ovarian cancer cell line OVCAR3 [Abdollahi T et al 2003]. These findings are reinforced in hepatocellular, gastric, pancreatic and prostate cancers, in which CXCL8 and its receptor(s) have been found on immunohistochemistry of surgically resected neoplasms [Akiba J et al 2001, Eck M et al 2003, Hussain F et al 2010, Kuwada Y et al 2003, Murphy C et al 2005]. Additionally, in biopsy tissue obtained from human ovarian carcinomas, neuroblastomas and squamous cell carcinomas of the head and neck, both

CXCL8 and its receptor, CXCR2 are expressed by malignant cells. This suggests CXCL8 could also function in an autocrine pathway for these tumours [Ferrer FA et al 2000, Ivarsson K et al 2000, Richards BL et al 1997].

CXCL1 (GRO α) was originally identified and purified from serum-free culture supernatants of a malignant melanoma cell line, Hs294T, and characterized as an autocrine growth factor for melanoma cells [Bordoni R et al 1990, Richmond A and Thomas HG 1986]. Two highly related CXC chemokines CXCL2 (GRO β) and CXCL3 (GRO γ) have additionally been shown to be involved in melanocyte transformation and tumour growth [Owen JD et al 1997]. All three share the receptor CXCR2. CXCL1 has also been shown to act as an autocrine growth factor for some human adenocarcinoma cell lines derived from the lung and stomach [Fujisawa N et al 2000] and in human malignant colonic, pancreatic, and oesophageal cell lines [Li A et al 2004, Takamori H et al 2000, Wang B et al 2006]. In a murine model CXCL1 is an autocrine mitogenic agent for squamous cell carcinoma [Loukinova E et al 2000]. In gastric carcinoma further verification has been provided by immunohistochemistry on patient samples [Eck M et al 2003, Junnila S et al 2010].

CXCL12 has been found to stimulate glioblastoma cell proliferation [Barbero S et al 2003]. The expression of the receptor for CXCL12 ligand, CXCR4, has been observed to be upregulated in human glioblastomas and inhibition of this receptor blocks tumour cell proliferation [Barbero S et al 2003, Seghal A et al 1998, Seghal A, Ricks S et al 1998]. Interestingly, Bajetto A et al 2001 and Bajetto A, Bonavia R et al 2001 demonstrated the concomitant expression of the CXCL12 ligand (SDF-1) with its receptor CXCR4 leads to autocrine and paracrine regulation of cell growth in cultured

astrocytes. Also, using 12 primary cultures from human meningioma tissue Barbieri F et al 2006 established that CXCL12 - CXCR4 interaction stimulated meningioma cell proliferation through the extracellular signal-regulated kinase (ERK) - 1/2 pathway. Kang H et al 2005 have established the role of the autocrine CXCL12 – CXCR4 pathway in the proliferation of breast cancer cell lines; Marchesi F et al 2004 and Sutton A et al 2007 have confirmed the same axis in pancreatic and hepatocellular cancer respectively using cell lines and human tissue.

In prostate cancer cell lines, PC3, DU145 and LNCaP, CCL5 (RANTES) was confirmed to promote cell proliferation via the CCR5 receptor in an autocrine fashion, which could be inhibited by a CCR5 antagonist [Vaday GG et al 2006, Zhang X et al 2010]. Both CCL5 and CCR5 were also detected in human prostate cancer tissues [Vaday GG et al 2006]. Additionally, Lu Y et al 2006, demonstrated CCL2 (MCP-1) acted as a paracrine and autocrine growth factor in prostate cell lines.

Chemokines in the modulation of angiogenesis and angiostasis

Angiogenesis is a normal physiological process that takes place during embryonic development and wound healing. It is also required for solid tumours to grow beyond 1 mm in diameter and for their subsequent rapid growth [Folkman J 1995, Foulds L 1964, Gimbrone M et al 1974]. CXCL4 (PF-4) and CXCL8 are members of the CXC chemokine subfamily, but they differ in that CXCL8 contains the ELR motif (ELR+; Glu-Leu-Arg) at its NH₂ terminus. It has been demonstrated that CXCL4 has angiostatic properties, which was initially demonstrated by Maione TE et al 1990, who observed that it inhibited endothelial cell proliferation, angiogenesis in the chick chorioallantoic

membrane assay and tumour growth in immunodeficient mice. Lewis lung carcinoma cells transfected with human CXCL4, when injected intravenously, had significantly impaired ability to form lung metastases due to inhibition of neovascularisation in vivo [Yagamuchi K et al 2005]. In fact a variant of CXCL4 has been discovered, known as CXCL4-L1 or PF-4var, which differs from CXCL4 in only three amino acids, but is much more potent in inhibiting angiogenesis in tumours such as melanoma and lung carcinoma [Struyf S et al 2004, Struyf S et al 2007]. It has been established that it is the short terminal COOH fragment or terminal peptides of both CXCL4 and CXCL4L1 that determine the potent antiangiogenic effect of these molecules [Hagedorn M et al 2002, Vandercappellen J et al 2010]. Also of interest is the fact that CXCL4 is able to inhibit the migration and proliferation of lymphatic endothelial cells in a dose dependent manner in vitro, suggesting that it may be implicated in the control of lymphangiogenesis [Shao XJ and Xie FM 2005].

In contrast, CXCL8 was the first chemokine shown to stimulate endothelial cell chemotaxis, proliferation and in vivo angiogenesis (using a rat corneal micropocket assay) [Koch AE et al 1992]. In human umbilical vein endothelial cells (HUVECs) and human dermal microvascular endothelial cells, recombinant human CXCL8 induced endothelial cell proliferation and capillary tube organization (via CXCR2 and CXCR1) whilst neutralization by anti-CXCL8 antibody blocked capillary tube organization [Li A et al 2003]. Incubation of endothelial cells with CXCL8 inhibited endothelial cell apoptosis [Li A et al 2003]. CXCL8 is critical to glial tumour [Brat DJ et al 2005] and melanoma [Gabellini C et al 2009] neovascularity (via CXCR2 and CXCR1) and in glial neoplasms levels of the chemokine correlate with histological grade in glial neoplasms

[Brat DJ et al 2005]. In prostate cancer, CXCL8 has been particularly well studied as regards its role in neoangiogenesis and prognosis. Significant levels of CXCL8 are observed in prostate tumour cells, but not in normal or benign hyperplastic cells [Ferrer FA et al 1998]. Antibody to CXCL8 secreted by the cell line PC-3 has been shown to reduce tumour growth and tumour-related angiogenesis in a SCID mouse model [Moore BB et al 1999]. In LNCaP cells CXCL8 confers androgen-independent growth [Araki S et al 2007, Lee F et al 2004] and Aalinkeel R et al 2004 have suggested that the metastatic potential of prostate cancer cells in vitro correlates with the expression of proangiogenic factors including CXCL8. Clinically, serum CXCL8 (ELR+) is elevated in prostate cancer patients [Veltri RW et al 1999] with a significant elevation of CXCL8 in men with bone metastases when compared to men with localised disease [Lehrer S et al 2004]. Additionally, CXCL8 mRNA levels in radical prostatectomy specimens are positively correlated with an advanced pathologic stage [Uehara H et al 2005] and cytoplasmic expression of this chemokine has been established to correlate with microvessel density on immunohistochemistry [Murphy C et al 2005]. In pancreatic cancer, Matsuo Y et al 2009 measured ELR+ CXC chemokine levels in supernatants from multiple pancreatic cell lines and confirmed significantly higher expression from those derived from malignant cells. Paracrine effects of these ELR+ chemokines on human umbilical vein endothelial cells (HUVEC) was investigated and results confirmed significantly enhanced proliferation, invasion, and tube formation of HUVEC. These biological effects were significantly inhibited by treatment with a neutralizing antibody against the CXCR2 receptor.

Strieter RM et al 1995 hypothesised that the presence of the ELR motif is critical for determining the effect a CXC chemokine has on angiogenesis. They showed that substitution of the ELR motif in CXCL8 with the amino acids TVR (Thr-Val-Arg) or DLQ (Asp-Leu-Gln) resulted in an ELR- mutated CXCL8 that was unable to stimulate endothelial chemotaxis or in vivo angiogenesis. The mutated CXCL8 actually inhibited angiogenesis. In contrast, the addition of ELR to CXCL9 (MIG), an ELR- chemokine, resulted in its conversion from an angiostatic to an angiogenic agent. The angiogenic members of the CXC chemokine family include CXCL1, CXCL2, CXCL3, CXCL5, CXCL6, CXCL7 and CXCL8, which are all ELR+. Only CXCL8 and CXCL6 specifically bind to the receptor CXCR1, whereas, all ELR+ CXC chemokines bind to CXCR2 [Addison CL et al 2000, Strieter RM et al 2004]. The ability of all ELR+ CXC chemokine ligands to bind to CXCR2 supports the notion that this receptor mediates the angiogenic activity of ELR+ CXC chemokines. The angiostatic ELR- CXC chemokines such as CXCL4, CXCL9, CXCL10 and CXCL11 mediate their activity through the CXCR3 receptor [Strieter RM et al 2004].

Luan J et al 1997 tested the biological consequence of overexpression of CXCL1, CXCL2, CXCL3 (GRO α , GRO β , GRO γ : all ELR+) chemokines following their transfection of non-tumourigenic immortalised mouse melanocytes. This resulted in the formation of highly vascular tumours in nude mice. Antibodies to these three proteins slowed or inhibited the formation of tumours in the SCID mouse model (accompanied by a reduction in the number of viable endothelial cells in tumours) and blocked the angiogenic response to conditioned medium from tumourigenic transfectants in the rat corneal micropocket assay. In colorectal cancer, CXCL1 released from carcinoma cells

induced microvascular endothelial cell migration and tube formation in vitro [Wang D et al 2006]. Furthermore, PGE₂ (a proinflammatory mediator) promoted tumour growth in vivo by induction of CXCL1 expression, which resulted in increased tumour microvessel formation in vitro [Wang D et al 2006]. A correlation between CXCL1 cytoplasmic immunostaining and microvessel density was revealed in a series of human oral squamous cell carcinomas [Shintani S et al 2004] and it has been noted that in patients with metastatic renal cell cancers CXCL1 and CXCL3 levels are raised (as well as several other proangiogenic chemokines) [Mestas J et al 2005]. Collectively, these results indicate that CXCL1 inhibitors in particular should be evaluated further as potential anti-angiogenic agents for treatment of cancers.

Amongst the angiostatic chemokines the most studied has been CXCL10 (IP-10), which is ELR⁻. This molecule inhibits growth of new blood vessels stimulated by either vascular endothelial growth factor (VEGF) or angiogenic CXC chemokines in the rat corneal micropocket assay [Belperio JA et al 2000]. Using a mouse matrigel neovascularisation model, CXCL10 was shown to inhibit angiogenesis stimulated by basic fibroblast growth factor in vivo [Angiolillo AL et al 1995]. In HUVECs, CXCL10 resulted in dose-dependent and selective inhibition of proliferation and countered the proliferative effects of vascular endothelial growth factor as well as leading to potent and selective induction of apoptosis [Feldman ED et al 2006]. Treatment of endothelial cells with CXCL10 in the presence of VEGF inhibited endothelial cell tube formation in vitro and significantly inhibited VEGF-induced endothelial motility, via the CXCR3 receptor [Bodnar RJ et al 2006]. Burkitt's lymphoma cells transfected to overexpress CXCL10 had reduced ability to form subcutaneous tumours in nude mice, which was attributed to

its ability to decrease tumour angiogenesis [Sgadari C et al 1996]. Similarly, in melanoma, CXCL10 resulted in decreased tumour growth and microvessel density in vivo by binding the CXCR3 receptor [Yang J and Richmond A 2004]. In renal cancer, intratumour CXCL10 mRNA levels were inversely correlated with microvessel density in patient samples and thus high CXCL10 expression levels were a favourable prognostic factor [Kondo T et al 2004].

Interestingly, one ELR– CXC chemokine actually stimulates, rather than inhibits, angiogenesis: SDF-1 or CXCL12. Gupta SK et al 1998 demonstrated that the CXCR4 receptor is expressed on endothelial cells and that its ligand CXCL12 was an efficacious chemoattractant for these cells. Additionally, CXCL12 induces angiogenesis from cross-sections of leukocyte-free rat aorta in vitro [Salcedo R et al 1999] and the formation of capillary-like structures by endothelial cells in culture [Molino M et al 2000]. Endothelial progenitor cells (EPC) from healthy volunteers also express the CXCR4 receptor and anti-CXCR4 antibodies significantly inhibited CXCL12 induced EPC migration, EPC induced angiogenesis as well as reducing EPC incorporation and impairing blood flow recovery in ischaemic hind limbs of nude mice [Walter DH et al 2005]. Related to this, Ara T et al 2005 have observed that CXCL12 acts on arterial endothelial cells of large arteries to up-regulate CXCR4 and mediate the connection between the larger artery and neighbouring capillary plexus. Recently, using in vitro experiments in glioma cells, VEGF has been shown to exert its effects by upregulation of CXCL12 and CXCR4 expression [Hong X et al 2006], and in ovarian carcinoma it was shown that VEGF upregulates CXCR4 expression on vascular endothelial cells and synergises CXCL12 mediated vascular endothelial cell migration in vivo [Kryczek I et al 2005]. Additionally,

CXCL12 synergised VEGF mediated vascular endothelial cell expansion and hypoxia induced both tumour CXCL12 and VEGF production. This suggests that hypoxia triggered tumour CXCL12 and VEGF form a synergistic angiogenic axis in vivo [Kryczek I et al 2005]. From this evidence, it is likely that anti-VEGF treatments, which have been introduced, act partly via down-regulation of the CXCL12 – CXCR4 axis. Interestingly, using tumor xenografts of the C6 glioma cell line containing cancer stem cells (CSC; which are predicted to be critical drivers of tumour progression due to their self-renewal capacity and limitless proliferative potential) Folkins C et al 2009 demonstrated that that CSC contribute to tumour angiogenesis by promoting both local endothelial cell activity and systemic angiogenic processes involving bone marrow-derived endothelial progenitor cells. This was found to be the result of increased VEGF and CXCL12 by the CSC. It should be noted that there is now some emerging evidence that CXCL12 exerts its biological effects in endothelial cells through a receptor different from CXCR4 [Hatse S et al 2006].

These studies suggest the presence of both stimulators and inhibitors of angiogenesis among the CXC chemokine subfamily. It is postulated that CXC chemokines form a balanced network of angiogenic and angiostatic regulators that are disrupted in cancer. Importantly, the balance of ELR+ and ELR– chemokines produced by a tumour and its stroma may determine the degree of angiogenesis surrounding the tumour and thus, the consequent invasiveness of the tumour [Moore BB et al 1998, Strieter RM et al 2004].

Chemokines in local tumour invasion and adhesion

Several studies have shown that chemokines are important in stimulating cancer cells to produce and secrete protease enzymes, which aid invasiveness through the ECM. For example, CXCL8 expression by human melanoma cells induces transcriptional activation of expression of the gene encoding MMP-2 and augmented collagenase activity in these tumour cells, which leads to increased invasiveness [Luca M et al 1997].

In prostate cancer, CXCL8 over-expression induces the expression of MMP-9, leading to increased tumour cell invasiveness and metastatic potential in nude mice [Inoue K et al 2000a]. Invasion through ECM components by malignant prostate cell lines (LNCaP and/ or PC3) in response to CXCL12 was shown to be a result of increased MMP expression (specifically MMP-1, MMP-2, MMP-3, MMP-9, MMP-14) [Chinni SR et al 2006, Hu W et al 2008, Singh S et al 2004a]. CXCL12 – CXCR4 interaction, resulting in increased MMP-9 and MMP-2 expression, has been implicated in perineural invasion of prostate cancer using human tissue and cell lines [Zhang S et al 2008]. Hu W et al 2008 suggested that exogenous CXCL16 interacted with the CXCR4 receptor in prostate cancer cells to promote significant MMP-9 and MMP-2 activity in LNCaP but not in PC3. Additionally, the CCL25 ligand has been shown to enhance expression of MMP-2 and MMP-9 in prostate cancer cells in vitro, via the CCR9 receptor, resulting in increased invasive capacity [Singh S et al 2004b].

In bladder cancer it has been suggested that CXCL8 exerts its action through an autocrine and paracrine loop by inducing adjacent tumour cells and stromal cells to express increased levels of MMP-2 and MMP-9, which facilitates tumour invasion, and metastases [Inoue K et al 2000b]. Also Eisenhardt A et al 2005 noted a distinct rise in

intracellular actin stress fibre formation, chemotactic activity and invasion through matrigel coated membranes in the bladder cancer cell lines J82 and T24 upon stimulation with CXCL12, which was blocked in the presence of a specific CXCR4 receptor antibody. More recently, Kawanishi H et al 2008, once again using the highly invasive human bladder cancer cell line T24 in addition to the poorly invasive human bladder carcinoma cell line RT112, demonstrated that CXCL1, secreted from malignant cells, promoted cancer cell invasiveness via the increased expression of MMP-13. They also showed that urinary CXCL1 levels were significantly higher in patients with invasive bladder cancer (pT1-4) than those with non-invasive pTa tumours and normal control, thus suggesting its use as a potential urinary biomarker for invasive bladder cancer.

Tang CH et al 2010 found that human chondrosarcoma tissues had significant expression of the chemokine ligand CCL5 and its receptor CCR5, which was higher than that in normal cartilage. They also found CCL5 increased MMP-3 expression in human chondrosarcoma cells (JJ012 cells). Interestingly, it has been noted that human adipose tissue derived stem cells (hASCs), when co-cultured with breast cancer cells in vitro, resulted in increased neoplastic cell invasion through matrigel due to secretion of CCL5 by hASCs, which resulted in raised MMP-9 activity in cancer cells [Pinilla S et al 2009].

Chemokines are also implicated in mediating the expression of integrins, which as discussed earlier, are involved in the formation of tumour cell – ECM or tumour cell – endothelial cell adhesions during invasion and migration. For example, increased tumour cell adhesion to the fibronectin of ECM is related to the CXCL12 stimulation of numerous ovarian cancer cell lines to upregulate β 1-integrin [Scotton CJ et al 2001]. In small cell lung cancer cells (SCLC) CXCL12 stimulation has been demonstrated to

induce firm adhesion to marrow stromal cells via activation of $\alpha 4\beta 1$ integrin and also induce SCLC cell invasion into the ECM [Burger M et al 2003]. In the B16 melanoma experimental metastasis model, CXCR4 transfected cells were observed to enhance adhesion to dermal and pulmonary microvascular endothelial cells [Murakami T et al 2002]. Under flow conditions, these transfected cell lines showed no evidence of rolling before arrest and adhesion was dependent on $\beta 1$ integrin expression and adhesion of transfectants to endothelial cells both in vitro and in vivo was inhibited by anti- $\beta 1$ antibodies [Cardones AR et al 2003]. Engl T et al 2006 have established that CXCL12 – CXCR4 interaction resulted in enhanced expression of $\alpha 5$ and $\beta 3$ integrins in LNCaP and DU145 cell lines, which enabled increased adhesion of these cells to human endothelium or to ECM proteins (laminin, collagen, fibronectin), thereby promoting tumour invasion. Also it has been noted that lung derived CXCL12 (chondrosarcoma shows a predilection for metastasis to lungs) enhances the invasiveness of chondrosarcoma cell lines by increasing $\alpha 5\beta 3$ integrin expression through the CXCR4/ ERK/ NF-kappaB signal transduction pathway [Lai TH et al 2009].

Additionally, Singh S et al 2009a, established that in prostate cancer, CXCL13, the only ligand for CXCR5, was produced by human bone marrow endothelial (HBME) cells, and was able to induce prostate cancer cell line adhesion to HBME cells and also increase their invasive ability in a CXCR5-dependent manner. This CXCL13 – CXCR5 interaction promoted the clustering of $\alpha 5\beta 3$ integrin in the prostate cancer cells. CXCL13-mediated prostate cancer cell adhesion to HBME cells and $\alpha 5\beta 3$ clustering was abrogated by CXCR5 blockade.

Chemokines in the organ specific directional migration of cancer cells

As discussed in an earlier section, metastasis is not a random process and different cancer types have specific metastatic sites. There is increasing support for the “homing” theory of organ specific metastasis stating that different organs have special abilities to attract, through chemotactic factors, specific types of cancer cells [Moore MA 2001, Muller A 2001, Ben-Baruch A et al 2008]. Importantly there is growing evidence that chemokines and their receptors play a pivotal role in this directional migration of cancer cells.

In a seminal publication by Muller A et al 2001, they researched into the mechanisms involved in the metastasis of breast cancer to specific organs. They found that amongst 17 different chemokine receptor genes, CXCR4 and CCR7 were highly expressed in human breast cancer cells lines, malignant breast tumours and metastases relative to the levels in normal mammary epithelial cells. They then screened a panel of normal human organs for the ligands of these receptors, CXCL12 and CXCL21 respectively, and found they exhibited peak levels of expression in organs preferred for breast cancer metastases. In vitro, using breast cancer cell lines, these ligands stimulated pseudopodia formation and directional migration in cells in addition to local invasion through extracellular matrix and basement membrane. Also, extracts of organs targeted by breast cancer (lung, liver, bone marrow and lymph node) had chemotactic activity for breast cancer cells that could be neutralised by anti-CXCR4 antibody, thus suggesting CXCL12 was the active agent. Neutralising anti-human CXCR4 monoclonal antibody suppressed lymph node and lung metastases in a metastatic model of human breast cancer (MDA-MB-231 cell line injected either orthotopically into the mammary fat pad or

intravenously in immunodeficient SCID mice). The same group found that melanoma cell lines express receptors CCR7 and CCR10 and that skin and lymph nodes, the two major sites of metastatic melanoma, selectively express ligands for both these receptors. At the time of this discovery CXCL12 (SDF-1) had already been well known for its homing effect on immature (CD34-positive) progenitor cells in the process of bone marrow repopulation [Aiuti A et al 1997].

CXCR4 is, in fact, the chemokine receptor most commonly found in human and murine cancer cells [Balkwill F 2004a and b] and its involvement in directional metastasis has been suggested in a variety of tumours, including small-cell lung cancers, pancreatic cancers, astroglomas, myelomas, B cell lymphomas, chronic lymphocytic leukaemias, kidney cancer and rhabdomyosarcoma [Balkwill F 2004b]. Studies have also reported that VEGF induces CXCR4 expression in tumour cells [Bachelder RE et al 2002]. This observation raises the possibility that anti-VEGF agents may exert their anti-tumour effects partly through CXCR4. The evidence for the role of the CXCL12 – CXCR4 axis in the directional migration of a variety of cancers is discussed in detail in the final chapter.

Wiley H et al 2001 have reported that transfection of a normally non-metastatic melanoma cell line with CCR7 rendered it able to migrate to the lymph nodes in vivo. Takanami I 2003 reported the expression of CCR7 correlated highly with the ability of non-SCLC to metastasize to the regional lymph nodes. CCR7 negative tumours, in contrast, very rarely were found in the regional lymph nodes. CCR7 positive gastric carcinoma cells have a high incidence of lymph node metastasis, and patients with CCR7-positive tumours have a significantly poorer prognosis than those with CCR7-

negative tumours [Mashimo K et al 2002]. Similar observations have been made in oesophageal carcinoma patients [Ding Y et al 2003] and it has also been noted that in an analysis of 78 human oesophageal squamous cell cancers, high CCR7 mRNA expression in neoplastic cells was found to be an independent predictive factor for lymph node metastases [Ishida K et al 2009]. CCR7 expression by malignant cells has additionally been implicated in the metastasis of SW620 colon cancer cells in vitro and in vivo [Yu S et al 2008]. It is suggested that CCR7 is a key receptor in determining lymph node metastasis in particular [Takanami I 2003]. Interestingly, Kochetkova M et al 2009, using breast cancer cell lines, reported a novel property of the chemokine receptors CCR7 and CXCR4 (both expressed on malignant breast cells) in inhibiting detachment-induced cell death - anoikis, which is believed to be one of the major blocks in the metastatic spread of various neoplasms.

Other chemokine receptors implicated in chemokine dependent tumour cell attraction to certain tissues include CCR4, which is often expressed in adult T-cell leukaemias that preferentially invade the skin, where one of the CCR4 ligands, CCL17 (TARC), can be expressed [Ishida T et al 2003]. Lee JH et al 2009 found that 6 out of 8 gastric carcinoma cell lines expressed functional CCR4, as demonstrated by migration assays using its ligand CCL17; migration was inhibited by anti-CCR4 antibodies. Additionally, human CCR4 positive gastric tumours had a significantly poorer patient prognosis.

Using immunohistochemical techniques, a unique cohort of 21 primary lung cancers with matched adrenal metastases were studied for chemokine receptor expression [Raynaud CM et al 2010]. It was discovered that CCR6 was clearly overexpressed in

adrenal metastases, compared with corresponding primary tumors. Moreover, CCL20, the ligand of CCR6, was preferentially expressed in adrenal tissues that developed metastases [Raynaud CM et al 2010].

CCR3 has been demonstrated to be expressed in CD30+ cutaneous lymphomas, and its ligand CCL11 (eotaxin) is often expressed in the tumour cells and tumour associated skin lesions [Kleinhans M et al 2003]. In prostate cancer cells CCR9 expression also correlates with enhanced chemotaxis and directional migration when induced by the ligand of CCR9, CCL25. Inhibition of CCL25 – CCR9 interactions effectively reduced the migration (and invasive competence) of LNCaP and PC3 cells [Singh S et al 2004b].

Of the CXCR group of receptors (excluding CXCR4, whose role in metastasis is discussed in detail in the final chapter), CXCR2 or CXCR3 have recently been verified in the organ specific metastasis of human melanoma [Singh S et al 2009b], colon cancer [Cambien B et al 2009] and osteosarcoma [Pradelli E et al 2009].

In prostate cancer, the chemokine ligand CCL2 has been implicated in promoting metastatic activity [Mizutani K et al 2009, Zhang J et al 2010], which can be significantly decreased in vitro by curcumin (the active phytochemical ingredient of turmeric and a dietary supplement, which is often self-prescribed to promote prostate health) [Herman JG et al 2009]. Also, in four hepatoma cell lines, following CCL3 stimulation, obvious pseudopodia formation as well as increased cell migration of hepatoma cells was observed, as a result of CCL3 interaction with its receptor CCR1, found on malignant cells [Yuan Y et al 2010]. CCL3 facilitated the migration of hepatoma cells by increasing the concentration of intracellular calcium.

All of these studies mentioned support the hypothesis that certain chemokine ligands and their receptors are involved in the homing of metastatic tumour cells to specific organs.

SECTION 1.5

Hypothesis and aims

It was hypothesised that chemokine ligand - receptor interactions may be important in the non-random and organ selective metastasis of prostate cancer.

This hypothesis was structured after studying the literature on the role of chemokines and their receptors in all aspects of cancer development, progression and migration and especially following the publication of the seminal paper in “Nature” by Muller A et al 2001, which demonstrated that the chemokine receptor : ligand interactions CCR7 : CCL21 and particularly CXCR4 : CXCL12 had a critical role in the directional migration of malignant breast cancer cells to specific metastatic sites such as bone marrow and lymph nodes.

In order to test this hypothesis we had the following aims:

- 1) The first aim was to perform a semi-quantitative analysis, at mRNA level, using RT-PCR, of the chemokine receptors in the CXCR and CCR groups in prostate cell lines derived from normal prostate epithelium and stroma, primary prostate cancers and metastatic prostate cancers.
- 2) If the pattern of expression of any chemokine receptor was found to be of interest in the prostate cell lines (eg. upregulation in metastatic cells), the next aim was to perform a

more accurate quantitative analysis of the mRNA of the specific receptor of interest in the prostate cell lines and in benign and malignant tissue derived from human prostates.

3) Following this, the next step was to demonstrate protein expression of the receptor of interest in prostate cells.

4) Once protein expression of chemokine receptor was established, the subsequent aim was to determine whether the receptor was functional (using prostate cell lines) by stimulating the receptor with its appropriate ligand.

CHAPTER 2

THEORY OF TECHNIQUES

SECTION 2.1

Polymerase chain reaction and reverse transcriptase – polymerase chain reaction

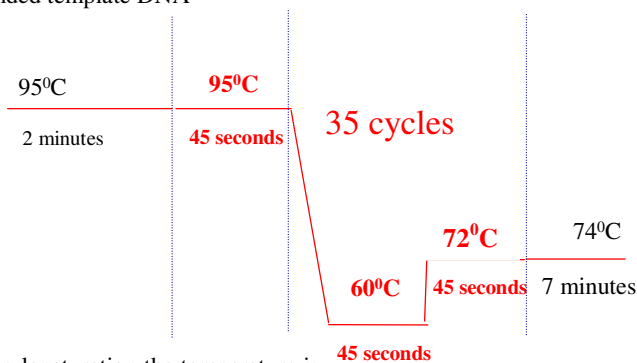
The polymerase chain reaction (PCR) is a technique which allows the exponential amplification of a specific region of DNA by repeating a 3 step process: denaturation, annealing and synthesis (extension). This process is shown in figure 2.1.

Reverse transcriptase – PCR (RT-PCR) investigates gene expression at the mRNA level. The enzyme reverse transcriptase synthesizes a complementary DNA (cDNA) strand from a RNA strand. This cDNA is then used as a template for PCR analysis.

Figure 2.1: The polymerase chain reaction

Figure 2.1: The Polymerase Chain Reaction

1) The template DNA is denatured by heating to 95°C, disrupting the hydrogen bonds between the base pairs resulting in two single strands of DNA from the one double stranded template DNA



4) The 3 step process of denaturation, annealing and extension is typically repeated for 25-35 cycles. At the end of 30 cycles there will be up to 2^{30} double stranded DNA molecules identical to the initial template DNA fragment.

2) After denaturation the temperature is reduced to approximately 60°C to allow primers to bind with high specificity to their complementary bases on the template DNA. Annealing temperature varies depending on the nucleotide composition of the primer selected

3) After annealing the primers, the temperature is increased to 72-74°C, the optimal temperature for Taq DNA polymerase activity. Beginning at the primer annealing site, Taq DNA polymerase synthesises new DNA by adding complementary nucleotide bases to the denatured single stranded template DNA resulting in two double stranded DNA molecules identical to the initial template DNA.

SECTION 2.2

Real-time quantitative PCR

Methodology background

Theoretically one copy of a specific sequence can be amplified and detected in PCR. The PCR reaction generates copies of a DNA template exponentially. This results in a quantitative relationship between the amount of starting target sequence and amount of PCR product accumulated at any particular cycle. Due to inhibitors of the polymerase reaction found with the template, reagent limitation or accumulation of pyrophosphate molecules, the PCR reaction eventually ceases to generate template at an exponential rate (i.e., the plateau phase) making the end point quantitation of PCR products unreliable. Therefore, duplicate reactions may generate variable amounts of PCR product. Only during the exponential phase of the PCR reaction is it possible to extrapolate back in order to determine the starting quantity of template sequence. The measurement of PCR products as they accumulate (i.e., real-time quantitative PCR) allows quantitation in the exponential phase of the reaction and therefore removes the variability associated with conventional PCR.

Since the first documentation of real-time PCR [Higuchi R et al 1993], it has been used for an increasing and diverse number of applications including mRNA expression studies, DNA copy number measurements in genomic or viral DNAs [Gómez-Curet I et al 2007, Gubina NE et al 2010, Murata H et al 2009], allelic discrimination assays [Castillejo A et al 2007], expression analysis of specific splice variants of genes [Dales JP et al 2010] and gene expression in paraffin-embedded tissues [Harbeck N et al 2008] and laser captured microdissected cells [Hoffmann AC et al 2009].

Fluorogenic probes and the Taqman real-time assay

Real-time quantitative PCR allows the reliable detection and measurement of products generated during each cycle of the PCR process which are directly proportional to the amount of template prior to the start of the PCR process. Holland and coworkers demonstrated that the thermostable enzyme *Thermus aquaticus* (i.e., Taq) DNA polymerase had 5' to 3' exonuclease activity [Holland PM et al 1991]. This group also showed that cleavage of a target probe during PCR by the 5' nuclease activity of Taq polymerase can be used to detect amplification of the target-specific product [Holland PM et al 1991]. An oligonucleotide probe, which was designed to hybridize within the target sequence, was introduced into the PCR assay. This probe was labeled with ³²P at its 5' end and was nonextendable at its 3' end to ensure it could not act as a primer. Annealing of probe to one of the PCR product strands during the course of amplification generated a substrate suitable for exonuclease activity. Also, during amplification, the 5' to 3' exonuclease activity of Taq DNA polymerase (when the enzyme extended from an upstream primer into the region of the probe) degraded the probe into smaller fragments that could be differentiated from undegraded probe. This dependence on polymerization ensured that cleavage of the probe occurred only if the target sequence was being amplified. After PCR, cleavage of the probe was measured by using thin-layer chromatography to separate cleavage fragments from intact probe.

The introduction of dual-labeled oligonucleotide fluorogenic probes allowed the elimination of post-PCR processing for the analysis of probe degradation [Lee LG et al 1993]. The probe has a reporter fluorescent dye at the 5' end and a quencher dye attached to the 3' end. Whilst the probe is intact, the close proximity of the quencher significantly

decreases the fluorescence emitted by the reporter dye. A fluorescence signal is only emitted on cleavage of the probe, based on the fluorescence resonance energy transfer (FRET) principle [Cardullo RA et al 1988].

In the real-time quantitative TaqMan® assay a fluorogenic non-extendable probe, termed the “TaqMan” (hydrolysis) probe is used in conjunction with a forward and reverse primer (figure 2.2) [Heid CA et al 1996]. The probe has a fluorescent reporter dye covalently bonded to its 5′ end and a quencher dye at its 3′ terminus. Various fluorescent reporter dyes are in use including 6-carboxyfluorescein (FAM), 6-carboxy-4,5-dichloro-2,7-dimethoxyfluorescein (JOE), tetrachloro-6-carboxyfluorescein (TET), hexachloro-6-carboxyfluorescein (HEX), or VIC (this is an acronym – Applied Biosystems have not released the chemical composition of this dye). Quenchers include either 6-carboxytetramethylrhodamine (TAMRA) or 4-(dimethylaminoazo)benzene-4-carboxylic acid (DABCYL). If the target sequence is present, the fluorogenic probe anneals downstream from one of the primer sites and is cleaved by the 5′ nuclease activity of the Taq polymerase enzyme during the extension phase of the PCR [the most commonly used enzyme is Taq polymerase (Holland PM et al 1991) but any enzyme with 5′ nuclease activity can be used (Gut M et al 1999)].

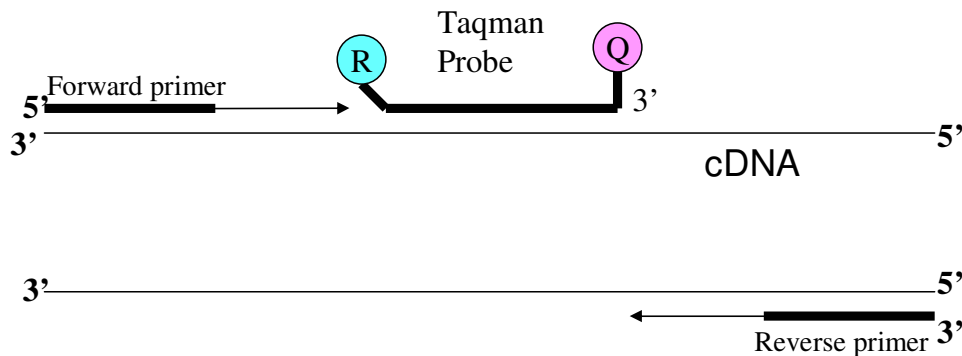
Whilst the probe is intact the proximity of the reporter and quencher dyes permits FRET and the fluorescence emission of the reporter dye is absorbed by the quenching dye. Cleavage of the probe by Taq polymerase during PCR separates the reporter and quencher dyes, thereby increasing the fluorescence emission from the former. Additionally, cleavage removes the probe from the target strand, allowing primer extension to continue to the end of template strand, thereby not interfering with the

exponential accumulation of PCR product. Additional reporter dye molecules are cleaved from their respective probes with each cycle, leading to an increase in fluorescence intensity directly proportional to the amount of amplicon produced. The TaqMan chemistry is the most widely used real-time PCR assay and has been used for multiple purposes [Bustin SA et al 2005, Kubista M et al 2006]. The various available chemistries using fluorogenic probes for real-time PCR include Taqman (hydrolysis) probes, dual hybridization probes, molecular beacons and scorpion probes.

Figure 2.2: The Taqman real time quantitative PCR assay (hydrolysis probes)

Figure 2.2: The Taqman assay (hydrolysis probes)

a) Denaturation and annealing

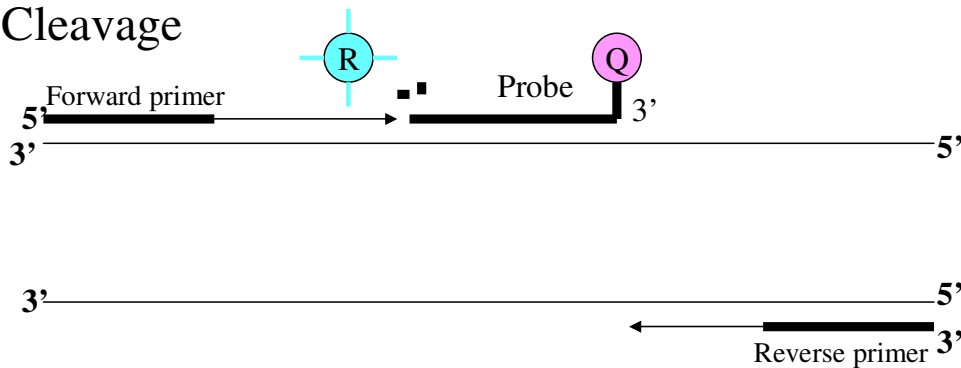


Two fluorescent dyes, a reporter (R) and a quencher (Q), are attached to the 5' and 3' ends of a TaqMan[®] probe.

When the Taqman probe is intact, the reporter and quencher dyes stay close to each other, and fluorescence emission is quenched. The primer and Taqman probe anneal to the complementary DNA strand following denaturation

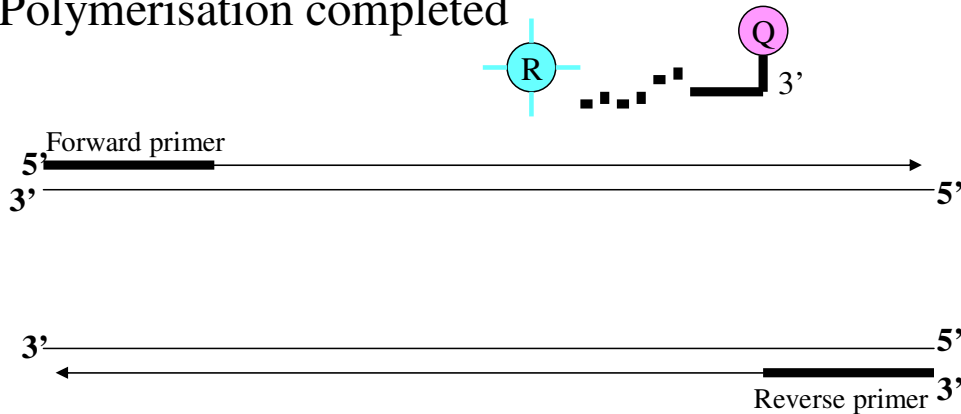
Figure 2.2 continued

b) Cleavage



After hybridisation and during each extension cycle, the 5' endonuclease activity of the Taq DNA polymerase cleaves the probe and separates the reporter and quencher dyes.

c) Polymerisation completed



Once separated from the quencher, the reporter dye emits its characteristic fluorescence.

In addition to fluorescent probes the other chemistry available for amplicon detection are the double-stranded (ds) DNA-intercalating agents (DNA-binding dyes). These include SYBR Green 1 or ethidium bromide and this is the simplest and most cost-effective method as amplicon-specific labelled hybridization probes are not required. SYBR Green 1 only fluoresces when intercalated into dsDNA. The intensity of the fluorescence signal is therefore dependent on the quantity of dsDNA present in the reaction. The main disadvantage of this method is that it is not specific since the dye binds to all dsDNAs formed during the PCR reaction (i.e. non-specific PCR products and

primer-dimers). With fluorogenic probes, non-specific amplification due to mispriming or primer-dimer artifact does not generate signal as specific hybridization between probe and template is necessary for fluorescence emission. Also, fluorogenic probes can be labelled with different and distinguishable reporter dyes, thus allowing the detection of amplicons that may have been produced by one or several primer pairs in a single PCR reaction – termed multiplex real-time PCR.

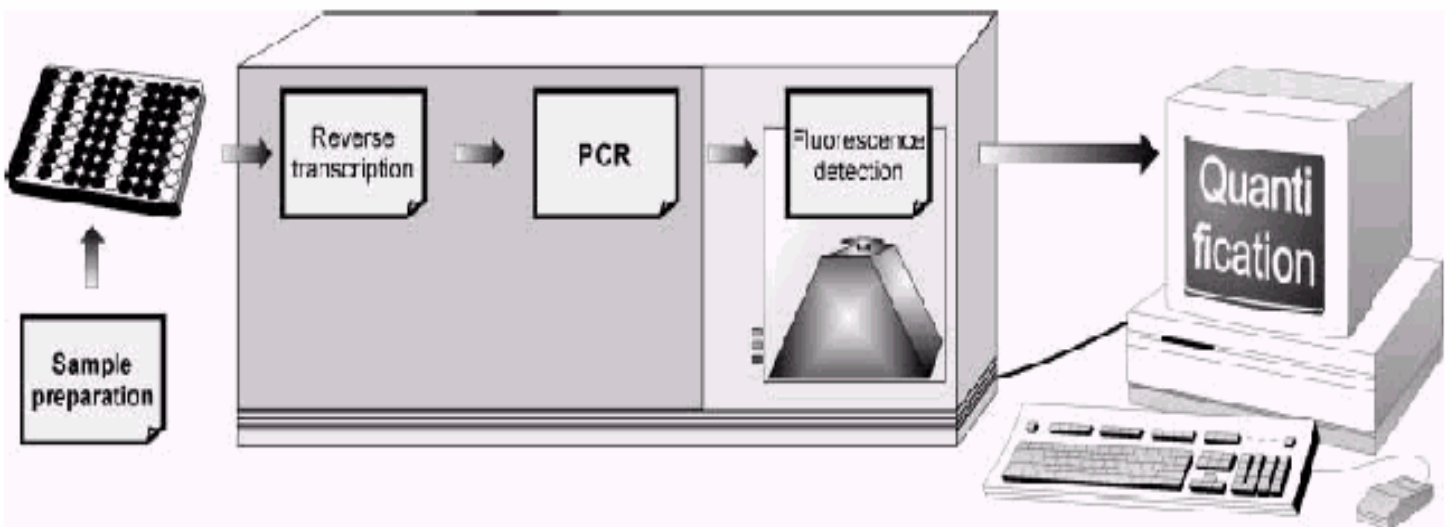
It is important to note that because of the enormous amplification possible with PCR, contamination of new PCRs with trace amounts of amplification products, i.e. carry-over contamination, can yield false positive results. Other sources of contamination could be from samples with high DNA levels or from positive control templates. Carry-over contamination can be controlled by incorporating dUTP in place of dTTP as a dNTP substrate in all PCRs of cDNA [Longo MC et al 1990]. All subsequent fully pre-assembled starting PCR reactions should then be treated with the enzyme uracil DNA glycosylase (uracil N-glycosylase or UNG), followed by thermal inactivation of UNG. UNG cleaves the uracil base from the phosphodiester backbone of uracil-containing DNA, but has no effect on natural (i.e. dTTP or thymine-containing) DNA (also, UNG has no effect on RNA). The resulting apyrimidinic sites block replication by DNA polymerases, and are very labile to acid/base hydrolysis. Because UNG does not react with dUTP, and is also inactivated by heat denaturation prior to the actual PCR, carry-over contamination of PCRs can be controlled effectively if the contaminants contain uracils in place of thymines.

Instrumentation

The ABI PRISM® 7700 Sequence Detection System (Perkin-Elmer–Applied Biosystems, Foster City, CA, USA) (figure 2.3) was used in the performance of all real time quantitative PCR assays in our experiments.

Figure 2.3: The ABI PRISM ® 7700

The ABI PRISM 7700. Amplification is performed in closed, optical tubes of a 96-well microplate that is placed in a combined thermal cycler/detector, the ABI 7700. Fluorescence is induced by a laser directed to each of the 96 sample wells, and the fluorescence emission data for each sample are collected once every few seconds as the PCR products are being generated. Simultaneous use of more than one reporter dye or fluorescent probe is possible. The starting copy number is determined by monitoring when PCR product is first detected – the higher the starting copy number of the target, the sooner a significant increase in fluorescence is observed. The data are fed to a computer that analyses and displays the results, which eliminates the need for post-PCR processing.



The 7700 system has a built-in thermal cycler and a laser directed via fibre-optic cables to each of the 96 sample wells. Fluorescence is induced during the PCR by distributing laser light to all 96 samples contained in thin-walled reaction tubes via the multiplexed array of optical fibres. This fluorescence emission data for each sample is

collected once every few seconds as the PCR products are being generated and travels back through the cable fibres to be directed to a spectrograph with a charge-coupled device (CCD) camera. The starting copy number is determined by monitoring when PCR product is first detected – the higher the starting copy number of the target, the sooner a significant increase in fluorescence is observed. The data are fed to a computer, which analyses and displays the results, eliminating the need for post-PCR processing. Because each well is irradiated sequentially, the dimensions of the CCD array can be used for spectral resolution of the fluorescent light. Also, as the 7700 instrument detects an entire fluorescence spectrum (500 – 660nm), the system is capable of distinguishing and quantitating multiple fluorophores in each sample well.

The software analyzes the data by first calculating the contribution of each component dye to the experimental spectrum. Each reporter signal is then divided by the fluorescence of an internal reference dye (ROX) in order to normalize for non-PCR related fluorescence fluctuations occurring well-to-well or over time. The use of this internal reference dye, enabled by the ability to distinguish fluorophores, increases the precision of the data obtained with the 7700 system. The other advantage of distinguishing fluorophores is that probes labelled with different reporter dyes can be used so that more than one PCR target can be detected in a single tube. By plotting the increase in fluorescence versus cycle number, the system produces amplification plots that provide a more complete picture of the PCR process than assaying product accumulation after a fixed number of cycles.

This instrument can be used for assays based on DNA-binding dyes, molecular beacons and hydrolysis (Taqman) probes. RT-PCR reactions typically take 2 hours to

complete. Its description by the manufacturer as a real-time technique is not strictly correct as, unlike competing systems, the progress of the PCR reaction can be analysed only after termination of the amplification run. Although the ABI Prism® 7700 Sequence Detection System from Applied Biosystems was the first commercially available thermocycler for real-time PCR, it has now been discontinued. It has recently been replaced by the ABI Prism 7900HT, which has similar specifications to the 7700 but is completely automated and designed especially for very high throughput applications (384 samples per run).

Real-Time PCR Quantitation

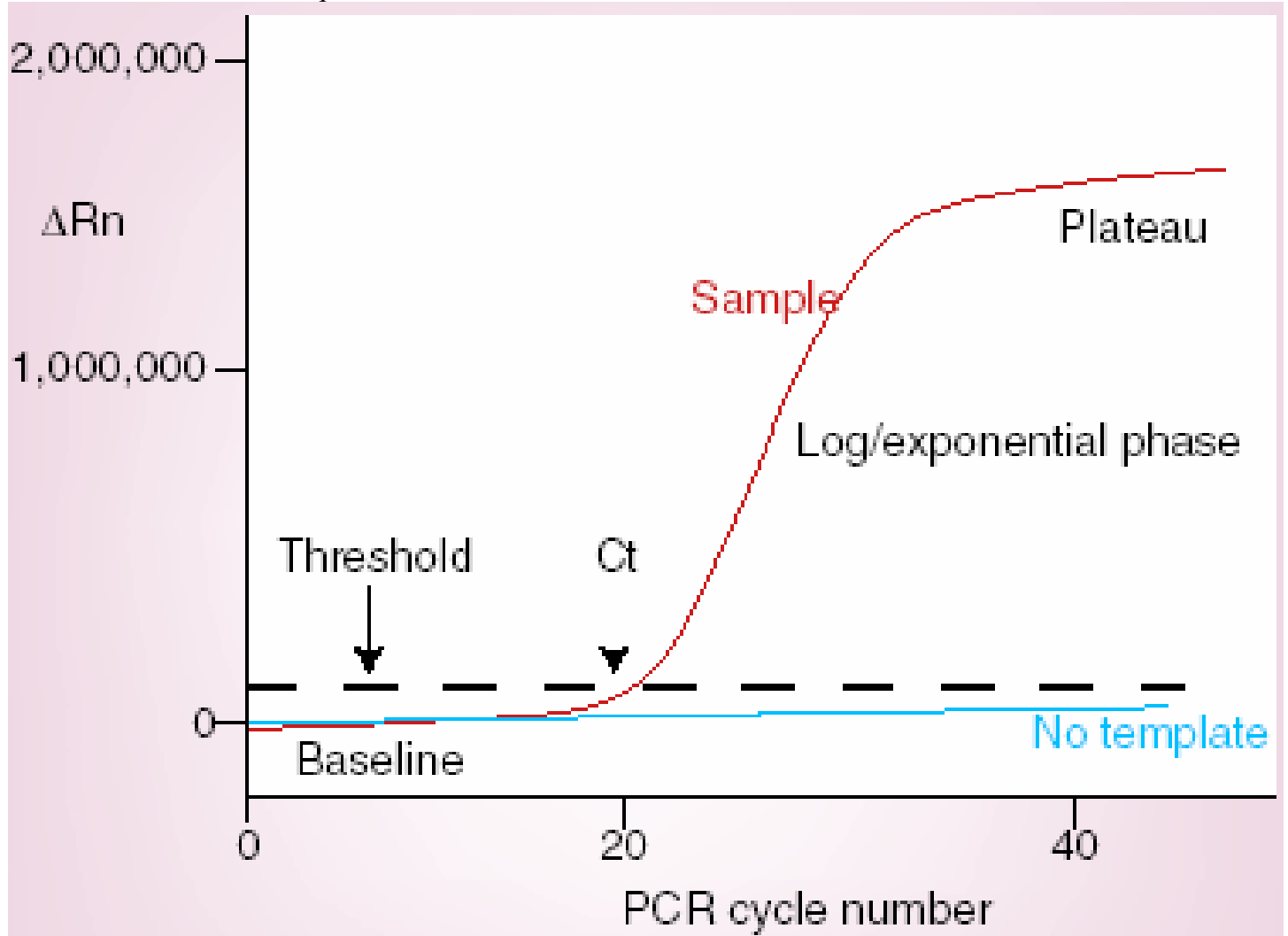
a) Definition of terms

Described here are the definitions of the terms used in quantitation analysis.

- Amplification plots

As mentioned earlier, using any of the developed chemistries, the increase in fluorescence emission during the PCR reaction can be detected in real time by a modified thermocycler. The computer software constructs amplification plots using the fluorescence emission data that are collected during the PCR amplification. An amplification plot is the plot of fluorescence signal versus PCR cycle number. Figure 2.4 demonstrates a representative amplification plot.

Figure 2.4: Model of a single amplification plot illustrating the nomenclature commonly used in real-time quantitative PCR



ΔR_n = Fluorescence emission of the product at each time point – fluorescence emission of the baseline

Ct = Threshold cycle

- Baseline

The baseline is defined as the PCR cycles in which a reporter fluorescent signal is accumulating but is beneath the limits of detection of the instrument. By default, the

computer software sets the baseline from cycles 3 to 15; however, this often needs to be changed manually.

- R_n

The reporter signal is normalised to the fluorescence of an internal passive reference dye [ROX (Applied Biosystems) – this is composed of a 25 μ M solution of 5-carboxy-X-rhodamine in 10mM Tris-HCL (pH 8.6), 0.1mM EDTA and 0.01% Tween® 20] to allow for well-to-well corrections in fluorescent fluctuations caused by changes in concentration or volume (the passive reference dye does not participate in PCR amplification). R_n is this normalised reporter signal and is calculated by the computer software program. It represents the fluorescence signal of the reporter dye divided by the fluorescence signal of the passive reference dye (ROX™).

$$\text{Therefore } R_n = \frac{\text{fluorescence signal of reporter dye}}{\text{fluorescence signal of the passive reference dye (ROX)}}$$

During PCR, this number will increase as amplicon copy number increases until the reaction reaches a plateau.

- ΔR_n

A computer software program calculates a ΔR_n using the equation $\Delta R_n = R_{np} - R_{nb}$, where R_{np} is the fluorescence emission of the product at each time point (normalized to ROX) and R_{nb} is the fluorescence emission of the baseline (normalized to ROX) established in the first few cycles of PCR.

Similar to R_n , ΔR_n increases during PCR as amplicon copy number increases until the reaction approaches a plateau. The ΔR_n values are plotted versus the cycle number in an

amplification plot. During the early cycles of PCR amplification, ΔRn values do not exceed the baseline.

- Threshold

An arbitrary threshold is chosen by the computer, based on the variability of the baseline. It is calculated as ten times the standard deviation of the average signal of the baseline fluorescent signal between cycles three to 15. A fluorescent signal that is detected above the threshold is considered a real signal that can be used to define the threshold cycle (Ct) for a sample. If required, the threshold can be manually changed for each individual experiment so that it is in the region of exponential amplification across all amplification plots (this region is depicted in the log view of the amplification plots as the portion of the plot, which is linear).

- Ct

This is defined as the fractional PCR cycle number at which the reporter fluorescence is greater than the minimal detection level (i.e., the threshold). The Ct (threshold cycle) is a basic principle of fluorescence based real-time PCR and is an essential component in producing accurate and reproducible data. Fluorescence values are recorded during every cycle and represent the amount of product amplified to that point in the amplification reaction. The presence of more template at the start of the reaction leads to a fewer number of cycles reaching the point at which the fluorescent signal is recorded as statistically significant above background. This Ct value will always occur during the exponential phase of target amplification, which occurs during the early

cycles of PCR. As reaction components become limiting, the rate of target amplification decreases until the PCR reaction is no longer generating template at an exponential rate (plateau phase) and there is little or no increase in PCR product. The quantity of PCR product observed at the end of the reaction is very sensitive to slight variations in reaction components. This is because endpoint measurements are generally made when the reaction is beyond the exponential phase and a slight difference in a limiting component can have a major effect on the final amount of product. For example, side reactions, like formation of primer dimers, can consume reagents to different extents from tube to tube. Thus, it is possible for a sample with a higher starting copy number to end up with less accumulated product than a sample with a lower starting copy number. This is the main reason why Ct is a more reliable measure of starting copy number than an endpoint measurement of the amount of accumulated PCR product. During the exponential phase none of the reaction components is limiting and therefore Ct values are very reproducible for replicate reactions with the same starting copy number. A Ct value of 40 or higher means no amplification (i.e. no detectable fluorescence after 40 cycles of PCR). Thus, the essential principle of real-time quantitative PCR is that reactions are characterized by the point in time during cycling when amplification of a PCR product is first detected rather than the amount of PCR product accumulated after a fixed number of cycles and the higher the starting copy number of the nucleic acid target, the sooner a significant increase in fluorescence is observed.

b) Quantitation methods

Two methods are available to quantify real-time RT- PCR results:

i) Standard-curve or absolute quantitation

As shown by Higuchi and coworkers, the plot of the log of initial target copy number for a set of known standards (five- or tenfold serial dilution) versus Ct is a straight line (the standard curve) [Higuchi R et al 1993]. Quantitation of the amount of target in the “unknown” samples of interest is accomplished by measuring Ct and using the standard curve to determine starting copy number. The most common source of a known sample is a plasmid for the gene of interest and the standard curve is generated based on a serial dilution of a starting amount. Another option, and easier to generate if a plasmid is unavailable, is the use of a synthetic single-stranded sense oligonucleotide for the entire amplicon. The advantage of this approach is that it significantly simplifies the process of obtaining a standard curve for amplicons up to 100 bp, which encompasses most real-time PCR amplicons. Furthermore, it is also less susceptible to bias when quantified by a spectrophotometer due to the relative purity of the oligonucleotide. Together with the greater precision of measurement of the standard and the possibility of calculating the moles of oligonucleotide (hence, number of copies), it is possible to approximate the number of copies of a template in an unknown sample, although not in terms of absolute copy number. One final option for a standard curve is to use a cell line with a known copy number or expression level of the gene of interest. The standard curve method is used in circumstances when absolute quantitation is critical for the investigator [eg. when measuring a small number of genes in either a few or many samples (Dumur CI et al 2002, Jurado J et al 2003)] and in quantitation of viral load [Ngaosuwankul N et

al 2010]. The entire process of calculating Cts, preparing a standard curve, and determining starting copy number for unknowns is performed by the software of the 7700 system.

ii) Relative quantitation

Relative quantitation is also known as the comparative threshold method ($2^{-\Delta\Delta Ct}$ method). This method eliminates the need for standard curves and mathematical equations are used to calculate the relative expression levels of a target relative to a reference control or calibrator such as a non-treated sample, RNA from normal tissue or relative to another treated sample. The amount of target, normalized to an endogenous housekeeping gene and relative to the calibrator, is then given by $2^{-\Delta\Delta Ct}$, where $\Delta\Delta Ct = \Delta Ct(\text{sample}) - \Delta Ct(\text{calibrator})$, and ΔCt is the Ct of the housekeeping gene subtracted from the Ct of the target gene. The equation thus represents the normalized expression of the target gene in the unknown sample, relative to the normalized expression of the calibrator sample. For this calculation to be valid and in order to obtain reliable results, it is imperative that the amplification efficiencies of the housekeeping and target gene are approximately equal and at or above 90%. This can be established by looking at how Ct (of both target and housekeeping gene) varies with template dilution. If the plot of starting RNA/ cDNA quantity versus ΔCt is close to zero, it implies that the amplification efficiencies of the target and housekeeping genes are very similar. If a housekeeping gene cannot be found whose amplification efficiency is similar to the target, the standard curve method is then preferable. Alternatively, new primers can be designed and/or optimized to achieve a similar efficiency for the target and housekeeping gene amplicons.

The solutions to the following equations need to be calculated in a sequential manner in order to elucidate relative expression levels.

A) $\Delta Ct = Ct \text{ target gene (eg. CXCR4)} - Ct \text{ housekeeping gene (eg. } \beta\text{-actin)}$

In real-time quantitative PCR experiments specific errors will be introduced due to minor differences in the starting amount of RNA, quality of RNA or differences in efficiency of cDNA synthesis and PCR amplification. In order to minimize these errors and correct for sample-to-sample variation, a cellular RNA is simultaneously amplified with the target, which serves as an internal reference against which other RNA values can be normalized [Karge WH et al 1998]. The most common genes used for normalization, termed housekeeping genes, are: β -actin, a cytoskeletal protein; glyceraldehyde-3-phosphate dehydrogenase (GAPDH), a glycolytic enzyme; ribosomal RNA (rRNA). These genes should theoretically be expressed at a constant level amongst different tissues of an organism and at all stages of development, and their expression levels should also remain relatively constant in different experimental conditions. However, none of these housekeeping genes are ideal. It has been shown that GAPDH expression may be variable in different tissues [Barber RD et al 2005] with expression levels also being altered by glucose, insulin, heat shock and cellular proliferation and additionally β -actin levels may be modified by experimental treatments [Bustin SA 2000, Chervoneva I et al 2010, Rhoads RP et al 2004, Steele BK et al 2002, Yperman J et al 2004]. rRNA production is less likely to vary under conditions affecting mRNA transcription [Dheda K et al 2004, Bas A et al 2004]. However, it is not always a good representative of total mRNA population in a cell as rRNA is expressed at a much higher level than mRNA.

Other alternative housekeeping genes have been proposed but none have been entirely satisfactory and no single unequivocal reference gene has yet been identified. Some authors have suggested the use of several housekeeping genes in a single experiment and that the mean expression of these multiple housekeeping genes can be used for normalization [Vandesompele J et al 2002].

Importantly, selection of the housekeeping gene for each specific experiment should be made very carefully as the reliability of the results depends on the choice of the most relevant housekeeping gene according to the cells of interest and specific experimental treatments. We have used β -Actin mRNA as an internal standard to normalise patterns of gene expression when using the Taqman assay.

B) $\Delta\Delta Ct = \Delta Ct \text{ sample} - \Delta Ct \text{ calibrator}$ (eg. 1542 CPT3X; see chapter 5)

The normalised amount of target gene (eg. CXCR4) is a unitless number that can be used to compare the relative amount of target in different samples. One way to make this comparison is to designate one of the samples as a calibrator. This sample with the lowest detectable expression level of the target is usually chosen as the calibrator (eg. 1542 CPT3X CXCR4 mRNA expression in our experiments in chapter 5). This calculation can in fact be considered a second normalisation step where all samples are normalised to the calibrator sample.

C) $Relative \text{ quantitation} = 2^{-\Delta\Delta Ct}$

The final equation thus represents the normalised expression of the target gene in the unknown sample, relative to the normalised expression of the calibrator sample.

Importantly, as mentioned earlier, the $2^{-\Delta\Delta CT}$ method can only be used if the efficiency of PCR amplification for the target gene is approximately equal to that for the housekeeping gene. For every target gene this has to be tested by plotting the ΔCT against varying RNA dilutions of target and housekeeping genes. If the slope of this line is <0.1 , this reflects similar efficiencies. The advantage of this system is that no standards have to be constructed. A disadvantage is that the efficiencies of amplification of housekeeping and target gene have to be similar to obtain reliable results.

Primer, probe & amplicon design

Great care should go into the design of the assay. Primers, probes and amplicons are designed to very exacting specifications and the TaqMan system provides its own primer/probe design software from Applied Biosystems known as Primer Express®, which is probably the most widely used oligonucleotide design program for developing real-time quantitative PCR assays. Primer3, a free program from Massachusetts Institute of Technology, USA can also be used to generate good real-time PCR assays.

- **Amplicon Design**

The amplicon length for the PCR product using real-time RT-PCR should be as small as reasonably possible, the optimal being 50 – 150 base pairs in length for designs using hybridisation probes (includes the Taqman assay). Shorter amplicons amplify more efficiently than longer ones and are more tolerant of reaction conditions. This is because they are more likely to be denatured during the 92–95⁰C step of the PCR, allowing the probes and primers to compete more effectively for binding to their complementary

targets. As the extension rate of Taq polymerase is between 30 and 70 bases/second, it also means that polymerisation times as short as 15 seconds are sufficient to replicate the amplicon, making amplification of genomic DNA contaminants less likely and reducing the time it takes to complete the assay. Higher efficiency also means that the assays are more likely to work the first time. In addition, high-efficiency assays enable relative quantitation to be performed using the comparative threshold method ($2^{-\Delta\Delta CT}$). This method increases sample throughput by eliminating the need for standard curves when looking at expression levels of a target relative to a reference control.

- Primer /Probe Design

A summary of the primer and probe design guidelines using Primer Express® (the primer/probe design programme for the Taqman system) is shown in table 2.1.

The optimal length for single-stranded primers is 15–20 bases with a G/C content in both primers and probes of 20–80%. Regions with a G/C content in excess of this may not denature well during thermal cycling, leading to a less efficient reaction. In addition, G/C-rich sequences are susceptible to non-specific interactions that may reduce reaction efficiency and produce non-specific signal. For this same reason, primer and probe sequences containing runs of four or more G bases should be avoided. A/T-rich sequences require longer primer and probe sequences in order to obtain the recommended T_m . This is rarely a problem for quantitative assays; however, probes approaching 40 base pairs can exhibit less efficient quenching and produce lower synthesis yields.

Table 2.1. Shown here is a summary of the primer and probe design guidelines used by the primer/probe design program, Primer Express®, for real-time quantitative Taqman PCR.

Taqman® Probe Guidelines	Sequence Detection Primer Guidelines (for Taqman® Assays or SYBR Green Assays)
Probe selected first and primers designed as close as possible to the probe without overlapping it (amplicons of 50 – 150 base pairs strongly recommended)	
G/ C content kept in 20 – 80% range	
Runs of identical nucleotide avoided; this is especially true for guanine, where runs of four or more Gs should be avoided	
When using Primer Express® software the T _m should be 68 – 70°C	When using Primer Express® software the T _m should be 58 – 60°C
No G on the 5' end	The five nucleotides at the 3' end should have no more than two G and/ or C bases
The strand that gives the probe more C than G bases should be selected	

Selecting primers and probes with the recommended T_m is one of the factors that allows the use of universal thermal cycling parameters. The T_m for TaqMan primers should be in the range of 68–70°C. Having the probe T_m 8–10 °C higher than that of the primers ensures that the probe is fully hybridized during primer extension.

Primer Express® software does not select Taqman probes with a G on the 5' end. The quenching effect of a G base in this position on reporter fluorescence will be present even after probe cleavage. This can result in reduced normalized fluorescence values (R_n), which can impact the performance of an assay. Having G bases in positions close to the 5' end, but not on it, has not been shown to compromise assay performance. Another observation is that probes with more C than G bases will often produce a higher R_n. Since Primer Express® software does not automatically screen for this feature, it must be checked manually. If a probe is found to contain more G than C bases, the complement of

the probe selected by Primer Express® software should be used, ensuring that a G is not present on the 5' end.

Non-specific priming is minimized by selecting primers that have only one or two G/Cs within the last five nucleotides at the 3' end. Under certain circumstances, however, such as a G/C-rich template sequence, this recommendation may have to be relaxed to keep the amplicon under 150 base pairs in length. It should, however, be followed as often as possible, and even when it is not possible, primer 3' ends extremely rich in G and/or C bases should be avoided.

Universal Thermal Cycling Parameters

All quantitative assays designed using Primer Express® software or their guidelines can be run using the same universal thermal cycling parameters. This eliminates any optimisation of the thermal cycling parameters and means that multiple assays can be run on the same plate without sacrificing performance. Table 2.2 shows the universal thermal cycling parameters for quantitative TaqMan® when using DNA or cDNA as the substrate.

Table 2.2: Universal Thermal Cycling Parameters for real-time quantitative TaqMan® PCR

Times and Temperatures			
Initial Steps		Each of 40 Cycles	
		Melt	Anneal / Extend
HOLD	HOLD	CYCLE	
2 min* 50 °C	10 min** 95 °C	15 sec 95 °C	1 min 60 °C

*The 2 min hold at 50 °C is required for optimal AmpErase® UNG activity.

** The 10 min hold at 95 °C is required for AmpliTaq Gold® DNA Polymerase activation.

Also, 10-min incubation at 95 °C is necessary to cleave the dU-containing PCR product generated in the low temperature (18 to 50°C) incubation, to substantially reduce AmpErase UNG activity, and to denature the native DNA in the experimental sample. Because UNG is not completely deactivated during the 95 °C incubation, it is important to keep the reaction temperatures greater than 55 °C, to prevent amplicon degradation.

SECTION 2.3

Flow cytometry

What is flow cytometry?

“*Cytometry*” refers to the measurement of the physical and chemical characteristics of cells. “*Flow cytometry*” refers to the technique where these measurements are made individually of single particles (e.g. cells, nuclei, chromosomes) suspended within a stream of liquid as they pass through a light source, usually a laser, focused at a very small region. All parameters measured can be divided into two main groups:

- 1) those related to light scattering, which mainly reflects the size of the cell and its internal complexity, and
- 2) those related to fluorescence. These are associated with the presence of one or more fluorochromes inside the cell or attached to the cell surface membrane, either in a natural (autofluorescence) or artificial (i.e. using fluorochrome conjugated monoclonal antibodies) way.

The emitted fluorescence and light scatter of each particle is collected, filtered and converted to digital values that are stored on a computer. The important feature of flow cytometry is that measurements are made on each individual particle within the suspension in contrast to measuring an average property for the entire population. Average measurements do not detect subpopulations that have small differences from the overall population. In addition to measuring the physical and chemical characteristics of single cells, it is possible using this technique to physically separate or *sort* subpopulations from the larger pool of particles. A very large number of particles can be

evaluated in a very short time; some systems can run particles at rates approaching 100,000 particles per second while collecting 10 to 20 parameters from each particle. Also, particles of almost any size can be evaluated by flow cytometry. These range from particles that are below the resolution limits of visible light, as they can be detected by their fluorescent signatures, to those particles as large as several thousand microns.

There are numerous applications of flow cytometry in both basic and clinical research, with this technology providing rapid and accurate measurements of a relatively broad range of cell characteristics that include DNA and/or RNA cell content, enzyme activity, the detection and quantitation of cell antigens, the analysis of multidrug cell resistance, membrane potential, mitochondria and chromosomes, the measurement of intracellular pH or ions such as free Ca^{2+} . [Givan AL 2004, Ibrahim SF and van den Engh G 2007, Krishhan VV et al 2009, Preffer F and Dombkowski D 2009]. In addition, flow cytometry allows sorting of cells and subcellular components such as the chromosomes [Givan AL 2004, Ibrahim SF and van den Engh G 2004, Ibrahim SF and van den Engh G 2007].

It should be noted that flow cytometry is a generic term, whilst FACS (Fluorescence Activated Cell Sorter) is a trademark of the Becton-Dickinson Corporation.

Historical aspects of flow cytometry and the flow cytometer

The beginnings of flow cytometry date back to the synthesis of dyes in the late 1800s and to the seminal work by Caspersson and Schultz published in “Nature” in 1938 [Caspersson T and Schultz J 1938]. They demonstrated that DNA content, measured by

ultraviolet and visible light absorption in unstained cells, doubled during the cell cycle. In the 1940s, Papanicolaou demonstrated that he could identify cells as being cancerous from cervical cancer, by observing the staining patterns obtained by staining tissues with specifically designed stains [Papanicolaou GN and Traut R 1941].

However, it was not until 1950, when Coons and Kaplan reported on the improved detection of antigens using fluorescence antibody methods [Coons AH and Kaplan MH 1950], that it was realised that fluorescence measurements could offer more advantages than absorption. Since then, fluorescein remains the most common label for quantitative immunofluorescence analysis, and now for routine flow cytometric applications in scientific research.

The automated flow analysis of single cells had its beginnings when Moldovan reported a photoelectric method for counting individual cells flowing through a capillary tube mounted on a microscope stage [Moldovan A 1934]. The system had major technical difficulties but in 1956 there was a breakthrough in flow cytometry when an apparatus was built by WH Coulter in which blood cells, in saline suspensions, passed one by one through a small orifice and were detected by changes of electrical impedance at the orifice [Coulter WH 1956]. This instrument was the forerunner of the modern flow cytometers.

In the 1960s Louis Kametsky began the drive to design and build single-cell analyzers. Kametsky was interested in using optical character recognition techniques to identify cancer cells. Because of the lack of computation, this became a difficult goal and in place of image-based technology, Kametsky focused on single-cell analysis and the design of a cytometer that measured absorption and scatter and used it to measure the

nucleic acid content and light scattering of unstained mammalian cells in a flow stream [Kamentsky LA et al 1965]. Later the same year, the first flow sorter was described by Fulwyler [Fulwyler MJ 1965]. The instrument separated biological cells according to their volume, which was determined as they passed through a Coulter aperture.

Thus, flow cytometry was based mainly on light scattering and fluorescence and the first applications were measurement of nuclear DNA (using stoichiometric DNA stains) and cell surface antigens (using immunofluorescence). Methodologies and applications since then have expanded rapidly.

Fluorescence

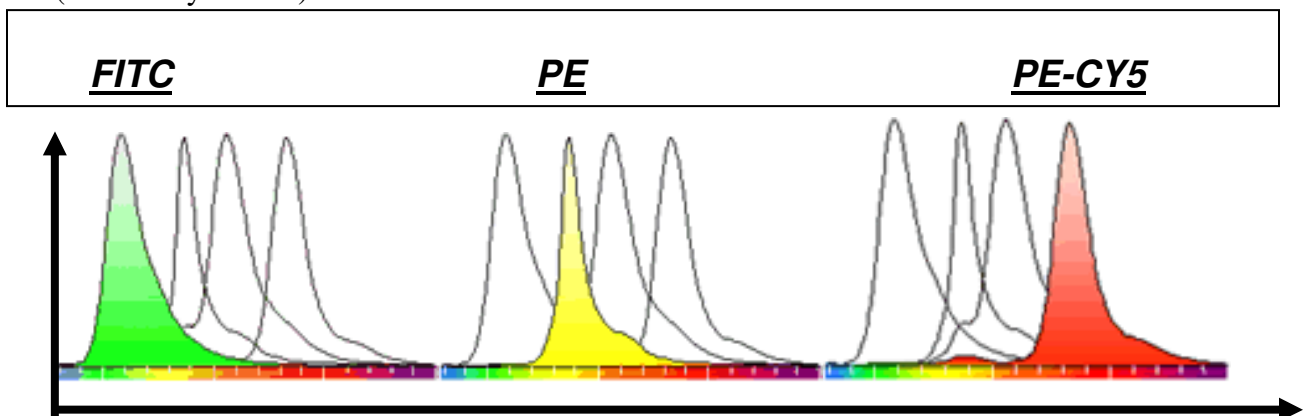
The principles of fluorescence are a key concept in flow cytometry. When a compound absorbs light, electrons are raised from the ground state to an excited state. The electrons return to the ground state via a variety of routes; some routes such as the loss of the energy by heat do not result in fluorescence, but certain molecules lose energy by a process of radiative transfer, termed fluorescence. When stimulation of the fluorescent compound is stopped by removing the exciting light source, fluorescence emissions cease rapidly. Therefore fluorescence is a property of molecules to absorb light energy at one wavelength, termed the excitation wavelength, and then rapidly re-radiate some of that energy as light of a longer or emission wavelength eg. fluorescein isothiocyanate (FITC) excited with pure blue light appears to fluoresce greenish-yellow. Fluorescence is always of a lower energy, and hence longer wavelength, than the exciting light.

Immunofluorescence is a technique that allows visualization of cellular features or structures by linking these to a fluorescent molecule i.e. one that emits light when stimulated by light at a separate wavelength. These fluorescent molecules may be either dyes that bind directly to structures in or on the cell, or they may be fluorochromes (figure 2.5) conjugated to a ligand such as monoclonal antibodies. The fluorochromes (and dyes) used for flow cytometry must be compatible with the laser in the cytometer. This means that the fluorochromes must be excited at the wavelength of the laser light source and should fluoresce at a wavelength distinct from the laser light.

The characteristic distribution of radiated energy for a fluorochrome is called its emission spectrum (figure 2.5). The emission spectrum of each fluorochrome has a clear peak, significantly different and distinct from the others (and which visually gives the fluorochrome a particular color). This allows flow cytometric assays to use multiple different fluorochromes in one experiment to simultaneously evaluate different cell features without significant overlap or interference from individual emission spectra.

Figure 2.5: Emission spectra for 3 common fluorochromes.

X axis – light wavelength; Y axis – intensity of emission. FITC – fluorescein isothiocyanate. PE – phycoerythrin. PE-CY5 - a tandem conjugate of two fluorochromes (PE and Cyanine-5).



Light scatter

The flow cytometer is able to detect (and quantitate) immunofluorescence as well as light scatter signals. The light scatter signals are the result of the laser light reflecting and refracting off the cells. Two types of light scatter are measured.

1) Light scatter measured in the forward direction i.e. along the same axis that the laser light is traveling or near 180° from the point at which the laser beam intersects the cell, is called forward, or low angle, scatter. This forward scatter roughly correlates with cell size and surface properties of cells eg. cell ruffling. Therefore it can be used to distinguish cell size as well as live from dead cells.

Note – in the forward direction it is necessary to use a blocker bar to eliminate *unscattered* laser light.

2) Light scatter measured at a right angle to the direction of the laser beam is termed orthogonal or side light scatter. This is detected in the side or 90° scatter channel and its intensity correlates with the granularity of the cell.

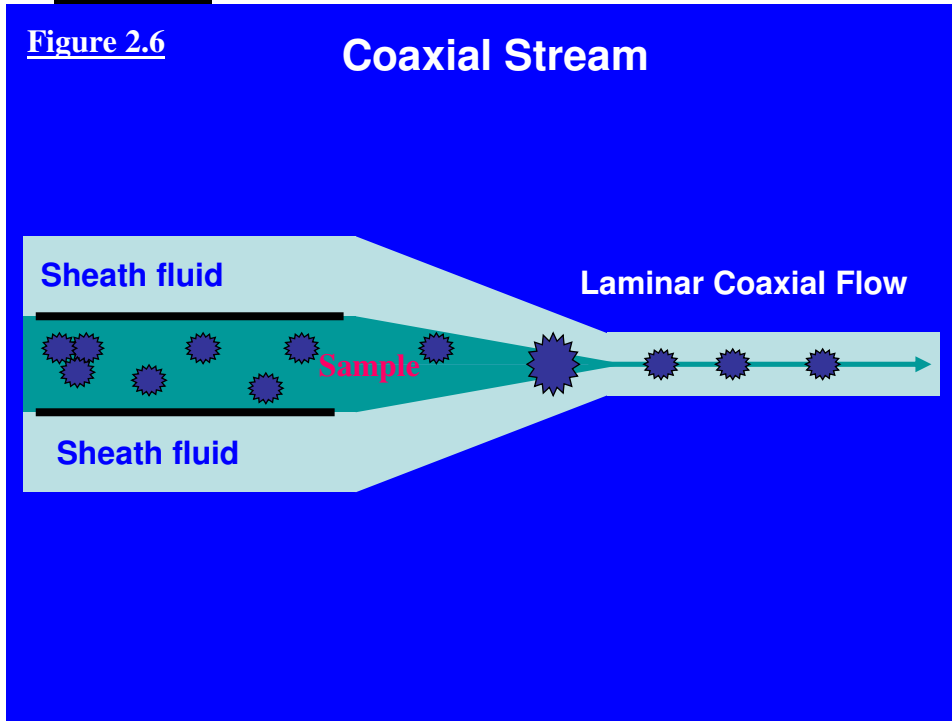
The modern flow cytometer

- *Fluidic system* (figure 2.6)

The role of the fluidic system is to focus the cells/ particles in a fine stream and move them, one at a time, past a precise point to intersect the laser and the optical path for the detectors. Also, the fluidic system is essential in cell sorting by flow cytometry. Initially, a suspension of fluorescently labelled single cells is introduced into the flow cytometer. Whilst flowing rapidly through a narrow channel in the instrument, a small amount of cell suspension joins a larger amount of cell-free buffer, called "sheath fluid". This is

termed a *coaxial stream* i.e. a stream within a stream, and therefore consists of an inner sample stream surrounded by an outer sheath stream; the fluids in the two streams do not mix (figure 2.6).

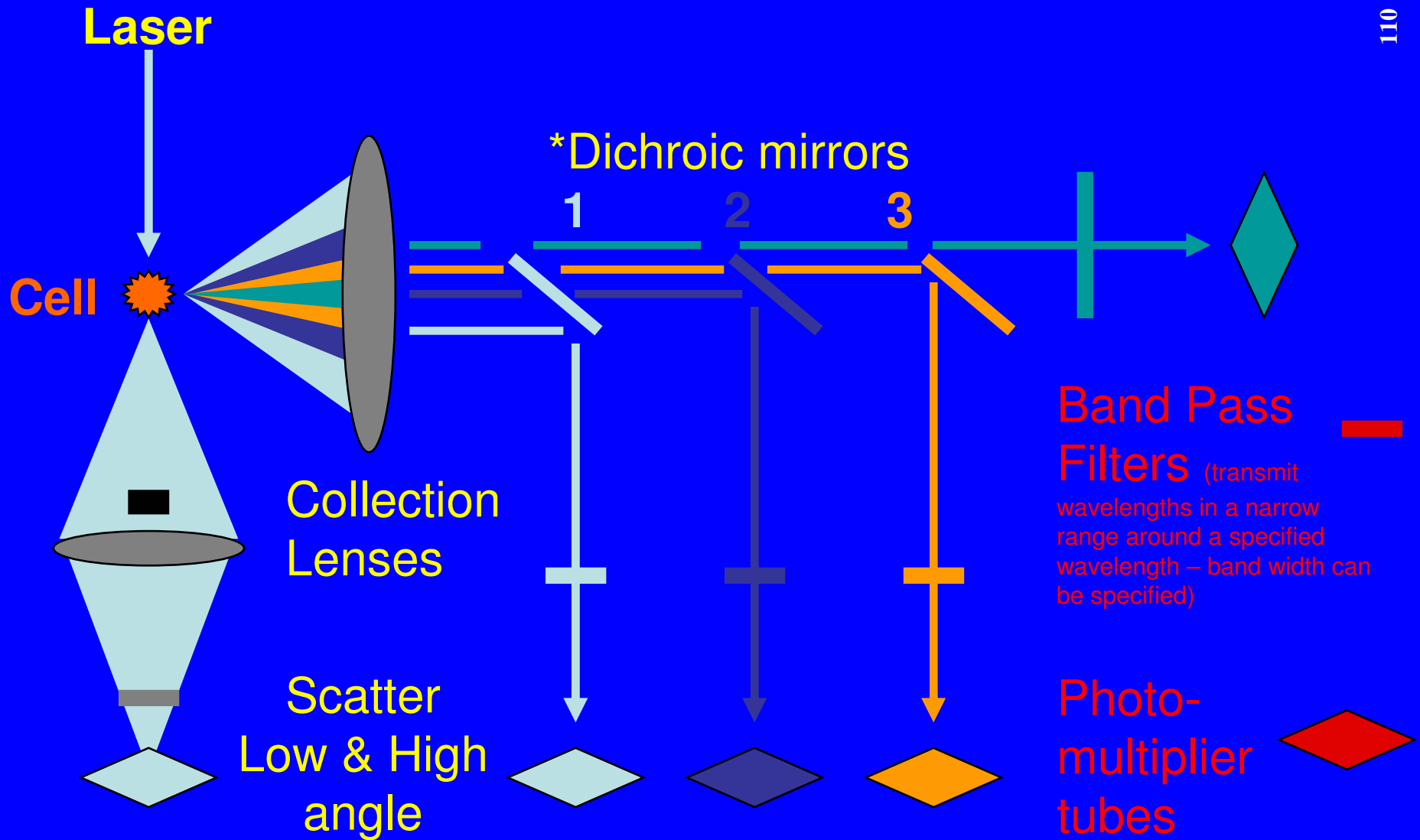
Figure 2.6: The coaxial stream



The outer sheath stream focuses the inner stream and minimizes the turbulence arising from the resistance of the tubing. The coaxial stream ensures the cells are spaced out sequentially and that they pass the laser beam(s) one at a time. Additionally, the coaxial stream keeps the cells centered in the flowing stream so that they pass the laser beam optimally centered. The flow channel is positioned vertically to the laser beam.

Positive air pressure acting on the sample reservoir keeps the sample fluid flowing continuously. In a similar manner, sheath fluid flow is controlled by a second positive air pressure regulator acting on the sheath chamber. A purge line is connected to the sheath inlet to allow a vacuum to be applied for clearing blockages and air bubbles.

Figure 2.7 Basic Optics of a Flow Cytometer



* Dichroic mirror – when filter placed at 45° angle to light source light which would have been transmitted by filter is still transmitted but light that would have been blocked is reflected at 90°. Used this way filter called dichroic mirror

- *Optical system and analysis* (figure 2.7)

The optical system has two components:

a) a light source, usually a laser, which is necessary to appropriately excite the cells, in addition to the lens and mirrors needed to focus and direct the laser beam to the flow chamber containing the cells. Lasers, which emit light at specific peak emission wavelengths, need to be matched with the fluorochromes used for immunofluorescent staining analyzed on the cytometer.

b) a variety of mirrors and filters (materials that absorb certain wavelengths whilst transmitting others), which are needed for the collection of light emitted from, or scattered by, the cells (figure 2.7). These include dichroic mirrors, which reflect light above a specific wavelength and only permit light below that wavelength to pass through; short pass filters (that permit only light below a specified wavelength to pass through); long pass filters (that permit only light above a specified wavelength to pass through); bandpass filters (that permit light in a specified range of wavelengths to pass through).

These mirrors and filters also separate and direct emissions of different wavelengths to the corresponding detectors or photomultipliers (PMT). In the PMTs, the incident light is converted into electronic signals. Further electronic and computational processing results in graphic display and statistical analysis of the measurements being made.

Some modern cytometers are capable of analyzing up to 13 parameters for each cell (forward scatter, side scatter, and as many as 11 colours of immunofluorescence) [De Rosa SC et al 2001, Wood B 2006] allowing size, protein content, DNA content, lipid content, antigenic properties, enzyme activity, etc for each cell to be measured, and

therefore permitting a multidimensional representation of a population to be obtained. It is almost always possible to analyze at least 1,000 cells per second. With appropriate specimens, some cytometers can analyse up to 100,000 cells per second without a significant sacrifice in the quality of data [Ashcroft RG and Lopez PA 2000, Ibrahim SF and van den Engh G 2007].

- *Colour Assignment*

A signal emitted by a fluorochrome is detected by its associated photo-multiplier tube (PMT) and converted to a parameter for acquisition. The series of optical filters and mirrors is used to allow only a specific region of the spectrum to reach each of the PMTs (figure 2.7). In the flow cytometer the PMT detectors are labeled FL1, FL2, FL3 and onwards, with each detecting light of only a specific emission wavelength.

In the Becton Dickinson FACScan there is an argon laser with a strong emission at 488 nm and there are three PMTs each detecting fluorescence (with an additional two for detecting forward and side scatter) at specific wavelengths produced by the excitation of several commonly used fluorochromes and dyes (table 2.3).

Table 2.3: Photomultiplier detection of light emission produced by common fluorochromes/ dyes in the Becton Dickinson FACScan
 FITC - fluorescein isothiocyanate; PE – phycoerythrin; PI – propidium iodide;
 PE–CY5 - a tandem conjugate of two fluorochromes (PE and Cyanine-5)

Photomultiplier	Light emission wavelength detected (colour)	Fluorochrome
FL1	515-545 nm (green)	FITC
FL2	564-606 nm (yellow-orange)	PE / PI
FL3	650-675 nm (red)	PE-CY5

A wide variety of fluorochrome conjugated ligands (eg. monoclonal antibodies) and dyes are available for directly estimating cellular parameters such as nucleic acid content (DNA, mRNA). Analysis of cell cycle position by quantitation of cellular DNA was one of the earliest applications of flow cytometry. It is still the method of choice for fast, accurate determination of cell cycle distributions. In the simplest method, cellular DNA is detected using a fluorescent dye that binds preferentially to DNA. A key feature of DNA dyes is that they are stoichiometric i.e. the number of molecules of probe bound is equivalent to the number of molecules of DNA. Propidium iodide is the most commonly used. Fluorescent molecules in flow cytometry are now also used in measuring enzyme activity, calcium flux, membrane potential, pH and the density and distribution of cell-surface and cytoplasmic determinants and receptors, as well as allowing functional subpopulations of cells to be identified.

Analysis of data

- *Histograms and dot plots.*

As mentioned earlier light from a specific region of the spectrum is detected by a PMT. This converts it via an amplifier to a voltage i.e. electrical output that is proportional to the original fluorescence intensity and the voltage on the PMT. These electrical pulses are then processed by a series of linear and log amplifiers. The use of a logarithmic scale to measure fluorescence is indicated in most biological situations and the effect is to normalise the distribution. The use of a logarithmic scale is also required when there is a broad range of fluorescence (again true of most biological distributions) as this type of amplification expands the scale for weak signals and compresses the scale for “strong” or specific fluorescence signals.

These voltages, which are a continuous distribution, are converted to a discrete distribution by an Analog to Digital converter (ADC) which places each signal into a specific channel depending on the level of fluorescence. These channels correspond to the original voltage generated by a specific "light" event detected by the PMT detector. Thus the ADC assigns a channel number based on the pulse height for individual events. Therefore, brighter specific fluorescence events will yield a higher pulse height and thus a higher channel number when displayed as a histogram. The greater the resolution of the ADC, the closer this reflects the continuous distribution. The ADCs in the FACScan are 10-bit, i.e., they divide data into four decades across 1024 channels with 256 channels per decade. For the FACScan, the number of decades is fixed.

The flow cytometry data is most often represented as histograms or dot plots. A histogram is a graph of the fluorescent intensity on x-axis and the number of cells in each channel on the y-axis. Using the FACScan, histograms have 1,024 channels (with higher channel numbers representing a higher signal intensity of a fluorescent/ scatter after amplification) displayed on the 'x' axis using a 4-log decade logarithmic scale (256 channels per decade). Only the intensity of one parameter (scatter or fluorescence) can be represented on a histogram.

In contrast to histograms, dot plots (also known as bivariate display, two parameter histograms, scattergram, bitmap) show the correlated distribution of intensity for two parameters (eg. forward scatter versus side scatter) and each cell is represented by a dot, positioned on the X and Y scales (often both 1024 channels, 4-log decade logarithmic scales) according to the intensities detected for that cell. Dot plots can be

divided into quadrants, which divide the light intensity channels into areas of interest. The number of particles in each of the defined areas can then be counted.

Both histograms and dot plots can reveal whether there are discrete subpopulations of cells with different intensities.

- *Gating and negative controls.*

Usually data only from single, viable cells is required and data from cell debris (particles smaller than cells), dead cells, and clumps of 2 or more cells needs to be eliminated. Subcellular debris and clumps can be distinguished from single cells by size (estimated by the intensity of low angle forward scatter). Dead cells have lower forward-scatter and higher side-scatter than living cells. These differences are accurately preserved following formaldehyde fixation (despite the fact that after fixation, all the cells are dead). The computer can be configured to display the fluorescence signals only from those particles with a specified set of scatter properties, namely, living single cells. This is called a scatter-gated fluorescence analysis. It is actually possible to "gate" on any set of signals in order to analyse the specific data of either the main cell population or a subpopulation.

Quadrant gates can be subjectively set on dot plots using the background levels of fluorescence of either the respective unstained negative control (contains only the fluorochrome-conjugated secondary antibody without the primary antibody) or fluorochrome isotype matched control population of cells (when a fluorochrome-conjugated primary antibody is used). These negative control samples are needed to demonstrate the amount of non-specific binding that one may get with the antigen

specific antibody. It should be noted that the fluorochrome isotype matched control primary antibody has no specificity to any epitope on the cells being analysed, is the same species and isotype, is used at the same concentration and is conjugated with the same fluorochrome as the antigen specific primary antibody.

When quadrant gates are used on the graph, each quadrant then demonstrates the following:

- 1) Lower-left quadrant represents cells negative for the descriptors on both the x- and y-axis
- 2) Upper-right quadrant represents cells dual-positive for the descriptors on both the x- and y-axis
- 3) Upper-left quadrant represents cells positive for the y-axis descriptor, but negative for the x-axis descriptor
- 4) Lower-right quadrant represents cells positive for the x-axis descriptor, but negative for the y-axis descriptor

Important aspects of sample preparation for flow cytometry

The aim of sample preparation is to produce a single cell suspension with minimal aggregation, termed a "monodisperse suspension". The sample should contain as little debris and as few dead cells and clumps as possible. The latter disrupts the smooth flow of fluid or blocks tubes within the flow cytometer. With all preparative methods great care needs to be taken to ensure that the technique itself does not bias the results. For example, enzymatic preparative techniques can alter cell-surface antigens and affect cell viability.

The monodisperse cells are labelled, by incubation under appropriate conditions, with a fluorescent tag. This can be a fluorescent dye, fluorescent-conjugated antibody or ligand. For accurate interpretation of results, it is important that the staining is specific for and proportional to the feature to be measured. It is not unusual for fluorescent probes and monoclonal antibodies to bind non-specifically and care needs to be taken to block cross-reactions. Data can be acquired in the flow cytometer with the cells either alive or fixed with formaldehyde/ paraformaldehyde. With fixed cells, the fluorescence and light scatter properties are stable, and data acquisition can be postponed for days or weeks.

SECTION 2.4

Cell migration assays

The most common method used to study cell motility in vitro was first described by Boyden S in 1962. Transwell® migration assays are one of the modifications of the Boyden Chamber system and were used by us to study the chemotaxis of cells in response to the ligand for CXCR4 i.e. CXCL12. Increased motility of cells in this assay is matched by increased migration and invasion of cells in vivo [Klemke RL et al 1998]. The Boyden Chamber system and Transwell® migration assays use a hollow plastic chamber (upper compartment), sealed at one end with a porous filter membrane (refer to chapter 3, figure 3.2). This chamber is suspended over a larger well (lower compartment) which may contain medium and/or chemoattractants. Cells are placed inside the upper compartment chamber and allowed to migrate through the pores, to the other side of the membrane. Migratory cells are then stained and counted.

The pore size has to be chosen small enough in relation to the size of the cells being investigated so that the cells actively migrate through the pores and cannot passively pass across the membrane by just dropping through them. The pore diameter of the Transwell® membrane usually ranges from 3-12µm (commercially available), and is selected to suit the subject cells. Smaller pore size results in a greater challenge for the migrating cells. Most cells range in size from 30-50µm and can migrate efficiently through 3-12µm pores. The majority of cell migration assays use an 8µm pore size, as this is appropriate for the majority of cell types. This pore size supports optimal migration for most epithelial, fibroblast and tumour cells. The assay runs only for a few (3 to 6) hours, although this is dependent on cell type. In this assay, the investigator

analyzes the migratory activity by counting the transmigrated cells on the lower side of the filter (after 3 hours) or the cells in the lower compartment (after 6 hours). The “Boyden Chamber” assay is a very common assay and its standardized performance allows a high comparability of results.

CHAPTER 3

MATERIALS AND METHODS

SECTION 3.1

MATERIALS AND METHODS USED IN CHAPTER 4: ELUCIDATION OF CHEMOKINE RECEPTOR EXPRESSION (CXCR AND CCR GROUPS) IN PROSTATE CELL LINES

Standard materials

All chemicals and solvents were purchased from either Sigma-Aldrich Co. Ltd., UK or British Drug Houses (BDH) Ltd., UK unless otherwise stated.

Cell culture reagents

All materials used in routine cell culture were purchased from GibcoBRL (Life Technologies Ltd., UK). Foetal bovine/ calf serum (FBS) was purchased from Sigma-Aldrich Co. Ltd., UK. All plastic ware for cell culture use was manufactured by Nunc Ltd., UK.

Continuous cell lines

Details of the origins of human cell lines used and their growth media are shown in **table 3.1**.

Routine Maintenance

All cell lines were maintained under identical conditions as monolayers in 25cm² / 80cm² flasks in 5ml / 15ml of their required medium at 37⁰C or 33⁰C in a humidified atmosphere of 5% CO₂ in air. At least twice per week, the medium from the culture flasks was removed and replaced with an equal quantity of fresh medium. Cells were subcultured when they reached 70-80% confluency. This was done by first washing the monolayers with phosphate buffered saline (PBS) and then incubating with 1x trypsin

(1ml and 2mls for a 25cm² and 80cm² flask respectively) for 3 minutes at 37⁰C. The cells were detached from the culture surface by a gentle tap on each side of the flask, which was also sufficient to produce a crude single cell suspension. The detached cells were then taken up into 20ml medium and distributed into four 25cm² flasks or two 80cm² flasks. The medium in the flasks was replaced with fresh medium 24 hours after passaging to remove unattached cells.

Preparation of a Single Cell Suspension

When cells were required for experiments, exponentially growing cells (70-80% confluent) were detached from the culture surface by first washing with PBS and incubating with 1x trypsin (1ml and 2mls for a 25cm² and 80cm² flask respectively) for 3 minutes at 37⁰C. The detached cells were taken up in 10-15mls medium and a fine single cell suspension was produced by passing cells through a 19 gauge needle prior to counting. To 100µl of this cell suspension was added the same volume of 0.1% trypan blue and viable cell number was assessed using a haemocytometer (Freshney 1983). The number of cells per millilitre was calculated as follows:

Mean number of viable cells (in 4 squares) x 2 (dilution factor) x 10⁴ = number of cells/ml.

An appropriate dilution of cells was made to produce the final cell number required for experiments.

Table 3.1: Details of continuous human cell lines used

Cell Line	Derivation	Primary Reference	Growth Medium (incubation temp ⁰ C)
DU145	Established from a metastatic CNS lesion of prostatic adenocarcinoma in 69 years old patient	Stone KR et al, 1978	RPMI (Roswell Park Memorial Institute Medium) 1640 medium supplemented with 8% *FBS and 2mM L-glutamine (37 ⁰ C)
PC3	Established from a metastatic bone marrow lesion of prostatic adenocarcinoma in 62 years old patient	Kaighn ME et al, 1979	RPMI 1640 medium supplemented with 8% *FBS and 2mM L-glutamine (37 ⁰ C)
LNCaP	Established from a metastatic supraclavicular lymph node lesion of prostatic adenocarcinoma in 50 years old patient	Horoszewicz JS et al, 1980	RPMI 1640 medium supplemented with 8% *FBS and 2mM L-glutamine (37 ⁰ C)
1542 CPT3X	Established from a primary prostatic adenocarcinoma in a radical prostatectomy specimen	Bright RK et al, 1997	Keratinocyte – SFM (serum free medium) supplemented with 4% *FBS, 2mM L-glutamine, 30µg/ml bovine pituitary extract (BPE), 5ng/ml EGF (37 ⁰ C)
1542 NPTX	Established from normal prostatic epithelium in same individual as 1542 CPT3X	Bright RK et al, 1997	Keratinocyte – SFM supplemented with 4% *FBS, 2mM L-glutamine, 30µg/ml bovine pituitary extract, 5ng/ml human recombinant EGF (37 ⁰ C)
Pre 2.8	Established from normal prostatic epithelium in a 71 years old patient	Alam TN et al, 2004	PrEGM (prostate epithelial-specific growth medium) supplemented with BPE 2ml, insulin 0.5ml, hydrocortisone 0.5ml, GA1000 0.5ml, retinoic acid 0.5ml, transferrin 0.5ml, triiodothyronine 0.5ml, epinephrine 0.5ml, hEGF 0.5ml (33 ⁰ C)
S2.13	Established from stroma in same individual as Pre 2.8	Daly-Burns B et al 2007	RPMI 1640 medium supplemented with 8% *FBS and 2mM L-glutamine (33 ⁰ C)
MDA-MB-231	Established from epithelial cells in pleural effusion of 51years old patient with stage IV invasive ductal carcinoma	Cailleau R et al 1974	RPMI 1640 medium supplemented with 8% *FBS and 2mM L-glutamine (37 ⁰ C)

* Each new 500ml bottle containing FBS was heated to 56⁰C for 1 hour to inactivate complement prior to storage in 25ml aliquots at -20⁰C.

Primers: designing primers and primer details

Designing primers

Primers were designed and their specificity checked using the Basic Local Alignment Search Tool (BLAST) database at the National Centre for Biotechnology Information (NCBI) website (www.ncbi.nlm.nih.gov). Using the GI numbers (GenInfo Identifier sequence identification number) for the genomic and cDNA sequences (obtained from Genbank, which is part of the Nucleotide database at NCBI) of specific genes the BLAST 2 sequences tool produced the alignment of these two given sequences using the BLAST engine for local alignment. Thus intron-spanning primers could be designed so that products amplified from cDNA (complementary deoxyribose nucleic acid – has no introns) during polymerase chain reaction (PCR) could be differentiated from products amplified from genomic DNA (containing introns and therefore much larger). Often if the introns were long, the genomic DNA product would not be amplified because of the poor PCR efficiency of this longer product.

The following principles were followed when designing primers:

- Primers were usually 20-30 base pairs long to allow a reasonably high annealing temperature (longer than 30 does not improve primer specificity).
- Primer annealing was improved by having guanine or cytosine at the 3' end, as the three H⁺ bonds formed by guanine to cytosine are stronger than the two formed between adenine and thymine / uracil .

- Primers were designed so that a total of 50 or more hydrogen bonds form when the primers anneal and primers contained approximately equal numbers of purines (adenine and guanine) and pyrimidines (thymine and cytosine).
- Repetitive sequences and stretches of more than 3 of the same base were avoided to ensure specificity.
- Complementary sequences either within a primer or between a primer pair were minimised to prevent the formation of primer dimers - an artifact where the primer itself acts as a template resulting in a short length product.
- The distance between the sense and the antisense primer i.e. the length of desired product did not exceed 10 kilobases (the polymerase enzyme is less effective at amplifying the cDNA after 3kb).
- When performing reverse transcriptase-PCR (RT-PCR) there is a risk of cDNA contamination by genomic DNA. This was overcome by designing intron spanning primers in adjacent exons. The genomic DNA segment including the intron is too large to amplify. However, the intron is spliced out in the formation of mRNA so the cDNA can be amplified.

Primer details

Primer sequences, annealing temperatures used and product size details are shown in table 3.2.

Table 3.2: Details of chemokine receptor primers used in PCR.

The expression of the receptor CXCR6 was not elucidated as it was not formally named until 2002 [Murphy PM 2002]. Similarly, CXCR7 was not named until 2005 [Balabanian K et al 2005]. Additionally, there is no information publicly available at this time to confirm whether this designation for CXCR7 has been accepted by the International Union of Immunological Societies (IUIS) / World Health Organisation (WHO) Subcommittee on Chemokine Nomenclature (also, the function of the CXCR7 receptor is currently controversial with some studies suggesting it is a non-signalling scavenger receptor for CXCL11 and CXCL12 [Naumann U et al 2010]).

The CCR11 receptor has been disqualified as a chemokine receptor [Murphy PM 2002].

We did not elucidate the expression of the CCR4 and CCR10 receptors.

Receptor	Sense (5' to 3')	Antisense (5' to 3')	Annealing temperature (°C)	Product size (base pairs)
CXCR1	TCT GAC TGC AGC TCC TAC TG	GAA TTG TTT GGA TGG TAA GC	60	627
CXCR2	CTC CAC CTT CAG ACT GGT AG	CAA AGC TGT CAC TCT CCA TG	60	411
CXCR3	GCC CAG CCA TGG TCC TTG AG	CGT AGA AGT TGA TGT TGA AG	60	417
CXCR4	AAC CAG CGG TTA CCA TGG AG	CAT CTG CCT CAC TGA CGT TG	60	558
CXCR5	AGC CTC TCA ACA TAA GAC AG	GGC AAG ATG AAG ACC AGC AG	60	367
CCR1	AGA CTT CAC GGA CAA AGT CC	TAC CTG TCA ATC GTC AGC AG	60	438
CCR2	GAC TGC CTG AGA CAA GCC AC	CAA TAG CCA GGT ATC TAT CG	60	505
CCR3	TCT TCC ACA GGC ACT TGC TC	ACT ATC TAA CAT TCA GGT GC	60	414
CCR5	CTG TGT AGT GGG ATG AGC AG	GAG GAT GAC CAG CAT GTT GC	63	455
CCR6	GTC ATC ACA TTG GTG AGC TG	GGA TGT CTG CAA TGG CCA TG	63	458
CCR7	TTT ACC GCC CAG AGA GCG TC	CGT AGC GGT CAA TGC TGA TG	63	485
CCR8	CAT TGA GCT GCA CTC ACA TG	GTA CCT GTC CAC ACT CAT GA	63	496
CCR9	CCA GAC ACT GAG AGC TGG TG	ACG CTG ATG CAC ATG ATC AG	63	462
CXCL12	ACA GAT GCC CAT GCC GAT TC	CCT GCA CAG CTC AGA GAA TC	60	630
GAPDH	TCC TGC ACC ACC AAC TG	GCC TGC TTC ACC ACC TT	60	450

Cell line RNA: RNA extraction from cell lines

RNA was extracted using the silica-gel-based RNeasy® Mini kit (Qiagen Ltd., UK) using the manufacturer's instructions. With the RNeasy procedure, all RNA molecules longer than 200 nucleotides are isolated. The procedure provides enrichment of mRNA since most RNAs <200 nucleotides (such as 5.8S rRNA, 5S rRNA, and tRNAs, which together comprise 15–20% of total RNA) are selectively excluded.

Cells grown to 70-80% confluence in a 80cm² flask were harvested by trypsinisation and subsequently lysed with a mixture of β-mercaptoethanol (Sigma-Aldrich Co. Ltd., UK) and RLT buffer [guanidine isothiocyanate (GITC)-containing lysis buffer]. The latter is highly denaturing and immediately inactivates RNases to ensure isolation of intact RNA. Complete lysis or disruption, with GITC-containing buffer, of plasma membranes of cells and organelles was required to release all the RNA contained in the sample (incomplete disruption results in significantly reduced yields). The cell lysate was homogenized using a QIA shredder spin column. Homogenization was necessary to reduce the viscosity of the cell lysates produced by disruption. Homogenization shears the high-molecular-weight genomic DNA and other high-molecular-weight cellular components to create a homogeneous lysate. Incomplete homogenization results in inefficient binding of RNA to the RNeasy membrane and therefore significantly reduced yields. An equal volume of 70% ethanol was then added to the homogenized lysate to ensure selective binding of RNA onto the silica based RNeasy spin column, and the sample was loaded onto the RNeasy column. A wash with RW1 buffer (composition not released) followed by two washes with RPE buffer (composition not released) removed sheared genomic DNA, and protein contaminants.

RNA was eluted from the RNeasy spin column with 30µl DEPC-treated water and recovered by centrifugation. It was stored at -70°C .

Leucocyte RNA: isolation of RNA from leucocytes

Whole blood (5mls) was collected into a commercially available tube containing ethylenediaminetetraacetic acid (EDTA). The blood (5mls) was carefully pipetted into a tube containing Ficoll-Hypaque (5mls) (Sigma-Aldrich Co. Ltd., UK) and the solution centrifuged (2000rpm for 20 minutes). With great care the buffy coat was pipetted off and subsequently washed twice in phosphate buffered saline (PBS) (500µl), the latter being removed each time after separation of the leucocytes by centrifuging (2000rpm for 1 minute). RNA could then be extracted from the isolated leucocytes by using the the Nucleospin® Nucleic Acid Purification Kit (CLONTECH) (the RNeasy® Mini kit (Qiagen Ltd., UK) was not suitable for extraction of RNA from body fluids according to the manufacturer's instructions). Similar principles were involved as to RNA extraction from cell lines but an extra step involving incubation of the sample with DNase 1 enzyme at room temperature for 15 minutes was included.

Measurement of RNA concentration

RNA concentrations were measured by UV spectrophotometry using a DU650 series spectrophotometer (Beckman Ltd., UK). 4µl of eluted RNA was diluted with sterile water to 400µl (1/100) and added to a microcuvette. The spectrophotometer was blanked with

water following which the absorbance, or optical density (OD), of the sample was measured at 260nm and at 280nm and the RNA concentration was calculated as follows:

$$OD_{260} \times 40\mu\text{g/ml} \times \text{dilution factor} = \text{RNA concentration } \mu\text{g/ml}$$

An absorbance of 1 unit at 260nm corresponds to 40 $\mu\text{g/ml}$ of RNA. This relation is valid only for measurements in water. The ratio of the readings at 260 nm and 280 nm provides an estimate of the purity of RNA with respect to contaminants that absorb in the UV spectrum, such as protein. The 260nm/280nm ratio of pure RNA in water is approximately 2.0.

Performance of RT-PCR

mRNA was derived from cell lines using one of the commercially available kits (refer to earlier section). Table 3.3 demonstrates the protocol followed for the RT reaction. After reverse transcription the cDNA can be amplified by PCR immediately or stored for several months at -20°C.

PCR was carried out in a Perkin Elmer-Gene Amp 2400 thermal cycler (Perkin Elmer Ltd., UK). All primers were synthesized by Invitrogen (GibcoBRL, UK) and supplied as lyophilised stock. For each primer an equal volume of sterile water (in μl) as the amount of nmoles supplied was added to provide a stock of 1000 μM . For experiments 2 μl aliquots of this stock solution were made up with sterile water to 200 μl i.e. a 10 μM solution.

Table 3.3: Constituents of a 20µl reverse transcriptase reaction

1µg mRNA is diluted to 11µl in RNAase free [diethylpyrocarbonate (DEPC) treated] water

*Add 1µl of OligodT 12-18 (0.5µg/µl) primer (to make 12 µl solution)

The 12µl solution is heated to 70⁰C for 10 minutes

Centrifuge for few seconds and put solution on ice

Add 4µl of 5x first strand buffer, 2µl of 0.1M DTT (dithiothreitol) and 1µl of 10mM dNTPs (the single nucleotides or deoxynucleoside triphosphates dATP, dTTP, dGTP, dCTP)

**Heat at 42°C for 50 minutes, but after two minutes 1µl (200units) SUPERScript™ II (reverse transcriptase) is added to each tube

***Heat at 70°C for 10 minutes

*mRNA has several adenosine (A) nucleotides at its 3' end – the polyA tail. A primer, made up of several thymidine (T) nucleotides - oligo-deoxythymidine (oligodT), is complementary and will bind to this polyA tail. The heat removes the secondary structure of the mRNA and allows the oligodT to anneal to the polyA tail.

** reverse transcriptase hybridises the single deoxynucleoside triphosphates (dNTPs) to their complementary base sequentially from the oligodT primer, to make cDNA.

***this step inactivates the reverse transcriptase enzyme

To perform PCR a master mix was made, using multiples of the ingredients shown in table 3.4, depending on the number of samples to be used. The master mix was added to 3µl of cDNA in PCR tubes on ice. A drop of mineral oil was also added to prevent evaporation during the PCR process.

Table 3.4: PCR master mix for 1x 50µl reaction

1. 5 µl 10x buffer
2. 5 µl dNTP (2mM)
3. 3 µl MgCl₂ (25mM)
4. 2 µl sense primer (10µM=10pmol/µl)
5. 2 µl antisense primer (10µM =10pmol/µl)
6. 29.5 µl H₂O

The samples were then placed in a pre-programmed PCR machine and heated at 95⁰C for 3 minutes before 0.5µl (2.5Units) of Red Hot DNA polymerase (Advanced Biotechnologies Ltd., UK) was added and the programme started. This “hot start” minimizes non-specific annealing of primers to non-target DNA sequences and reduces the incidence of primer oligomerisation therefore resulting in a more specific and efficient PCR reaction. The PCR cycle that was used is shown here but described in more detail in chapter 2, figure 2.1.

95⁰C –2 minutes

95⁰C – 45 seconds

60⁰C – 45seconds

72⁰C – 45seconds

74⁰C – 7 minutes

35 cycles

Controls

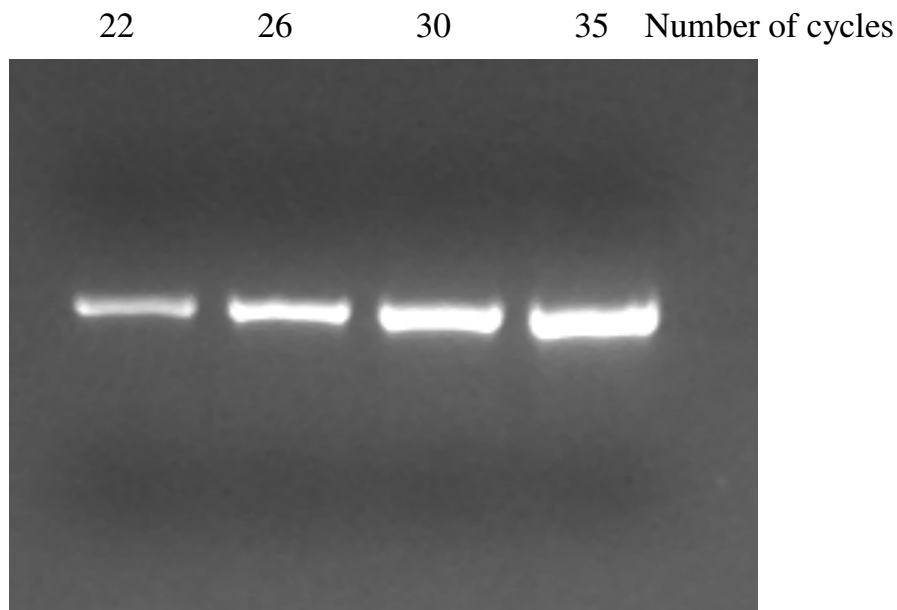
To confirm the presence of amplifiable DNA in samples PCR is simultaneously performed with primers for an alternative target eg. glyceraldehyde 3-phosphate dehydrogenase (GAPDH). Also, if PCR is to be used for quantitative applications

GAPDH amplification is performed as a standard in order to confirm similar starting concentrations of cDNA (and therefore indirectly RNA) template between samples. To do this GAPDH PCR should be performed at a number of cycles during which amplification is linear (i.e. before the plateau phase is reached for the reaction; for more details of this refer to Taqman real time quantitative PCR in chapter 2). We amplified GAPDH at several different numbers of cycles and elucidated that amplification is still in the linear range at 26 cycles (figure 3.1).

Figure 3.1: Optimisation of GAPDH PCR cycles. This shows an agarose gel viewed on an ultraviolet transilluminator and captured using the Gel doc system (Quantity One Software, Biorad Ltd, UK).

GAPDH was amplified at several different numbers of cycles and it can be seen that amplification was still in the linear range at 26 cycles.

Figure 3.1 **Optimisation of GAPDH PCR cycles**



To avoid PCR amplification of contaminating genomic RNA/ DNA a mRNA negative control (therefore cDNA negative) was also included in each reverse

transcriptase reaction (12µl DEPC water used in this control reverse transcriptase reaction).

Due to the enormous amplification possible with PCR, special laboratory practices are necessary in order to avoid false positive amplifications. Sources of sample contamination may be from carryover from previous PCR reactions or from samples with high DNA levels or from positive control templates. In order to minimize this we followed the following procedures:

a) Clean laboratory coat was worn (not previously worn while handling amplified PCR products or used during sample preparation) and also clean gloves when preparing samples for PCR amplification.

b) Separate areas and dedicated equipment and supplies were maintained for:

- Sample preparation
- PCR setup
- PCR amplification
- Analysis of PCR products

c) Amplified PCR products were never brought into the PCR setup area.

d) Reactions and components were capped as much as possible to avoid splashing PCR samples.

e) Laboratory benches and equipment were periodically cleaned with 10% bleach solution.

It should be noted the presence of multiple products does not necessarily imply contamination. It may be due to lack of primer specificity. By reducing the number of cycles or increasing the annealing temperature the specificity improves. A small product [20-30 base pairs (bp)] may represent primer dimers (see primer design).

Agarose Gel Electrophoresis

Once PCR was complete agarose gel electrophoresis was used to visualize the amplified products. A 1-3% gel was used depending on product size - higher concentrations allow better discrimination of smaller products. The desired amount of agarose was dissolved in 1x TAE (tris acetate EDTA) buffer for 5-10 minutes at full power in a conventional microwave oven. The gel was then cooled to 50⁰C, supplemented with 1µg/ml ethidium bromide and poured onto a clean plastic gel plate to set at room temperature. Prior to loading, an appropriate volume of 5x DNA loading buffer was added to each sample. In addition, a product size-marking DNA ladder [1 kilobase (kb)] was loaded onto the agarose gel and an electric current (125V) was passed across the gel in a horizontal gel tank (Hybaid, UK). Gels were viewed on an UV transilluminator (ethidium bromide binds to DNA and fluoresces in ultra-violet light), images captured using Gel Doc system (Quantity One software, Biorad Ltd., UK) and printed on thermal paper (Mitsubishi P91 thermal printer).

DNA extraction from agarose gel

DNA (for later sequencing) was purified from agarose gel using the silica based QIAquick Gel Extraction Kit (Qiagen Ltd., UK). This protocol was designed to extract and purify DNA of 70 bp to 10 kb from agarose gels in TAE. Initially, amplified PCR product (40µl) was run on a 1x TAE agarose gel. Using a clean scalpel blade the fragment of interest was cut out from the gel as quickly as possible to minimize UV-mediated DNA damage. DNA was then extracted and purified according to the manufacturer's instructions. Briefly, buffer QG (3 volumes) (solubilisation buffer; exact composition not released), containing guanidine thiocyanate, solubilized the agarose gel

slice at 50°C for 10 minutes and provided the appropriate conditions for binding of DNA to the silica membrane in the QIAquick spin column. The adsorption of DNA to the membrane was efficient only at pH 7.5. Buffer QG contained a pH indicator, which was yellow at pH 7.5 and orange or violet at higher pH. If the color of the mixture was orange or violet, 10 µl of 3 M sodium acetate, pH 5.0, was added until the color of the mixture turned to yellow. Isopropanol (1 volume) was then added to the sample to increase the yield of DNA fragments <500bp and >4kb. The mixture was then centrifuged in the QIAquick spin column with DNA adsorbing to the silica-gel membrane whilst contaminants (eg. salts, enzymes, unincorporated nucleotides, agarose, dyes, ethidium bromide) passed through the column. Salts were quantitatively washed away by centrifuging with ethanol-containing buffer PE (0.75ml) (wash buffer; exact composition not released). DNA was eluted with 30 µl of the buffer EB (elution buffer; 10 mM Tris·Cl, pH 8.5). Buffer EB provided the basic (pH 7.0 and 8.5) conditions necessary for maximum elution efficiency. DNA was stored at -20°C.

DNA sequencing

The chain terminator method for DNA sequencing was employed using the ABI PRISM® dRhodamine Terminator Cycle Sequencing Ready Reaction Kit. The principles of the chain terminator method for DNA sequencing were first described by Sanger et al 1977. 2µl of the agarose gel extracted DNA was mixed with an equal amount of 5x loading buffer and run on a 1.5% agarose gel in order to visually check the concentration and quality of the purified DNA. An appropriate volume of gel-extracted DNA (depending on its concentration judged visually by running on 1.5% agarose gel, as mentioned earlier) was diluted in sterile water to a total volume of 14.5µl. Sense primer,

0.5µl of a 4µM solution (4pmol/µl), was added followed by sequencing reaction mix (5µl of Terminator Ready Reaction Mix from the ABI PRISM® dRhodamine Terminator Cycle Sequencing Ready Reaction Kit) containing AmpliTaq DNA Polymerase FS (fluorescent sequencing), dNTPs, ddNTPs (di-deoxynucleosides ddATPs, ddTTPs, ddCTPs, ddGTPs - in relatively low concentration compared to dNTPs), magnesium chloride and Tris-HCl buffer (Ph 9.0). Each ddNTP was fluorescently tagged with 1 of 4 different fluorescent dyes [either rhodamine 6G (R6G), tetramethyl-6-carboxyrhodamine (TAMRA), rhodamine 110 (R110) or ROX] that emitted a specific wavelength of light when excited by a laser. Also ddNTPs were chain terminators because they lack the 3'OH residue of the deoxyribose backbone and when incorporated into the growing DNA strand, they prevent phosphodiester bond formation with the next dNTP. The solution was then placed in a Perkin Elmer-Gene Amp 2400 thermal cycler (Perkin Elmer Ltd., UK) and PCR performed under the following conditions:

96⁰C –1minute,
96⁰C – 30seconds
50⁰C – 15seconds
60⁰C – 4 minutes
4⁰C – hold

25 cycles

DNA replication in the presence of both dNTPs and ddNTPs terminated the growing DNA strand at each base and resulted in many copies of different sized DNA fragments being produced. Moreover each new DNA fragment was labelled with a fluorescent dye, which was specific for the terminal base. Precipitation of PCR products was subsequently performed by incubating with a mixture of 95% ethanol and 3M sodium acetate (50µl and 2µl respectively) for 15 minutes on ice followed by centrifugation (25minutes at maximum speed) and pipetting of the supernatant. The

remaining DNA pellet was washed with 70% ethanol (100µl) and the alcohol left to evaporate. The pellet was stored in the dark until automated sequencing was performed by running the fluorescently labelled DNA fragments on the ABI PRISM® 377 DNA Sequencer (this automated sequencing was performed at the Ludwig Institute, UCL by a colleague scientist). Basically these fragments were loaded into the top of a polyacrylamide gel with fragments separating into distinct bands according to size. Near the base of the gel the bands passed through the beam of a constantly scanning laser, which excited the fluorophores or fluorescent dyes attached to DNA bands (i.e. ddNTP). The wavelengths of the resulting light emissions were then identified and the signal quantitated. Thus the emitted wavelength or colour identified the terminal base characteristic of each band, and the quantitation of each band's fluorescent signal gave the relative number of fragments within each band. In addition to nucleotide sequence text files the automated sequencer also provided trace diagrams termed electropherograms.

SECTION 3.2

MATERIALS AND METHODS USED IN CHAPTER 5:

QUANTITATION OF CXCR4 mRNA EXPRESSION IN CELL LINES

AND PATIENT PROSTATE TISSUE SAMPLES

Quantitation of CXCR4 mRNA was performed using the TaqMan® real time quantitative PCR assay (principles of this technique are described in chapter 2).

All reactions were conducted in the ABI PRISM® 7700 Sequence Detection System (Perkin-Elmer–Applied Biosystems, Foster City, CA, USA) (chapter 2, figure 2.3) using the universal thermal cycling parameters detailed in chapter 2, table 2.2. Also, all reactions were run in triplicate on a MicroAmp® Optical 96-well reaction plate (Applied Biosystems) and each reaction mixture was made up to a total of 25µl with RNase free water. Every reaction additionally contained Taqman® Universal PCR Master Mix (Applied Biosystems). This mix is optimized for the Taqman® reactions and contains AmpliTaq Gold® DNA polymerase, AmpErase® Uracil N-Glycosylase (UNG), dNTPs with dUTP, Passive Reference dye (ROX) and optimized buffer components. The following components were added when necessary to this reaction mixture:

a) CXCR4 primers and probe

The reverse complement (i.e. the sequence reversed and then its complementary base pairs) of the CXCR4 mRNA target sequence was used to generate the primer and

probe sequences (using Primer Express® software) as it was not possible to devise these with the original sequence and fulfill the strict criteria for their design (table 3.5).

Table 3.5: CXCR4 Primers, Probe and Amplicon Details (designed using Primer Express® software and supplied by Applied Biosystems)

*Labelled with 6-FAM fluorescent dye covalently linked to the 5' end and TAMRA quencher dye at the 3' end

	Sequence (5' to 3')	Length (no of bases)	T_m (°C)	Concentration (pmol/μl)
Forward primer (junction spanning)	AGGGCCTGAGTGCTCCAGTAG	21	59.5	9.60
Reverse primer	CGGTGTAGTTATCTGAAGTGTATATACTGATC	32	58.3	9.60
*Probe	CTCCATGGTAACCGCTGGTTCTCCAGA	27	69.5	5
Amplicon	-	90	-	-

b) Housekeeping gene (β-actin) primers and probe

Pre-developed Taqman® assay reagents control kit (Applied Biosystems) containing control (i.e. housekeeping gene) primers and probe reagent. This product contained a pre-mixed solution of β-actin primers and probe. The probe was labelled with a VIC™ fluorescent dye (VIC™ is an acronym – Applied Biosystems have not released the chemical composition of this dye). The sequence of the β-actin primers and probe was not provided by Applied Biosystems. The volume of the mixture necessary for a 50μl reaction was advised.

c) cDNA from cell lines

Cell line extracted RNA was reverse transcribed into cDNA as described earlier in this chapter. In several optimisation experiments, a mixture of cDNA derived from DU145/ LNCaP/ PRE 2.8 cell lines was used.

d) Patient prostate RNA samples

Table 3.6 summarises available information on the patient samples. These RNA samples were provided by H. Klocker at the University of Innsbruck in Austria: nine fresh primary prostate tumours (radical prostatectomy specimens) were initially frozen and later cut into 50µm sections. Tumour cells were laser microdissected and RNA extracted using the Stratagene RNA isolation kit and following the manufacturer's instructions. Tumour stage in these RNA samples ranged from pT2c to pT3a with no evidence of local lymph node spread on histological examination and no evidence of distant metastasis on radiological staging. Combined Gleason grade varied from 5 to 9. Benign epithelial prostatic tissue was also obtained from 6 of these patients with primary prostate cancer (again using using laser capture microscopy) and RNA extracted using the Stratagene RNA isolation kit (one patient had benign tissue isolated from two different areas). Another 2 samples were from benign areas in patients with prostatic carcinoma, but no sample was taken from the neoplasm.

The patient samples were labelled from number 1 to 18 (during experiments we were not aware as to the derivation of each sample). In our laboratory, from each sample, 20µl cDNA was made from 200ng of RNA using the SUPERSCRIPT™ II reverse

transcriptase kit (Invitrogen - GibcoBRL, UK) - thus 10ng RNA was equivalent to 1µl cDNA in these patient samples.

Table 3.6: Clinically localized patient primary prostate tumour and benign prostate samples - summary of available information (all tissue derived from frozen fresh radical prostatectomy specimens). Samples were randomly labelled from numbers 1 to 18 (during experiments we were not aware as to the derivation of each sample)

Sample No.	Carcinoma/ Benign	Prostate weight - grams (without SV)	pT	N	M	Gleason grade	Combined Gleason grade
1 2 13	Carcinoma Benign Benign TS Zone	37	3a	0	0	3+2	5
3 4	Carcinoma Benign	40	2c	0	0	3+3	6
5 6	Carcinoma Benign	47	2c	0	0	3+3	6
7 8	Carcinoma Benign TS Zone	34	3a	0	0	3+3	6
9 10	Carcinoma TS Zone Benign	20	2c	0	0	3+2	5
11 12	Carcinoma Benign TS Zone	45	2c	0	0	3+4	7
14	Carcinoma	31	3a	0	0	4+5	9
15	Benign	19	2c	0	0	3+4	7
16	Carcinoma	24	2c	0	0	3+3	6
17	Carcinoma	15	2c	0	0	3+3	6
18	Benign	40	2a	0	0	3+3	6

Reactions for optimisation of CXCR4 primer concentrations

This experiment was done in order to elucidate the concentration of reverse and forward primers necessary for optimal assay performance and determine the minimum primer concentrations giving the maximum ΔR_n .

These reactions contained a constant concentration of fluorogenic probe (5pmol - equivalent to 1 μ l), DU145/LNCaP/PRE cDNA mixture (equivalent to a total of 100ng starting RNA) and 12.5 μ l of Taqman® Universal PCR Master Mix (Applied Biosystems). However, varying concentrations of CXCR4 forward and reverse primers were added, resulting in 50 nM to 900 nM solutions of forward or reverse primer.

Reactions for optimization of starting RNA quantity

Optimisation of starting RNA quantity was necessary in order to elucidate the minimal amount of RNA necessary for the reaction to proceed.

These reactions contained a constant concentration of fluorogenic probe (5pmol - equivalent to 1 μ l), forward/ reverse primers (500nM solution) and Taqman® Universal PCR Master Mix (Applied Biosystems) (12.5 μ l). Also, varying dilutions of cDNA (again derived from a mixture of DU145/LNCaP/PRE RNA) equivalent to a range of starting RNA quantities (0.001ng – 100ng) was added to each reaction mixture.

Reactions used in calculating the relative efficiency plot

This was necessary to check that the amplification efficiencies of the target (CXCR4) and endogenous control (β -actin) were approximately equal.

CXCR4 reactions - these reactions contained a constant concentration of CXCR4 specific fluorogenic probe (2.5pmol equivalent to 0.5 μ l), forward/ reverse primers

(300nM solution - elucidated from previous experiment) and Taqman® Universal PCR Master Mix (Applied Biosystems) (12.5µl). Variable dilutions of DU145/LNCaP/PRE 2.8 cDNA mixture, equivalent to a range of starting RNA amounts (9.375ng - 120ng), were included.

β-actin reactions - these reactions contained a constant concentration of β-actin specific fluorogenic probe – primers mix (1.25µl – as advised by Applied Biosystems for a 25µl reaction) and Taqman® Universal PCR Master Mix (Applied Biosystems) (12.5µl). Variable dilutions of DU145/LNCaP/PRE 2.8 cDNA mixture, equivalent to a range of starting RNA amounts (9.375ng - 120ng), were included.

Final reactions used in determining CXCR4 mRNA levels in cell lines and patient samples (using real time quantitative PCR)

Final results for real time quantitation of CXCR4 mRNA in all cell lines and patient samples were obtained. Therefore the wells contained either cell lines or patient tissue and within these CXCR4 or β-actin cDNA was amplified.

Cell line wells containing CXCR4 reactions - these reactions contained the equivalent of 10ng cell line RNA which had been reverse transcribed into cDNA (0.2µl), 2.5pmol fluorogenic probe (0.5µl), forward/ reverse primers 300nM solution, and Taqman® Universal PCR Master Mix (Applied Biosystems) (12.5µl).

Cell line wells containing β-actin reactions - these reactions contained the equivalent of 10ng cell line RNA which had been reverse transcribed into cDNA (0.2µl), constant volume of fluorogenic probe – primers mix (1.25µl) and Taqman® Universal PCR Master Mix (Applied Biosystems) (12.5µl).

Patient samples wells - volumes as above but 10ng of RNA (which had been reverse transcribed into cDNA) was contained in 1 μ l of sample.

SECTION 3.3

MATERIALS AND METHODS USED IN CHAPTER 6: **ELUCIDATION OF CELL MEMBRANE CXCR4 CHEMOKINE** **RECEPTOR (PROTEIN) EXPRESSION IN PROSTATE CELL** **LINES**

The principles of sample preparation using the protocols described below were that using individual cell lines, a monodisperse cell suspension was prepared and incubated initially with primary anti-CXCR4 antibody and then subsequently with a fluorochrome conjugated secondary antibody (note that one of the primary anti-CXCR4 antibodies was also fluorochrome conjugated; all antibodies used are shown in table 3.7a and b). The control reaction contained only fluorescent secondary and no primary anti-CXCR4 antibody (note that when using the fluorochrome conjugated primary antibody no secondary antibody was needed and the control contained a fluorochrome isotype matched primary control antibody, which did not bind to cellular antigens). The specimen was finally fixed in formaldehyde prior to determining cell surface CXCR4 receptor expression by using the Becton Dickinson FACScan.

The Becton Dickinson FACScan uses an air-cooled argon gas laser with fixed wavelength emission of 488 nm. The FACScan can measure up to five parameters including forward light scatter, side light scatter and three fluorescence parameters:

- *Green fluorescence signal* received by the PMT, FL1, which measures emitted light in the green range of the spectrum (515 to 545 nm) eg. FITC.

- *Yellow-orange fluorescence signal* received by the PMT, FL2, which measures emitted light in the yellow-orange range of the spectrum (564-606 nm) eg. PE and PI.
- *Red Fluorescence signal* received by the PMT, FL3, which measures emitted light in the red range of the spectrum (above 650-675nm) eg. PE-CY5.

The FACScan can analyze cell suspensions at the rate of several hundred cells per second. Typically, approximately 10,000 cells per sample are acquired (or anywhere in the range 5,000 – 15,000). In the FACScan, fluorescence/ scatter is represented on a logarithmic scale with the data divided into four decades across 1024 channels with 256 channels per decade.

Data was analysed using CellQuest™ software.

In our experiments a total of 10,000 events were analysed in each sample using the Becton Dickinson FACScan, with data due to dead cells/cell debris and non-specific binding of the secondary antibody being gated out of the final results when appropriate. All experiments were repeated in triplicate in order to confirm the results and representative histograms and dot plots are shown in the results (chapter 6).

Primary and secondary antibodies

Antibodies - all primary and secondary antibodies used are shown in tables 3.7a and 3.7b.

Table 3.7: Details of primary and secondary antibodies used

Table 3.7a) i) Primary anti-CXCR4 antibodies

Host/ Isotype	Mono/ polyclonal	Epitope in CXCR4	Clone	Source	Concentration/ Dilution used	Fluoro chrome
Rabbit/ IgG	polyclonal	ECL2 (partly transmembrane region - amino acids 176-293)	H-118 (Fusin)	Santa Cruz Biotechnology, Inc.	200µg/ml 1/1	-
*Mouse/ IgG2a, κ	monoclonal	on ECL2 and ECL1	12G5	BD PharMingen	12.5µg/ml 1/1	PE
Mouse/ IgG2a	monoclonal	on ECL2	44708.1 11	R&D Systems	100µg/ml 1/1	-
Mouse/ IgG2b	monoclonal	on ECL2	44716.1 11	R&D Systems	100µg/ml 1/1	-
Mouse/ IgG2b	monoclonal	on ECL2	44717.1 11	R&D Systems	100µg/ml 1/1	-

*Fluorochrome isotype matched primary antibody is necessary for use in the control population of cells. Details of this are given in table 3.7a) ii).

Table 3.7a) ii) Fluorochrome isotype matched control primary antibody (for use in control experiment for primary anti-CXCR4, PE conjugated mouse IgG2a, κ shown in table 3.7a)i))

*Mouse/ IgG2a, κ	monoclonal	does not bind to CXCR4	MOPC- 173	BD PharMingen	12.5µg/ml 1/1	PE
---------------------	------------	---------------------------------------	--------------	---------------	------------------	----

Table 3.7b) Secondary antibodies

Host species	Antigen	Source	Concentration/ Dilution	Fluorochrome
Goat	anti-rabbit IgG	Sigma	1mg/ml 1/50	FITC
Goat	anti-mouse IgG2a (γ 2a chain specific)	SouthernBiotech	1mg/ml 1/50	FITC
Goat	anti-mouse IgG2b (γ 2b chain specific)	SouthernBiotech	1mg/ml 1/50	FITC
Goat	Anti-mouse IgG F(ab') ₂ (γ 2b chain specific)	SouthernBiotech	1mg/ml 1/50	FITC

Reaction protocols

All procedures were performed in a hood to keep all solutions and antibodies sterile. The protocols followed are described.

a) Protocol using non-fluorescent primary anti-CXCR4 antibody and FITC-conjugated secondary antibody

The protocol described here was the same for all experiments involving non-fluorescent primary antibodies and FITC-conjugated secondary antibodies. The dilutions of the antibodies given are for primary mouse IgG2b clone 44717.111 (R&D Systems) and secondary anti-mouse IgG2b, γ 2b chain specific (SouthernBiotech). The dilutions used for the other antibodies are given in tables 3.7a and 3.7b.

Cells in a 80cm²/ 25cm² flask were dissociated with undiluted non-enzymatic Cell Dissociation Solution (Sigma) and resuspended in the appropriate culture medium. The cells were counted with a haemocytometer, centrifuged and resuspended in 1% bovine serum albumin in phosphate buffered saline (BSA-PBS) at 2.5 x 10⁶ cells/ml. 200µl of this cell suspension (500,000 cells) was then distributed in a well within a round 96 well plate (two wells for each cell line) prior to being incubated on ice for 20-30 minutes. Following centrifugation at 1500 rpm for 3-5 minutes, supernatant was removed with a pipette. The cells were subsequently resuspended in 20µl of the primary anti-CXCR4 antibody diluted at 100µg/ml in sterile PBS (the dilution for mouse IgG2b clone 44717.111 - R&D Systems) or in 20µl sterile PBS only (control). Following this, incubation for 1 hour on ice was necessary. After this, two washes with 1% BSA-PBS were performed by first centrifuging the incubated cells at 1500rpm for 3 minutes, removing supernatant, resuspending the cells in 200µl 1% BSA-PBS and then repeating the procedure. Once again the supernatant was removed before the addition to the cells of 1/50 concentration of secondary FITC antibody (anti-mouse IgG2b, γ2b chain specific - SouthernBiotech) (1µl of secondary FITC antibody in 49µl 1% BSA-PBS). Incubation for 30 minutes in the dark was then essential, and this was followed by another 2 washes in 1% BSA-PBS. The cells were then fixed by resuspending in 200µl of 3.7% formaldehyde and incubation on ice for 15 minutes in the dark. 300µl PBS was then added and the cells stored at 4⁰C in the dark in a 5mls FACS tube. FACS analysis was performed within 24 hrs.

b) Protocol using PE conjugated primary anti – CXCR4 antibody

The method was exactly the same as that described for non-PE conjugated primary antibodies described above except that there was no need for incubation with a secondary antibody. The reactive anti-CXCR4 antibody used was PE conjugated mouse IgG2a, κ chain specific clone 12G5 (BD PharMingen), and the non-reactive isotype control antibody was PE conjugated mouse IgG2a, κ chain specific clone MOPC-173 (BD PharMingen). Dilutions of the antibodies used are given in tables 3.7a and 3.7b.

SECTION 3.4

MATERIALS AND METHODS USED IN CHAPTER 7:

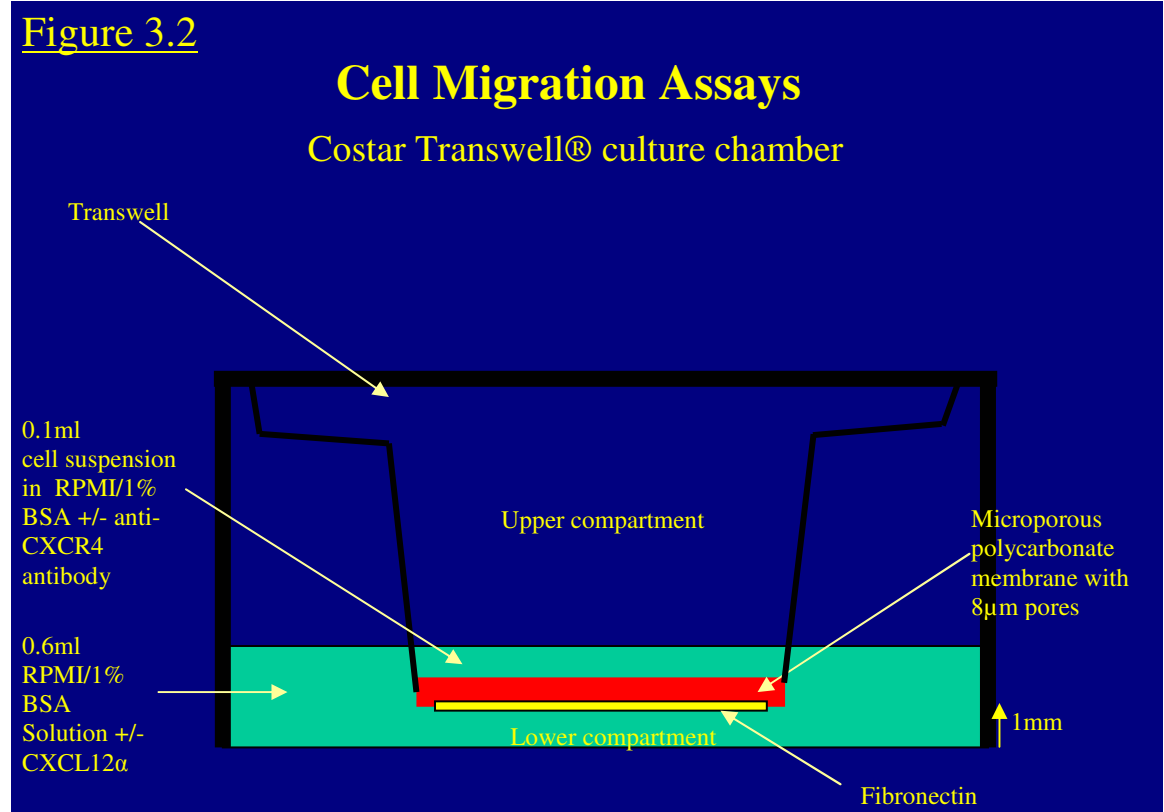
ESTABLISHING THAT THE CXCR4 RECEPTOR IS FUNCTIONAL

IN CELL LINES DERIVED FROM PROSTATE CANCER

METASTASES

In cell migration assays the cell lines DU145, PC3 and 1542 NPTX were used (the latter was used as a control because 1542 NPTX had been shown in the results from chapter 6 to have extremely low or absent CXCR4 protein expression). The protocol was based on that described by Muller A et al 2001.

Figure 3.2: Costar Transwell® culture chamber



Cell migration assays were conducted using Transwell® 24 well cell culture chambers (Costar) (figure 3.2). Each Transwell® was 6.5mm in diameter with a translucent polycarbonate membrane attached to the bottom of the well. The polycarbonate membrane was 10µm thick with 8µm pores. Stock 0.1% (1mg/ml) fibronectin from bovine plasma (Sigma-Aldrich) was diluted 1/100 with PBS to create a 10µg/ml solution. 50µl of this diluted solution was coated onto the lower surface of the polycarbonate membrane of each Transwell® and left to dry at room temperature for 2 hours.

Serum free RPMI 1640 with 1% BSA and L-glutamine was filter sterilized by syringing through a 0.2µm syringe filter (Nalgene). Recombinant human SDF1α/CXCL12 was made up with 1ml 0.1% BSA to form a 10µg/ml stock solution. This CXCL12 stock solution was diluted in serum free RPMI / 1% BSA to 150ng/ml (30µl stock solution made up to 2000µl). 600µl of this solution was added to the lower chamber (cluster plate well). In the control experiments 600µl serum free RPMI / 1% BSA alone (without SDF1α) was added to the lower chamber.

Appropriate cell lines were resuspended in serum free RPMI / 1% BSA at a concentration of 4×10^5 cells/ ml. 100µl of this cell suspension was added to the upper compartment of the Transwell®. When necessary, IgG2b anti-CXCR4 monoclonal antibody (clone 44717.111) (R & D Systems) was added to the cells (100µg in 1ml PBS stock antibody solution). To do this, the cells were spun down and serum free RPMI / 1% BSA aspirated. The cells were then resuspended in the antibody solution at room temperature for 5 minutes (20µl, equivalent to 2µg, of stock antibody solution per 500µl

of centrifuged cell suspension) before the aspirated serum free RPMI / 1% BSA was again added (thus IgG2b antibody concentration 4µg/ml). 100µl of this cell suspension and antibody solution was then added to the upper compartment of the Transwell®. Simultaneously in other wells without antibody, cells were spun down and resuspended for 5 minutes in serum free RPMI / 1% BSA alone (without antibody).

All wells were incubated for 3 hours at 37⁰C in a humid atmosphere of 5% CO₂ / 95% air. After incubation the Transwell® was removed from the cluster plate and the upper surface of the polycarbonate membrane was wiped gently with a cotton wool bud to remove cells from the upper surface. The Transwell® was then suspended in PBS (1 minute) followed by fixation of cells in the fibronectin layer with 3.7% formaldehyde (BDH Laboratories) (15 minutes). The Transwell® was again washed in PBS (1 minute) and then the cells were stained by leaving the well in haematoxylin (Gill's formula; Vector Laboratories) (10-12 minutes). This was followed by one final wash in PBS.

Stained cells were then counted using a microscope. This was done under x200 magnification and the mean number of cells per three high power fields (the central and the two vertically adjacent fields) for each well was calculated.

All experiments were repeated on three separate occasions using four Transwell® wells each time for each CXCL12 ligand concentration.

The results of the migration assays were assessed with the "Student's t test". The level of significance was defined as $p < 0.05$.

CHAPTER 4

ELUCIDATION OF CHEMOKINE RECEPTOR mRNA EXPRESSION (CXCR AND CCR GROUPS) IN PROSTATE CELL LINES

SECTION 4.1

INTRODUCTION AND AIMS

The hypothesis stated that prostate cancer may use chemokine receptor – ligand interactions in the process of metastasis to preferred sites. In order to pursue this hypothesis the first aim was to determine the expression, at mRNA level (messenger ribonucleic acid), of the chemokine receptors in the CXCR and CCR groups in prostate cell lines (the expression of thirteen receptors in total was demonstrated).

Several cell lines were used which were derived from normal prostate epithelium and stroma, primary prostate cancer and metastatic prostate cancers. As all CXCR and CCR receptors and the CXCL12 ligand are expressed by various subsets of human leucocytes, RNA extracted from leucocytes was thus used as a positive control in all experiments involving chemokine receptor (or ligand) expression.

mRNA expression was assessed in the cells using standard reverse transcriptase polymerase chain reaction (RT-PCR). By analysing these initial results and the pattern of expression of the chemokine receptors being screened we would be able to elucidate whether any specific receptor may be important in the metastasis of prostate cancer (eg. over-expression in metastatic cells). Any receptor of interest could then be studied in more detail in further experiments in an attempt to verify the hypothesis.

SECTION 4.2

RESULTS

1) **Chemokine receptors and ligand expression** - the expression of the known chemokine CXCR and the majority of the CCR receptors was demonstrated. This was done to investigate whether there was differential expression of any of these receptors between the benign, primary and metastatic prostate cancer cell lines, which would indicate whether they may have a role in the organ specific metastatic process. In addition, the expression of the CXCL12 ligand was elucidated in the prostate cell lines. The positive controls were leucocytes obtained from human whole blood, which are known to express the chemokine receptors and ligands (refer to chapter 1). A negative control was routinely used for all assays to confirm the absence of contamination. For these negative controls, RNA was omitted from the RT reaction mixture and the reverse transcription was carried out as described in chapter 3.

As Muller A et al 2001 had shown (using real-time quantitative PCR techniques) there were high levels of CXCR4 RNA in the MDA-MB-231 breast cancer cell line, we performed standard RT-PCR to confirm these results with a view to using these cells as a positive control in experiments related to CXCR4 expression.

Therefore following agarose gel electrophoresis of amplified PCR products, starting mRNA quantitation of chemokine receptors was estimated initially by visual comparison of band intensities (real-time quantitative PCR would later be performed for any receptors of interest). Several different patterns of receptor expression were observed, which are shown in figures 4.1a - n and summarized in table 4.1:

- receptor mRNA undetectable in all cell lines (CXCR5, CCR3, CCR7, CCR8)

- receptor detected at low/ very low levels in only one metastatic cell line (CXCR1, CXCR3, CCR2, CCR9)
- expression at low/ very low concentrations in one or more malignant and benign cell lines (CXCR2, CCR1, CCR5, CCR6)
- upregulation of receptor expression with high/ moderate levels in metastatic cells (in addition to the stromal cell cultures S2.13) and very low or no detectable mRNA in the primary prostate and benign epithelial cell lines (CXCR4).

Importantly, it was noted that there was no detectable CXCR4 expression in the breast ductal carcinoma cell line MDA-MB-231.

CXCL12 ligand mRNA was not detected in any of the prostate cell lines.

Figures 4.1a – n:

All the images in this figure are of agarose gels viewed on an ultraviolet transilluminator and captured using the Gel doc system (Quantity One Software, Biorad Ltd, UK).

The images demonstrate the expression of CXCR and CCR chemokine receptors and CXCL12 ligand in cell lines using standard RT-PCR performed at 35 cycles. A 1kb DNA ladder was used.

Lane 1 – no RNA control, 2 – DU145, 3 – LNCaP, 4 – PC3, 5 – 1542 CPT3X, 6 – 1542 NPTX, 7 – Pre 2.8, 8 – S2.13, 9 – leucocytes, 10 – MDA-MB-231

Figure 4.1a

CXCR1 and GAPDH Expression

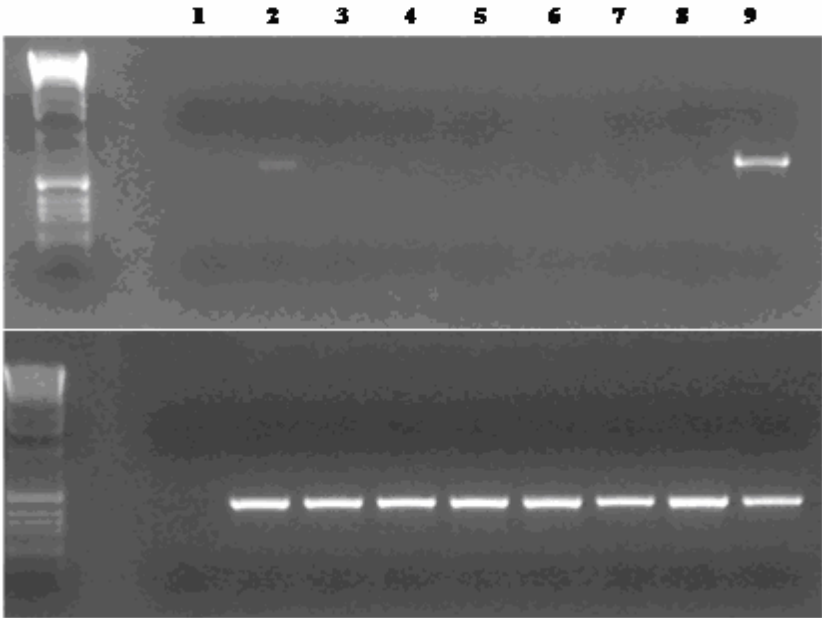


Figure 4.1b

CXCR2 and GAPDH Expression

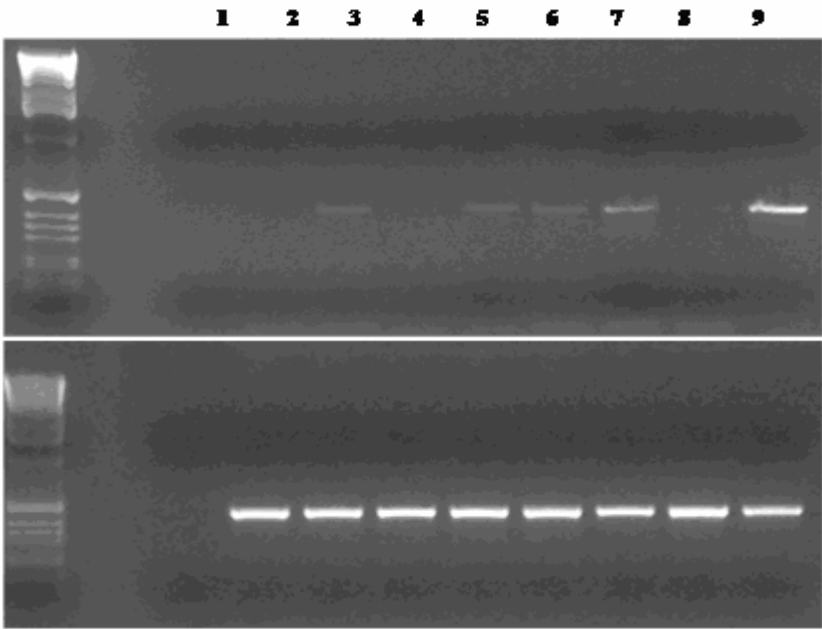


Figure 4.1c

CXCR3 and GAPDH Expression

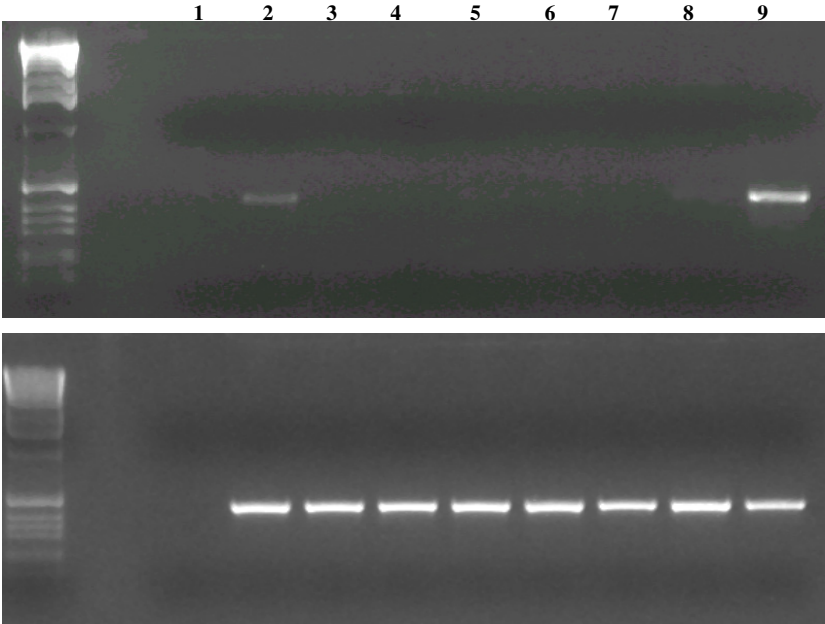


Figure 4.1d

CXCR4 and GAPDH Expression

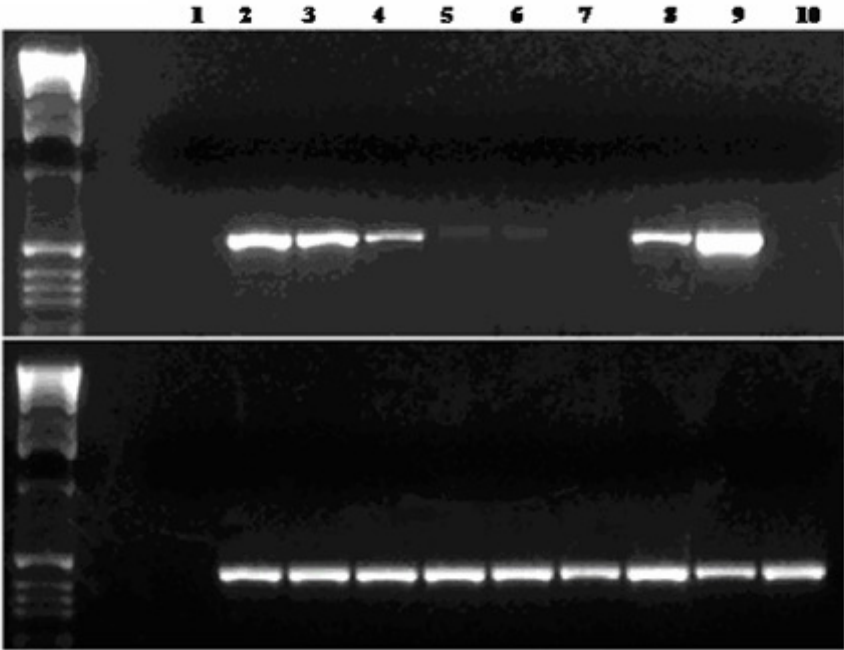


Figure 4.1e CXCR5 and GAPDH Expression

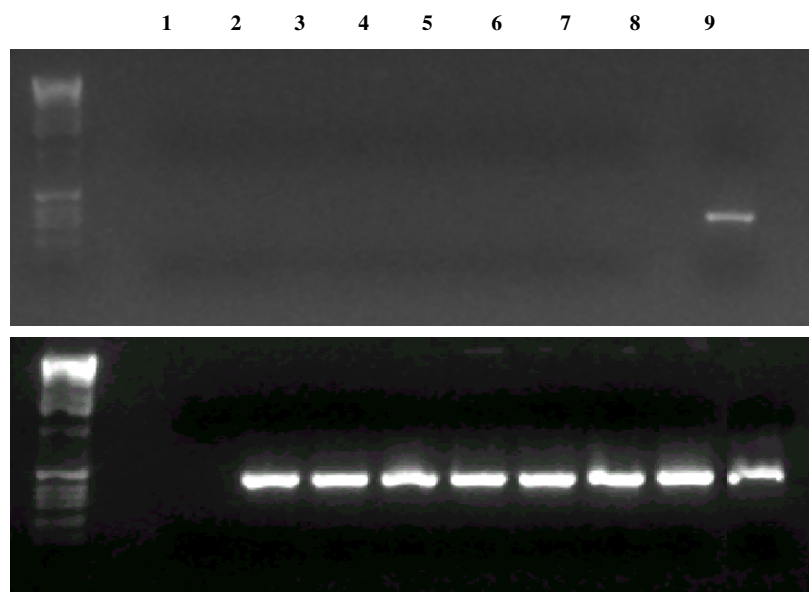


Figure 4.1f CCR1 and GAPDH Expression

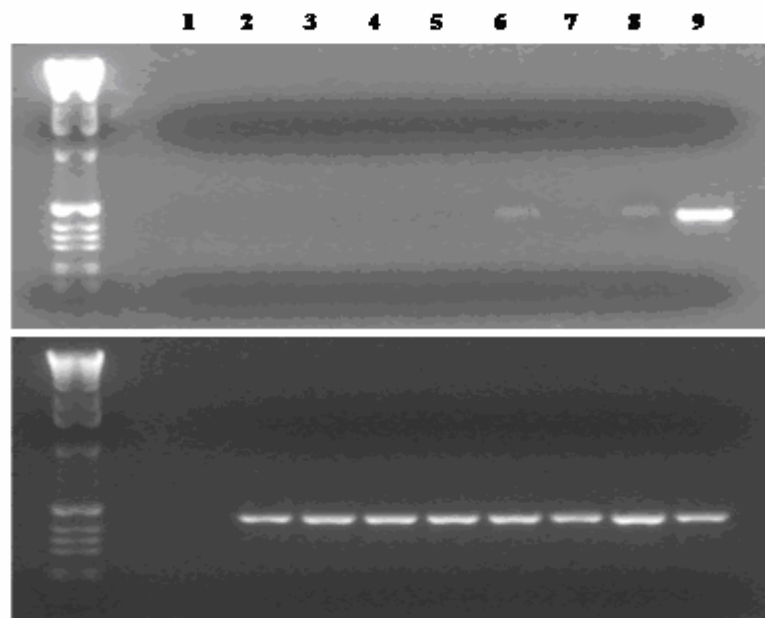


Figure 4.1g **CCR2 and GAPDH Expression**

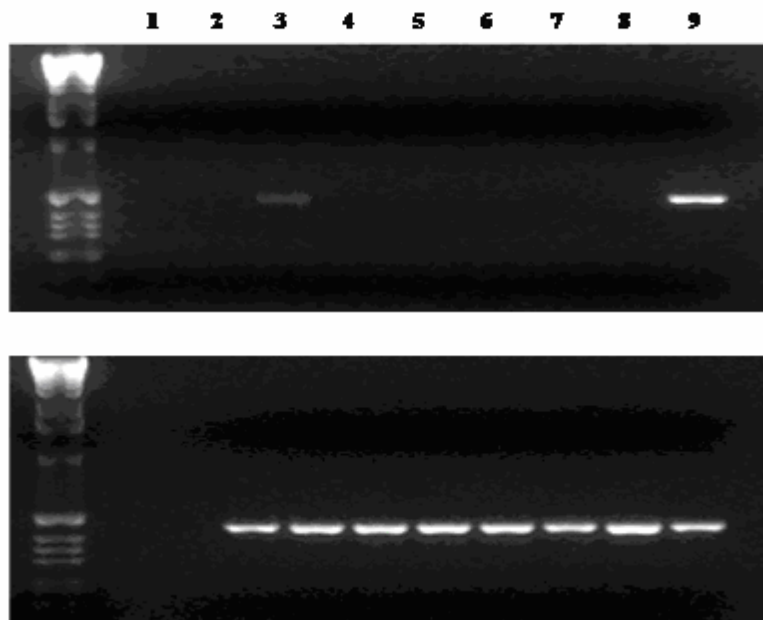


Figure 4.1h **CCR3 and GAPDH Expression**

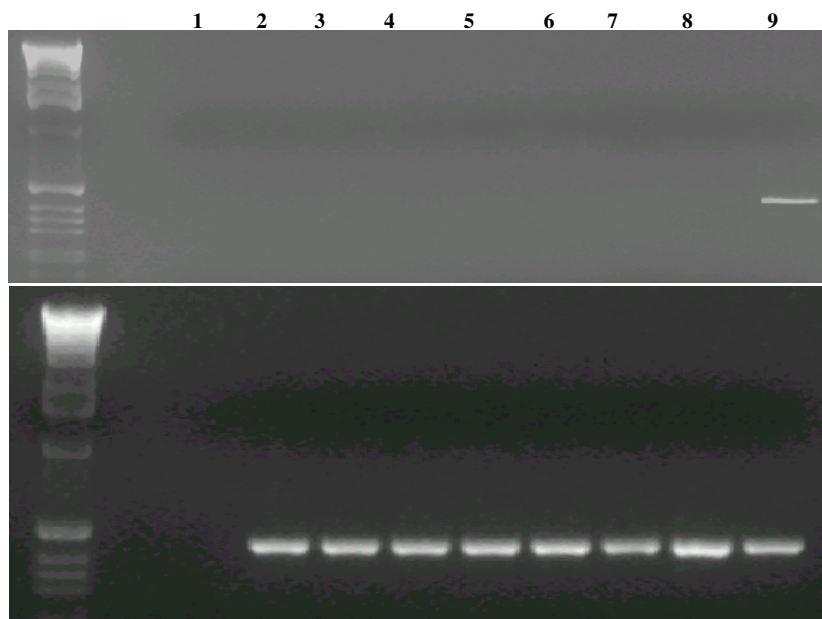


Figure 4.1i **CCR5 and GAPDH Expression**

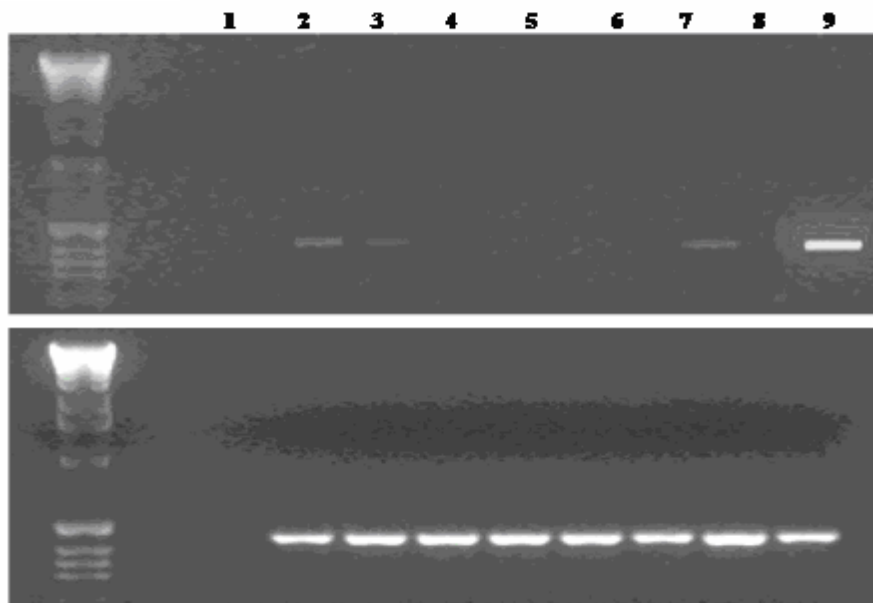


Figure 4.1j **CCR6 and GAPDH Expression**

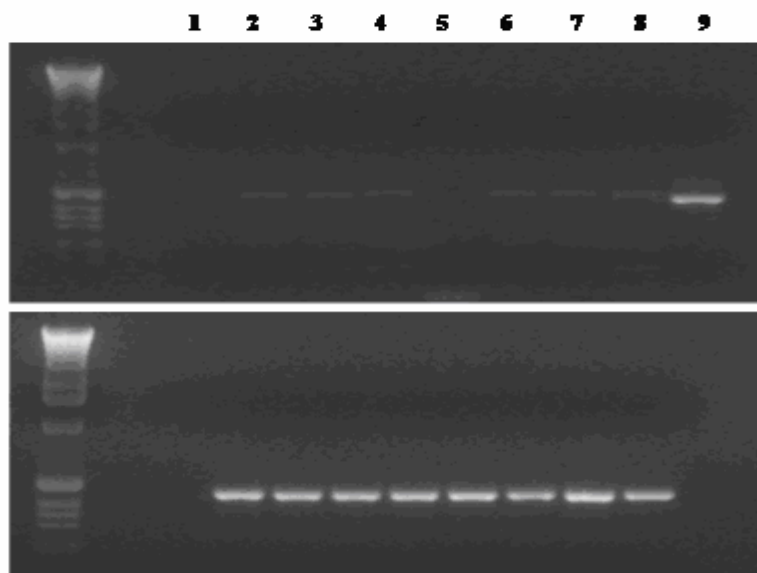


Figure 4.1k

CCR7 and GAPDH Expression

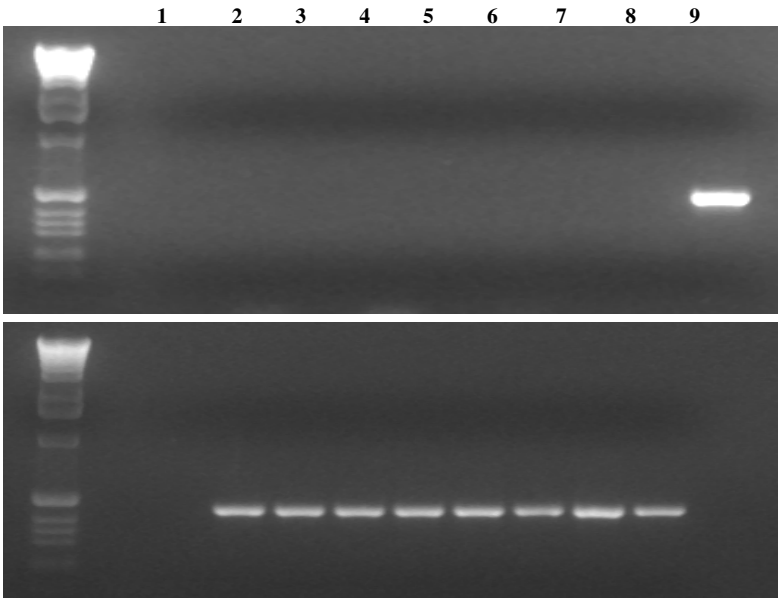


Figure 4.1L

CCR8 and GAPDH Expression

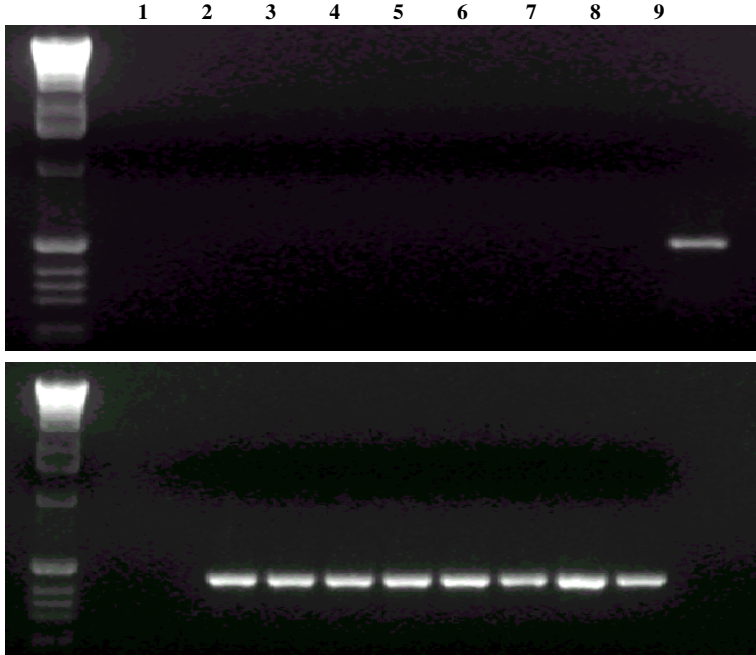


Figure 4.1m

CCR9 and GAPDH Expression

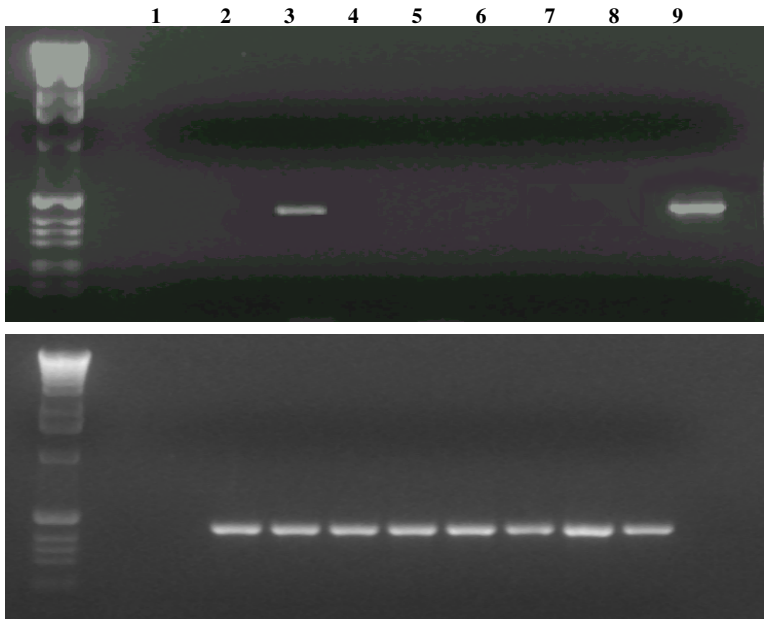


Figure 4.1n

CXCL12 and GAPDH Expression

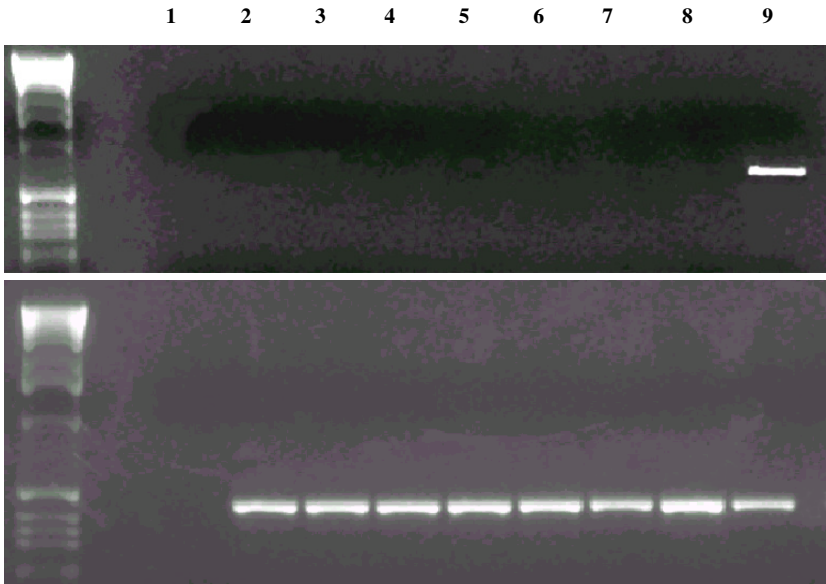


Table 4.1: Summary of CXCR and CCR receptor and CXCL12 ligand expression observed in cell lines.

This was estimated by visual comparison of band intensities on agarose gel electrophoresis of amplified PCR products shown in figure 4.1a - n.

VL - very low expression, L – low expression, M – moderate expression, H – high expression, empty box - no detectable expression, nt – not tested.

	Cell lines							
	DU145	LNCaP	PC3	1542 CPT3X	1542 NPTX	PRE 2.8	S2.13	MDA- MBA-231
CXCR1	VL							nt
CXCR2		VL		VL	VL	L		nt
CXCR3	L							nt
CXCR4	H	H	M	VL	VL		M	
CXCR5								nt
CCR1					VL		VL	nt
CCR2		VL						na
CCR3								nt
CCR5	L	VL				L		nt
CCR6	VL	VL	VL		VL	VL	VL	nt
CCR7								nt
CCR8								nt
CCR9		L						nt
CXCL12								nt

2) **Sequencing of CXCR4 receptor** – for the leucocyte positive control and the cell line DU145, we extracted and purified the CXCR4 PCR product from the agarose gel and subsequently used it in sequencing reactions. This sequencing was done to ensure the correct product was being amplified. A representative electropherogram is shown in figure 4.2.

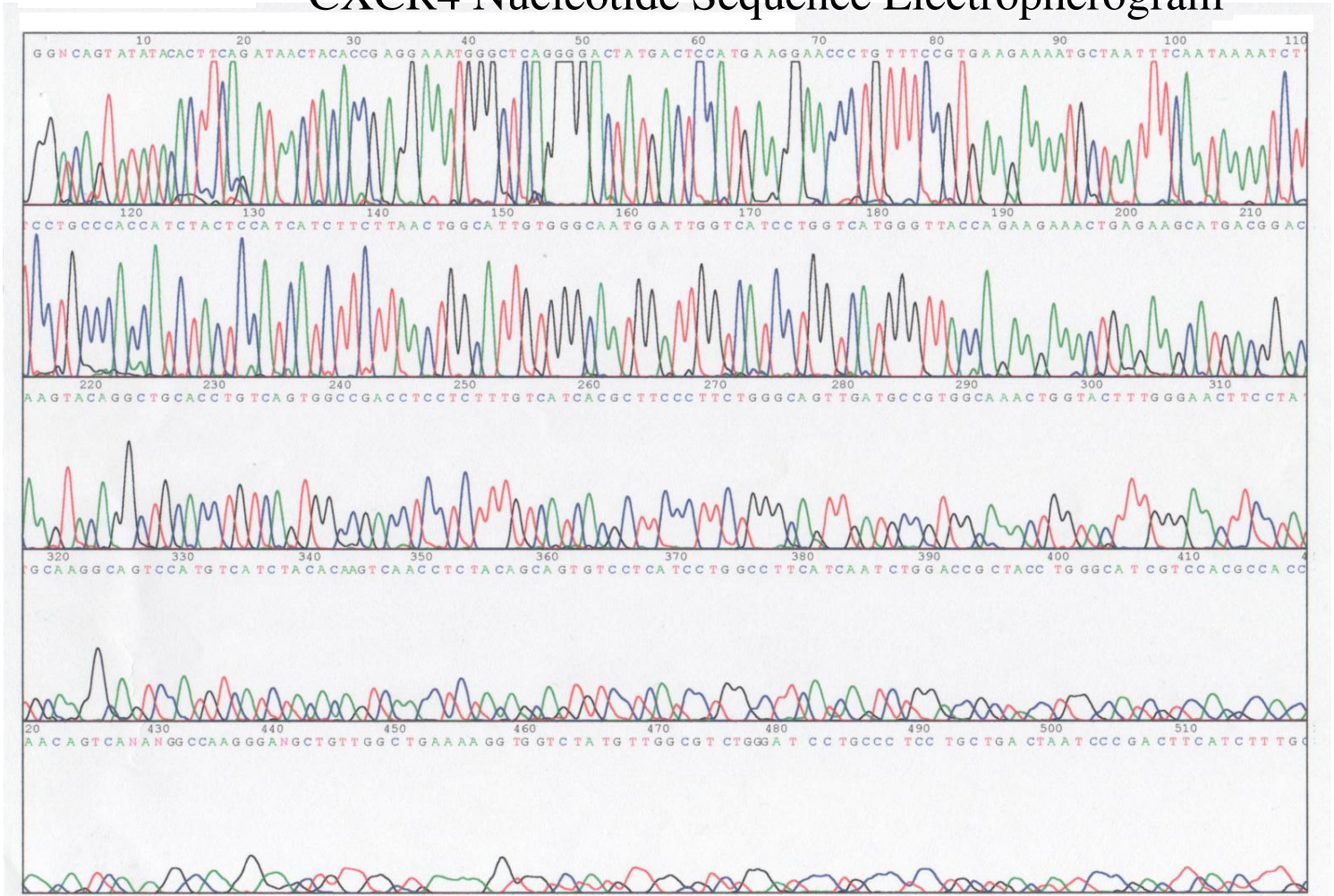
Using the NCBI BLASTN programme, which compares a nucleotide “query” sequence against a nucleotide sequence database, we confirmed that this sequence in figure 4.2 (using a region of 416 nucleotide bases) corresponded to that of human CXCR4 mRNA transcript variant 2 (this only differs from transcript variant 1 by encoding a CXCR4 isoform with a shorter N-terminus, Gupta SK and Pillarisetti K 1999). This gene is located on chromosome 2q21. The bit score and expectation (e) - value were 793 and 0 respectively (derived from BLASTN search), suggesting that it is extremely improbable that this exact alignment occurred by chance alone. There was no evidence of any mutations in this section of the DU145 CXCR4 cDNA sequence.

Figure 4.2: Nucleotide sequence electropherogram obtained by extracting the CXCR4 PCR product from an agarose gel using the DU145 cell line. A similar electropherogram was obtained using the CXCR4 PCR product from leucocytes. Using the NCBI BLASTN programme, we confirmed that this sequence corresponded to that of human CXCR4 mRNA (transcript variant 2).

Note that the automated sequencing and production of this nucleotide sequence electropherogram was performed by a colleague scientist at the Ludwig Institute, UCL.

Figure 4.2

CXCR4 Nucleotide Sequence Electropherogram



SECTION 4.3

DISCUSSION

These results demonstrated that the CXCR4 receptor is upregulated particularly in metastatic prostate cancer cell lines (DU145, LNCaP, PC3) as compared with prostate cancer cell lines derived from a primary tumour (1542 CPT3X) and those originating from normal prostate epithelium (1542 NPTX, Pre 2.8) (figure 4.1d). It appeared from the results that presence of the androgen receptor was not related to CXCR4 mRNA expression as on the agarose gels DU145 and LNCaP were observed to have high CXCR4 mRNA levels whereas PC3 expressed moderate levels (DU145 and PC3 do not express androgen receptor in contrast to LNCaP cells which do). Of note is that it has been recently demonstrated that androgens increased the levels of both CXCR4 mRNA and functional protein in LNCaP prostate cancer cells [Frigo DE et al 2009].

The cell line S2.13 established from stroma derived from a non-malignant prostate also expressed CXCR4 mRNA at moderate levels (figure 4.1d) – this is in accordance with fibroblast chemokine receptor expression in other tissues [Bourcier T et al 2003, Eck SM et al 2009, Franco OE et al 2010, Mishra P et al 2010] where chemokine receptors and their ligands are thought to be associated in the control of stromal cell proliferation, viability or differentiation.

It was surmised that the CXCR4 receptor, in a similar manner to breast cancer as observed by Muller A et al 2001, may play a significant role in the directional migration of metastatic prostate cancer cells to specific organs and further experiments were performed to clarify this (chapters 4, 5 and 6). Also, by extracting and sequencing the CXCR4 PCR product from the agarose gel for the leucocyte positive control and the cell

line DU145, we ensured that the correct product was being amplified with no evidence of any mutations in this section of the DU145 CXCR4 cDNA sequence.

In our results, the pattern of expression of the remaining CXCR and CCR receptors did not suggest a very significant role for their involvement in the metastasis of prostate cancer. However, the results did demonstrate that mRNA of CXCR3 and CCR9 was observed at low levels in only the metastatic cell lines DU145 and LNCaP respectively (figures 4.1c and 4.1m). The CXCR3 receptor has not previously been shown to be involved in prostate cancer progression but has been noted to be involved in the organ specific metastasis of human melanoma [Singh S et al 2009b], colon cancer [Cambien B et al 2009] and osteosarcoma [Pradelli E et al 2009]. However, Singh S et al 2004b have established that functional CCR9 is expressed by LNCaP and is associated with increased chemotaxis of these cells via its ligand CCL25.

After it was noted that CXCR4 receptor mRNA levels were elevated particularly in DU145, LNCaP and PC3 cells, expression of its ligand, CXCL12, was demonstrated. However, CXCL12 mRNA was not expressed in any of the cell lines (figure 4.1n), signifying that this ligand does not have an autocrine or paracrine effect on the regulation of growth and progression in these cells. This is in contrast to a variety of tumour cell lines (already discussed in the introduction) where chemokines have been shown to be involved in stimulating cell proliferation in vitro and in vivo via an autocrine or paracrine pathway [Araki K et al 2009, Hussain F et al 2010, Lo BK et al 2010, Raychaudhuri B and Vogelbaum MA 2010, Sauv e K et al 2009]. Also of interest is that autocrine production of CXCL12 by primary tumours has been shown by some investigators to be deleterious to the formation of metastasis [Gilbert DC et al 2009, Mirisola V et al 2009].

It is proposed that this is due to a combination of the loss of CXCL12 gradients that might otherwise attract cells away from the primary tumour and also saturation of the CXCR4 receptor through autocrine CXCL12 production, which may reduce chemotaxis towards CXCL12-releasing metastasis target tissues thus decreasing the number of metastases formed. As mentioned in chapter 1, CXCL12 ligand has, in fact, been observed in several studies to be constitutively expressed by stromal cells in tissues which are the preferred site of prostate cancer metastasis, with highest expression in bone marrow (fibroblasts, osteoblasts, endothelial cells), lymph nodes, lung, and liver and markedly lower expression levels in the small intestine, skin and skeletal muscle [Bradstock KF et al 2000, Imai K et al 1999, Muller A et al 2001, Ponomaryov T et al 2000, Sun YX et al 2005, Taichman RS et al 2002, Zou YR et al 1998].

As Muller A et al 2001 had established, using real time quantitative PCR, that CXCR4 mRNA was expressed at significant levels in the breast ductal carcinoma cell line MDA-MB-231, we had intended to use these cells as a positive control in this and further experiments related to CXCR4 expression and functionality. However, using RT-PCR we were not able to confirm the expression of CXCR4 mRNA in the MDA-MB-231 cell line (obtained from Michael O'Hare at University College London) (figure 4.1d). An email was sent by Professor J. Masters to the authors of the paper and Dr A. Zlotnik, the senior author, replied that their MDA-MB-231 cells had been obtained from a colleague at Schering-Plough who had selected them on the basis of their potent metastatic potential *in vivo*. Importantly, Dr Zlotnik agreed that other sources of these breast cancer cells, eg. The American Type Culture Collection (ATCC), were cells with low to no CXCR4 expression. Therefore, in these and further experiments, RNA extracted from

leucocytes was used as a positive control as all CXCR and CCR receptors and the CXCL12 ligand are expressed by various subsets of human leucocytes (the evidence for this has been reviewed in chapter 1).

Prostate cell lines had been used in the experiments in this chapter as in vitro models of human prostate cancer or benign tissue and on the assumption that cell lines reflect the genotypic and phenotypic characteristics of in vivo prostate malignancy/benign tissue in humans. There are several advantages to using cell lines including the fact that they are easy to handle and represent an unlimited self-replicating source that can be grown in almost infinite quantities. In addition, they exhibit a relatively high degree of homogeneity and are easily replaced from frozen stocks if lost through contamination. Importantly, cancer cell lines are free of contaminating stromal cells or other non-malignant cells. Additionally, cell lines are generally good models of the characteristics of in vivo human neoplasms retaining the properties of the cancer of origin with limitations mainly occurring if they are handled incorrectly. One problem that can arise is that cell lines evolve as they are grown continuously over a large number of passages. In fact, genotypic and phenotypic variants constantly appear in the cancer cell line populations, and selection occurs of those with superior growth properties. This may change the characteristics of a cell line drastically. Also this genetic instability can occur due to the uncontrolled passing of cells between laboratories and their exposure to different environments (eg. media, sera, trypsin, carbon dioxide levels, humidity temperature). The solution to this is that the cells should not be grown indefinitely and passed in an uncontrolled manner between laboratories. Adequate frozen stocks of each cell line should be produced, and users should return to frozen stocks at regular intervals.

If this is done the cell lines retain most of the features of the cancers from which they were derived [Masters JR 2000].

Also cross-contamination between cell lines is a persistent problem and often results in scientific misrepresentation. It has been estimated that 17 - 36% of cell lines are of a different origin or species to that claimed [Stacey GN 2000]. Cross-contamination can result from poor culture technique when two cell lines accidentally get into the same culture. After a few passages, there is no trace of the slower-growing cell line, and it has been completely displaced by the faster-growing cell line. Also, cross-contamination can occur due to clerical error - mislabelling of growing cells or frozen stocks. It is suggested that as an essential quality control, all cell lines should be short tandem repeat (STR) profiled [Barallon R et al 2010, Masters JR et al 2001].

Mycoplasmal infection of cell lines can also occur but this can be prevented by regular checking of laboratory cell stock with simple tests.

However, in our laboratory, cells in culture underwent a maximum of ten passages before a return to frozen stock and regular quality control measures were implemented. Thus we infer that the cell lines used in our experiments were representative models of *in vivo* human neoplasms or benign tissue. Consequently results obtained from the prostate cell lines could be correlated to human tissue *in vivo*.

CHAPTER 5

QUANTITATION OF CXCR4 mRNA EXPRESSION IN CELL LINES AND PATIENT PROSTATE TISSUE SAMPLES

SECTION 5.1

INTRODUCTION and AIMS

Conventional RT-PCR had demonstrated that levels of CXCR4 receptor mRNA were relatively high in the metastatic prostate cell lines DU145, PC3 and LNCaP, in comparison to those cell lines derived from primary prostate tumour (1542 CPT3X) and normal prostate epithelium (1542 NPTX and Pre 2.8). The first aim in this chapter was to accurately quantitate and compare CXCR4 mRNA expression between the individual cell lines. Additionally, patient prostate RNA samples, acquired by extracting RNA from laser microdissected benign and malignant areas within radical prostatectomy specimens, had been provided by H. Klocker at the University of Innsbruck, Austria. Thus, our aim was also to quantitate CXCR4 mRNA levels in these primary prostate cancer specimens and benign human prostate tissue samples.

In the cell line mRNA studies, using conventional RT-PCR in Chapter 4, each chemokine receptor RT-PCR reaction was performed in conjunction with a GAPDH control. This was done not just to confirm the presence of amplifiable DNA in samples, but also to confirm similar starting concentrations of cDNA (and therefore indirectly RNA) template between samples as GAPDH PCR was performed at a number of cycles during which amplification was linear (i.e. before the plateau phase was reached for the reaction; for more details of this refer to chapter 2 and chapter 3). Therefore, following agarose gel electrophoresis of amplified PCR products, relative starting mRNA quantitation of chemokine receptors was estimated by visual comparison of band intensities. However, this visual quantitation is not accurate. More precise agarose gel quantitation can be achieved by densitometric measurement of band intensity.

Unfortunately, this technique can also be prone to error (eg. variability in ethidium bromide staining with gel concentration and thickness and DNA quantities $\leq 10\text{ng}$). Subsequently, in order to quantitate CXCR4 mRNA levels in cell lines, and also in patient samples, we used a real-time quantitative PCR assay (TaqMan).

SECTION 5.2

RESULTS

a) Optimisation

i) Optimisation of CXCR4 primer concentrations

By independently varying CXCR4 forward and reverse primer concentrations, the concentrations that provide optimal assay performance can be identified. Primers are always in large molar excess during the exponential phase of PCR amplification and the purpose of this procedure is to determine the minimum primer concentrations giving the maximum ΔR_n . By spanning a concentration range of 50nM – 900nM solutions for each primer, the most favourable primer concentrations were identified. The primer concentrations used in the primer optimisation matrix are shown in table 5.1.

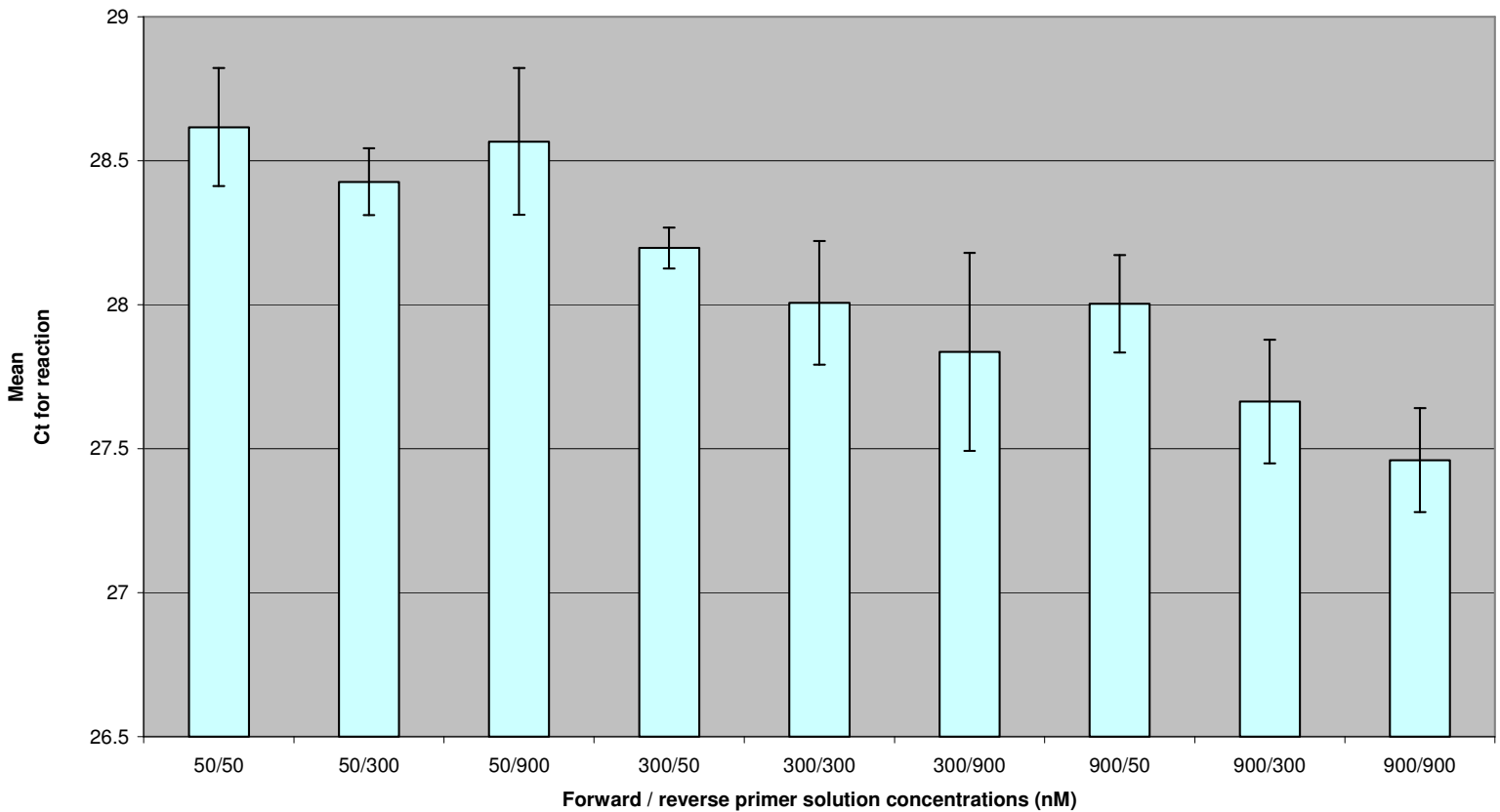
Table 5.1: Combinations of CXCR4 forward and reverse primer concentrations for optimisation (all primer concentrations are nM solutions)

50 forward 50 reverse	50 forward 300 reverse	50 forward 900 reverse
300 forward 50 reverse	300 forward 300 reverse	300 forward 900 reverse
900 forward 50 reverse	900 forward 300 reverse	900 forward 900 reverse

The mean Ct value for each triplicate reaction was calculated and is presented graphically in figure 5.1.

Figure 5.1: Optimisation of CXCR4 primer concentrations. By spanning a range of concentrations for forward and reverse primers the most favourable primer concentrations were identified. The mean Ct +/- SD is shown for each reaction. The 300 nM reaction solution of both forward and reverse primers provided an economical as well as an acceptably efficient reaction (mean Ct 28.01 +/- 0.21).

Figure 5.1 OPTIMISATION OF CXCR4 PRIMER CONCENTRATIONS



The reaction with the lowest Ct value was the most efficient i.e. that containing 900nM of both forward and reverse primers (mean Ct - 27.46). However, as this constituted a relatively large volume of each primer solution we decided to use the 300nM concentrations of both primers as this was both economical and provided an acceptably efficient reaction (mean Ct 28.01).

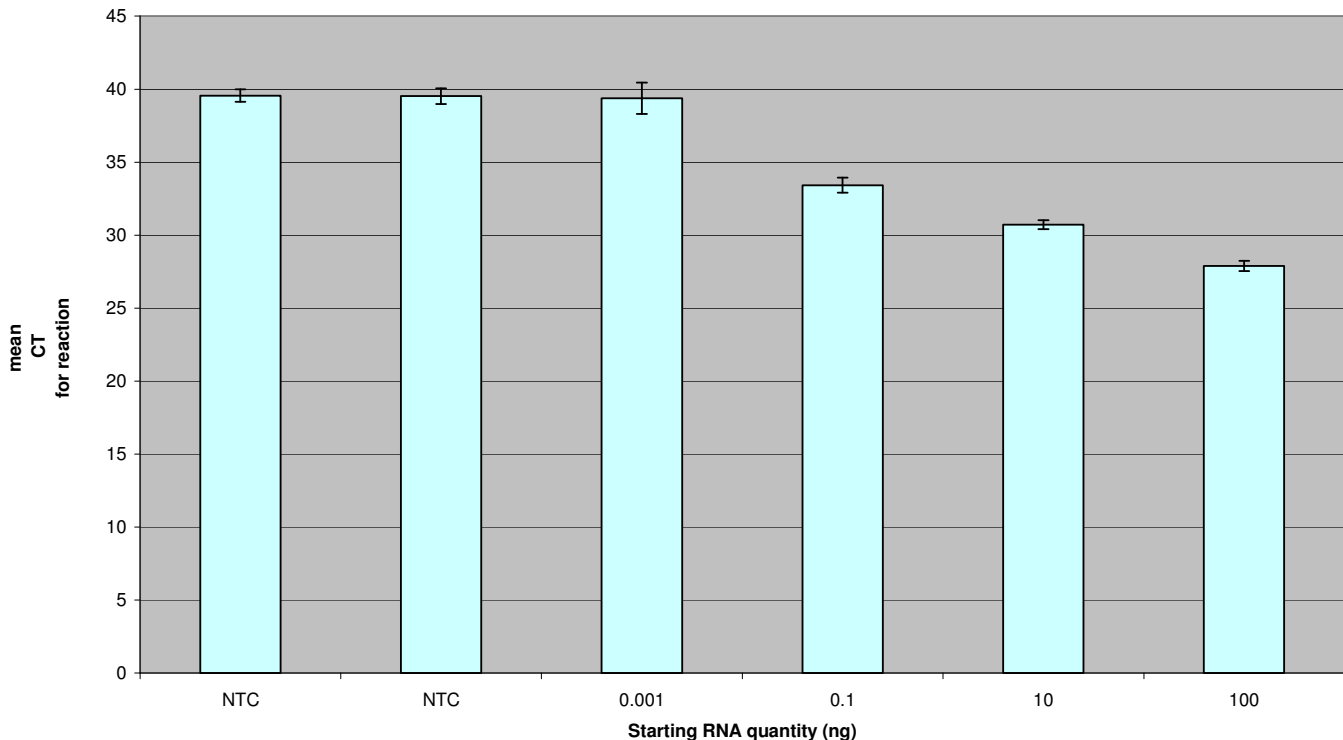
It was not necessary to optimize probe concentrations.

ii) Optimisation of starting RNA quantity

The mean Ct value for each triplicate reaction, using varying quantities of starting RNA, was calculated and is presented graphically in figure 5.2. The reaction did not progress with a starting RNA quantity of 0.001ng, as its mean Ct value of 39.38, was similar to that of the two no template controls (NTC), which contained no cDNA (39.56 and 39.53). At 0.1, 10 and 100ng of RNA the reaction did proceed with the latter having the lowest mean Ct (27.88). However, in order to conserve the scarce patient mRNA, we decided that 10ng of starting RNA (mean Ct 30.72) was sufficient for use in future experiments as the reaction proceeded efficiently with this starting quantity.

Figure 5.2: Optimisation of starting RNA quantity. The mean Ct +/- SD is shown for each reaction. The target gene does not amplify with a starting RNA quantity of 0.001ng, as its mean Ct of 39.38 is similar to that of the two no template controls (NTC – Cts 39.56 and 39.53). At a starting RNA concentration of 10ng, the reaction proceeds satisfactorily (mean Ct 30.72).

Figure 5.2 OPTIMISATION OF RNA CONCENTRATION



iii) Relative efficiency plot

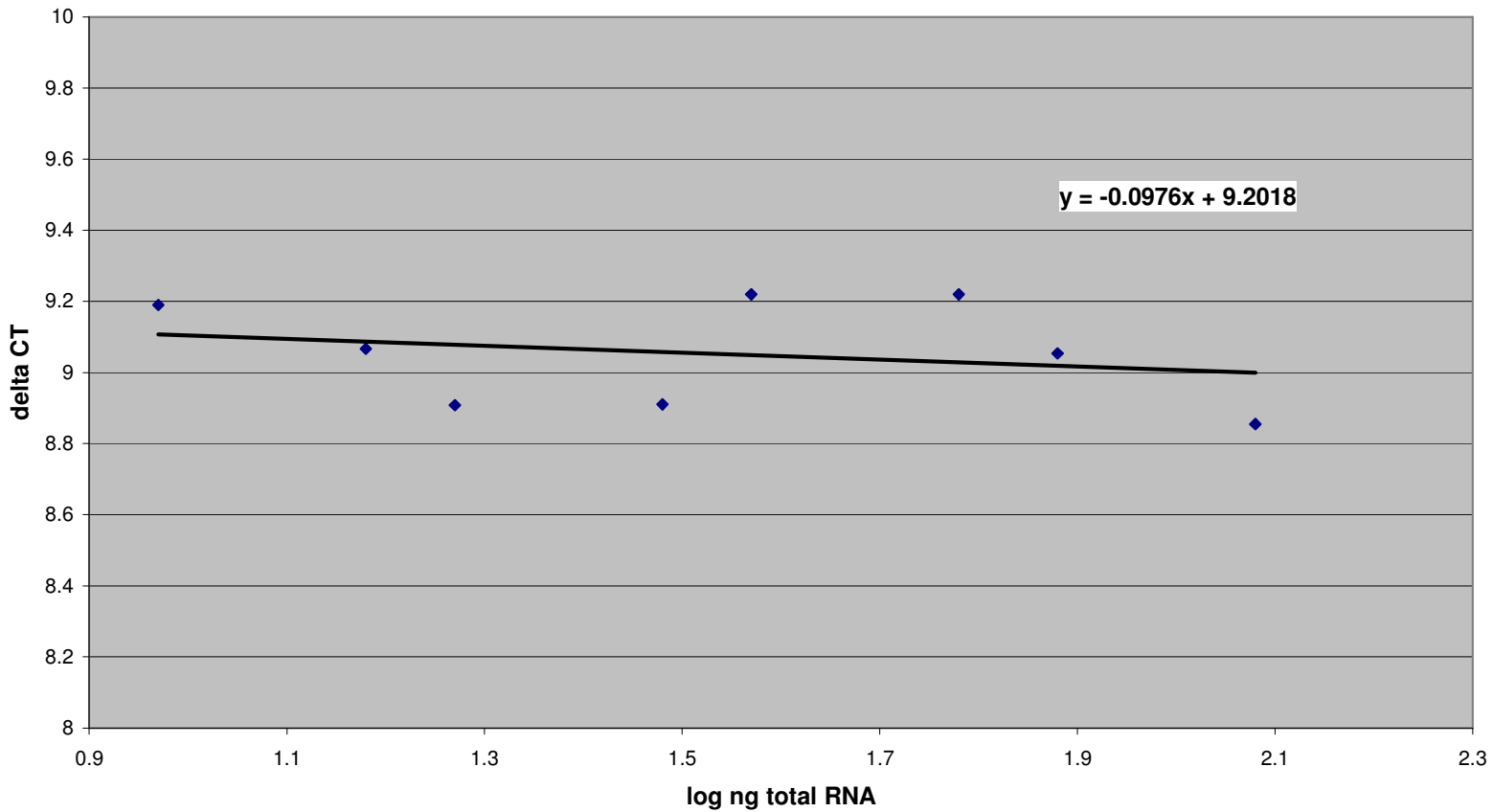
As mentioned earlier (in chapter 2) the comparative Ct method ($2^{-\Delta\Delta C_t}$) can only be used if the amplification efficiencies of the target (CXCR4) and endogenous control (β -actin) are approximately equal. Therefore ΔC_t (where $\Delta C_t = C_t \text{ CXCR4} - C_t \beta\text{-actin}$) must be plotted against varying total RNA levels of both genes to ensure that it stays constant across this range. If the ΔC_t remains constant, the slope of the graph, ΔC_t vs log total RNA, will be <0.1 (i.e. close to zero) and thus reflect similar amplification efficiencies. Figure 5.3 demonstrates that the slope of the line was -0.0976 (close to zero) and this consequently suggested similar amplification efficiencies of both genes (CXCR4 and β -actin) between total RNA quantities of 9.375ng and 120ng and therefore the comparative Ct method could be used.

Figure 5.3:

Relative amplification efficiency scatter plot.

The ΔC_t (where $\Delta C_t = C_t \text{ CXCR4} - C_t \beta\text{-actin}$) is plotted against log total RNA (ng) in the reaction. The mean ΔC_t is shown for each reaction. The best fit straight line is shown (as calculated by the Excel programme). As the slope of the line is close to zero (-0.0976), it suggests similar amplification efficiencies of both genes (CXCR4 and β -actin) between total RNA quantities of 9.375ng and 120ng and thus the comparative Ct method can be used.

Figure 5.3 **_CXCR4 / b-ACTIN RELATIVE EFFICIENCY PLOT**



b) Background to analysis of final results

For CXCR4 mRNA expression analysis, the baseline was manually adjusted on the amplification plots between 3 – 22, when analysing all results. The threshold was manually adjusted to 0.02.

For β -actin mRNA expression analysis the baseline was manually adjusted on the amplification plots between 3 – 16. The threshold was manually adjusted to 0.03.

It should be noted that patient samples were randomly numbered 1-18 and we were blinded as to which samples were benign/ malignant until analysis of relative gene expression was completed.

CXCR4 mRNA expression was normalised in each cell line and patient sample to β -actin expression (i.e. ΔCt calculated, where $\Delta Ct = \text{mean sample Ct CXCR4} \textit{ minus } \text{mean sample Ct } \beta\text{-actin}$). Following this 1542 CPT3X was used as the calibrator and $\Delta\Delta Ct$ calculated where $\Delta\Delta Ct = \Delta Ct \text{ sample} \textit{ minus } \Delta Ct \text{ 1542 CPT3X}$. Finally $\Delta\Delta Ct$ values were used in the equation $2^{-\Delta\Delta Ct}$ to give expression levels of normalised CXCR4 for each sample relative to 1542 CPT3X (see tables 5.2a – c in final results section).

PRE 2.8 and MDA-MB-231 cell lines were not used as the calibrator samples as they showed no detectable CXCR4 mRNA expression as the mean CXCR4 Ct for both was 40, or more, which suggested no (CXCR4) cDNA amplification (it should be noted that cDNA was present in each of these two cell lines as there was satisfactory β -actin amplification – see table 5.2a in results section).

c) Final results

Table 5.2a demonstrates the results and calculation of relative quantitation, using the comparative threshold ($2^{-\Delta\Delta Ct}$) method, for one experiment consisting of three samples for each cell line.

The final results, for three separate experiments, are tabulated in tables 5.2b and 5.2c and presented in graphical form in figures 5.4a and b.

Table 5.2a

This demonstrates calculation of relative quantitation, using the comparative threshold ($2^{-\Delta\Delta Ct}$) method, for one experiment consisting of three samples for each cell line. CXCR4 mRNA expression for each individual cell line, relative to CXCR4 mRNA expression in the cell line 1542 CPT3X, is shown with standard deviation. 1542 CPT3X was used as the calibrator as it had the lowest detectable expression of CXCR4 mRNA. Pre 2.8 and MDA-MB-231 had no detectable CXCR4 expression as the mean CXCR4 Ct for each was 40 cycles (or more), which suggests no cDNA amplification (it should be noted that cDNA was present in each of these two cell lines as there was satisfactory β -actin amplification) Human leucocytes were used as a positive control. Each experiment was repeated in triplicate (i.e. twice more – table 5.2b). The second decimal place of all results is shown.

* ΔCt = mean Ct CXCR4 (target gene) – mean Ct β -actin (housekeeping gene). The standard deviation of the difference is calculated using

the formula:
$$s = \sqrt{(s_1)^2 + (s_2)^2}$$

where S is the new standard deviation,

S₁ is the standard deviation of β -actin expression,

S₂ is the standard deviation of CXCR4 expression.

** $\Delta\Delta Ct$ = ΔCt sample – ΔCt calibrator (i.e. 1542CPT3X). The normalised amount of target gene, CXCR4, is a unitless number that can be used to compare the relative amount of target in different samples. This sample with the lowest detectable expression of CXCR4 was chosen as the calibrator; 1542 CPT3X in our experiments. As this is subtraction of an arbitrary constant, the standard deviation of $\Delta\Delta Ct$ is the same as the standard deviation of the ΔCt value.

*** $2^{-\Delta\Delta Ct}$ This final equation represents the normalised expression of CXCR4 (target gene) in the unknown sample, relative to the normalised expression of the calibrator sample (1542 CPT3X).

Table 5.2a

Cell line	β -actin Ct			Mean β -actin Ct	CXCR4 Ct			Mean CXCR4 Ct	* Δ Ct	** $\Delta\Delta$ Ct	*** $2^{-\Delta\Delta$ Ct
	Sample 1	Sample 2	Sample 3		Sample 1	Sample 2	Sample 3				
LNCaP	20.87	21.13	21.18	21.06 +/-0.16	31.28	31.34	31.36	31.32 +/- 0.04	10.26 +/-0.17	-8.25 +/-0.17	305.14 (270.92-343.67)
DU145	19.61	19.69	19.54	19.61 +/-0.07	28.22	28.19	28.06	28.15 +/-0.08	8.54 +/-0.11	-9.97 +/-0.11	1007.57 (931.38-1089.98)
PC3	19.1	19.02	18.81	18.97 +/-0.14	32.92	33.42	33.11	33.15 +/-0.25	14.17 +/-0.29	-4.34 +/-0.29	20.34 (16.60-24.93)
1542 CPT3X	19.28	19.17	19.31	19.25 +/- 0.07	37.1	37.89	38.33	37.77 +/-0.62	18.52	0	1
1542 NPTX	19.14	19.37	19.42	19.31 +/- 0.14	36.77	36.19	37.02	36.66 +/-0.42	17.35 +/-0.45	-1.17 +/-0.45	2.25 (1.64-3.07)
Pre 2.8	20.02	20.17	20.12	20.10 +/- 0.07	40	40	40	40 +/-0	N/A	N/A	0
S2.13	17.87	18.06	17.99	17.97 +/-0.09	31.7	31.87	31.91	31.82 +/-0.11	13.85 +/-0.14	-4.66 +/-0.14	25.39 (22.93-28.12)
Blood leucocytes	18.44	18.4	18.18	18.34 +/-0.14	23.52	23.48	23.88	23.62 +/-0.22	5.28 +/-0.26	-13.23 +/-0.26	9630.08 (8036.26-11540.01)
MDA-MB-231	18.33	18.62	18.4	18.45 +/-0.15	40	40	40	40 +/-0	N/A	N/A	0

Table 5.2b:

This shows mean relative CXCR4 mRNA expression in cell lines (with standard deviation) for the three samples run in experiments 1, 2 and 3. The overall mean relative CXCR4 expression and standard deviation were calculated. This same data is also presented graphically in figure 5.4a.

Cell line	First experiment: relative CXCR4 expression	Second experiment: relative CXCR4 expression	Third experiment: relative CXCR4 expression	Overall mean relative CXCR4 expression
LNCaP	408.25 (385.20-432.69)	507.28 (387.80-663.58)	305.14 (270.92-343.67)	406.89 (347.97- 499.98)
DU145	1165.44 (1008.35-1347.01)	1686.71 (1427.66-1992.76)	1007.57 (931.38-1089.98)	1286.57 (1122.46 – 1476.58)
PC3	15.56 (11.69-20.71)	26.84 (22.53-31.97)	20.34 (16.60-24.93)	20.91 (16.94 – 25.87)
1542 CPT3X	1	1	1	1
1542 NPTX	1.67 (1.28-2.17)	2.13 (1.46-3.11)	2.25 (1.64-3.07)	2.01 (1.46 – 2.78)
Pre 2.8	not detected	not detected	not detected	not detected
S2.13	32.97 (28.24-38.49)	37.44 (30.29-46.27)	25.39 (22.93-28.12)	31.93 (27.15 – 37.63)
Blood leucocytes	11558.5 (10483.52-12743.71)	14868.79 (12891.1-17149.9)	9630.08 (8036.26-11540.01)	12019.13 (10470.29 – 13811.21)
MDA-MB-231	not detected	not detected	not detected	not detected

Table 5.2c

Represented here are the results of the mean relative CXCR4 mRNA expression for the laser microdissected patient samples, numbered 1 to 18 (refer to chapter 3, table 3.6).

*Samples derived from primary prostate tumour cells (clinically localized neoplasms); the remaining were from benign prostatic tissue (samples were provided by H. Klocker at the University of Innsbruck, Austria). Histological details of these prostate specimens and patient staging are shown in chapter 3, table 3.6. Calculations were performed in the same way as for table 5.2a. In order to conserve patient RNA for further experiments, only 3 reactions were run in only one experiment for each of the 18 prostate samples. We were not aware as to the derivation of each sample during experiments (i.e. as to which sample was derived from benign or malignant prostate tissue). This same data is also presented graphically in figure 5.4

Table 5.2c

Patient sample	β -actin Ct			Mean β -actin Ct	CXCR4 Ct			Mean CXCR4 Ct	Δ Ct	$\Delta\Delta$ Ct	$2^{-\Delta\Delta$ Ct
	Sample 1	Sample 2	Sample 3		Sample 1	Sample 2	Sample 3				
*1	22.9	22.78	23.41	23.03+/-0.33	29.87	29.44	29.81	29.70+/-0.23	6.67+/-0.40	-11.84+/-0.40	3674.50 (2770.13-4874.12)
2	21.24	21.2	21.27	21.23+/-0.03	29.66	29.4	29.87	29.64+/-0.23	8.40+/-0.23	-10.11+/-0.23	1107.68 (939.19-1306.4)
*3	24.02	24.06	24.02	24.03+/-0.02	32.69	33.31	32.86	32.95+/-0.32	8.92+/-0.32	-9.6+/-0.32	776.04 (621.15-969.56)
4	24.61	24.57	24.49	24.55+/-0.06	33.1	33.2	32.86	33.05+/-0.17	8.49+/-0.18	-10.02+/-0.18	1040.69 (915.37-1183.17)
*5	24.08	23.8	23.94	23.94+/-0.14	31.03	31.01	30.16	30.73+/-0.49	6.79+/-0.51	-11.72+/-0.51	3389.05 (2370.028-4846.22)
6	24.14	24.08	24.01	24.07+/-0.06	30.12	30.29	30.42	30.27+/-0.15	6.2+/-0.16	-12.32+/-0.16	5113.16 (4564.02-5728.37)
*7	21.9	22.09	21.76	21.91+/-0.16	28.89	29.03	29.33	29.08+/-0.22	7.16+/-0.27	-11.35+/-0.27	2616.33 (2155.95-3175.03)
8	22.37	22.36	22.45	22.39+/-0.04	29.54	29.43	29.67	29.54+/-0.12	7.15+/-0.12	-11.36+/-0.12	2640.63 (2413.30-2889.36)
*9	24.2	24.43	24.36	24.33+/-0.11	29.61	29.43	29.51	29.51+/-0.90	5.18+/-0.14	-13.33+/-0.14	10321.27 (9312.14-11439.76)
10	26.08	25.93	25.89	25.96+/-0.10	33.08	32.75	33.14	32.99+/-0.21	7.02+/-0.23	-11.49+/-0.23	2889.62 (2459.24-3395.32)
*11	23.65	23.68	23.52	23.61+/-0.08	29.75	29.45	29.51	29.57+/-0.15	5.95+/-0.18	-12.56+/-0.18	6066.57 (5354.64-6873.16)
12	22.57	22.75	22.35	22.55+/-0.20	28.09	28.26	28.17	28.17+/-0.08	5.61+/-0.21	-12.90+/-0.21	7661.08 (6588.3-8908.53)
13	26.47	26.58	26.47	26.50+/-0.06	34.45	34.05	34.46	34.32+/-0.23	7.81+/-0.24	-10.70+/-0.24	1671.19 (1412.77-1976.88)
*14	21.85	22	21.62	21.82+/-0.19	27.8	27.89	27.64	27.77+/-0.12	5.95+/-0.22	-12.56+/-0.22	6066.57 (5174.39-7112.58)
15	23.21	22.93	23.29	23.14+/-0.18	29.47	29.5	29.68	29.55+/-0.11	6.40+/-0.22	-12.11+/-0.22	4430.74 (3802.68-5162.53)
*16	24.03	24.03	24.1	24.05+/-0.04	31.19	31.18	31.13	31.16+/-0.03	7.11+/-0.05	-11.40+/-0.05	2714.86 (2619.41-2813.80)
*17	22.87	22.76	22.76	22.79+/-0.63	30.03	29.9	30.68	30.20+/-0.41	7.40+/-0.42	-11.11+/-0.42	2215.37 (1652.73-2969.53)
18	21.13	21.3	21.26	21.23+/-0.08	27.72	27.53	27.58	27.61+/-0.09	6.38+/-0.13	-12.14+/-0.13	4513.40 (4116.87-4948.12)

Figure 5.4a and b:

The graphs show relative CXCR4 mRNA expression in prostate cell lines and patient samples using real-time (Taqman) quantitative RT-PCR. These figures are the graphical representation of the data from table 5.2b and table 5.2c. CXCR4 mRNA expression for each sample, including patient samples, are shown relative to 1542 CPT3X (as this cell line had the lowest detectable expression of CXCR4 mRNA). Human leucocytes were used as a positive control. DU145, LNCaP and PC3 had 1287, 407 and 21 times CXCR4 mRNA levels respectively, relative to 1542 CPT3X. The cell line 1542 NPTX, derived from normal prostate epithelial cells, had similar CXCR4 mRNA expression to that of 1542 CPT3X (the former having only twice the quantity) and results for Pre 2.8 are not shown as these cells had undetectable levels of receptor mRNA (similar to MDA-MB-231).

In the laser microdissected patient clinically localized primary tumour samples and patient benign tissue specimens mean relative CXCR4 mRNA expression for tumours was 4205 (range 776 – 10,321); mean relative expression for benign samples was 3542 (range 1040 – 7661). Thus expression in both these two groups was significantly greater than that of the primary prostate cancer cell line 1542 CPT3X.

Figure 5.4a Real time quantitative (Taqman) PCR for prostate cell lines

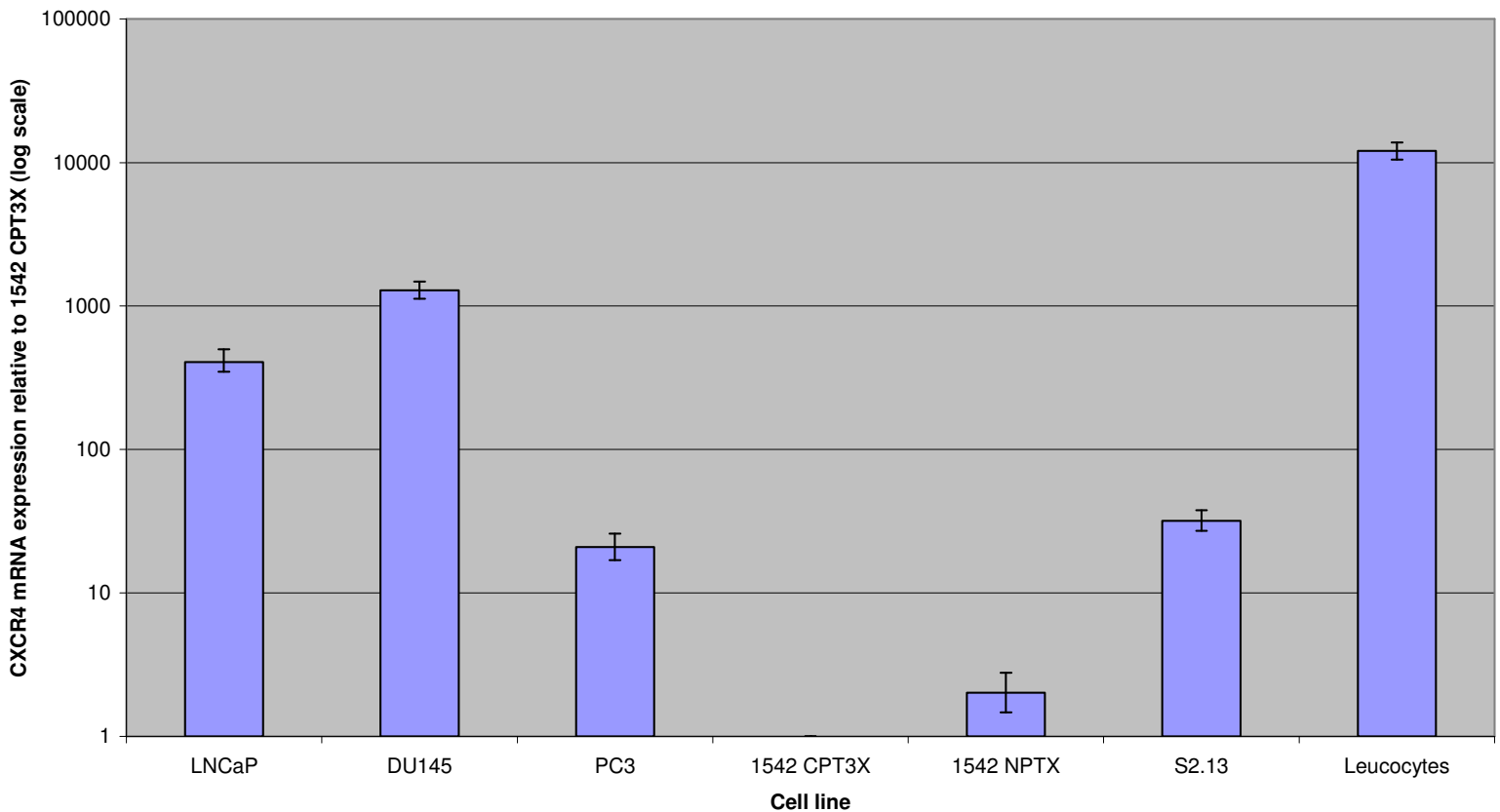
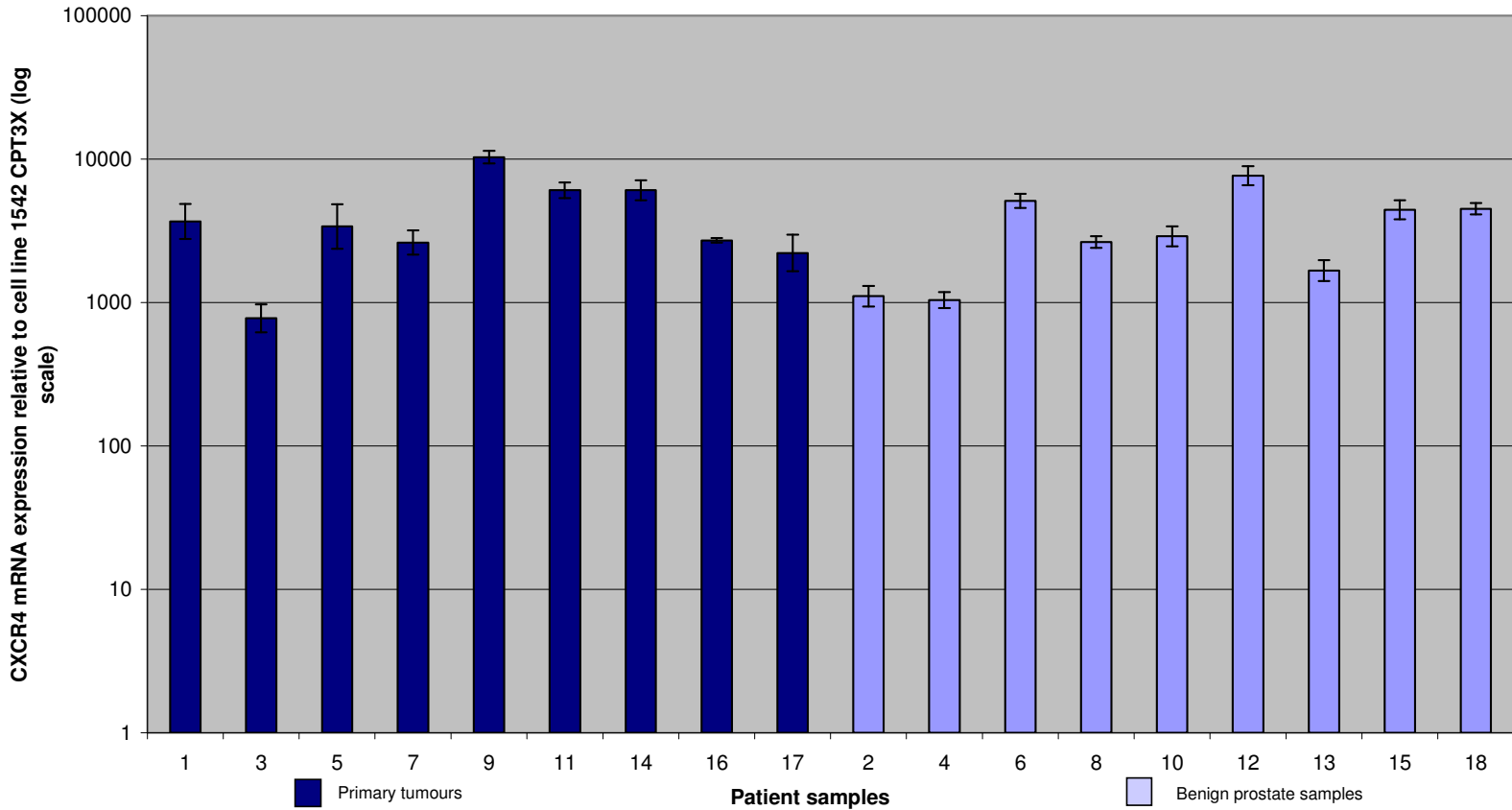


Figure 5.4b Real time quantitative (Taqman) PCR for laser microdissected patient samples



It can be seen from figure 5.4a that highest relative mRNA CXCR4 expression is seen in the positive control sample derived from blood leucocytes (12,019 times that of 1542 CPT3X). Also from figure 5.4a (and table 5.2b) it is obvious that there is great variation in CXCR4 mRNA expression with the metastatic cell lines DU145, LNCaP and PC3 having approximately 1287, 407 and 21 times CXCR4 mRNA respectively, relative to the primary prostate tumour cell line 1542 CPT3X. Additionally, Pre 2.8 had no

detectable CXCR4 expression and 1542 NPTX had a mean relative expression approximately twice that of the 1542 CPT3X. Thus these two cell lines derived from normal prostate epithelial cells, have very little CXCR4 mRNA expression in comparison to all 3 metastatic cell lines but particularly in comparison to DU145 and LNCaP.

In the laser microdissected clinically localized patient primary tumour samples, CXCR4 mRNA expression (mean relative expression for primary tumours was 4205) was higher than that of the metastatic cell lines, DU145, LNCaP and PC3 (mean relative expression 1287, 407 and 21 respectively), and thus significantly greater than that of the primary prostate cancer derived cell line 1542 CPT3X (figure 5.4b).

Benign patient prostate epithelial tissue samples demonstrated similar CXCR4 mRNA levels to the primary tumour samples (mean relative expression 3542 in benign samples). Using the unpaired Student's t test there was no significant difference in CXCR4 gene expression between patient primary prostate tumour samples and benign prostate tissue.

SECTION 5.3

DISCUSSION

Real time quantitative PCR had been used to quantitate CXCR4 mRNA expression in cell lines and patient samples. The results were calculated for all samples (cell lines and human tissue) relative to 1542 CPT3X (the calibrator) as this had the lowest *detectable* level of CXCR4 mRNA expression. It was demonstrated that the 3 metastatic cell lines had significantly greater CXCR4 mRNA expression in comparison to the cells derived from primary tumour (1542 CPT3X) and those of normal prostate epithelial origin. DU145 cells particularly had relatively high levels in comparison even to LNCaP and PC3 (1287, 407 and 21 times respectively that of the calibrator). This large difference in expression between DU145 and LNCaP had not been apparent on visual inspection when using conventional PCR, as both appeared to have comparable band densities on the agarose gel (refer to chapter 4). However, other results from conventional PCR were confirmed as Pre 2.8 and MDA-MB-231 had no detectable CXCR4 mRNA expression and 1542 NPTX and 1542 CPT3X had similar levels (the former only twice that of the latter; both were described as having very low levels on agarose gel electrophoresis). From these cell line results, which confirmed our previous observations using conventional RT-PCR, we could hypothesise that CXCR4 mRNA expression may be related to metastasis of prostate cancer.

Interestingly, laser microdissected clinically localised primary prostate tumour samples (mean relative CXCR4 mRNA expression 4205) and benign prostate epithelial tissue (mean relative CXCR4 mRNA expression 3542) from patients both had CXCR4 mRNA levels much higher than that of DU145 (the cell line expressing the highest levels

of CXCR4 mRNA). Certainly, 1542 CPT3X cells (derived from a primary prostate malignancy) were not representative of primary prostate tumours in vivo as regards quantity of CXCR4 receptor mRNA. Statistically (using the unpaired Student's t test) there was no significant difference in CXCR4 gene expression between patient primary prostate tumour samples and benign prostate tissue. However, Sun YX et al 2003, have suggested that post-transcriptional modification of the CXCR4 receptor plays a major role in regulating protein expression; in fact this group observed that CXCR4 mRNA levels were highest in human BPH tissue but actual protein levels were highest in metastatic prostate tissue (see chapter 8). Therefore in our patient samples, although CXCR4 mRNA levels are high in primary tumour samples and in patient benign tissue specimens, protein expression may be much lower.

Alternatively, if high CXCR4 mRNA levels are translated into high protein expression in clinically localized patient primary tumours, this may be the result of a survival benefit in primary cancer cells expressing this receptor in vivo, and these tumours may be more aggressive and likely to metastasise. Mochizuki H et al 2004 have noted in human prostate tissue that positive expression of CXCR4 protein was an independent and superior predictor for bone metastasis to Gleason sum and Darash-Yahana M et al 2004 demonstrated that high levels of CXCR4 induced a more aggressive phenotype in prostate cancer cells in vivo. Additionally, in vivo CXCR4 expression may promote proliferation and neoangiogenesis in primary tumours leading to rapid local growth. Related to this is the finding that subcutaneously injected prostate cancer cells transfected with CXCR4 grew larger tumours with increased muscle invasion compared with parental cells [Darash-Yahana M et al 2004]. Unfortunately, we were unable to

obtain follow-up details (from Austria) of these patients with primary tumours to investigate whether they relapsed locally or systemically. It is possible that in vivo metastatic cells may express CXCR4 mRNA at even higher levels than primary tumour but we were not able to obtain fresh prostate metastatic tissue from patients, which could be laser microdissected and analysed.

It should, however, be noted that although mRNA levels are high and subsequently the majority of this translated into protein, actual protein levels may still be low due to regulation of cellular protein. As regards CXCR4, it has been demonstrated that this receptor undergoes significant spontaneous endocytosis and that recycling of internalized receptors is not efficient [Tarasova NI et al 1998]. Therefore in the patient samples, or the cell lines derived from metastases, levels of functional protein may be depleted.

It is also possible, although less likely, that primary prostate cancer and/ or benign prostate tissue samples had high CXCR4 mRNA expression because these samples may have contained stromal or other non-cancerous contaminating tissue. Stromal cells are known both in vitro (S2.13 mean relative CXCR4 mRNA expression was 31.93) and in vivo to express high levels of this chemokine receptor [Bourcier T et al 2003, Hosokawa Y et al 2005, Puxeddu I et al 2006].

Consequently, having established CXCR4 mRNA levels, our next goal was to elucidate protein expression of this chemokine receptor.

CHAPTER 6

ELUCIDATION OF CELL MEMBRANE CXCR4 CHEMOKINE RECEPTOR (PROTEIN) EXPRESSION IN PROSTATE CELL LINES

SECTION 6.1

INTRODUCTION AND AIMS

Using conventional RT – PCR followed by real time quantitative PCR, we had established that CXCR4 *mRNA* expression was particularly high in metastatic prostate cell lines DU145, LNCaP and PC3 and significantly lower in those cell lines derived from primary prostate tumour (1542 CPT3X) and normal prostate epithelium (1542 NPTX and Pre 2.8).

However, mRNA expression is a useful but not a consistently reliable predictor of cellular protein levels. For example, transcript and protein concordance in LNCaP has been reported to vary from 32% [Waghray A et al 2001] to 83% [Lin B et al 2005]. There can be several reasons for the poor correlation between the level of mRNA and the level of protein, and these may not be mutually exclusive. First, there are many complicated and varied post-transcriptional mechanisms involved in turning mRNA into protein that are not yet sufficiently well defined to be able to compute protein concentrations from mRNA; second, regulation may actually occur at the protein level eg. short in vivo protein half life or endocytosis of cell surface proteins with inefficient recycling of internalized receptors [latter has been reported in relation to the CXCR4 receptor by Tarasova NI et al 1998]; and/or third, there may be a significant amount of error and noise in both protein and mRNA experiments that limit our ability to get a clear picture.

Levels of protein expression in cells may be established by using various methods including immunohistochemistry, Western blotting or flow cytometry. However, using flow cytometry, one can obtain accurate data for individual cells. Also, the technique has the ability to identify distinct cell populations as defined by their size and granularity, the

capacity to gate out dead cells and additionally one can definitively localize the position of a protein to the cell surface.

Therefore our aim in this section was to quantitate CXCR4 protein expression in each individual cell line and simultaneously confirm that the CXCR4 receptor was expressed on the cell membrane. We achieved these aims by using flow cytometry.

SECTION 6.2

RESULTS

Note that in all experiments a total of 10,000 events were analysed in each sample with data due to dead cells/cell debris and non-specific binding being gated out of the results only when appropriate. All experiments were repeated in triplicate in order to confirm the results and representative histograms and dot plots are shown.

a) Optimisation of conditions

1) Optimisation of cell dissociation

On performing flow cytometry analysis, enzymatic digestion of adherent cells in culture with trypsin presumably resulted in damage to the epitope on the CXCR4 receptor as no binding of primary antibody occurred when trypsin based cell dissociation solution was used. Therefore non-enzymatic cell dissociation solution (Sigma) was used for cell preparation in all experiments.

2) Optimisation of primary antibody isotype

Anti-CXCR4 primary antibodies initially used for flow cytometry analysis, using the DU145 cell line, were poorly reactive for cell membrane CXCR4 receptor detection. In total five primary antibodies were used (see chapter 3, table 3.7a). The results of differential antibody binding (using DU145 cells), using each of these five different primary anti-CXCR4 antibodies, are summarized in table 6.1 with graphical representation, via histograms and dot plots, in figures 6.1a - e.

The increase in the geometric mean fluorescent intensity (GMFI - also known as the geometric mean channel fluorescence), demonstrated on the histograms, is given for each primary antibody in table 6.1. This was derived by:

GMFI with primary anti-CXCR4 antibody minus GMFI in negative control (latter without primary anti-CXCR4 antibody i.e. experiment contains only secondary antibody).

(It should be noted that with log-amplified data the geometric mean is better suited for use, rather than the arithmetic mean, as it takes into account the weighting of the data distribution and is a good indicator of the central tendency of the population).

Additionally the percentage of DU145 cells showing CXCR4 receptor positivity, detected by each antibody, was calculated using the dot plots by:

% of cells in right upper quadrant using primary anti-CXCR4 antibody minus % of cells in right upper quadrant in negative control (latter without primary anti-CXCR4 antibody i.e. experiment contains only secondary antibody; these are cells remaining in the right upper quadrant after subjective insertion of the quadrant gates).

Both of the above calculations are each individually derived from either the histogram or dot plots. The increase in GMFI was a more accurate method of analysing our data (dot plots are a better method for visualizing subpopulations within a specimen).

It can be seen that mouse IgG2b monoclonal antibody clone 44717.111 (R&D Systems) recognized a much greater proportion of cell surface CXCR4 (figures 6.1a - e and table 6.1) than any of the other primary antibodies used, and thus demonstrated greater specificity for binding the CXCR4 receptor. This monoclonal antibody was therefore used in all further experiments for CXCR4 receptor detection in prostate cell lines.

Table 6.1: The results of differential primary antibody binding to the cell membrane CXCR4 receptor in the DU145 cell line using each of five different primary anti-CXCR4 antibodies. The results are derived from figures 6.1a - e. The increase in geometric mean fluorescent intensity (geometric mean channel fluorescence) is relative to the negative control. It can be seen that mouse IgG2b monoclonal antibody clone 44717.111 (R&D Systems) bound to a much greater proportion of cell surface CXCR4.

Antibody	Increase in geometric mean fluorescent intensity (channels)	% of cells demonstrating CXCR4 receptor positivity
Rabbit IgG clone H-118 (Fusin)	15.48	13.16
Mouse IgG2a, κ, clone 12G5	5.87	20.09
Mouse IgG2a clone 44708.111	59.29	60.15
Mouse IgG2b clone 44716.111	32.47	50.44
Mouse IgG2b clone 44717.111	204.56	77.61

Figures 6.1a – e

The data from this figure is summarized in table 6.1.

This figure shows representative flow cytometry histograms and dot plots for the results of differential primary anti-CXCR4 antibody binding to DU145 cells using five different primary antibodies. A total of 10,000 cells were analysed in each sample and no cells were gated out of these results.

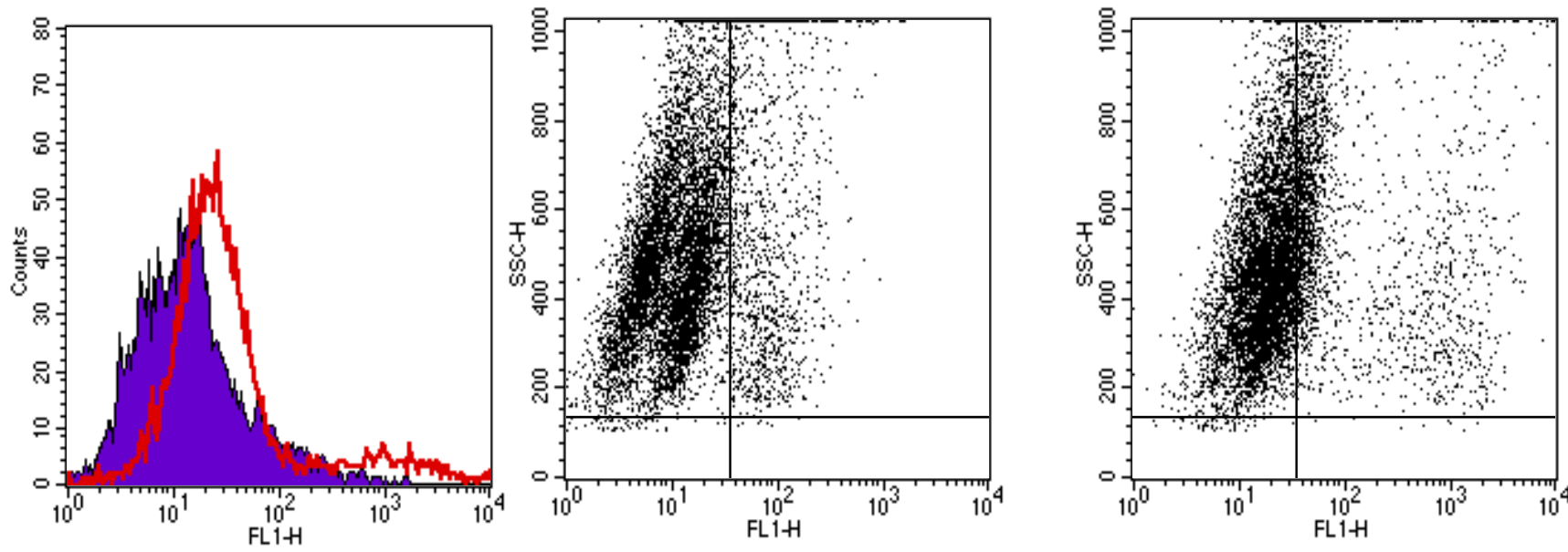
On both the histograms and dot plots the x-axis shows fluorescence intensity (channel number) on 1024 channels encompassing 4-log decades (i.e. logarithmic scale).

On the histograms the y-axis shows cell counts in each channel, whereas on the dot plots, the y-axis shows side scatter intensity - SSC (channel number) on a linear scale.

Quadrant gates were set on the dot plots using the background levels of fluorescence of either the respective unstained negative control (contains only the fluorochrome-conjugated secondary antibody without the primary antibody – figures 6.1a, c, d, e) or fluorochrome isotype matched control population of cells (when a fluorochrome-conjugated primary antibody is used – figure 6.1b). Cells in the right upper quadrant were taken as positive for CXCR4 receptor expression (the percentage of cells in the right upper quadrant in the negative control samples was subtracted out of the final results).

GMFI refers to geometric mean fluorescent intensity (geometric mean channel fluorescence).

Figure 6.1a: Results of flow cytometry using primary anti-CXCR4 antibody IgG clone H-118 (Fusin)



Histogram

Dot plot - negative control
- contains secondary
antibody only

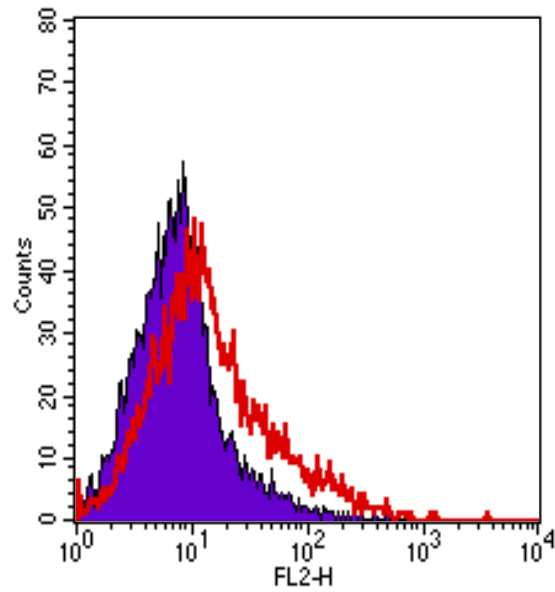
Dot plot -
contains primary and
secondary antibody

■ Negative Control – contains secondary antibody only
— Contains primary and secondary antibody

Increase in GMFI (channels)
15.48

% of cells demonstrating CXCR4 receptor positivity
13.16

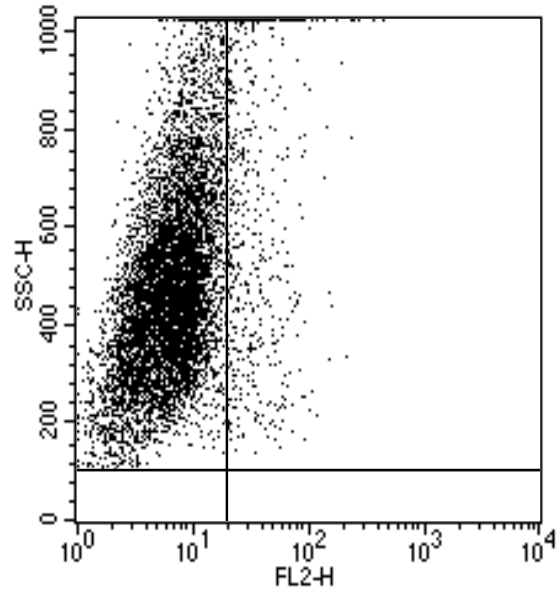
Figure 6.1b: Results of flow cytometry using primary anti-CXCR4 antibody IgG2a, κ , clone 12G5



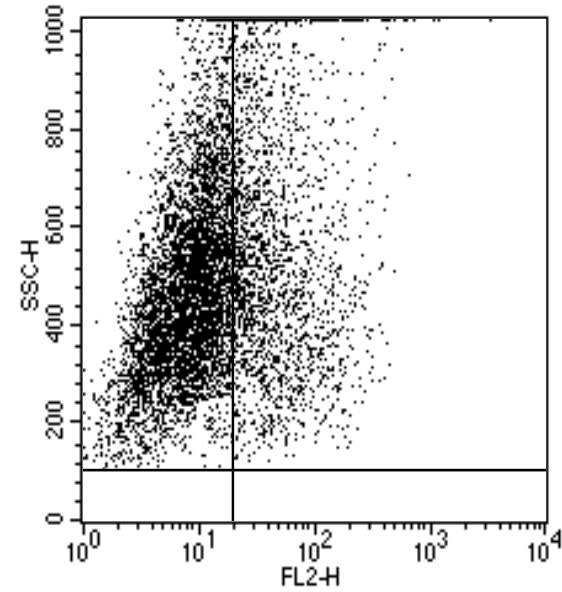
Histogram

- Negative Control – contains non-reactive PE-conjugated isotype control antibody
- Contains PE conjugated primary anti-CXCR4 antibody

Increase in GMFI (channels)
5.87



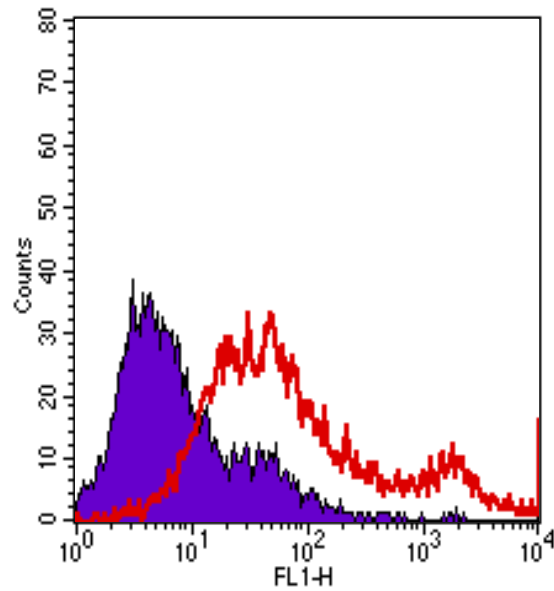
Dot plot - contains non-reactive PE-conjugated isotype control antibody



Dot plot - contains PE-conjugated primary anti-CXCR4 antibody

% of cells demonstrating CXCR4 receptor positivity
20.09

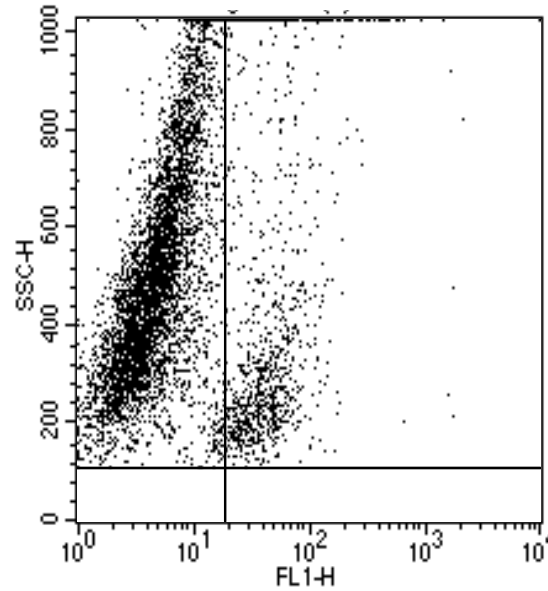
Figure 6.1c: Results of flow cytometry using primary anti-CXCR4 antibody IgG2a clone 44708.111



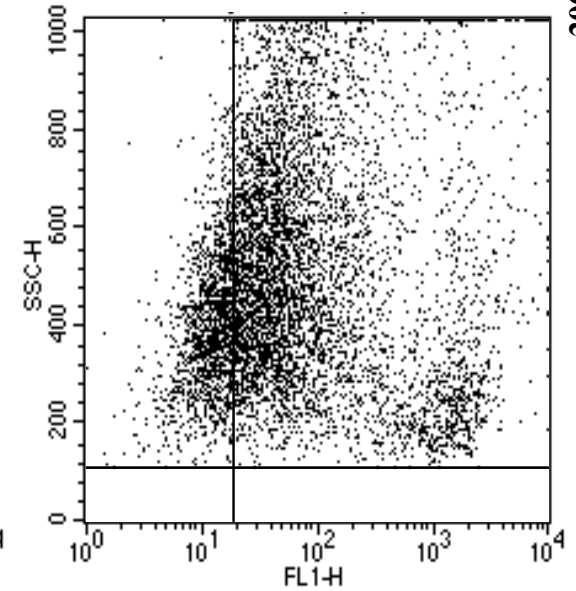
Histogram

- Negative Control – contains secondary antibody only
- Contains primary and secondary antibody

Increase in GMFI (channels)
59.29



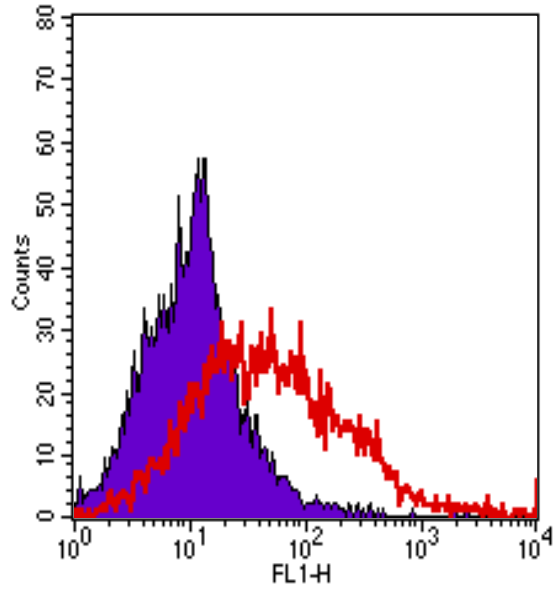
Dot plot - negative control
– contains secondary
antibody only



Dot plot -
contains primary and
secondary antibody

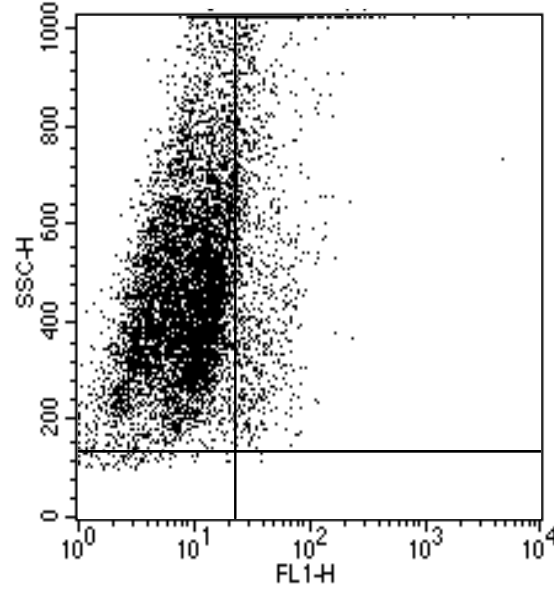
% of cells demonstrating CXCR4 receptor positivity
60.15

Figure 6.1d: Results of flow cytometry using primary anti-CXCR4 antibody IgG2b clone 44716.111

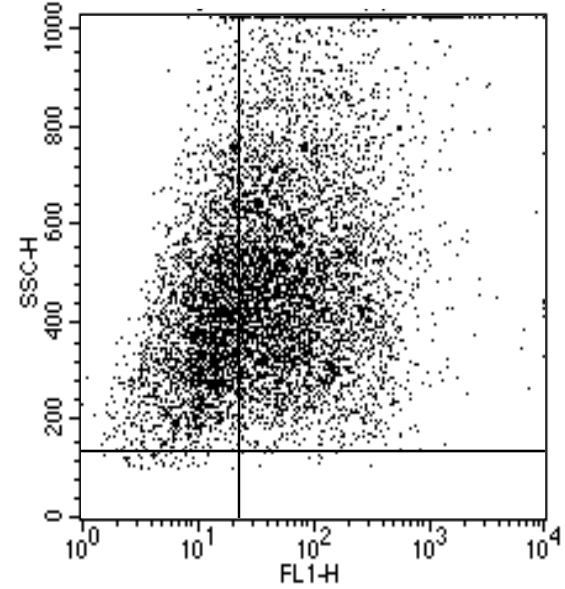


Histogram

■ Negative Control – contains secondary antibody only
— Contains primary and secondary antibody



Dot plot - negative control
– contains secondary
antibody only

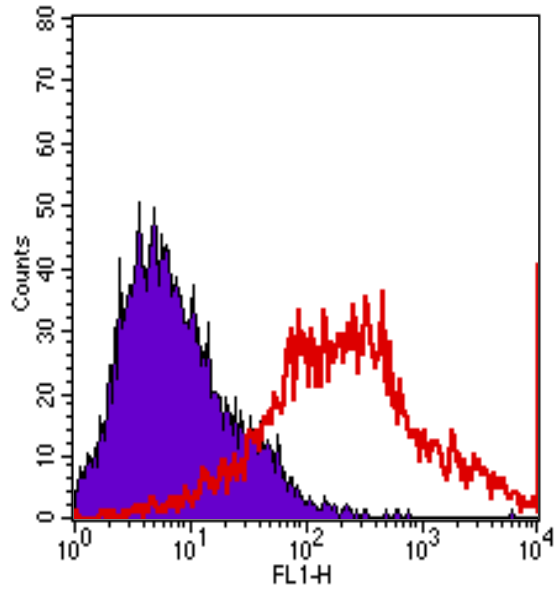


Dot plot -
contains primary and
secondary antibody

Increase in GMFI (channels)
32.47

% of cells demonstrating CXCR4 receptor positivity
50.44

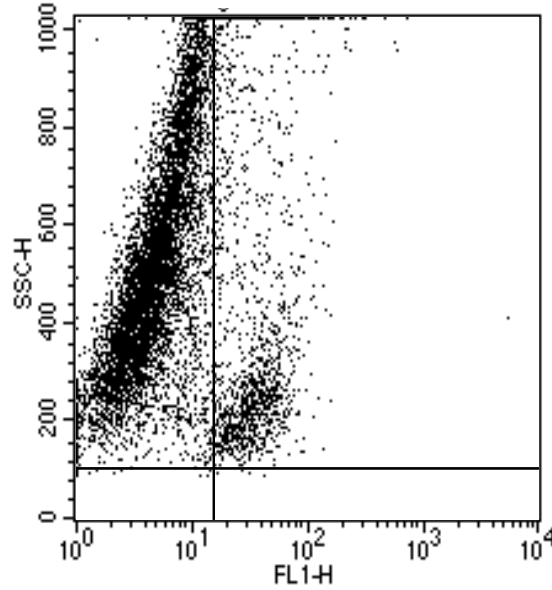
Figure 6.1e: Results of flow cytometry using primary anti-CXCR4 antibody IgG2b clone 44717.111



Histogram

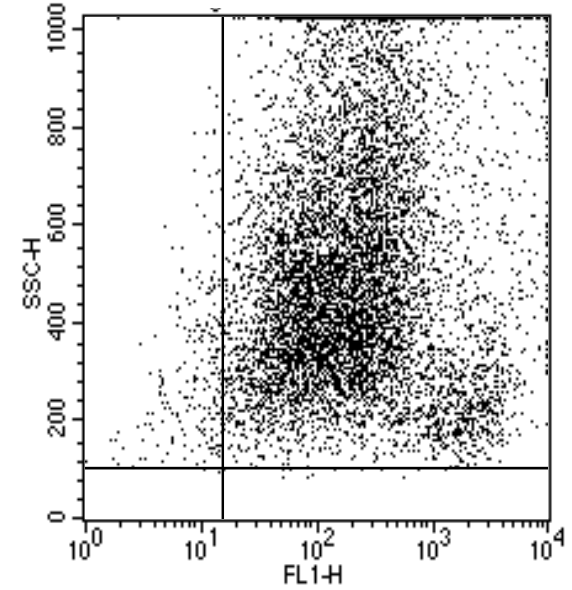
■ Negative Control – contains secondary antibody only
— Contains primary and secondary antibody

Increase in GMFI (channels)
204.56



Dot plot - negative control
– contains secondary
antibody only

% of cells demonstrating CXCR4 receptor positivity
77.61



Dot plot -
contains primary and
secondary antibody

3) Non-specific binding of secondary antibody

As the primary antibody of choice in obtaining the final results was mouse IgG2b monoclonal antibody clone 44717.111 (R&D Systems) the appropriate secondary antibody for use was FITC-conjugated anti-mouse IgG2b (γ 2b chain specific) (SouthernBiotech) (see chapter 3, table 3.7b). However, non-specific binding of this secondary antibody needed to be eliminated or optimised.

Figure 6.2a shows DU145 cell autofluorescence when no fluorescent tag is added to the cells. This autofluorescence comes from normal cell components which fluoresce, such as riboflavin and flavoproteins. In the negative control sample (figure 6.2b), when only FITC-conjugated secondary antibody, anti-mouse IgG2b γ 2b chain specific, SouthernBiotech (see chapter 3, table 3.7b), 1/50 dilution is added to the cells, non-specific binding of the secondary antibody is seen which is maintained when the primary anti-CXCR4 antibody (IgG2b clone 44717.111 - R&D Systems) is present (figure 6.2c). We attempted to decrease this non-specific cell binding by dilution of the secondary antibody to 1/100. Unfortunately this was unsuccessful and non-specific binding still persisted (figure 6.2d). Non-specific binding can also be due to Fc mediated binding, but it was established that FITC-labelled secondary F(ab')₂ anti-mouse IgG2b fragments (γ 2b chain specific) (SouthernBiotech) did not bind to the primary antibody as shown in figure 6.2e (also refer to discussion at the end of this chapter). Thus on final analysis of the data this non-specific cell binding of the secondary antibody was gated out of the results (and 1/50 dilution of anti-mouse IgG2b (γ 2b chain specific) secondary antibody was used in further experiments).

4) Optimisation of primary antibody dilution

Dilution of *primary* antibody resulted in markedly decreased binding to its epitope. Thus it was necessary to incubate cells in 20µl of the undiluted primary anti-CXCR4 antibody (mouse IgG2b monoclonal antibody clone 44717.111) stock solution. This, in combination with using non-enzymatic cell dissociation solution for cell preparation, did lead to some clumping of cells, which had to be accepted in order to achieve optimal primary antibody binding.

Figures 6.2a - e

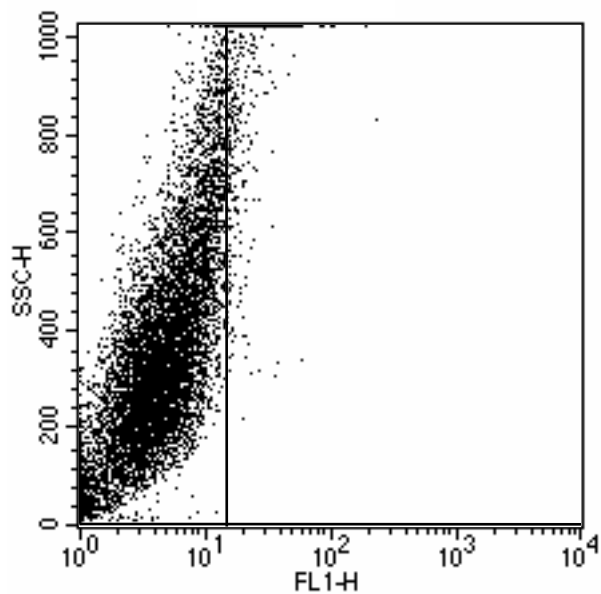
Dot plots demonstrating autofluorescence and non-specific binding of secondary antibody.

The x-axis shows fluorescence intensity (channel number) on 1024 channels encompassing 4-log decades (i.e. logarithmic scale). The y-axis shows side scatter intensity (channel number) on a linear scale.

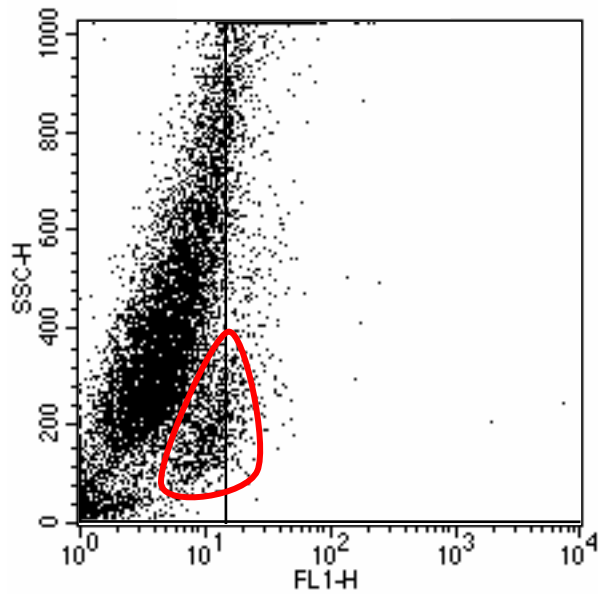
The primary antibody used was mouse IgG2b clone 44717.111 and the secondary antibodies used were FITC-conjugated anti-mouse IgG2b ($\gamma 2b$ chain specific) (SouthernBiotech) or FITC-conjugated anti-mouse IgG F(ab')₂ ($\gamma 2b$ chain specific) (SouthernBiotech).

Areas bound by red border represent non-specific secondary antibody binding.

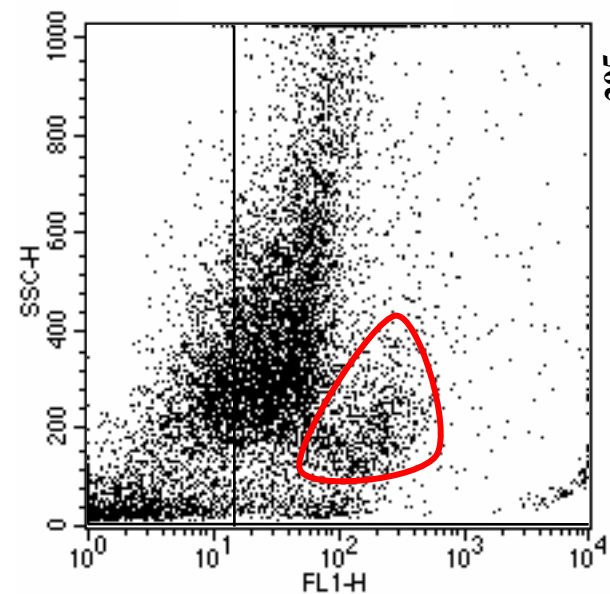
Figure 6.2: a) Autofluorescence – no primary or secondary antibody



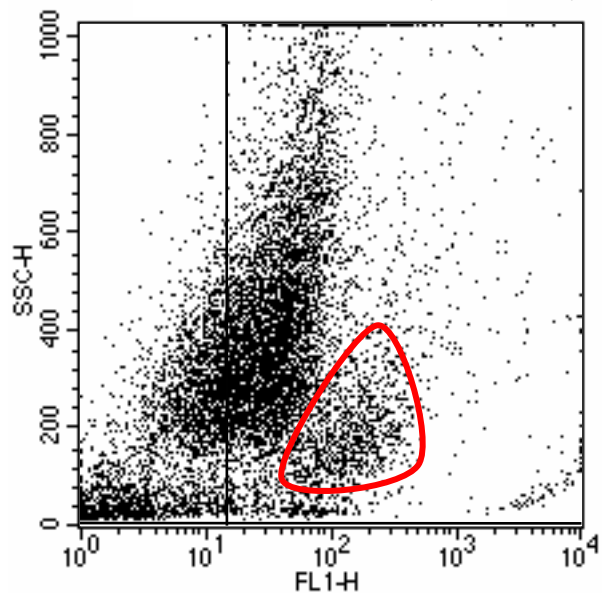
b) No primary and 1/50 dilution of secondary antibody



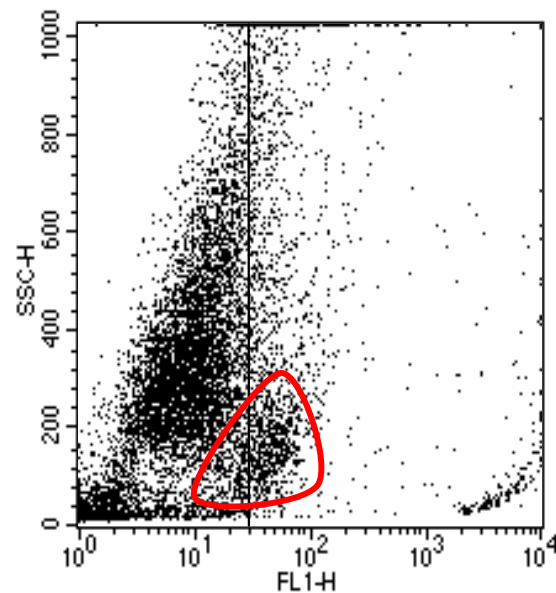
c) anti-CXCR4 primary antibody and 1/50 dilution secondary antibody



c) anti-CXCR4 primary antibody and 1/100 dilution secondary antibody



e) Anti-CXCR4 primary antibody and F(ab')₂ fragments secondary antibody



b) Final results

Representative flow cytometry results for CXCR4 receptor expression in cell lines are shown in figure 6.3 and summarized in table 6.2 [using undiluted anti-CXCR4 primary mouse IgG2b monoclonal antibody clone 44717.111 (R&D Systems) together with 1/50 dilution of FITC labeled anti-mouse IgG2b (γ 2b chain specific) (SouthernBiotech) secondary antibody].

Table 6.2: This summarises the results data from figure 6.3 and shows the results from one experiment elucidating cell membrane CXCR4 receptor expression in cell lines.

	DU145	LNCaP Cell Population 1 2		PC3	1542- CPT3X	1542- NPTX	Pre 2.8	S2.13	MDA- MB-231
Increase in GMFI (channels)	166.48	11.66	214.98	99.27	8.07	10.1	3.71	51.7	11.58
% of cells demonstrating CXCR4 receptor positivity	87.44	34.28	64.83	71.99	26.47	32.52	21.68	88.52	26.17

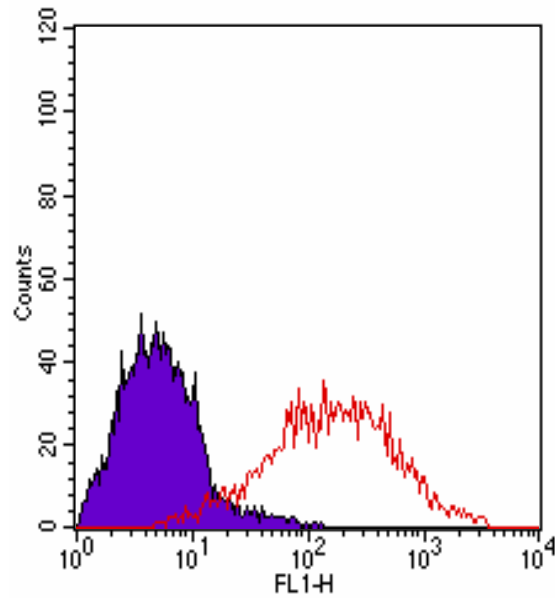
Figures 6.3a – h:

Representative flow cytometry histograms and dot plots are shown for cell membrane CXCR4 receptor expression in each cell line. A total of 10,000 events were analysed in each sample, with data due to dead cells/cell debris and non-specific binding of the secondary antibody being gated out of the final results when appropriate (note that it is not possible to completely gate out this data). The histogram and dot plot axes are labelled in the same manner as described in the legend to figure 6.1a - e.

The results, from this figure, for all cell lines are summarized in table 6.2.

Note that undiluted anti-CXCR4 primary mouse IgG2b monoclonal antibody clone 44717.111 (R & D Systems) together with 1/50 dilution of FITC labelled anti-mouse IgG2b (γ 2b chain specific) (SouthernBiotech) secondary antibody was used in all experiments.

Figure 6.3a: Results of flow cytometry for DU145

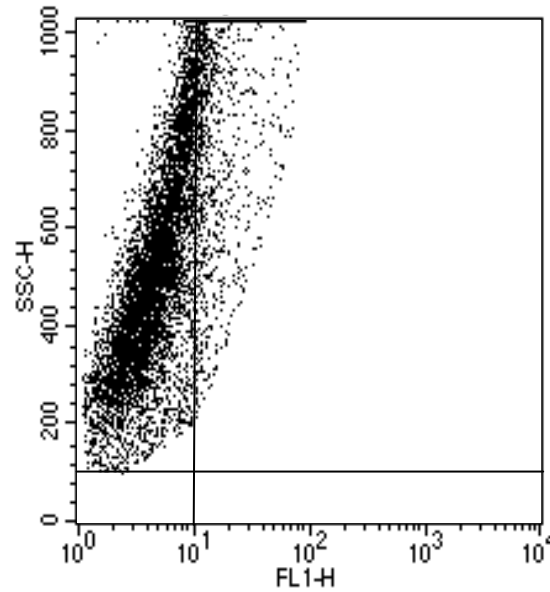


Histogram

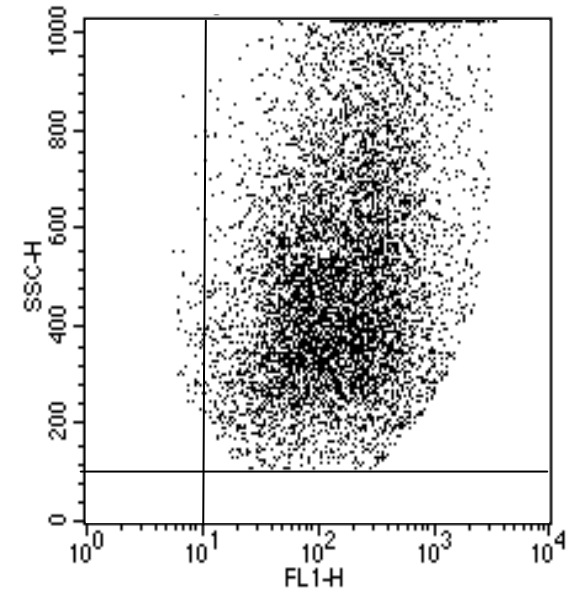
■ Negative Control – contains secondary antibody only

— Contains primary and secondary antibody

Increase in GMFI (channels)
166.48



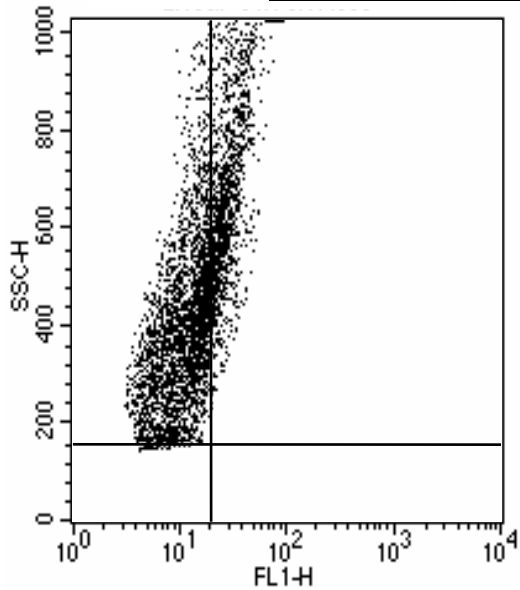
Dot plot - negative control
– contains secondary
antibody only



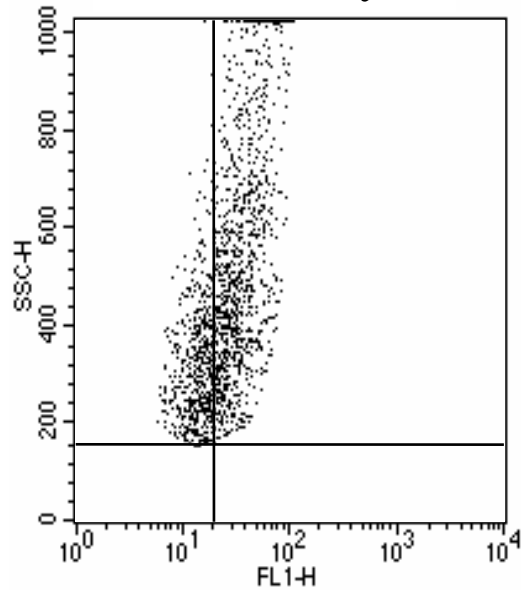
Dot plot -
contains primary and
secondary antibody

% of cells demonstrating CXCR4 receptor positivity
87.44

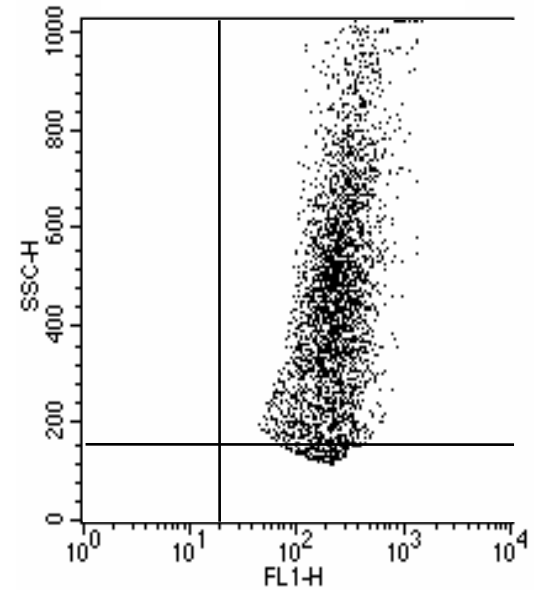
Figure 6.3b: Results of flow cytometry for LNCaP



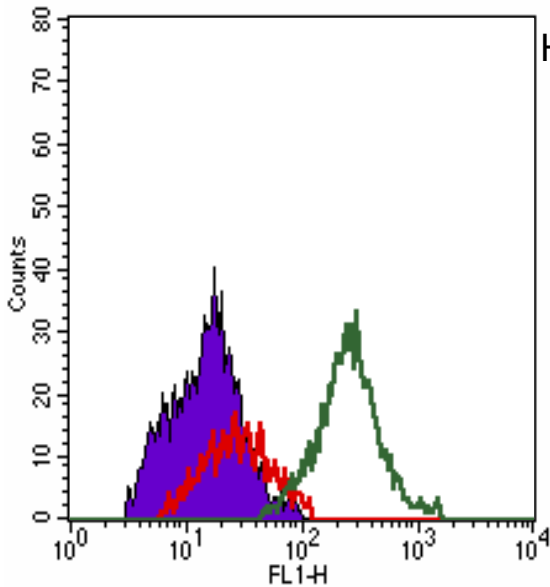
Dot plot - negative control
– contains secondary antibody only



Dot plot – subpopulation 1
contains primary and secondary antibody



Dot plot – subpopulation 2
contains primary and secondary antibody



Histogram

- Negative Control
– contains secondary antibody only
- Subpopulation 1 - contains primary and secondary antibody
- Subpopulation 2 - contains primary and secondary antibody

% of cells demonstrating CXCR4 receptor positivity

Subpopulation 1 – 34.28

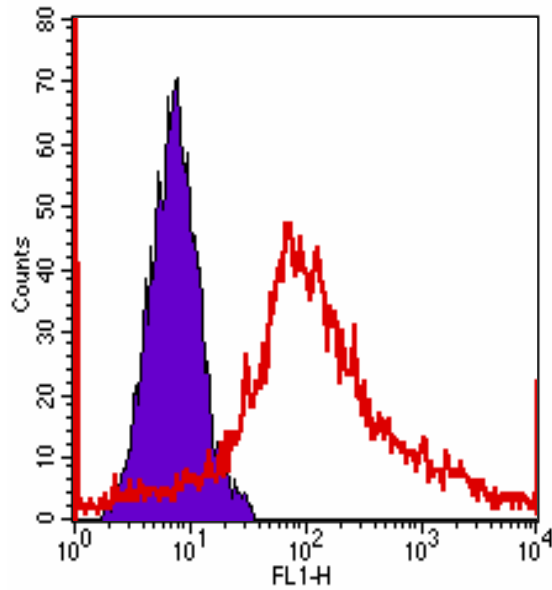
Subpopulation 2 – 64.83

Increase in GMFI (channels)



Subpopulation 1 – 11.66

Subpopulation 2 – 214.98

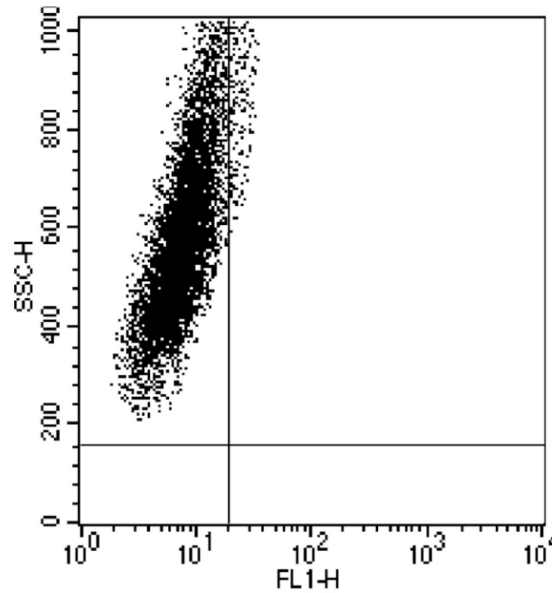
Figure 6.3c: Results of flow cytometry for PC3



Histogram

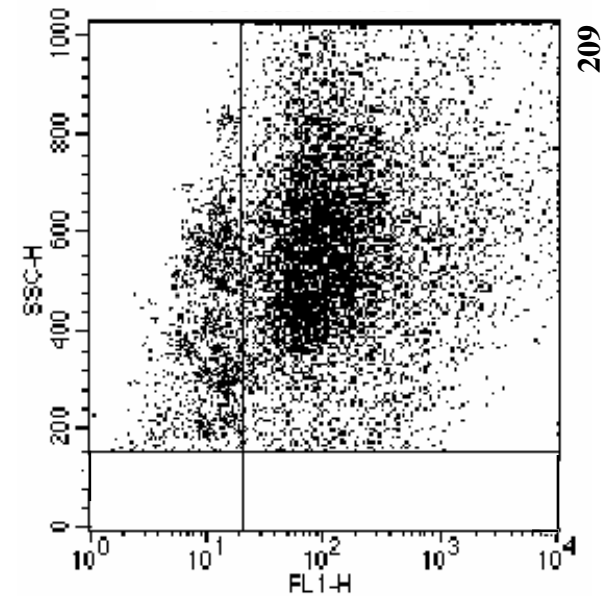
-  Negative Control – contains secondary antibody only
-  Contains primary and secondary antibody

Increase in GMFI (channels)
99.27



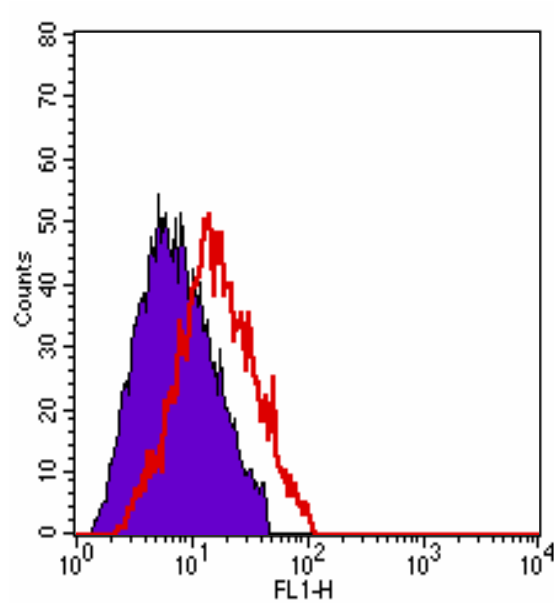
Dot plot - negative control
– contains secondary
antibody only

% of cells demonstrating CXCR4 receptor positivity
71.99



Dot plot -
contains primary and
secondary antibody

Figure 6.3d: Results of flow cytometry for 1542 CPT3X

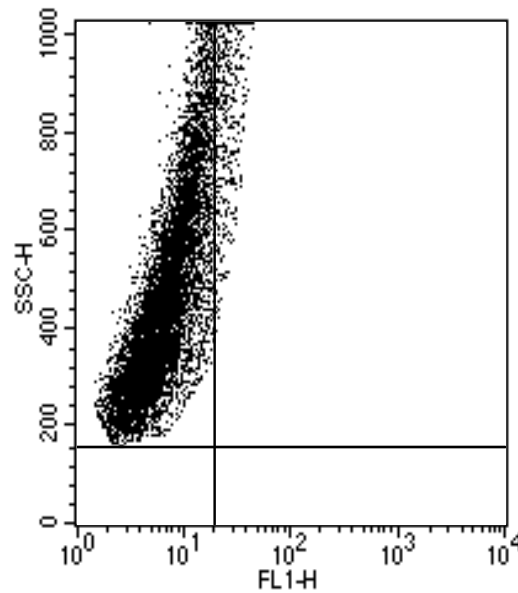


Histogram

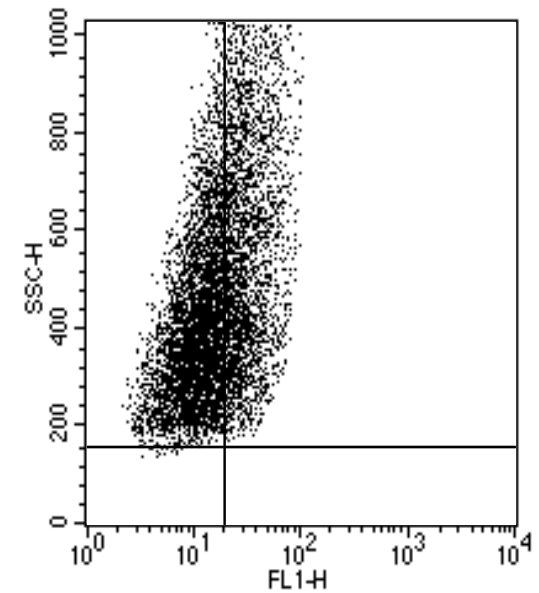
- Negative Control – contains secondary antibody only
- Contains primary and secondary antibody

Increase in GMFI (channels)

8.07



Dot plot - negative control
– contains secondary
antibody only

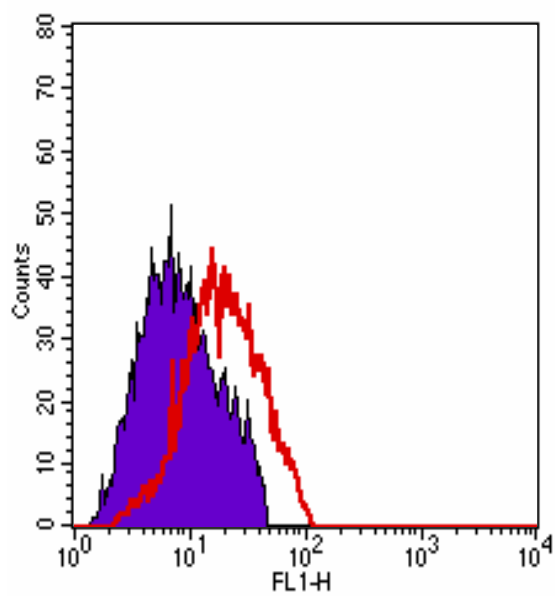


Dot plot -
contains primary and
secondary antibody

% of cells demonstrating CXCR4 receptor positivity

26.47

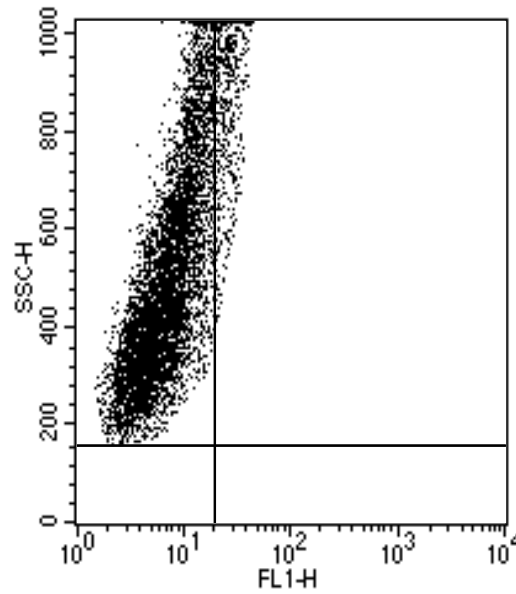
Figure 6.3e: Results of flow cytometry for 1542 NPTX



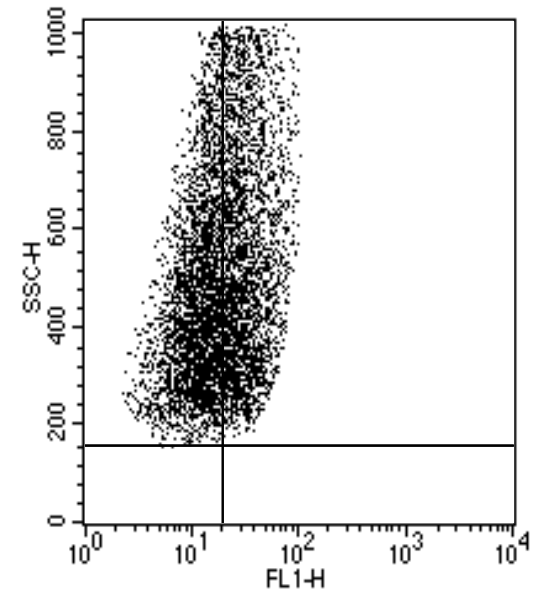
Histogram

- Negative Control – contains secondary antibody only
- Contains primary and secondary antibody

Increase in GMFI (channels)
10.1



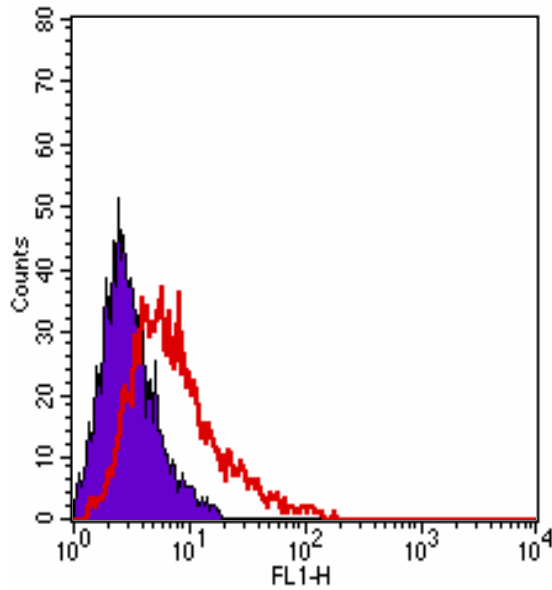
Dot plot - negative control
– contains secondary
antibody only



Dot plot -
contains primary and
secondary antibody

% of cells demonstrating CXCR4 receptor positivity
32.52

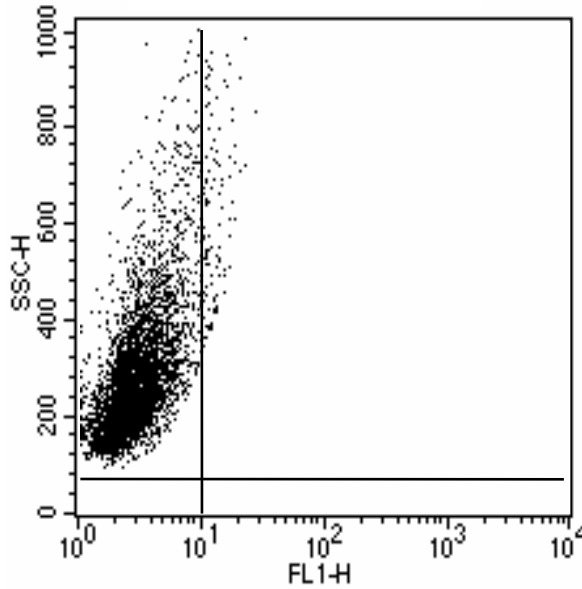
Figure 6.3f: Results of flow cytometry for Pre 2.8



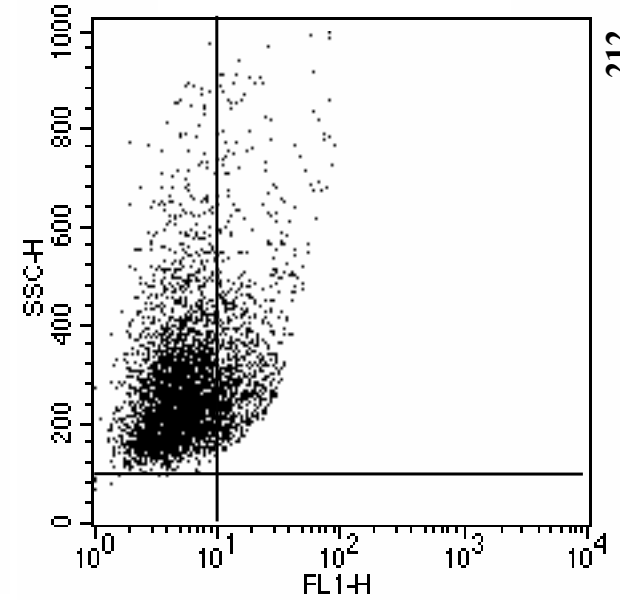
Histogram

- Negative Control – contains secondary antibody only
- Contains primary and secondary antibody

Increase in GMFI (channels)
3.71



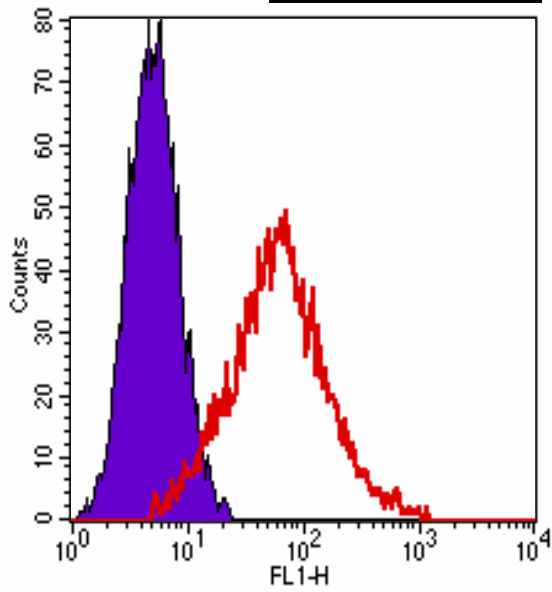
Dot plot - negative control
– contains secondary
antibody only



Dot plot -
contains primary and
secondary antibody

% of cells demonstrating CXCR4 receptor positivity
21.68

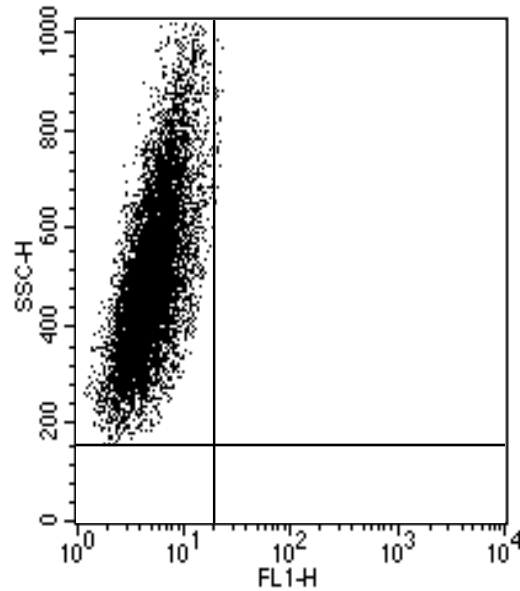
Figure 6.3g: Results of flow cytometry for S2.13



Histogram

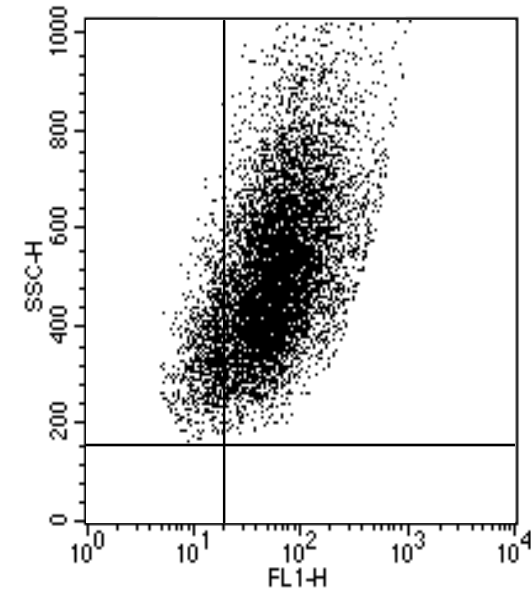
■ Negative Control – contains secondary antibody only
— Contains primary and secondary antibody

Increase in GMFI (channels)
51.7



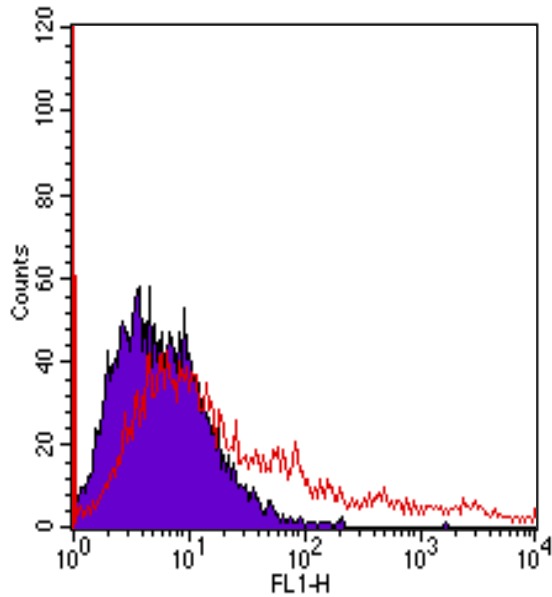
Dot plot - negative control
– contains secondary
antibody only

% of cells demonstrating CXCR4 receptor positivity
88.52



Dot plot -
contains primary and
secondary antibody

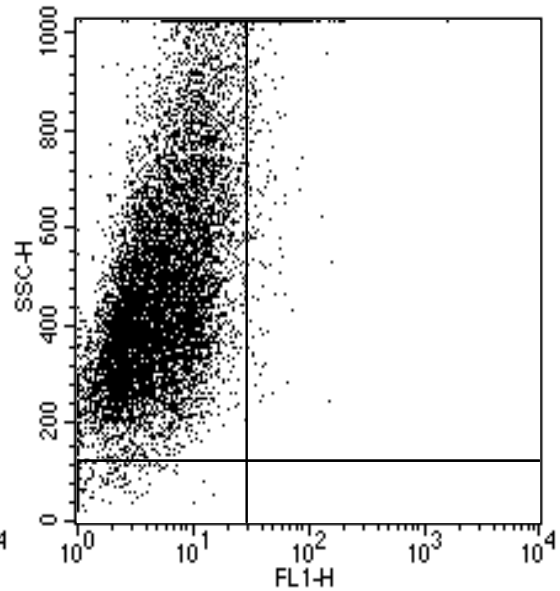
Figure 6.3h: Results of flow cytometry for MDA-MB-231



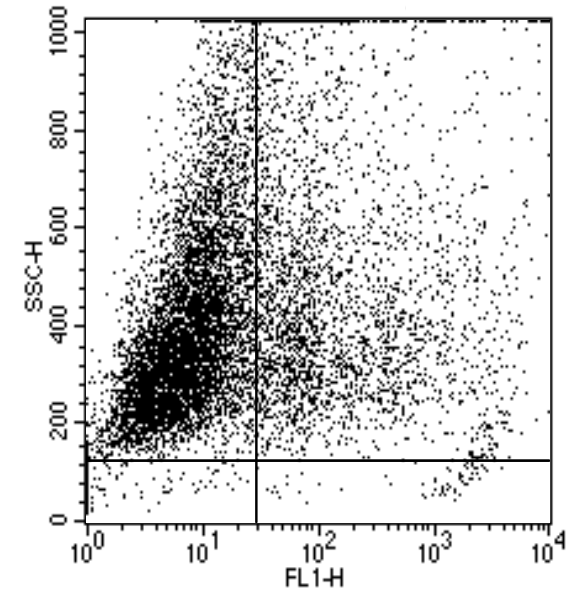
Histogram

- Negative Control – contains secondary antibody only
- Contains primary and secondary antibody

Increase in GMFI (channels)
11.58



Dot plot - negative control
– contains secondary
antibody only



Dot plot -
contains primary and
secondary antibody

% of cells demonstrating CXCR4 receptor positivity
26.17

In scrutinizing the results, the increase in GMFI detailed in the histograms was a more accurate method of analyzing our data as compared to calculating the percentage of cells exhibiting CXCR4 positivity from the dot plots. This is well demonstrated on reviewing the data for the LNCaP cell line (figure 6.3b). There are clearly two subpopulations of cells, which exhibit different concentrations of CXCR4 expression, and despite the fact that the first subpopulation has a small increase in the GMFI (11.66 channels), a significant number of cells (34.28%) are, however, considered positive for the CXCR4 receptor as they appear in the right upper quadrant of the dot plot. Theoretically, a situation could arise using the dot plots where *all* of the cells of both subpopulations appear in the right upper quadrant and are therefore considered totally positive for CXCR4 expression (i.e. 100% of cells demonstrate receptor positivity in both subgroups), with the two cell clusters being distinguished in their concentration of plasma membrane CXCR4 receptor, only by calculating a mean GMFI for each subpopulation. Therefore the advantage of the histogram data is that it enables weak and strong CXCR4 expression to be easily distinguished *numerically* by the increase in the mean GMFI.

Three separate experiments were performed for each cell line and the overall mean increase in GMFI +/- standard deviation was calculated (table 6.3).

Table 6.3: The overall mean GMFI +/- standard deviation (SD) has been calculated from 3 separate flow cytometry experiments investigating CXCR4 receptor expression in each cell line.

	Increase in GMFI (3 separate experiments)			Overall mean increase in GMFI +/- SD
	1	2	3	
DU145	166.48	176.51	190.90	177.93 +/- 12.27
LNCaP	i)11.66 ii) 214.98	i) 15.04 ii) 180.70	i) 20.67 ii) 190.02	i) 15.79 +/- 4.55 ii) 195.23 +/- 17.72
PC3	99.27	93.94	97.17	96.79 +/- 2.68
1542 CPT3X	8.07	5.36	7.43	6.95 +/- 1.42
1542 NPTX	10.1	7.88	4.91	7.63 +/- 2.60
Pre 2.8	3.71	2.61	4.47	3.60 +/- 0.94
S2.13	51.7	49.61	45.30	48.87 +/- 3.26
MDA-MB-231	11.58	5.37	2.87	6.61 +/- 4.84

DU145 expressed quantities of CXCR4 receptor second to that only of a subset of LNCaP cells (mean increase in GMFI for DU145 was 177.93 +/- 12.27 channels). LNCaP cells exhibited one subpopulation with a relatively low CXCR4 concentration (mean increase in GMFI 15.79 +/- 4.55 channels), and the other manifested a much higher quantity of the receptor (mean increase in GMFI 195.23 +/- 17.72 channels). Additionally, PC3 cells demonstrated comparatively high CXCR4 protein levels (mean increase in GMFI 96.79 +/- 2.68). The remaining cell lines, except the stromal derived cells S2.13 (mean increase in GMFI 48.87 +/- 3.26 channels), displayed relatively low quantities of cell surface CXCR4 receptor (mean increase in GMFI 1542 CPT3X = 6.95 +/- 1.42; 1542 NPTX = 7.63 +/- 2.60; Pre 2.8 = 3.60 +/- 0.94; MDA-MB-231 = 6.61 +/- 4.84).

SECTION 6.3

DISCUSSION

a) Optimisation - the results of optimisation of primary antibody isotype demonstrated that mouse IgG2b monoclonal antibody clone 44717.111 (R&D Systems) recognised a much greater proportion of cell surface CXCR4 (figures 6.1a - e and table 6.1) in comparison to the other primary antibodies used, and thus demonstrated greater specificity for binding the CXCR4 receptor. CXCR4 possesses four extracellular domains (chapter 1 figure 1.3): an N-terminal region and three extracellular loops (ECL1, ECL2, and ECL3). Using a panel of monoclonal antibodies to CXCR4, Baribaud F et al 2001 demonstrated that CXCR4 on both primary and transformed T cells as well as on primary B cells exhibited considerable antigenic heterogeneity. This antigenic heterogeneity in CXCR4 was the result of conformational differences most likely in CXCR4 ECL domains, and in particular in ECL2. The conformational antigenic heterogeneity is responsible for differential antibody binding in most cell types. It is thought that the epitope recognized by the poorly reactive monoclonal antibodies is occluded on a variable portion of cell surface CXCR4 receptors. Several explanations for conformational differences in CXCR4 have been proposed and investigated. The CXCR4 receptor (similar to other seven-transmembrane receptors) is subject to a number of factors that could alter receptor conformation. The CXCR4 receptor is glycosylated (contains two N-linked glycosylation sites, only one of which is used) (Berson JF et al 1996, Chabot DJ 2000) and sulfated (Farzan M et al, 1999) and can be phosphorylated as well (Orsini MJ et al 1999). Heterogeneity in any of these post-translational events would result in structurally distinct forms of CXCR4. However, several researchers have shown

that these post-translational modifications have little or no effect on antibody reactivity (Baribaud F et al 2001, Berson JF et al 1996, Chabot DJ 20003, Farzan M et al 1999). Additionally, the CXCR4 receptor associates with other membrane proteins, such as CD4 in T lymphocytes and cytosolic pertussis toxin-sensitive G proteins (Lapham CK 1996). Heterogeneity in CXCR4 interactions with these proteins would not be unexpected between cell types, resulting in conformational heterogeneity. However, Baribaud F et al 2001 demonstrated that this may not be the case.

Other potential possibilities for CXCR4 conformational differences include changes in cell membrane lipid composition (in which the receptor resides), growth conditions, receptor oligomerisation, or interactions with as yet unidentified molecules. These associations are currently being investigated.

In our experiments, the epitopes recognized by the primary monoclonal antibodies in figures 6.1b, c, d, e, were composed of residues on ECL2. As discussed, it is probable that the determinant bound by the poorly reactive monoclonal antibodies in figures 6.1b, c, d, is occluded on a variable portion of the CXCR4 receptors. These monoclonal antibodies therefore detect only a fraction of available cell surface CXCR4 molecules with resultant gross underestimation of receptor density.

The monospecificity of monoclonal antibodies can sometimes limit their usefulness. This is apparent particularly when changes in the structure of an epitope, eg. as a consequence of conformational antigenic heterogeneity in CXCR4, markedly affects the binding of the monoclonal antibody. In this situation polyclonal antibodies may have better antigen specificity because they are heterogeneous and recognize a host

of antigenic epitopes. Therefore, when using a polyclonal antibody, the effect of change on a single or small number of epitopes is less likely to be significant.

We used a polyclonal anti-CXCR4 antibody, Fusin (H-118), but this in fact did not bind successfully during cell preparation for flow cytometry (figure 6.1a, table 6.1). The increase of GMFI when using this antibody was only 15.48. The unsuccessful binding of Fusin (H-118) may be explained by the fact that this polyclonal antibody is raised against a recombinant protein corresponding to amino acids 176 - 293 of the CXCR4 receptor, which actually maps partly within a transmembrane region of the receptor (chapter 1 figure 1.3).

Non specific binding of the secondary FITC-conjugated anti-mouse IgG2b (γ 2b chain specific) antibody (SouthernBiotech) (figure 6.2), could have been due to Fc mediated binding. The Fab fragment of the antibody forms the specific antigen-binding site, whereas the non-specific Fc domain allows the antibodies to recruit cells of the immune system, such as monocytes, macrophages and dendritic cells, by engaging the Fc receptors on these cells. However, tumour cells are also known to possess Fc receptors which by various mechanisms can actually result in a growth and survival advantage to the neoplasm (Cassard L et al 2002, Nitta T et al 1992, Ran M et al 1988, Ran M et al 1992). This can therefore result in problematic non-specific binding of the fluorescent secondary antibody during sample preparation for flow cytometry. The use of Fab or $F(ab')_2$ fragments, i.e. antibodies without their Fc ends, can sometimes help to significantly decrease or alleviate this difficulty. In our experiments the use of FITC-labelled secondary $F(ab')_2$ anti-mouse IgG2b fragments (SouthernBiotech) was

unsuccessful as this antibody did not in fact did not bind successfully to the primary antibody (figure 6.2e).

b) Final results - the final results obtained via flow cytometry regarding cell membrane CXCR4 protein concentrations confirmed our results from previous mRNA expression studies. These results additionally confirmed that CXCR4 receptor was present on the cell surface/ membrane.

The metastatic cell lines DU145, LNCaP and PC3 manifested the highest CXCR4 cell surface receptor levels (figure 6.3, table 6.3). However, LNCaP demonstrated two subpopulations of cells – approximately 34% had relatively low CXCR4 protein levels (mean increase in GMFI 15.79 channels) and approximately 65% were observed to have the highest CXCR4 levels amongst all the cell lines (increase in mean GMFI 195.23 channels) (figure 6.3b, table 6.3). The presence of these two LNCaP subpopulations is most likely explained by the finding that LNCaP cells display phenotypic and genotypic heterogeneity in culture [Horoszewicz JS et al 1983, Wan XS et al 2003]. This suggests that it would not have been surprising to find even more than two subpopulations of LNCaP exhibiting heterogeneity in levels of CXCR4 expression. As it has been recently demonstrated that androgens increased the levels of both CXCR4 mRNA and functional protein in LNCaP prostate cancer cells [Frigo DE et al 2009], it is possible that subpopulations of LNCaP cells with higher androgen receptor levels also manifested an increased quantity CXCR4 protein. Another explanation that was considered for the two different subpopulations within LNCaP, was that the LNCaP cells may have been exposed to hypoxic conditions during cell culture promoting the appearance of a subset of

cells with upregulated CXCR4 protein, as investigators have shown that hypoxia induces CXCR4 expression in tumour cells via increased levels of HIF-1 α (discussed in detail in chapter 8) [Dunn LK et al 2009, Schioppa T et al 2003, Staller P et al 2003, Zagzag D et al 2005]. However, as cell culture conditions were strictly controlled for all cell lines (see chapter 3) and the same results was obtained on at least three different occasions, this was regarded as an implausible explanation.

Although DU145 had the highest CXCR4 mRNA levels (see chapter 5), these cells were second to the subpopulation of LNCaP as regards cell surface CXCR4 protein expression (change in mean GMFI 177.93 and 195.23 respectively – table 6.3). This lack of correlation between CXCR4 mRNA and protein in DU145 cells may occur due to either post-transcriptional mechanisms or regulation of CXCR4 at the protein level. Tarasova NI et al 1998 have reported that CXCR4 undergoes endocytosis on binding of CXCL12 ligand but recycling of the internalized receptor is inefficient. Recently, Wagner PL et al 2009 established that CXCR4 receptor was present on the cell membrane as well as in the cytoplasm and nucleus of adenocarcinoma lung cells (the authors suggested only cytomembranous CXCR4 was functional). Therefore in DU145, using the protocol for flow cytometry described in chapter 3, we may have detected only cell membrane CXCR4 receptor. Cytoplasmic and nuclear CXCR4 could have been detected using flow cytometry by permeabilising the DU145 cells. Alternatively, total CXCR4 protein levels could have been measured and compared between cell lines using Western blotting.

The cell lines cultured and immortalized from normal prostate epithelium (Pre 2.8, 1542 NPTX) and primary prostate cancer (1542 CPT3X), exhibited relatively small increases in the mean GMFI, signifying extremely low or absent CXCR4 protein

expression (table 6.3). A similar result was obtained with the MDA-MB-231 breast cancer cells. Particularly for the cell lines in which no CXCR4 mRNA was detected in earlier experiments, such as Pre 2.8 and MDA-MB-231, the small changes in GMFI could be attributed to non-specific binding of the secondary antibody to dead cell remnants and cell clumps, which could not be eliminated.

Thus, our flow cytometry results, which confirmed over-expression of the cell surface CXCR4 chemokine protein in the cell lines derived from prostate cancer metastases, augmented our findings from prior experiments and provided further evidence that this seven-transmembrane receptor may be involved in the metastatic process of prostate cancer.

CHAPTER 7

ESTABLISHING THAT THE CXCR4 RECEPTOR IS FUNCTIONAL IN CELL LINES DERIVED FROM PROSTATE CANCER METASTASES

SECTION 7.1

INTRODUCTION AND AIMS

Up to this point we had determined that the cell lines derived from prostate cancer metastases (DU145, LNCaP, PC3) expressed relatively high levels of both CXCR4 mRNA and CXCR4 cell membrane protein in comparison to prostate cell lines that originated from benign prostate tissue (1542 NPTX, Pre 2.8, S2.13) and primary prostate cancer (1542 CPT3X). The next aim was to establish that the CXCR4 receptor in the metastatic cell lines was functional. We aimed to do this by studying the motility or chemotaxis of the cells in response to the CXCR4 ligand i.e. CXCL12 (SDF-1). In these experiments the cell lines DU145 and PC3 were used in addition to 1542 NPTX. The latter was used as a type of control experiment as 1542 NPTX cells had been previously shown to have little or no CXCR4 protein expression.

Cell migration is an essential characteristic of both physiological and pathological processes and tumour cell motility plays a critical role in the process of neoplastic invasion and metastasis. In 1863, Rudolf Virchow described his observation of motile cells, which he had isolated from the lymph fluid and from cartilage tissue [Virchow R 1863]. However, it is now recognised that, within an organism, only several groups of highly specialized cells are able to actively and autonomously migrate. These cells include stem cells, leucocytes, fibroblasts, and tumour cells. Neutrophils, which have a maximum speed of 15 to 20 $\mu\text{m}/\text{min}$, are the fastest cells of all [Entschladen F et al 2000, Werr J et al 1998] whereas, in comparison to these cells, fibroblasts are relatively sluggish (0.2 to 1 $\mu\text{m}/\text{min}$) [Park S et al 2005] and, surprisingly, tumour cells are one of

the slowest migrating cells (0.1 to 0.3 $\mu\text{m} / \text{min}$) [Entschladen F et al 2004, Irimia D and Toner M 2009, Niggemann B et al 2004, Niggemann B et al 1997].

It should be noted that there are two distinct cell motile behaviours: chemotaxis is defined as directional cell movement towards concentration gradients of solubilized attractants, whereas chemokinesis is defined as random cell movement in the absence of chemoattractant gradients. However, no substance has been described which influences only directional migration without an increase of migratory activity. Therefore, chemotaxis does not occur independently from chemokinesis.

Cell motility/migration/chemotaxis can be studied via several different methods, the most widely accepted of which is the “Boyden Chamber assay”, initially described by Boyden S in 1962. Variations of this chemotactic assay, eg. the Transwell® migration assay (which was used in our experiments), have been effectively used to study the motility of a variety of cell populations. It has been reported that increased cell migration in a Boyden Chamber system correlates with increased invasive properties in vivo [Klemke RL et al 1998].

SECTION 7.2

RESULTS

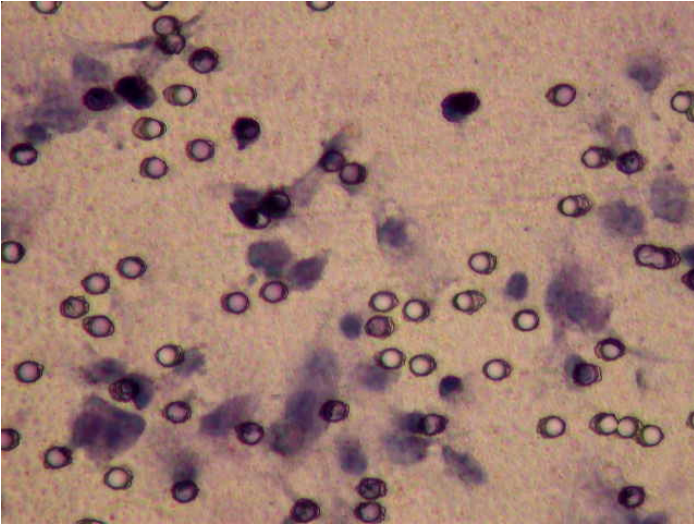
It should be noted that all experiments were repeated on three separate occasions using four Transwell® wells each time for each CXCL12 ligand concentration.

Stained cells were counted using a microscope. This was done under x200 magnification and the mean number of cells per three high power fields (the central and the two vertically adjacent fields) for each well was calculated (photographs of migrating cells at high power are shown in figure 7.1).

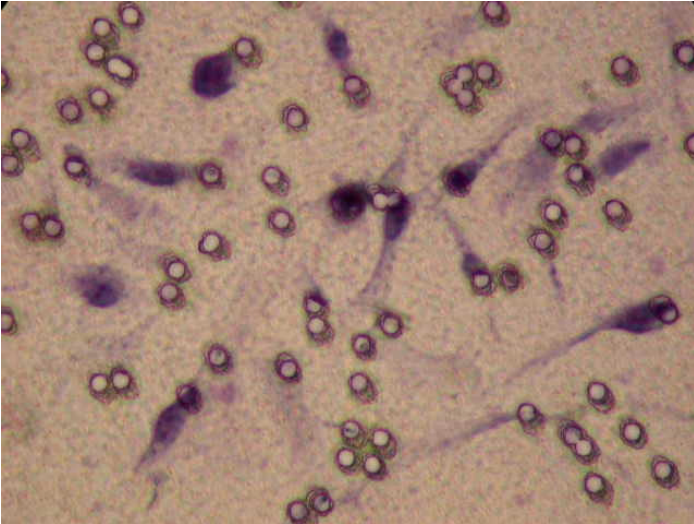
The results of the migration assays were assessed with the “Student’s t test”. The level of significance was defined as $p < 0.05$.

The results are presented in table 7.1 and summarized in graphical form in figures 7.2a - c.

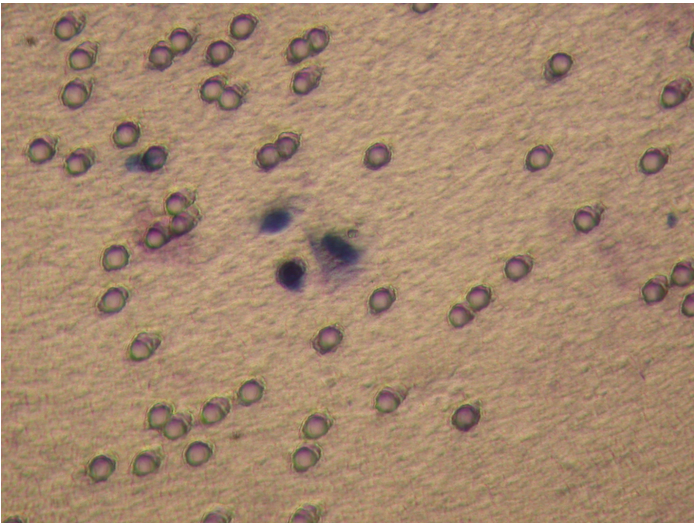
Figure 7.1: Photograph of migrating cells in one high power field in a Transwell® well at x200 magnification



DU145 Cells



PC3 cells



**1542 NPTX
Cells**

Transwell® wells 1-4 for each of three separate experiments. The mean number of cells per three high power fields (the central and the two vertically adjacent fields under x200 magnification) for each well was calculated and is tabulated.

	Well 1	Well 2	Well 3	Well 4	Well 1	Well 2	Well 3	Well 4	Well 1	Well 2	Well 3	Well 4	Mean (rounded to nearest whole number) +/- SE
DUI145 with no ligand	29	21	25	27	22	31	23	26	21	30	20	24	25 +/- 1.08
DUI145 with 50ng/ml ligand	38	37	44	41	48	47	38	44	47	36	37	50	42 +/- 1.45
DUI145 with 150ng/ml ligand	66	82	79	65	81	64	73	63	82	65	69	77	72 +/- 2.21
DUI145 with 300ng/ml ligand	78	82	100	98	73	87	76	85	94	76	82	93	85 +/- 2.63
DUI145 with 450ng/ml ligand	72	75	92	96	86	76	78	92	86	78	76	80	82 +/- 2.28
DUI145 with 150ng/ml ligand + Ab	56	42	48	39	51	50	39	39	36	49	54	40	45 +/- 1.97
PC3 with no ligand	11	18	12	16	14	18	15	16	18	12	12	18	15 +/- 0.79
PC3 with 150ng/ml ligand	11	12	18	12	9	13	10	12	15	14	12	14	13 +/- 0.69
PC3 with 300ng/ml ligand	25	25	20	19	18	24	22	19	24	18	21	27	22 +/- 0.89
PC3 with 300ng/ml ligand + Ab	16	10	13	11	13	17	12	12	16	12	9	15	13 +/- 0.72
1542 NPTX with no ligand	8	6	7	6	8	7	7	8	4	8	7	3	7 +/- 0.47
1542 NPTX with 150ng/ml ligand	7	3	6	8	6	5	6	4	5	6	5	3	5 +/- 0.43
1542 NPTX with 450ng/ml ligand	6	8	7	5	2	7	6	6	6	5	3	9	6 +/- 0.56
1542 NPTX with 150ng/ml ligand + Ab	4	9	9	6	7	2	5	8	8	5	8	7	7 +/- 0.62

Table 7.1. Results of cell migration assays (all results rounded up or down to the nearest whole number). All experiments were repeated on three separate occasions using four Transwell® wells each time. After 3 hours of incubation, the mean number of cells per three high power fields (the central and the two vertically adjacent fields under x200 magnification using light microscopy) for each well was calculated and is tabulated. The overall mean for all experiments on each cell line was then established in addition to the standard error of the mean (SE).

CXCL12 α ligand concentrations are in ng/ml and the anti-CXCR4 antibody (Ab) concentration is 4 μ g/ml.

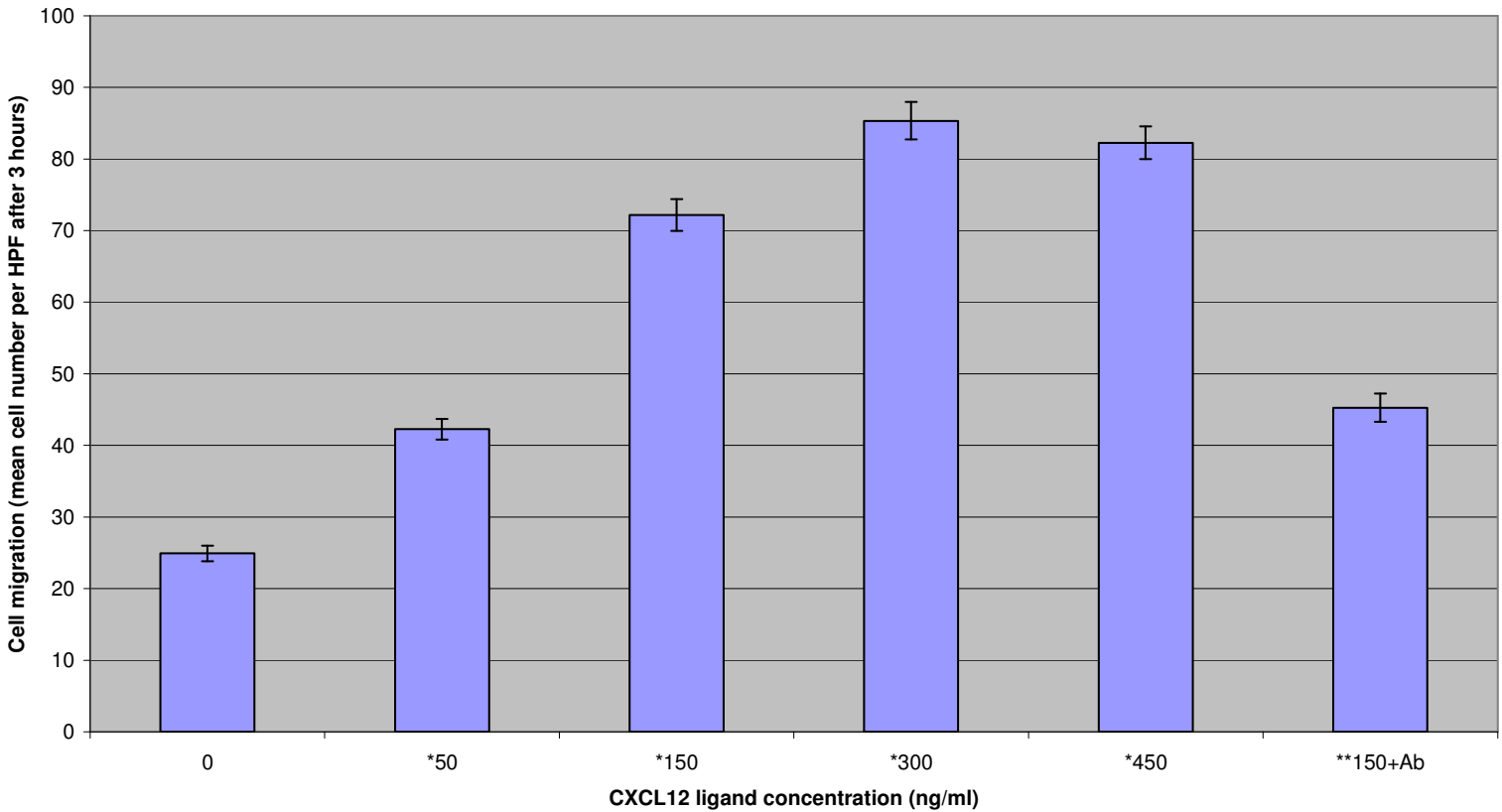
Figure 7.2a-c. Effect of CXCL12 α on chemotaxis of prostate cell lines (all results rounded up or down to the nearest whole number). Cells were placed in upper chamber with varying concentrations of CXCL12 α ligand in lower chamber of Transwell® (incubation period was 3 hours). When necessary, 4 μ g/ml of anti-CXCR4 IgG2b monoclonal antibody clone 44717.111 (Ab) was added to the upper compartment.

* Significant increase versus no ligand control (p<0.05, t test).

** Significant inhibition by anti-CXCR4 IgG2b monoclonal antibody (Ab) (p<0.05, t test).

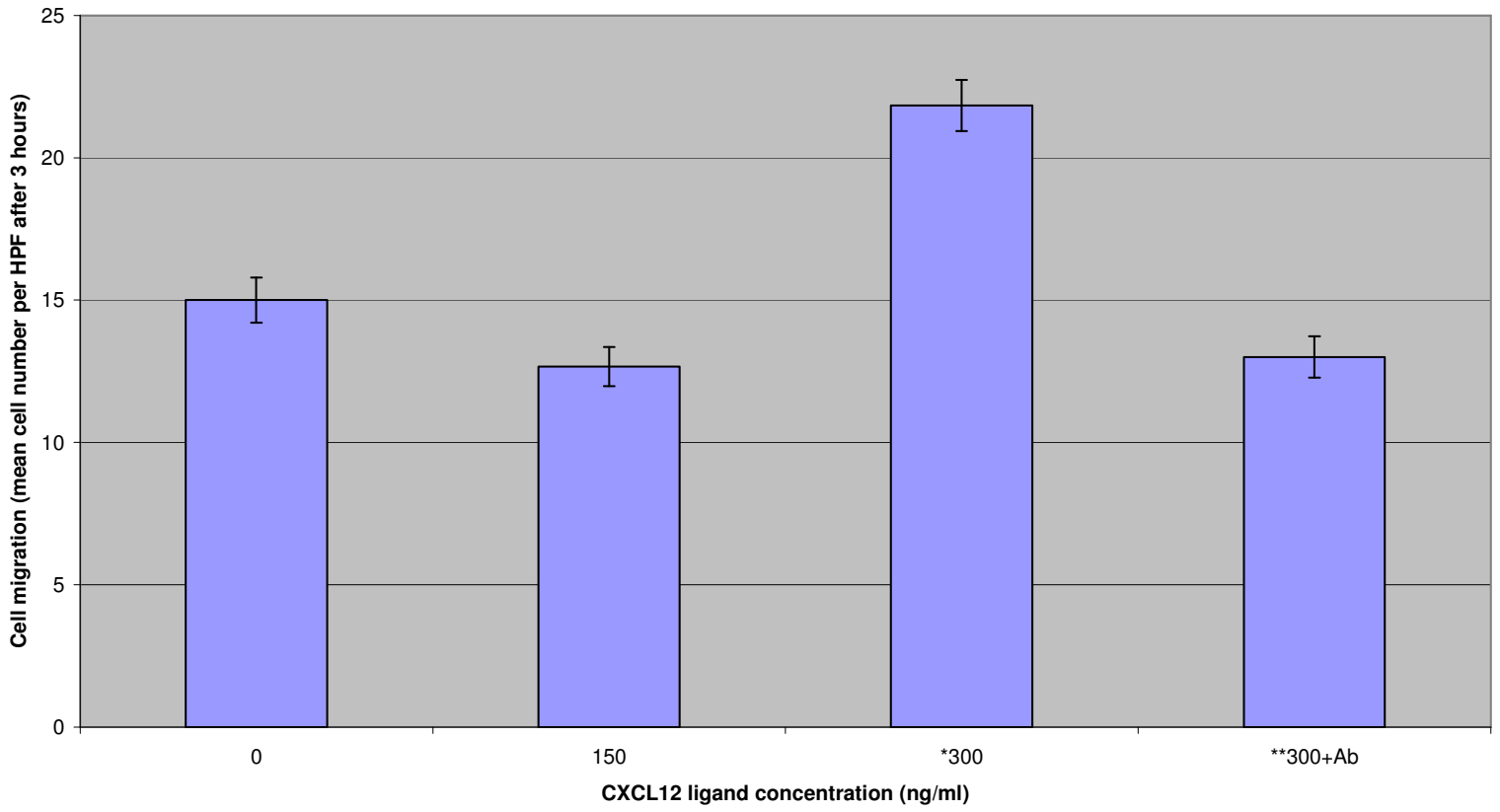
a)

DU145 Cell Migration



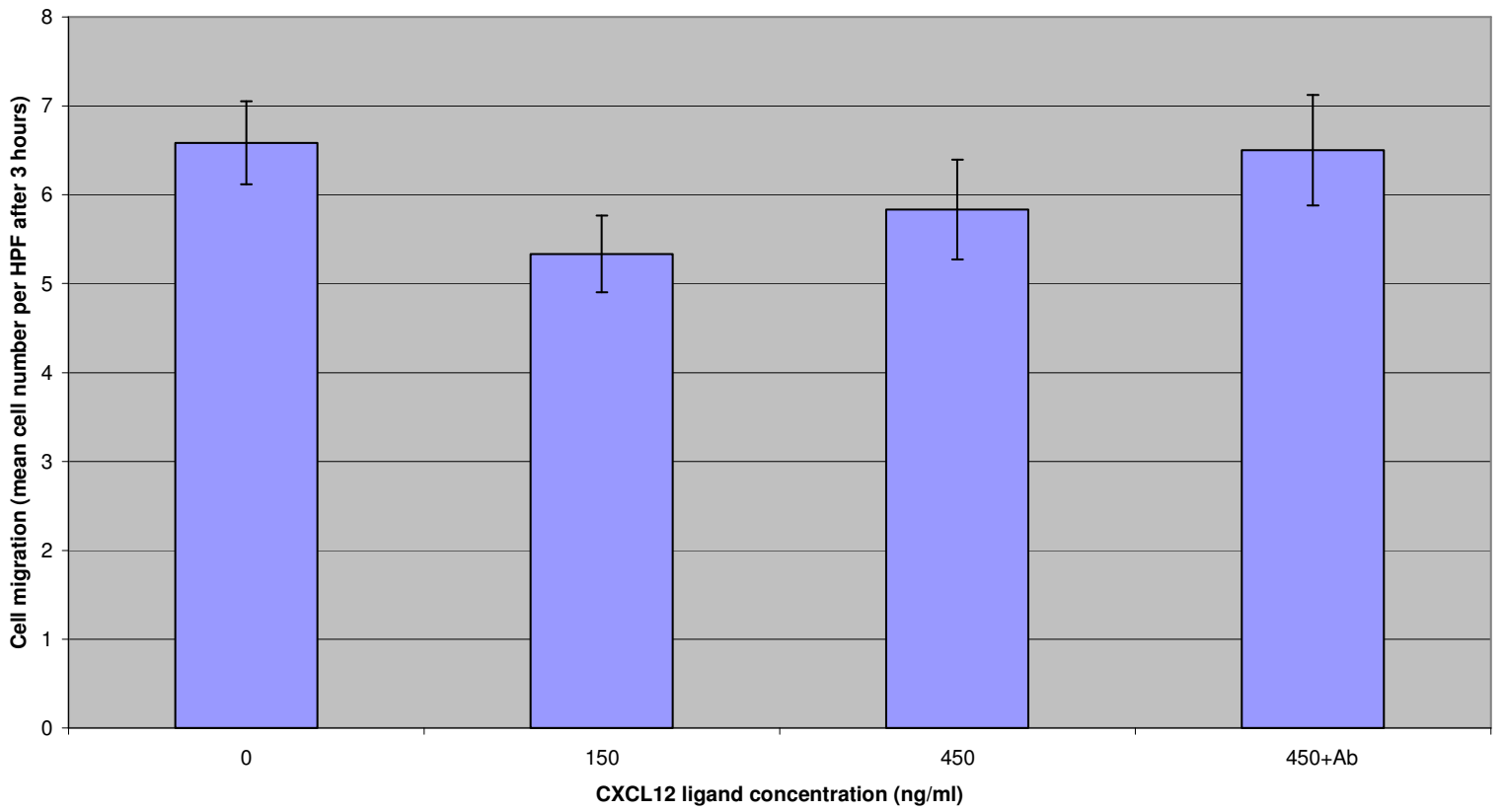
b)

PC3 Cell Migration



c)

1542 NPTX Cell Migration



In DU145 cells it was seen that the presence of the CXCR4 ligand, CXCL12 α , in the lower chamber promoted chemotaxis and increased cell migration into the lower chamber from a mean of 25 cells/HPF in the no ligand control to 42 cells/HPF ($p < 0.05$) and 72 cells/HPF ($p < 0.05$) with a ligand concentration of 50 ng/ml and 150 ng/ml respectively (table 7.1 and figure 7.2a). Increasing the concentration of ligand to 300 ng/ml increased the rate of cell migration to a mean of 85 cells/HPF but further increases did not affect the rate of cell movement. The addition of anti-CXCR4 IgG2b antibody clone 44717.111 (R & D Systems) (4 μ g/ml) into the upper chamber (with 150 ng/ml CXCL12 α in the lower) decreased cell migration to 45 cells/HPF ($p < 0.05$ in comparison with no antibody in upper chamber and 150 ng/ml CXCL12 α in the lower chamber).

With PC3 there was no significant increase in chemotaxis with a ligand concentration of 150 ng/ml as compared to the control experiment with no ligand (figure 7.2b). With CXCL12 α at 300 ng/ml, cell migration increased from a mean of 15 cells/HPF (no ligand control) to 22 cells/HPF ($p < 0.05$). The addition of antibody to the latter decreased migration to 13 cells/HPF ($p < 0.05$).

In contrast to DU145 and PC3, using 1542 NPTX cells, there was no significant increase in cell migration even when using a ligand concentration of 450 ng/ml (7 cells/HPF with no ligand and 6 cells/HPF with 450 ng/ml CXCL12 α) (figure 7.2c).

SECTION 7.3

DISCUSSION

In order to investigate the functionality of the CXCR4 receptor, we used the cell lines derived from metastases, DU145 and PC3, which we had shown had relatively high expression of CXCR4 on their cell membranes (chapter 6). 1542 NPTX was used as a control experiment as this cell line was derived from benign prostate epithelium and had been shown to have extremely low or absent CXCR4 protein expression (chapter 6). The main disadvantage of the Boyden Chamber / Transwell® migration assays is that a very large number of cells is applied, but only a small fraction of the cells are analysed i.e. the migratory active population of cells. Therefore, interpretations on the population as a whole can only be made when the cells behave as a homogeneous population. Therefore we did not use LNCaP cells in these experiments as it had been demonstrated in chapter 6, that there were two subpopulations of LNCaP cells, one with relatively low CXCR4 protein levels and the other expressing CXCR4 receptor at very much higher levels.

The results suggested that in the metastatic cell lines DU145 and PC3, the expressed CXCR4 receptor is functional as the ligand CXCL12 α promoted chemotaxis. This effect was concentration dependent as increasing the concentration of ligand in DU145 cells promoted increased cell migration until saturation was reached (at a ligand concentration of 300ng/ml). Also, this increased cell motility was specifically the result of CXCR4/ CXCL12 α interaction as the addition of anti-CXCR4 antibody decreased cell movement. PC3 cells did migrate in the presence of CXCL12 α but at a much slower rate than DU145 cells and also a much higher concentration of ligand was needed to promote cell migration (in the presence of 50ng/ml of CXCL12 α DU145 cells migrated, but in the

PC3 cell line no significant increase in movement was noted until a ligand concentration of 300ng/ml). This slower rate of PC3 chemotaxis may be explained by the finding from chapter 6 that PC3 cells had a much lower expression of CXCR4 protein as compared to DU145 cells. Additionally of note was that in the 1542 NPTX cell line there was no significant increase in cell migration in the presence of the ligand thus suggesting that cell movement was due only to chemokinesis (as opposed to chemotaxis). This result was not unexpected as Taqman real-time PCR and flow cytometry had established that 1542 NPTX cells had absent or very low levels of CXCR4 receptor expression.

Our results had determined that in the cell lines derived from metastases, DU145 and PC3, CXCR4 receptor was functional and its ligand CXCL12 promoted the chemotaxis of these cells. Of particular significance is the observation that *in vivo*, CXCL12 ligand is expressed and secreted at high levels by tissues which are the preferred site of prostate cancer metastasis, with highest expression in bone marrow (fibroblasts, osteoblasts, endothelial cells), lymph nodes, lung, and liver and markedly lower expression levels in the small intestine, skin and skeletal muscle [Bradstock KF et al 2000, Imai K et al 1999, Muller A et al 2001, Ponomaryov T et al 2000, Sun YX et al 2005, Taichman RS et al 2002, Zou YR et al 1998]. Therefore our *in vitro* experimental results suggested that the *in vivo* preferential metastasis of prostate cancer to specific sites, for example lymph nodes and bone, may be due to CXCL12 promoted chemotaxis.

CHAPTER 8

FURTHER DISCUSSION

SECTION 8.1

RESULTS SUMMARY AND EVALUATION

We hypothesized that prostate cancer may use chemokine ligand – receptor interactions in the process of metastasis to preferred sites.

In order to pursue this hypothesis we initially determined, using conventional RT-PCR, mRNA levels of the chemokine receptors in the CXCR and CCR groups in prostate cell lines derived from metastases (DU145, PC3, LNCaP), primary prostate cancer (1542 CPT3X) and benign epithelium or stroma (Pre 2.8, 1542 NPTX, S2.13). The expression of thirteen receptors in total was demonstrated. The results established that the expression of one chemokine receptor, CXCR4 (Fusin), was of particular interest because it was noted that CXCR4 mRNA was upregulated in DU145, LNCaP and PC3 cell lines i.e. cell lines developed from prostate malignancies that had spread to brain, lymph node and bone respectively. However, the RT-PCR results indicated that the cell lines derived from primary prostate tumour (1542 CPT3X) and normal prostate epithelium (1542 NPTX and Pre 2.8) manifested CXCR4 receptor mRNA at much lower or undetectable levels. The presence of the androgen receptor in the metastatic cells was not related to CXCR4 mRNA expression as DU145 and LNCaP were observed, using RT-PCR, to have high CXCR4 mRNA levels whereas PC3 expressed moderate levels (DU145 and PC3 do not express androgen receptor in contrast to LNCaP cells which do). However, at this stage, although high levels of CXCR4 mRNA had been elucidated in the metastatic cell lines, this may have been related to any process in the metastatic cascade including cell proliferation, neoangiogenesis, local invasion or chemotaxis.

The expression of the ligand for the CXCR4 receptor, CXCL12, was also investigated. However, CXCL12 mRNA was not observed in any of the prostate cell lines suggesting that it did not have an autocrine or paracrine effect on the regulation of growth and progression in these cells, which is in contrast to other malignancies where chemokines are involved in promoting cell proliferation in vitro and in vivo via an autocrine or paracrine pathway [Araki K et al 2009, Hussain F et al 2010, Lo BK et al 2010, Raychaudhuri B and Vogelbaum MA 2010, Sauv   K et al 2009]. Interestingly, a few researchers have proposed that the autocrine production of CXCL12 by primary neoplasms may actually decrease the incidence of metastases, firstly by saturating the CXCR4 receptor on primary malignant cells and secondly because CXCL12 chemotactic gradients are lost [Gilbert DC et al 2009, Mirisola V et al 2009]. Certainly, in vivo, chemotaxis towards CXCL12-releasing metastasis target tissues would be reduced. Sites which have been shown to secrete high levels of CXCL12 include bone marrow, where CXCL12 is constitutively produced by osteoblasts, fibroblasts and endothelial cells [Imai K et al 1999, Muller A et al 2001, Ponomaryov T et al 2000, Sun YX et al 2005, Zou YR et al 1998] and also lymph nodes [Muller A et al 2001]. Both bone and lymph nodes are favoured sites of metastasis of prostate cancer. It is important to point out that stromal and vascular endothelial cells in other tissues eg. skeletal muscle, cardiac muscle, skin and kidney do not secrete high levels of CXCL12 [Muller A et al 2001, Phillips RJ et al 2003, Sun YX et al 2005].

From the results obtained using conventional RT-PCR we concluded that the CXCR4 receptor warranted further investigation, and quantitation of CXCR4 mRNA was performed in all prostate cell lines using real-time quantitative PCR (TaqMan). This

technique confirmed previous RT-PCR results with DU145, LNCaP and PC3 having approximately 1287, 407 and 21 times CXCR4 mRNA levels respectively, relative to 1542 CPT3X (1542 NPTX had similar expression to 1542 CPT3X and expression in Pre 2.8 was undetectable by TaqMan PCR). This large difference in expression between DU145 and LNCaP had not been apparent on visual inspection when using conventional PCR, as both appeared to have comparable band densities on the agarose gel (refer to chapter 4).

CXCR4 cell membrane protein expression was subsequently elucidated in prostate cell lines using flow cytometry. This demonstrated that in accordance with high CXCR4 mRNA levels, the metastatic cell lines also had high cell surface receptor expression. In the remaining cell lines low CXCR4 mRNA correlated with low CXCR4 protein expression. However, it was observed that there were two subpopulations of LNCaP cells - one had relatively low CXCR4 protein levels and the other had the highest CXCR4 levels amongst all the cell lines. The occurrence of these two subpopulations is most likely explained by the finding that LNCaP cells display phenotypic and genotypic heterogeneity in culture [Horoszewicz JS et al 1983, Wan XS et al 2003]. It is possible that a subpopulation of LNCaP cells with increased androgen receptor levels also expressed an increased concentration of CXCR4 cell surface protein as it has been noted that androgens raised the levels of both CXCR4 mRNA and functional protein in LNCaP prostate cancer cells [Frigo DE et al 2009]. In our experiments, it would have been interesting to simultaneously quantitate androgen and CXCR4 receptor levels within the LNCaP subpopulations. Additionally, of note, is that the protocol that we used for flow cytometry only established cell membrane CXCR4 protein levels, whereas it is now

known that CXCR4 receptor is present on the cell membrane in addition to the cytoplasm and nucleus, with nuclear CXCR4 thought to be non-functional [Wagner PL et al 2009]. We could have demonstrated *total* CXCR4 protein levels within cells using Western blotting, or alternatively, cytoplasmic and nuclear CXCR4 receptor could have been detected using flow cytometry by permeabilising the cell membrane.

Cell migration assays were used to confirm the functionality of the CXCR4 receptor in response to its ligand, CXCL12. These studies of cell motility suggested that in the metastatic cell lines DU145 and PC3, the expressed CXCR4 receptor was functional as the ligand CXCL12 α promoted chemotaxis presumably by actin polymerization and subsequent pseudopodial invasion. This effect was concentration dependent as increasing the concentration of ligand in DU145 cells promoted increased cell migration until saturation was reached. Also, this increased cell motility was specifically the result of CXCR4/ CXCL12 α interaction as the addition of anti-CXCR4 antibody decreased cell movement. PC3 cells, which had been shown to have lower cell surface CXCR4 protein levels, did migrate in the presence of CXCL12 α but at a much slower rate than DU145 cells and a much higher concentration of ligand was needed to promote cell migration (at 50ng/ml of CXCL12 α DU145 cells migrated but in the PC3 cell line no significant increase in chemotaxis was noted until a ligand concentration of 300ng/ml). However, as demonstrated by Taqman real-time PCR and flow cytometry results, 1542 NPTX expressed CXCR4 at very low or absent levels and thus there was no significant increase in cell migration in the presence of the ligand. The main disadvantage of the Boyden Chamber / Transwell® migration assays is that a very large number of cells is applied, but only a small fraction of the cells are analysed i.e. the migratory active

population of cells. Therefore, interpretations on the population as a whole can only be made when the cells behave as a homogeneous population. It is possible that in the DU145 and PC3 cell lines that only a subpopulation of cells with functional cytomembranous CXCR4 receptor (as compared to those with non-functional nuclear localisation of CXCR4) were able to migrate in response to the CXCL12 ligand.

However, the *in vitro* cell migration results suggested that prostate cancer cells expressing CXCR4 receptor may migrate to preferred sites of metastasis, such as bone and lymph nodes, down a CXCL12 concentration gradient. The next step would have been to demonstrate that CXCL12 – CXCR4 mediated chemotaxis is important *in vivo* in the localization of prostate cancer cells to favoured sites of metastasis. This has since been verified by Sun YX et al 2005, who used a murine model to provide critical support for the CXCL12 – CXCR4 axis in prostate cancer skeletal metastasis.

Interestingly, laser microdissected primary tumour samples and benign prostate tissue from patients had CXCR4 mRNA levels higher than that of DU145. Sun YX et al 2003 have, however, suggested that post-transcriptional modification of the CXCR4 receptor plays a major role in regulating protein expression and therefore, although CXCR4 mRNA levels are high in primary tumour samples and in patient benign tissue specimens, protein expression may be low, particularly in the benign samples [Sun YX et al 2003]. Another explanation would be that high mRNA levels *in vivo* may not necessarily translate into high *in vivo* CXCR4 protein levels because it has been observed that CXCR4 undergoes significant spontaneous endocytosis and that recycling of internalized receptors is not efficient [Tarasova NI et al 1998]. Alternatively, high CXCR4 expression by patient primary tumours may be the result of a survival benefit in

primary cancer cells expressing this receptor in vivo, and these tumours may be more aggressive and likely to metastasise. In support of this theory is the discovery by investigators that hypoxia induces CXCR4 expression in malignant cells via increased levels of HIF-1 α [Dunn LK et al 2009, Schioppa T et al 2003, Staller P et al 2003, Zagzag D et al 2005]. Therefore CXCR4 may become expressed during primary tumour growth when partial pressures of oxygen diminish within the expanding tumour, thereby promoting the chemotaxis of cancer cells away from hypoxic areas into sites secreting high levels of CXCL12 (which are presumably also well oxygenated). Several researchers have confirmed that primary tumours expressing high levels of CXCR4 protein are likely to behave more aggressively. These include Mochizuki H et al 2004, who showed that, in a sample of 35 human primary prostate malignancies, positive expression of CXCR4 protein was an independent predictor of bone metastasis. Also, in neoplasms other than prostate, high CXCR4 expression in primary cancer of the breast [Chu QD et al 2010] and thyroid is associated with a poorer prognosis [Wagner PL et al 2008].

It is a possibility that in vivo metastatic prostate cells may, in fact, express CXCR4 mRNA at even higher levels than primary tumour but unfortunately we were unable to obtain fresh prostate metastatic tissue from patients, which could be laser microdissected. An alternative would have been to construct a tissue microarray of normal/benign prostate tissue, primary and metastatic prostate tumours [as achieved by Sun YX et al 2003] and compare CXCR4 protein expression using immunohistochemistry. This tissue microarray has now been constructed by subsequent

researchers in the department, although it contains only benign and malignant tissue from radical prostatectomy specimens (i.e. it does not contain tissue derived from metastases).

It should be noted that although the results had specifically suggested that CXCL12-CXCR4 interaction promotes the chemotaxis of prostate cancer cells to preferred metastatic sites, this pathway may also be involved in additional steps of the metastatic cascade such as neoplastic cell proliferation, neoangiogenesis and/ or local invasion. Also, the CXCL12-CXCR4 axis is only one of several pathways implicated in organ specific metastasis. Other factors include vascular flow patterns, adhesion with the endothelium in distant organs and interaction between tumour cells and their microenvironment at the secondary site. Establishment of successful cancer metastasis may fail as a result of a deficiency in any one of these processes. Additionally, chemotaxis of prostate cancer cells may occur in vivo in the absence of CXCL12-CXCR4 interaction as alternative (although less potent) chemoattractant molecules have been identified including osteonectin, TGF β 1, EGF and IGF1/ 2.

SECTION 8.2

CONFIRMATORY STUDIES OF CXCL12 – CXCR4 INTERACTION IN THE MIGRATION AND DISSEMINATION OF PROSTATE CANCER

Not surprisingly, following the paper relating the important role of CXCL12 – CXCR4 interaction in breast cancer metastasis by Muller A et al in 2001, many investigators throughout the world had the similar idea of demonstrating the significance

of this axis in a variety of human neoplasms. We and other researchers simultaneously investigated this pathway in prostate cancer. However, Taichman RS et al 2002 were the first to publish their research and provide evidence for the involvement of this chemokine ligand – receptor axis in prostate cancer metastasis to bone using in vitro studies with prostate cell lines. The same group followed up this publication with an important article approximately 1 year later with in vivo evidence for the hypothesis [Sun YX et al 2003]. They constructed a high-density tissue microarray from clinical prostate samples obtained from a cohort of over 600 patients. Immunostaining of the microarrays using CXCR4 monoclonal antibody revealed weak CXCR4 expression in normal/ benign prostate epithelium, moderate-to-strong CXCR4 protein expression in clinically localized prostate cancer samples and highest CXCR4 expression in metastatic lesions. However, on determining CXCR4 mRNA from a series of patient samples, they discovered that the CXCR4 mRNA levels in BPH, localized and metastatic cancers were elevated relative to normal adjacent tissues. In fact mean peak CXCR4 mRNA expression occurred in BPH tissue, followed by localised prostate cancer and lowest levels in metastatic prostate epithelium (but overall there was no statistical difference between the three). It was suggested that post-transcriptional regulation of the receptor plays a major role in regulating CXCR4 protein expression. More recently, the group have provided support for the CXCL12 – CXCR4 axis participating specifically in the localisation of metastatic prostate tumours to the bone marrow using a murine model [Sun YX et al 2005] and also demonstrated the activation of various signalling mechanisms on CXCL12 binding to CXCR4 [Wang J et al 2005]. Additional signalling pathways activated on CXCL12 –

CXCR4 interaction have been elucidated by Bendall LJ et al 2005, Goldsmith ZG and Dhanasekaran DN 2007, Kukreja P et al 2005, Mellado M et al 2001, Ward SG 2006.

The findings of Taichman's group have been both confirmed and extended by Xing Y et al 2008, who showed that the stable down-regulation of CXCR4 inhibited CXCL12 α -promoted prostate cancer cell adhesion to osteosarcoma and endothelial cells, inhibited migration plus invasion through Matrigel, and reduced the incidence of prostate cancer establishment and growth when the tumour cells were injected into the tibial bone of mice. Also, it has been observed that subcutaneously injected prostate cancer cells transfected with CXCR4 grew larger tumours with increased muscle invasion compared with parental cells [Darash-Yahana M et al 2004].

Vaday GG et al 2004 established that single chain Fv anti-CXCR4 antibodies inhibited prostate cancer cell migration and invasion in vitro and also reduced CXCL12 induced calcium mobilisation in PC3 and LNCaP cells. Invasion through ECM components by malignant prostate cell lines (LNCaP and/ or PC3) in response to CXCL12 was shown to be a result of increased MMP expression (specifically MMP-1, MMP-2, MMP-3, MMP-9, MMP-14) [Chinni SR et al 2006, Hu W et al 2008, Singh S et al 2004a]. CXCL12 – CXCR4 interaction, resulting in increased MMP-9 and MMP-2 expression, has been implicated in perineural invasion of prostate cancer using human tissue and cell lines [Zhang S et al 2008]. This increased expression of proteases on CXCL12 stimulation most likely creates a pathway for cell movement/ invasion.

Interestingly, Miwa S et al 2005, observed that in a mouse model the bisphosphonate, minodronate, may inhibit prostate cancer cell invasion into the bone matrix by repressing the expression of CXCR4 in bone metastasis lesions and Engl T et al

2006 have established that CXCL12 – CXCR4 interaction resulted in enhanced expression of alpha5 and beta3 integrins in LNCaP and DU145 cell lines, which enabled increased adhesion of these cells to human endothelium or to ECM proteins (laminin, collagen, fibronectin). These latter findings provide a link between chemokine receptor expression and integrin-triggered tumour dissemination.

Recently, it has been demonstrated that androgens increased the levels of both CXCR4 mRNA and functional protein in LNCaP prostate cancer cells [Frigo DE et al 2009]. Importantly, androgens enhanced the migration of LNCaP cells toward a CXCL12 gradient, an effect that could be blocked by a specific CXCR4 receptor antagonist [Frigo DE et al 2009]. This suggests that androgens may be involved in the regulation of pathways that are responsible for the homing of prostate cancer cells to select microenvironments.

Other investigators demonstrated, in a small clinical sample, that positive expression of CXCR4 protein was an independent and superior predictor for bone metastasis to Gleason sum [Mochizuki H et al 2004] and also that high levels of CXCR4 induced a more aggressive phenotype in prostate cancer cells in vivo [Darash-Yahana M et al 2004]. Additionally, in a series of prostate cancer samples obtained from 52 men with metastatic prostate cancer, Akashi T et al 2008, demonstrated that patients with a high expression of CXCR4 in tumours had poorer cancer-specific survival than those with low expression of CXCR4, thus suggesting that CXCR4 expression was a useful prognostic factor for patients with metastatic prostate cancer treated with androgen-withdrawal therapy.

Of particular note and of current interest is that immunostaining of clinical prostate specimens has shown that a subpopulation of tumour cells with a stem cell-like phenotype (i.e. possible prostate cancer stem cells which were CD133+) also expressed CXCR4 [Miki J et al 2007]. The authors suggested that the CXCL12 - CXCR4 pathway may be important in the chemotaxis of these possible cancer stem cells.

We published the results from our research in 2004 [Arya M et al 2004 – abstract in Appendix, page 309].

SECTION 8.3

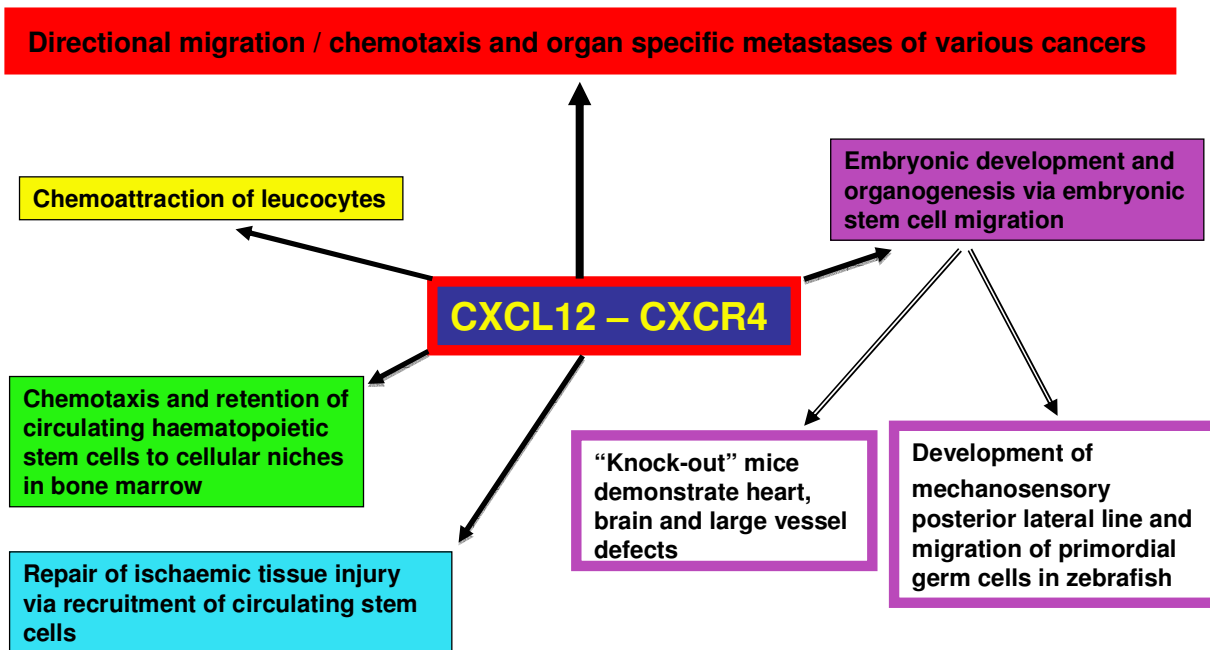
THE IMPORTANCE OF THE CXCL12 – CXCR4 AXIS IN TUMOUR CELL MIGRATION

We, and colleague scientists, have elucidated that CXCL12 – CXCR4 interaction has a distinctive biological role. Since the publication of the seminal paper in “Nature” by Muller A et al 2001, implicating the key role of this axis in the organ-specific metastasis of breast cancer, there has been great interest in this pathway, particularly in the promotion of cell migration, and the resulting implications for cancer therapy. A summary of the pathophysiological role of the CXCL12 – CXCR4 axis in relation to cellular migration/ chemotaxis (which is discussed in detail below), is shown in figure 8.1.

CXCL12 ligand is constitutively expressed by stromal cells in many tissues with highest expression in bone marrow (fibroblasts, osteoblasts, endothelial cells), lymph nodes, lung and liver and markedly lower expression levels in the small intestine, skin

and skeletal muscle [Bradstock KF et al 2000, Imai K et al 1999, Muller A et al 2001, Ponomaryov T et al 2000, Taichman RS et al 2002, Zou YR et al 1998]. Functional CXCR4 receptor is found in a wide variety of adult tissues including on peripheral blood T lymphocytes [Bleul CC et al 1997], monocytes [Bleul CC 1996 et al], plasma cells [Nakayama T et al 2003], subsets of natural killer cells [Hanna J et al 2003], dendritic cells [Zoetewij JP et al 1998], adult CD34+ bone marrow stem/progenitor cells [Aiuti A et al 1997], vascular smooth muscle cells [Schechter AD et al 2003], endothelial cells [Gupta SK et al 1998], intestinal [Dwinell MB et al 1999] and alveolar epithelial cells [Murdoch C et al 1999], microglia, neurons and astrocytes [Zou YR et al 1998].

Figure 8.1: A summary of the pathophysiological role of CXCL12 – CXCR4 interaction in cellular migration/ chemotaxis



Initial investigations on the CXCR4 receptor concentrated on its role in the pathogenesis of HIV infection. In 1996, the field of inflammation and HIV virology unexpectedly overlapped due to the discovery that chemokine receptors were identified as co-receptors and, that in conjunction with CD4, allowed HIV to infect the host cell [Feng Y et al 1996]. Approximately 90% of HIV strains infect using the CCR5 chemokine receptor (macrophage tropic) but the virus can mutate to use CXCR4 (T-cell tropic). Strains have been identified that can use other chemokine receptors, but all use either CCR5 or CXCR4.

Subsequently, CXCL12 – CXCR4 interaction was discovered to be involved in embryonic development and organogenesis. “Knock-out” mice studies have demonstrated that mice in which either CXCR4 or CXCL12 genes have been deleted do not develop normally and the majority die in utero with defects in heart, brain and large vessel development [Zou YR et al 1998, Ma Q et al 1998, Nagasawa T et al 1996, Tachibana K et al 1998]. The development of the mechanosensory posterior lateral line and migration of primordial germ cells in zebrafish is dictated by CXCR4 expressing cells, which respond to a CXCL12-like molecule [David NB et al 2002, Doitsidou M et al 2002]. Primordial germ cell migration in murine and fish embryos is also under the influence of CXCL12 - CXCR4 interactions and deletion or inhibition of CXCR4 or CXCL12 results in significantly decreased migration and ectopic location of the primordial germ cells [Ara T et al 2003, Knault H et al 2003]. These results suggest a pivotal role for CXCL12 – CXCR4 in organogenesis via the control of embryonic stem cell migration. Additionally, as these studies demonstrate that CXCR4 is expressed in early foetal development, this could partly explain the fact that tumour cells that originate in various

organs from the population of transformed or dedifferentiated cells often express cell surface CXCR4. This also implies that CXCL12 may influence tumour metastasis via the migration of CXCR4 positive tumour cells to specific sites, in a similar manner to its role in the migration of embryonic pluripotent stem cells.

As mentioned earlier, CXCL12 is constitutively secreted by adult bone marrow stromal cells. These create cellular niches in which CD34+ haematopoietic stem cells (HSCs) and progenitors are retained for growth and differentiation [Fuchs E et al 2004]. The chemotaxis or homing of circulating CXCR4 expressing HSCs to the cellular niches in the bone marrow, in addition to their subsequent retention in these sites, is controlled by CXCL12 [Aiuti A et al 1997, Broxmeyer HE et al 2003, Wright DE et al 2002]. These findings have been supported in clinical trials demonstrating that CXCR4 antagonists can result in leucocytosis due to rapid mobilization of HSCs [Broxmeyer HE et al 2005, DiPersio JF et al 2009, Dugan MJ et al 2010]. Besides HSCs, it has now been realised that functional CXCR4 is also expressed on the surface of various normal stem cells for different organs and tissues in adults (also referred to as tissue-committed stem cells, TCSCs) [Kucia M et al 2005]. Importantly, researchers have currently suggested that not only is CXCR4 expressed by embryonic stem cells and TCSCs but the receptor is additionally found on the cell membrane of cancer stem cells (CSCs) of various tissues and is vital in the homing of these CSCs to their specific metastatic site (following a CXCL12 chemotactic gradient) [Gelmini S et al 2008, Kucia M et al 2005, Visvader JE and Lindeman GJ 2008]. Thus CXCR4 can be considered a universal marker of all groups of stem cells.

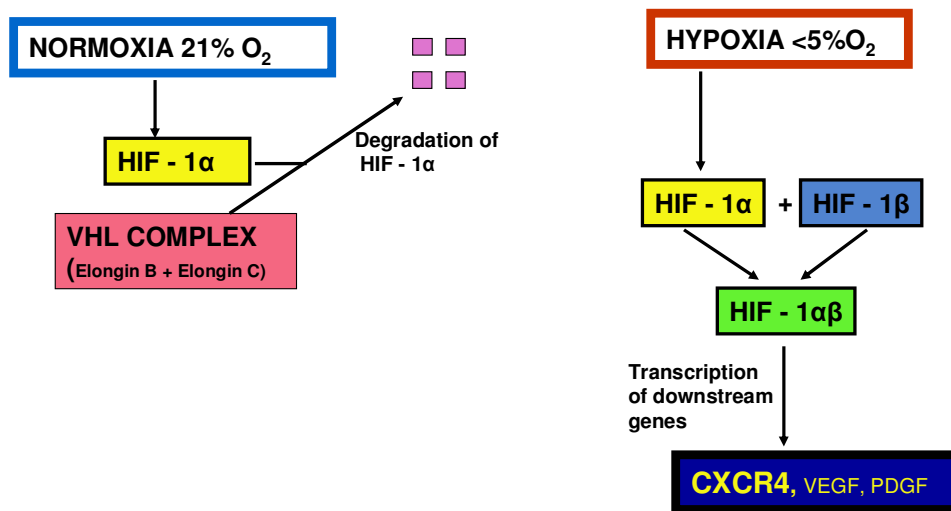
CXCL12 – CXCR4 interaction is also involved in the repair of ischaemic tissue injury, which involves the specific recruitment of circulating TCSCs or progenitor cells. Ceradini DJ et al 2004 observed that tissue hypoxia resulted in increased levels of hypoxia-inducible factor-1 α (HIF-1 α) in endothelial cells, which subsequently induced CXCL12 expression in the ischemic areas in direct proportion to reduced oxygen tension in vivo. Therefore, circulating progenitor/ stem cells migrate to areas of ischaemic tissue necrosis due to an increase in CXCL12 expression by endothelial cells, induced by HIF-1 α , to become involved in tissue repair. Once oxygen tension normalises and tissue regeneration has occurred expression of CXCL12 decreases [Ceradini DJ et al 2004]. Also, distinct niches of hypoxia are present in normal bone marrow that display increased levels of HIF-1 α induced CXCL12. Circulating CXCR4 positive progenitor cells of various tissues (i.e. TCSCs) such as muscle, liver, neural, retinal, renal tubular as well as HSCs, all localise within these niches and become mobilised during periods of tissue damage – a concept first described by Ratajczak M and colleagues [Ratajczak MZ et al 2004, Kucia M et al 2004]. Significantly, studies have suggested that hypoxia induces CXCR4 expression in tumour cells via HIF-1 α (in a similar manner to inducing CXCL12 in endothelial cells in ischaemic tissue injury) [Dunn LK et al 2009, Schioppa T et al 2003, Staller P et al 2003, Zagzag D et al 2005]. Initial studies confirming this related to the von Hippel-Lindau (VHL) protein, which is the product of the VHL tumour suppressor gene, and which promotes degradation of HIF-1 α under normoxic conditions (figure 8.2). However, under hypoxic conditions, or in renal cell cancers having deletions or inactivation of the VHL gene, this process is suppressed and thus HIF-1 α levels

increase and this promotes tumour cell expression of the CXCR4 receptor (figure 8.2) [Pan J et al 2006, Staller P et al 2003, Zagzag D et al 2005].

Figure 8.2: This demonstrates how hypoxia induces CXCR4 expression in renal clear cell cancer cells. Under normoxic conditions the VHL protein (a product of the VHL tumour suppressor gene) combines with Elongin B and C and promotes proteasomal degradation of HIF-1 α . However, under hypoxic conditions (or in renal cancer having inactivation of the VHL gene), HIF-1 α levels increase and this heterodimerises with HIF-1 β , which promotes tumour cell expression of the CXCR4 receptor in addition to several angiogenic factors (VEGF, PDGF).

VHL - von Hippel-Lindau protein, HIF-1 - hypoxia-inducible factor-1, VEGF – vascular endothelial growth factor, PDGF – platelet derived growth factor

Figure 8.2: The hypoxic control of CXCR4 expression in renal carcinoma cells



In fact, increased levels of CXCR4 in patients with renal clear cell cancers are associated with poor prognosis and decreased survival [Staller P et al 2003, Zagzag D et al 2005, Wang L et al 2009]. This may explain how CXCR4 becomes expressed during tumour development thus allowing the cancer cells to migrate from hypoxic areas, thereby

favouring metastasis as the oxygen concentration decreases within the tumour. This also demonstrates how the HIF-1 pathway, which is involved in controlling the expression of CXCL12 and CXCR4 in the homing of progenitor cells to injured tissues, may have been adapted by cancer cells to allow their directional migration down chemotactic gradients to specific organs secreting CXCL12, such as the bone marrow and lymph nodes.

CXCR4 is the most common chemokine receptor expressed in cancers and levels of its ligand, CXCL12, are highest in the common sites of metastases of many cancers i.e. lung, liver, bone marrow and lymph nodes [Bradstock KF et al 2000, Imai K et al 1999, Muller A et al 2001, Ponomaryov T et al 2000, Taichman RS et al 2002, Zou YR et al 1998]. This suggests that the CXCL12 – CXCR4 axis may be crucial in the organ specific metastasis of many cancers.

In vitro experiments observing the locomotion of individual cells using time-lapse monitoring have demonstrated that CXCL12 increases the motility of several human tumour cell lines derived from breast cancer, rhabdomyosarcoma and small cell lung cancer [Adams GB et al 2003, Libura J et al 2002]. Additionally, neoplastic cells migrated extensively in the presence of CXCL12, with CXCL12 increasing the final displacement, the average velocity of cell displacement and stimulating the formation of a leading edge in migrating cancer cells [Libura J et al 2002]. Many studies have also shown that CXCL12 promotes the directional migration or chemotaxis of neoplastic cells as well as invasion through Matrigel, endothelial cells, bone marrow stromal, or fibroblast monolayers, via the CXCR4 receptor [Balkwill F 2004a and b, Ben-Baruch A 2008, Zlotnik A 2008]. Also, in cell lines derived from malignancies such as small cell lung cancer and osteosarcoma, not only does CXCR4 activation induce migratory and

invasive responses, but it also results in activation and signaling of tumour-associated integrins that play an important role in tumour adhesion and progression [Hartmann TN et al 2005, Huang CY et al 2009]. In laryngeal and hypopharyngeal squamous cell carcinoma cell lines, motility and invasiveness were enhanced by CXCL12 acting through CXCR4, resulting in upregulation of MMP-13 [Tan CT et al 2008]. Interestingly, Bertran E et al 2009 treated hepatoma cells with TGF- β and selected the cells that survived its apoptotic effect and underwent epithelial-mesenchymal transition. The resultant mesenchymal, de-differentiated, phenotype had significantly elevated levels of CXCR4, which enhanced the cells' migratory abilities in response to CXCL12.

In vivo studies such as that by Bartolomé RA et al 2009 (using a xenograft mouse model) have shown that CXCR4 is required for melanoma metastasis to the lungs (specifically in the early phases of melanoma cell arrival in the lungs). Also, transfection of a melanoma cell line with CXCR4 redirected this cell line to metastasize to the lung instead of the lymph nodes [Murakami T et al 2002]. In pancreatic cancer, the soluble protein, pancreatic adenocarcinoma upregulated factor (PAUF), enhanced the metastatic potential of pancreatic cancer cells, at least in part, by upregulating CXCR4 expression in an orthotopic xenograft mouse model [Lee Y et al 2010]. Using bioluminescent imaging to quantify relative volumes of tumour burden after breast cancer cells were injected into the left cardiac ventricle, Huang EH et al 2009 indicated that treatment with a CXCR4 antagonist significantly reduced metastasis as well as primary tumour growth. Also, when non-small cell lung cancer cells are grown in SCID mice only 35% of cells in the primary tumour expressed CXCR4 compared with 99% of cells in metastases [Phillips RJ et al 2003].

In addition to in vitro and in vivo experiments there is now an increasing amount of evidence from retrospective clinical studies (using tissue samples derived from patients) that the CXCL12-CXCR4 pathway is involved in metastasis. Importantly, Muller A et al 2001 initially reported strong CXCR4 expression using immunohistochemistry in metastatic breast cancer tissue. This finding has been confirmed by Liu Y et al 2010, who demonstrated that high expression of CXCR4 (and CCR7) may be associated with lymph node metastasis. Moreover, the expression of these receptors served as an indicator of undesirable prognosis in patients with breast neoplasia. Also, high CXCR4 overexpression in primary tumours has been shown to be predictive of worse outcomes in hormone receptor-positive, node-negative breast cancer patients [Chu QD et al 2010]. Surprisingly, in another recent study, microarray gene expression analysis and immunohistochemistry revealed that increased expression of CXCL12 but not of CXCR4 significantly correlated with disease-free and overall survival in breast cancer and that CXCL12 was a strong, independent prognostic marker of this [Mirisola V et al 2009]. The group proposed that saturation of the CXCR4 receptor through autocrine CXCL12 production reduced chemotaxis towards CXCL12-releasing metastasis target tissues thus decreasing the number of breast cancer metastases formed [Mirisola V et al 2009]. In urological neoplasms, increased levels of CXCR4 in patient renal clear cell cancers are associated with poor prognosis and decreased survival [Zagzag D et al 2005, Staller P et al 2003]. Additionally, using immunohistochemistry, Wang L et al 2009 noted that renal cell carcinoma metastasis was associated with higher expression of CXCR4 (in comparison to primary tumours and normal tissue) but of particular note was the finding by these researchers that the interaction of CXCR4 and its ligand CXCL12

resulted in the internalization of CXCR4 from the cytoplasmic membrane. In bladder cancer, Nishizawa K et al 2010 identified that CXCR4 expression was induced in high-grade superficial bladder malignancies, including carcinoma-in-situ and invasive bladder tumours. Another group observed consistent expression of CXCR4 mRNA and protein in testicular germ cell tumours that accounted for their patterns of relapse in sites of known high CXCL12 expression [Gilbert DC et al 2009]. However, these scientists also found that expression of CXCL12 in stage I non-seminomas was significantly associated with organ-confined disease post-orchidectomy and reduced risk of relapse [Gilbert DC et al 2009]. They suggested that this may be through the loss of CXCL12 gradients that might otherwise attract cells away from the primary tumour. In oesophageal cancer, CXCR4 expression was identified as an independent variable that was most strongly associated with reduced disease specific survival [Kaifi JT et al 2005]. Interestingly, this study also showed that CXCR4 correlated with the presence of disseminated, potentially 'dormant' tumour cells in bone marrow and lymph nodes, implicating the receptor in early micrometastatic spread of single tumour cells. Additionally, expression of CXCR4 by papillary thyroid carcinoma correlated with indicators of tumour aggressiveness, including tumour size, extrathyroidal extension, angiolymphatic invasion and lymph node metastasis [Wagner PL et al 2008]. Also of note was the discovery that cytomembranous expression of CXCR4 in adenocarcinoma of the lung was an independent risk factor associated with worse disease-free survival, whereas nuclear immunostaining of the chemokine receptor conferred a survival benefit [Wagner PL et al 2009]. The authors suggested that these findings were consistent with a model in which CXCR4 promoted tumour cell proliferation and metastasis when present in the cytoplasm or cell membrane,

whereas localization of this molecule in the nucleus prevented it from exerting these effects.

SECTION 8.4

THERAPEUTIC IMPLICATIONS

The work in this thesis has demonstrated that the CXCL12 – CXCR4 pathway may be important in the organ specific metastasis of prostate cancer and this has been validated by other researchers. As discussed, the essential role of the CXCL12 – CXCR4 axis has additionally been shown to be pivotal in the chemotaxis of other neoplasms to specific metastatic sites. Therefore manipulation of this signaling pathway could be of therapeutic benefit to patients.

1) Small molecule CXCR4 antagonists

There have been great difficulties in the development of small molecule chemokine receptor antagonists. It was assumed that the search for chemokine receptor antagonists would be similar to that of other G-protein coupled receptors, but chemokine receptors are not typical of this receptor group. The number of ligands for a particular receptor, the ligand size, and the type of interaction between ligands and receptors are different [Onuffer J and Horuk R 2002]. Additional reasons for this slow progress include differences in affinity of the antagonists for human and animal chemokine receptors resulting in problems in the interpretation and relevance of preclinical trials. Another problem has been redundancy of the target i.e. several chemokine receptors may be

involved in the specific pathway or process of interest, which would mean that more than one receptor would have to be inhibited in order to demonstrate efficacy in clinical trials. Despite these difficulties, considerable progress has now been made and several small molecule chemokine receptor antagonists have now been developed, which may provide clinical benefit in cancer management.

a) Non-peptide CXCR4 antagonists - CXCR4 antagonists were first studied and developed in an effort to prevent the entry of the HIV-1 virus into its target cells, as this receptor (and CCR5) is known to be a co-receptor used by the HIV-1 virus for entry into T cells and macrophages (as already discussed in chapter 1). The bicyclams, in particular AMD3100 (plerixafor), are potent specific antagonists of CXCR4. AMD3100, a non-peptide CXCR4 antagonist, selectively and reversibly antagonizes the binding of CXCL12 to CXCR4. The critical role of the CXCR4-CXCL12 receptor-ligand interaction for CD34+ haematopoietic stem cell retention in the bone marrow has been discussed. It has been shown that AMD3100 can specifically mobilize CD34+ haematopoietic progenitor/ stem cells from the bone marrow, which is of considerable clinical benefit as a significant number of cancer patients cannot receive high-dose chemotherapy with subsequent peripheral blood progenitor cell transplantation because they fail haematopoietic stem/ progenitor cell mobilization.

In phase 3 clinical studies AMD3100 has been demonstrated to act synergistically with the established mobilizing agent, granulocyte colony-stimulating factor, for autologous stem-cell transplantation in non-Hodgkin's lymphoma and multiple myeloma patients [DiPersio JF et al 2009, Dugan MJ et al 2010]. AMD3100 was well tolerated with only mild, transient toxicity. Thus, patients can collect more haematopoietic

progenitors in fewer apheresis sessions, and patients that previously failed can now successfully collect sufficient peripheral blood progenitor cells for transplantation. In fact, AMD3100 was recently FDA-approved for stem cell mobilization in combination with granulocyte-colony stimulating factor in patients with non-Hodgkin's lymphoma and multiple myeloma. CXCR4 antagonists are the most exciting development in the field of peripheral blood progenitor cell mobilization for over a decade.

In promising studies related to solid cancers, administration of AMD3100 has been shown to prevent clonogenic growth, VEGF secretion, and intercellular adhesion molecule-1 expression of colorectal cancer cells in vitro [Ottiano A et al 2006]. Also, inhibiting CXCR4 with AMD3100 in murine 4T1 cells—a highly metastatic mammary cancer cell line and model for stage IV human breast cancer—substantially delayed the growth of metastatic 4T1 cells in the lungs of mice [Smith MC et al 2004]. In a mouse experiment of liver metastasis, intraperitoneal administration of AMD3100 blocked the metastatic potential of colon cancer cells [Matsusue R et al 2009].

b) Small peptide CXCR4 antagonists - another CXCR4 antagonist, T140 (and its analogues TN14003 and TC14012), has also been developed. This is classed as a small peptide CXCR4 antagonist. Studies on this 14-residue polypeptide, as well as AMD3100, found that each inhibits CXCR4 via different mechanisms. AMD3100 has weak partial agonist (CXCL12-like) activity, inducing CXCL12-like G-protein activation in cells with this receptor whereas T140 functions as an inverse agonist and does not induce any signaling on binding to CXCR4 [Trent JO et al 2003, Zhang WB et al 2002]. Since CXCR4 activation by a CXCR4 antagonist may be a disadvantage to the treatment of diseases in which CXCR4 activation provides a survival signal (e.g. prostate and breast

cancer), T140-derived CXCR4 antagonists might have an advantage over AMD3100. T140 CXCR4 antagonists have shown activity in animal tumour models and this provides a rationale for future clinical trials of these agents in patients with neoplastic disease [Takenaga M et al 2004, Tamamura H et al 2004]. In fact, the T140 analogue, TN14003 (BKT140), is currently under clinical development for patients with multiple myeloma [Burger JA et al 2011].

c) Monoclonal antibodies - therapeutic monoclonal antibodies targeting the CXCR4 receptor have also been developed but this has proved to be challenging as the CXCR4 receptor exhibits conformational heterogeneity, which is responsible for differential antibody binding in most cell types. These conformational differences may be the result of heterogeneity in post-translational events such as glycosylation [Chabot DJ 2000], sulfation [Farzan M et al 2002] or phosphorylation [Orsini MJ et al 1999] in cancer cells, which would result in structurally distinct forms of CXCR4. Other potential possibilities for CXCR4 conformational heterogeneity include changes in cell membrane lipid composition (in which the receptor resides), receptor oligomerisation or interaction with as yet unidentified molecules. However, neutralisation of CXCR4 using monoclonal antibodies has shown potential as a future cancer therapy in animal models of several neoplasms including those of the prostate [Engl T et al 2006] and endometrium [Gelmini S et al 2009] in which metastasis and progression was significantly impaired.

d) CXCL12 analogues - CTCE-9908, a peptide analogue of CXCL12, is a competitive antagonist of CXCR4. It has been shown to significantly reduce metastasis as well as primary tumour growth in mouse models of breast [Hassan S et al 2011, Huang EH et al 2009] and prostate cancer [Porvasnik S et al 2009]. In fact CTCE-9908 has now

received orphan drug status by the FDA for the treatment of osteogenic sarcoma. Importantly, CTCE-9908 is the only CXCR4 antagonist that has been used in clinical trials. In a phase I/II clinical trial enrolling 25 patients with metastatic solid cancers, which were resistant to standard treatment, CTCE-9908 showed good tolerability. Additionally, modest response rates were seen with 6 patients having overall stable disease after one cycle of the drug and 1 patient demonstrating a significant reduction in tumour size after less than one cycle of treatment [Kavsak PA et al 2009].

e) Novel CXCR4 antagonists being developed - small interfering RNAs (siRNA) inhibit the expression of a gene by inducing cleavage of the specific mRNA. Using a small interfering RNA retrovirus vector driven by human prostate-specific antigen promoter and targeting the CXCR4 gene, Du YF et al 2008 demonstrated that CXCR4 protein expression in LNCaP cells was blocked. In colorectal cancer, siRNA silencing CXCR4 expression abrogated CXCL12 induced migration of cells in vitro [Rubie C et al 2011]. These and other results have suggested great potential for RNA interference based therapeutic approaches for use in targeted cancer therapy.

Small molecular inhibitors of transcriptional coactivation of HIF-1 α are also being developed. This can result in downregulation of CXCL12 in various tissues and inhibit metastasis of CXCR4 positive tumour cells [Block KM et al 2009, Kung AL et al 2004].

A single domain antibody is an antibody fragment comprising a single monomeric variable antibody domain – these are termed nanobodies. Jahnichen S et al 2010 have reported the isolation and characterization of functional VHH-based (i.e. heavy chain) nanobodies against CXCR4. Two highly selective monovalent nanobodies, 238D2 and 238D4, competitively antagonised the chemoattractant effect of CXCL12 in CXCR4

expressing Jurkat leukaemia T cells. Only picomolar concentrations of these nanobodies was required, which represents the most potent CXCR4 inhibitors described up till now. These nanobodies provide a novel and promising method of inhibiting the CXCR4 receptor in cancer cells.

2. Immunotherapy

Chemokines may have great potential as agents in cancer immunotherapy. As they function physiologically as immunostimulatory molecules (i.e. promotion of chemotaxis and the effector function of leucocyte subpopulations), these proteins may be used to enhance antitumour immunity in the host. Several approaches have been used in the delivery of chemokines, such as CXCL12, into the tumour microenvironment.

a) Transduction of tumour cells with chemokine genes - as human tumours generally elicit only a weak host immune response, it would be greatly advantageous to render them immunogenic. Chemokines may be used to modify the tumour microenvironment and promote antitumor adaptive immune responses. Fushimi T et al 2006 showed that adenoviral gene transfer of CXCL12 into murine tumours resulted in the attraction of dendritic cells to the tumour and inhibition of tumour growth by activation of a cancer specific cellular immune response involving CD8+ cytotoxic T lymphocytes. An advantage of using chemokines is that, unlike tumour suppressor genes, it is theoretically not necessary for every tumour cell to be transduced.

b) The administration of tumour vaccine (combining tumour antigen and chemokines) - non-immunogenic tumour antigens can be rendered immunogenic when fused with chemokines. CXCL10 or CCL7 fusion to lymphoma immunoglobulin resulted

in variable regions eliciting leucocyte chemotactic responses in vitro and inducing inflammatory responses in vivo. Also, they enhanced protection against tumour challenge. Similarly, Zhang T et al 2005 have suggested that CXCL12 may be useful as an immunotherapeutic agent for cancer patients when fused with tumour antigen.

3. CXCR4/ CXCL12 as prognostic markers in cancer

The expression of CXCR4 in many malignancies may be used as a prognostic marker. For example, in primary breast cancer it has been shown that high expression of CXCR4 is associated with lymph node metastasis and indicates poor prognosis in patients with breast tumours [Chu QD et al 2010, Liu Y et al 2010]. Thus, this group of patients with high CXCR4 expression may benefit from adjuvant treatment post surgery. In human prostate cancer tissue CXCR4 expression is associated with perineural invasion [Zhang S et al 2008] and in 35 patient samples CXCR4 protein was an independent and superior predictor for bone metastases than Gleason sum [Mochizuki H et al 2004]. In 52 patients with metastatic prostate cancer, those cancers with high CXCR4 expression had poorer cancer specific survival than those with lower levels [Akashi T et al 2008]. These results suggest that high CXCR4 expression in prostate cancer is associated with a more aggressive phenotype. This can help to guide management as for example those clinically localized primary prostate cancers which have a high CXCR4 index may not be suitable for active surveillance or focal therapy. Additionally, as discussed previously, expression of CXCL12 in stage I non-seminomas was demonstrated to be associated with organ-confined disease post-orchidectomy with reduced risk of relapse [Gilbert DC et al 2009]. This is most likely due to the loss of CXCL12 gradients that might otherwise attract cells

away from the primary tumour. These patients may be avoided unnecessary post-orchidectomy treatments with their associated toxicities. Mirisola V et al 2009 used microarray gene expression analysis and immunohistochemistry in breast cancer samples from patients and demonstrated that CXCL12 expression by the neoplasms was an independent prognostic marker of disease-free and overall survival. The group proposed that saturation of the CXCR4 receptor through autocrine CXCL12 production reduced chemotaxis towards CXCL12-releasing metastasis target tissues.

CXCR4 may, in fact, offer a cell surface target for molecular imaging of metastases, assisting diagnosis, staging and therapeutic monitoring. Also, non-invasive detection of CXCR4 expression of a primary neoplasm may give an indication of metastatic potential of the lesion. Interestingly, Jacobson O et al 2011 developed a derivative of the CXCR4 peptide antagonist, T140-2D, which was labeled with the positron emission tomography (PET) isotope copper-64. The researchers used this agent to successfully identify CXCR4 positive tumour xenografts in a mouse model using PET imaging. In a similar study, Nimmagadda S et al 2010, reported the development and evaluation of [(64)Cu]AMD3100, a positron-emitting analogue of the stem cell mobilizing agent plerixafor, to image CXCR4 in human tumour xenografts preselected for graded expression of this receptor. This imaging method was evaluated in lung metastases derived from human MDA-MB-231 breast cancer cells, and the results confirmed the ability of [(64)Cu]AMD3100 to determine CXCR4 expression using PET. However, further research with imaging tracers targeting CXCR4 is required due to the concurrent high uptake of these substances in metabolic organs such as liver and kidneys.

SECTION 8.5

CONCLUDING REMARKS

The results from this thesis have implicated the CXCL12 – CXCR4 axis in the organ specific metastasis of prostate cancer. CXCL12 - CXCR4 chemokine ligand – receptor interaction has additionally been observed to be pivotal in the metastasis of a variety of other malignancies. However, the ultimate aim of elucidation of the genetics of a tumour is to incorporate it into the clinical treatment of patients i.e. therapeutic strategies that are individually constructed for every patient. These personalized management strategies based on the molecular profiling of each neoplasm will allow the stratification of disease aggressiveness and prognosis and therefore permit the selection of appropriate and specific treatment.

Importantly, during the past 10 years there has been a chemokine revolution in cancer and both scientists and physicians are now aware of their crucial role at all stages of neoplastic transformation and progression. Great strides have been made in a relatively short period in elucidating the often complex relationship between chemokines and their role in cancer. The next 5 - 10 years are likely to see further exciting progress in the field of chemokine research in relation to cancer but particularly as regards the manipulation of various chemokine ligand – receptor pathways for therapeutic intervention in cancer patients. There is little doubt that potent new compounds will emerge, which will have the ability to influence the migration of CXCR4 positive tumour cells in cancer metastasis but will have fewer unwanted effects and complications. These developments will translate into significant survival benefits to patients.

REFERENCES

Aalinkeel R, Nair MP, Sufrin G, et al. Gene expression of angiogenic factors correlates with metastatic potential of prostate cancer cells. *Cancer Res.* 2004; 64: 5311-21

Abdollahi T, Robertson NM, Abdollahi A, et al. Identification of interleukin 8 as an inhibitor of tumor necrosis factor-related apoptosis-inducing ligand-induced apoptosis in the ovarian carcinoma cell line OVCAR3. *Cancer Res.* 2003; 63: 4521-26

Adams GB, Chabner KT, Foxall RB, et al. Heterologous cells cooperate to augment stem cell migration, homing, and engraftment. *Blood.* 2003; 101: 45-51

Addison CL, Daniel TO, Burdick MD, et al. The CXC Chemokine Receptor 2, CXCR2, is the Putative Receptor for ELR(+) CXC Chemokine- Induced Angiogenic Activity. *J Immunol.* 2000; 165: 5269-77

Aiuti A, Webb IJ, Bleul C, et al. The chemokine SDF-1 is a chemoattractant for human CD34+ hematopoietic progenitor cells and provides a new mechanism to explain the mobilisation of CD34+ progenitors to peripheral blood. *J Exp Med.* 1997; 185: 111-20

Akashi T, Koizumi K, Tsuneyama K, et al. Chemokine receptor CXCR4 expression and prognosis in patients with metastatic prostate cancer. *Cancer Sci.* 2008; 99: 539-42

Akiba J, Yano H, Ogasawara S, et al. Expression and function of interleukin-8 in human hepatocellular carcinoma. *Int J Oncol.* 2001; 18: 257-64

Alam TN, O'Hare MJ, Laczko I, et al. Differential expression of CD44 during human prostate epithelial cell differentiation. *J Histochem Cytochem.* 2004; 52: 1083-90

Allavena P, Sica A, Solinas G, et al. The inflammatory micro-environment in tumor progression: the role of tumor-associated macrophages. *Crit Rev Oncol Hematol.* 2008; 66: 1-9

Al-Mehdi AB, Tozawa K, Fisher AB, et al. Intravascular origin of metastasis from the proliferation of endothelium-attached tumor cells: A new model for metastasis. *Nat Med.* 2000; 6: 100-102

Angiolillo AL, Sgadari C, Taub DD, et al. Human interferon-inducible protein 10 is a potent inhibitor of angiogenesis in vivo. *J Exp Med.* 1995; 182: 155-62

Ara T, Nakamura Y, Egawa T, et al. Impaired colonization of the gonads by primordial germ cells in mice lacking a chemokine, stromal cell-derived factor-1 (SDF-1). *Proc Natl Acad Sci U S A.* 2003; 100: 5319-23

Ara T, Tokoyoda K, Okamoto R, et al. The role of CXCL12 in the organ-specific process of artery formation. *Blood.* 2005; 105: 3155-61

Araki K, Shimura T, Yajima T, et al. Phosphoglucose isomerase/autocrine motility factor promotes melanoma cell migration through ERK activation dependent on autocrine production of interleukin-8. *J Biol Chem.* 2009; 284: 32305-11

Araki S, Omori Y, Lyn D, et al. Interleukin-8 is a molecular determinant of androgen independence and progression in prostate cancer. *Cancer Res.* 2007; 67: 6854-62

Arya M, Bott SR, Shergill IS, et al. The metastatic cascade in prostate cancer. *Surg Oncol.* 2006; 15: 117-28

Arya M, Patel HR, McGurk C, et al. The importance of the CXCL12-CXCR4 chemokine ligand-receptor interaction in prostate cancer metastasis. *J Exp Ther Oncol.* 2004; 4: 291-303

Ashcroft RG, Lopez PA. Commercial high speed machines open new opportunities in high throughput flow cytometry. *J Immunological Methods* 2000; 243:13–24

Autzen P, Robson CN, Bjartell A, et al. Bone morphogenetic protein-6 in skeletal metastases from prostate cancer and other common human malignancies. *Br J Cancer.* 1998; 78: 1219–23

Azenshtein E, Luboshits G, Shina S, et al. The CC chemokine RANTES in breast carcinoma progression: regulation of expression and potential mechanisms of promalignant activity. *Cancer Res.* 2002; 62: 1093–102

Baba M, Imai T, Nishimura M, et al. Identification of CCR6, the specific receptor for a novel lymphocyte-directed CC chemokine LARC. *J Biol Chem.* 1997; 272: 14893-8

Bachelder RE, Wendt MA, Mercurio AM. Vascular endothelial growth factor promotes breast carcinoma invasion in an autocrine manner by regulating the chemokine receptor CXCR4. *Cancer Res.* 2002; 62: 7203-6

Baggiolini M, Dewald B, Moser B. Interleukin-8 and related chemotactic cytokines CXC and CC chemokines. *Adv Immunol.* 1994; 55: 97-179

Baggiolini M, Dewald B, Moser B. Human chemokines: an update. *Annu Rev Immunol.* 1997; 15: 675-705

Baird JW, Nibbs RJ, Komai-Koma M, et al. ESkine, a novel b-chemokine, is differentially spliced to produce secretable and nuclear targeted isoforms. *J Biol Chem.* 1999; 274: 33496-503

Baird PN, D'Andrea RJ, Goodall GJ. Cytokine receptor genes: structure, chromosomal location, and involvement in human disease. *Leuk Lymph* 1995; 5: 373-83

Bais C, Santomasso B, Coso O, et al. G-protein-coupled receptor of Kaposi's sarcoma-associated herpesvirus is a viral oncogene and angiogenesis activator. *Nature*. 1998; 391: 86-9

Bajetto A, Barbero S, Bonavia R, et al. Stromal cell-derived factor-1alpha induces astrocyte proliferation through the activation of extracellular signal-regulated kinases 1/2 pathway. *J Neurochem*. 2001; 77: 1226-36

Bajetto A, Bonavia R, Barbero S, et al. Glial and neuronal cells express functional chemokine receptor CXCR4 and its natural ligand stromal cell-derived factor 1. *J Neurochem*. 1999; 73: 2349-57

Bajetto A, Bonavia R, Barbero S, et al. Chemokines and their receptors in the central nervous system. *Front Neuroendocrinol*. 2001; 22: 147-84

Balabanian K, Lagane B, Infantino S, et al. The chemokine SDF-1/CXCL12 binds to and signals through the orphan receptor RDC1 in T lymphocytes. *J Biol Chem*. 2005; 280: 35760-6

Balkwill F. Cancer and the chemokine network. *Nature Rev Cancer*. 2004a; 4: 540-50

Balkwill F. The significance of cancer cell expression of the chemokine receptor CXCR4. *Semin Cancer Biol*. 2004b; 14: 171-9

Barallon R, Bauer SR, Butler J, et al. Recommendation of short tandem repeat profiling for authenticating human cell lines, stem cells, and tissues. *In Vitro Cell Dev Biol Anim*. 2010 Jul 8. [Epub ahead of print]

Barber RD, Harmer DW, Coleman RA, et al. GAPDH as a housekeeping gene: analysis of GAPDH mRNA expression in a panel of 72 human tissues. *Physiol Genomics*. 2005; 21: 389-95

Barbero S, Bonavia R, Bajetto A, et al. Stromal cell-derived factor 1alpha stimulates human glioblastoma cell growth through the activation of both extracellular signal-regulated kinases 1/2 and Akt. *Cancer Res*. 2003; 63: 1969-74

Barbieri F, Bajetto A, Porcile C, et al. CXC receptor and chemokine expression in human meningioma: SDF1/CXCR4 signaling activates ERK1/2 and stimulates meningioma cell proliferation. *Ann N Y Acad Sci*. 2006; 1090: 332-43

Baribaud F, Edwards TG, Sharron M, et al. Antigenically Distinct Conformations of CXCR4. *J Virol*. 2001; 75: 8957-67

Bartolomé RA, Ferreiro S, Miquilena-Colina ME, et al. The chemokine receptor CXCR4 and the metalloproteinase MT1-MMP are mutually required during melanoma metastasis to lungs. *Am J Pathol*. 2009; 174: 602-12

Bas A, Forsberg G, Hammarstrom S, et al. Utility of the housekeeping genes 18S rRNA, beta-actin and glyceraldehyde-3-phosphate-dehydrogenase for normalization in real-time quantitative reverse transcriptase-polymerase chain reaction analysis of gene expression in human T lymphocytes. *Scand J Immunol.* 2004; 59: 566–73

Batson OV. Function of vertebral veins and their role in spread of metastases. *Ann Surg.* 1940; 112: 138-49

Bazan JF, Bacon KB, Hardiman G et al. A new class of membrane-bound chemokine with a CX3C motif. *Nature.* 1997; 5: 640-44

Belperio JA, Keane MP, Arenberg DA, et al. CXC chemokines in angiogenesis. *J Leukoc Biol.* 2000; 68: 1-8

Ben-Baruch A. Organ selectivity in metastasis: regulation by chemokines and their receptors. *Clin Exp Metastasis.* 2008; 25: 345-56

Ben-Baruch A, Xu L, Young PR, et al. Monocyte chemotactic protein-3 (MCP3) interacts with multiple leukocyte receptors: C-C CKR1, a receptor for macrophage inflammatory protein-1 alpha/Rantes, is also a functional receptor for MCP3. *J Biol Chem.* 1995; 270: 22123-8

Bendall LJ, Baraz R, Juarez J, et al. Defective p38 mitogen-activated protein kinase signaling impairs chemotactic but not proliferative responses to stromal-derived factor-1 α in acute lymphoblastic leukemia. *Cancer Res* 2005; 65: 3290–8

Bennaceur K, Chapman J, Brikci-Nigassa L, et al. Dendritic cells dysfunction in tumour environment. *Cancer Lett.* 2008; 272: 186-96

Bentley H, Hamdy FC, Hart KA, et al. Expression of bone morphogenetic proteins in human prostatic adenocarcinoma and benign prostatic hyperplasia. *Br J Cancer.* 1992; 66: 1159–63

Berson JF, Long D, Doranz BJ, et al. A seven transmembrane domain receptor involved in fusion and entry of T-cell-tropic human immunodeficiency virus type 1 strains. *J Virol.* 1996; 70: 6288–95

Bertran E, Caja L, Navarro E, et al. Role of CXCR4/SDF-1 alpha in the migratory phenotype of hepatoma cells that have undergone epithelial-mesenchymal transition in response to the transforming growth factor-beta. *Cell Signal.* 2009; 21: 1595-606

Besemer J, Hujber A, Kuhn B. Specific binding, internalization, and degradation of human neutrophil activating factor by human polymorphonuclear leukocytes. *J Biol Chem.* 1989; 264: 17409 – 15

Bingle L, Brown NJ, Lewis CE. The role of tumour associated macrophages in tumour progression: implications for new anticancer therapies. *J. Pathol.* 2002; 196: 254–265

Biragyn A, Tani K, Grimm MC, et al. Genetic fusion of chemokines to a self tumor antigen induces protective, T-cell dependent antitumor immunity. *Nature Biotechnol.* 1999; 17: 253-8

Blanpain C, Migeotte I, Lee B, et al. CCR5 binds multiple CC-chemokines: MCP-3 acts as a natural antagonist. *Blood.* 1999; 94: 1899-905

Bleul CC, Farzan M, Choe H, et al. The lymphocyte chemoattractant SDF-1 is a ligand for LESTR/fusin and blocks HIV-1 entry. *Nature.* 1996; 382: 829–33

Bleul CC, Wu L, Hoxie JA, et al. The HIV coreceptors CXCR4 and CCR5 are differentially expressed and regulated on human T lymphocytes. *Proc Natl Acad Sci USA.* 1997; 94: 1925–30

Block KM, Wang H, Szabó LZ, et al. Direct inhibition of hypoxia-inducible transcription factor complex with designed dimeric epidithiodiketopiperazine. *J Am Chem Soc.* 2009; 131: 18078-88

Bodnar RJ, Yates CC, Wells A. IP-10 blocks vascular endothelial growth factor-induced endothelial cell motility and tube formation via inhibition of calpain. *Circ Res.* 2006; 98: 617-25

Bokobza SM, Ye L, Kynaston HE, et al. GDF-9 promotes the growth of prostate cancer cells by protecting them from apoptosis. *J Cell Physiol.* 2010 May 10. [Epub ahead of print]

Bonecchi R, Polentarutti N, Luini W, et al. Up-regulation of CCR1 and CCR3 and induction of chemotaxis to CC chemokines by IFN-gamma in human neutrophils. *J Immunol.* 1999; 162: 474-9

Bordoni R, Fine R, Murray D, et al. Characterisation of the role of melanoma growth stimulating activity (MGSA) in the growth of normal melanocytes, nevocytes and malignant melanocytes. *J Cell Biochem.* 1990; 44: 207-19

Bottazzi B, Colotta F, Sica A, et al. A chemoattractant expressed in human sarcoma cells (tumor-derived chemotactic factor (TDCF)) is identical to monocyte chemoattractant protein-1/monocyte chemotactic and activating factor (MCP-1/MCAF). *Int J Cancer.* 1990; 45: 795–7

Bottazzi B, Polentarutti N, Acero R, et al. Regulation of the macrophage content of neoplasms by chemoattractants. *Science.* 1983; 220: 210–2

Bourcier T, Berbar T, Paquet S, et al. Characterization and functionality of CXCR4 chemokine receptor and SDF-1 in human corneal fibroblasts. *Mol Vis*. 2003; 9: 96-102

Boyden S: The chemotactic effect of mixtures of antibody and antigen on polymorphonuclear leucocytes. *J Exp Med* 1962, 115: 453-66

Bradstock KF, Makrynika V, Bianchi A, et al. Effects of the chemokine stromal cell-derived factor-1 on the migration and localization of precursor-B acute lymphoblastic leukemia cells within bone marrow stromal layers. *Leukemia*. 2000; 14: 882-8

Brat DJ, Bellail AC, Van Meir EG. The role of interleukin-8 and its receptors in gliomagenesis and tumoral angiogenesis. *Neuro-oncol*. 2005; 7: 122-33

Brew R, Erikson JS, West DC, et al. Interleukin-8 as an autocrine growth factor for human colon carcinoma cells in vitro. *Cytokine*. 2000; 12: 78-85

Breyer BN, Greene KL, Dall'Era MA, et al. Pelvic lymphadenectomy in prostate cancer. *Prostate Cancer Prostatic Dis*. 2008; 11: 320-4

Bright RK, Vocke CD, Emmert-Buck MR, et al. Generation and genetic characterization of immortal human prostate epithelial cell lines derived from primary cancer specimens. *Cancer Res*. 1997; 57: 995-1002

Brossner C, Ringhofer H, Hernady T et al. Lymphatic drainage of prostatic transition and peripheral zones visualized on a three-dimensional workstation. *Urology*. 2001; 57: 389-93

Brown JM, Vessella RL, Kostenuik PJ, et al. Serum osteoprotegerin levels are increased in patients with advanced prostate cancer. *Clin Cancer Res* 2001; 7: 2977-83

Broxmeyer HE, Cooper S, Kohli L, et al. Transgenic expression of stromal cell-derived factor-1/CXC chemokine ligand 12 enhances myeloid progenitor cell survival/antiapoptosis in vitro in response to growth factor withdrawal and enhances myelopoiesis in vivo. *J Immunol*. 2003; 170: 421-9

Broxmeyer HE, Orschell CM, Clapp DW, et al. Rapid mobilization of murine and human hematopoietic stem and progenitor cells with AMD3100, a CXCR4 antagonist. *J Exp Med*. 2005; 201: 1307-18

Bubendorf L, Schopfer A, Wagner U, et al. Metastatic patterns of prostate cancer: an autopsy study of 1,589 patients. *Hum Pathol*. 2000; 31: 578-83

Burger JA, Stewart DJ, Wald O, et al. Potential of CXCR4 antagonists for the treatment of metastatic lung cancer. *Expert Rev Anticancer Ther*. 2011; 11: 621-30

Burger M, Burger JA, Hoch RC, et al. Point mutation causing constitutive signalling of CXCR2 leads to transforming activity similar to Kaposi's sarcoma herpesvirus-G protein-coupled receptor. *J Immunol* 1999; 163: 2017-22

Burger M, Glodek A, Hartmann T, et al. Functional expression of CXCR4 (CD184) on small-cell lung cancer cells mediates migration, integrin activation and adhesion to stromal cells. *Oncogene*. 2003; 22: 8093-101

Bussard KM, Gay CV, Mastro AM. The bone microenvironment in metastasis; what is special about bone? *Cancer Metastasis Rev*. 2008; 27: 41-55

Bustin SA. Absolute quantification of mRNA using real-time reverse transcription polymerase chain reaction assays. *J Mol Endocrinol*. 2000; 25: 169-93

Bustin SA, Benes V, Nolan T, et al. Quantitative real-time RT-PCR—a perspective. *J Mol Endocrinol*. 2005; 34: 597-601

Cailleau R, Young R, Olive M, et al. Breast tumor cell lines from pleural effusions. *J Natl Cancer Inst*. 1974; 53: 661-74

Cambien B, Karimjee BF, Richard-Fiardo P, et al. Organ-specific inhibition of metastatic colon carcinoma by CXCR3 antagonism. *Br J Cancer*. 2009; 100: 1755-64

Campbell JJ, Bowman EP, Murphy K, et al. 6-C-kine (SLC), a lymphocyte adhesion-triggering chemokine expressed by high endothelium, is an agonist for the MIP-3beta receptor CCR7. *J Cell Biol*. 1998; 141: 1053-9

Cardones AR, Murakami T, Hwang ST. CXCR4 enhances adhesion of B16 tumor cells to endothelial cells in vitro and in vivo via beta(1) integrin. *Cancer Res*. 2003; 63: 6751-7

Cardullo RA, Agrawal S, Flores C, et al. Detection of nucleic acid hybridization by non-radiative fluorescence resonance energy transfer. *Proc. Natl Acad. Sci. USA*. 1988; 85: 8790-4

Caspersson T, Schultz J. Nucleic acid metabolism of the chromosomes in relation to gene reproduction. *Nature* 1938; 142: 294-7

Cassard L, Cohen-Solal JF, Galinha A, et al. Modulation of tumor growth by inhibitory Fc(gamma) receptor expressed by human melanoma cells. *J Clin Invest*. 2002; 110: 1549-57

Castellano G, Malaponte G, Mazzarino MC, et al. Activation of the osteopontin/matrix metalloproteinase-9 pathway correlates with prostate cancer progression. *Clin Cancer Res*. 2008; 14: 7470-80

Castillejo A, Mata-Balaguer T, Guarinos C, et al. The Int7G24A variant of transforming growth factor-beta receptor type I is a risk factor for colorectal cancer in the male Spanish population: a case-control study. *BMC Cancer*. 2009; 9: 406

Ceradini DJ, Kulkarni AR, Callaghan MJ, et al. Progenitor cell trafficking is regulated by hypoxic gradients through HIF-1 induction of SDF-1. *Nat Med*. 2004; 10: 858-64

Chabot DJ, Chen H, Dimitrov DS, et al. N-linked glycosylation of CXCR4 masks coreceptor function for CCR5-dependent human immunodeficiency virus type 1 isolates. *J Virol*. 2000; 74: 4404-13

Chambers AF, Groom AC, MacDonald AC, et al. Dissemination and growth of cancer cells in metastatic sites. *Nat Rev Cancer*. 2002; 2: 563-72

Chaput N, Conforti R, Viaud S, et al. The Janus face of dendritic cells in cancer. *Oncogene*. 2008; 27: 5920-31

Charo IF, Myers SJ, Herman A, et al. Molecular cloning and functional expression of two monocyte chemoattractant protein 1 receptors reveals alternative splicing of the carboxyl-terminal tails. *Proc Natl Acad Sci USA*. 1994; 91: 2752-6

Chervoneva I, Li Y, Schulz S, et al. Selection of optimal reference genes for normalization in quantitative RT-PCR. *BMC Bioinformatics*. 2010; 11: 253

Chinni SR, Sivalogan S, Dong Z, et al. CXCL12/CXCR4 signaling activates Akt-1 and MMP-9 expression in prostate cancer cells: the role of bone microenvironment-associated CXCL12. *Prostate*. 2006; 66: 32-48

Chu JH, Sun ZY, Meng XL et al. Differential metastasis-associated gene analysis of prostate carcinoma cells derived from primary tumor and spontaneous lymphatic metastasis in nude mice with orthotopic implantation of PC-3M cells. *Cancer Lett*. 2006; 233: 79-88

Chu QD, Holm NT, Madumere P, et al. Chemokine receptor CXCR4 overexpression predicts recurrence for hormone receptor-positive, node-negative breast cancer patients. *Surgery*. 2010 Jun 30. [Epub ahead of print]

Chung LW. Prostate carcinoma bone-stroma interaction and its biologic and therapeutic implications. *Cancer*. 2003; 97: 772-778

Chuntharapai A, Lee J, Hebert CA, et al. Monoclonal antibodies detect different distribution patterns of IL-8 receptor A and IL-8 receptor B on human peripheral blood leukocytes. *J Immunol*. 1994; 153: 5682-8

Cohen MC and Cohen S. Cytokine function. A study in biologic diversity. *Am J Clin Pathol* 1996; 5: 589-98

Cohen P, Peehl DM, Lamson G, et al. Insulin-like growth factors (IGFs), IGF receptors, and IGF-binding proteins in primary cultures of prostate epithelial cells. *J Clin Endocrinol Metab* 1991; 73: 401–7

Cole KE, Strick CA, Paradis TJ, et al. Interferon-inducible T cell alpha chemoattractant (I-TAC): a novel non-ELR CXC chemokine with potent activity on activated T cells through selective high affinity binding to CXCR3. *J Exp Med*. 1998; 187: 2009-21

Coleman RE. Skeletal complications of malignancy. *Cancer*. 1997; 80: 1588–94

Coleman RE. Metastatic bone disease: clinical features, pathophysiology and treatment strategies, *Cancer Treat Rev*. 2001; 27: 165–76

Combadiere C, Ahuja SK, van Damme J, et al. Monocyte chemoattractant protein-3 is a functional ligand for CC chemokine receptors 1 and 2B. *J Biol Chem*. 1995; 270: 29671-5

Conti I, Rollins BJ. CCL2 (monocyte chemoattractant protein-1) and cancer. *Semin Cancer Biol*. 2004; 14: 149-54

Coons AH, Kaplan MH. Localization of antigen in tissue cells. II. Improvements in a method for the detection of antigen by means of fluorescent antibody. *J Exp Med* 1950; 91: 1-4

Cooper CR, Chay CH, Gendernalik JD, et al. Stromal factors involved in prostate carcinoma metastasis to bone. *Cancer*. 2003; 97: 739-47

Cooper CR, Mclean L, Walsh M, et al. Preferential adhesion to prostate cancer cells to bone is mediated by binding to bone marrow endothelial cells as compared to extracellular matrix components in vitro. *Clin Cancer Res*. 2000; 6: 4839–47

Coulter WH. High speed automatic blood cell counter and cell size analyzer. *Proc Natl Electronics Conf* 1956; 12:1034-40

Cumming J, Hacking N, Fairhurst J, et al. Distribution of bony metastases in prostatic carcinoma. *Br J Urol*. 1990; 66: 411–14

Dai J, Keller J, Zhang J et al. Bone morphogenetic protein-6 promotes osteoblastic prostate cancer bone metastases through a dual mechanism. *Cancer Res*. 2005; 65: 8274-85

Dai Y, Siemann DW. BMS-777607, a small-molecule met kinase inhibitor, suppresses hepatocyte growth factor-stimulated prostate cancer metastatic phenotype in vitro. *Mol Cancer Ther*. 2010; 9: 1554-61

Dales JP, Beaufils N, Silvy M, et al. Hypoxia inducible factor 1alpha gene (HIF-1alpha) splice variants: potential prognostic biomarkers in breast cancer. *BMC Med.* 2010; 8: 44. [Epub ahead of print]

Daly-Burns B, Alam TN, Mackay A, et al. A conditionally immortalized cell line model for the study of human prostatic epithelial cell differentiation. *Differentiation.* 2007; 75: 35-48

Darash-Yahana M, Pikarsky E, Abramovitch R, et al. Role of high expression levels of CXCR4 in tumor growth, vascularization, and metastasis. *FASEB J* 2004; 18: 1240-2

Daugherty BL, Siciliano SJ, DeMartino JA, et al. Cloning, expression, and characterization of the human eosinophil eotaxin receptor. *J Exp Med.* 1996; 183: 2349-54

David NB, Sapede D, Saint-Etienne L, et al. Molecular basis of cell migration in the fish lateral line: role of the chemokine receptor CXCR4 and of its ligand, SDF1. *PNAS.* 2002; 99: 16297-302

De Rosa SC, Herzenberg LA, Roederer M. 11-color, 13-parameter flow cytometry: identification of human naive T-cells by phenotype, function, and T-cell receptor diversity. *Nature Medicine* 2001; 7:245 -8

Dheda K, Huggett JF, Bustin SA, et al. Validation of housekeeping genes for normalizing RNA expression in real-time PCR. *Biotechniques.* 2004; 37: 112-4, 116, 118-9

Ding Q, Bai YF, Wang YQ, et al. TGF-beta1 reverses inhibition of COX-2 with NS398 and increases invasion in prostate cancer cells. *Am J Med Sci.* 2010; 339: 425-32

Ding Y, Shimada Y, Maeda M, et al. Association of CC chemokine receptor 7 with lymph node metastasis of esophageal squamous cell carcinoma. *Clin Cancer Res.* 2003; 9: 3406-12

DiPersio JF, Micallef IN, Stiff PJ, et al. Phase III prospective randomized double-blind placebo-controlled trial of plerixafor plus granulocyte colony-stimulating factor compared with placebo plus granulocyte colony-stimulating factor for autologous stem-cell mobilization and transplantation for patients with non-Hodgkin's lymphoma. *J Clin Oncol.* 2009; 27: 4767-73

Dobner T, Wolf I, Emrich T, et al. Differentiation-specific expression of a novel G protein-coupled receptor from Burkitt's lymphoma. *Eur J Immunol.* 1992; 22: 2795-9

Doitsidou M, Reichman-Fried M, Stebler J, et al. Guidance of primordial germ cell migration by the chemokine SDF-1. *Cell.* 2002; 111: 647-59

Doranz BJ, Rucker J, Yi Y, et al. A dual-tropic primary HIV-1 isolate that uses fusin and the beta-chemokine receptors CKR-5, CKR-3, and CKR-2b as fusion cofactors. *Cell*. 1996; 85: 1149-58

D'Souza MP, Harden VA. Chemokines and HIV-1 second receptors - confluence of two fields generates optimism in AIDS research. *Nature Med*. 1996; 2: 1293-300

Du YF, Shi Y, Xing YF, et al. Establishment of CXCR4-small interfering RNA retrovirus vector driven by human prostate-specific antigen promoter and its biological effects on prostate cancer in vitro and in vivo. *J Cancer Res Clin Oncol*. 2008; 134: 1255-64

Dugan MJ, Maziarz RT, Bensinger WI, et al. Safety and preliminary efficacy of plerixafor (Mozobil) in combination with chemotherapy and G-CSF: an open-label, multicenter, exploratory trial in patients with multiple myeloma and non-Hodgkin's lymphoma undergoing stem cell mobilization. *Bone Marrow Transplant*. 2010; 45: 39-47

Dumur CI, Dechsukhum C, Wilkinson DS, et al. Analytical validation of a real-time reverse transcription polymerase chain reaction quantitation of different transcripts of the Wilms' tumor suppressor gene (WT1). *Anal Biochem*. 2002; 309: 127-36

Dunn LK, Mohammad KS, Fournier PG, et al. Hypoxia and TGF-beta drive breast cancer bone metastases through parallel signaling pathways in tumor cells and the bone microenvironment. *PLoS One*. 2009; 4: e6896

Dwinell MB, Eckmann L, Leopard JD, et al. Chemokine receptor expression by human intestinal epithelial cells. *Gastroenterology* 1999;117: 359-67

Ebisawa T, Tada K, Kitajima I, et al. Characterization of bone morphogenetic protein-6 signaling pathways in osteoblast differentiation. *J Cell Sci*. 1999; 112: 3519-27

Eck M, Schmausser B, Scheller K, et al. Pleiotropic effects of CXC chemokines in gastric carcinoma: differences in CXCL8 and CXCL1 expression between diffuse and intestinal types of gastric carcinoma. *Clin Exp Immunol*. 2003; 134: 508-15

Eck SM, Côté AL, Winkelman WD, et al. CXCR4 and matrix metalloproteinase-1 are elevated in breast carcinoma-associated fibroblasts and in normal mammary fibroblasts exposed to factors secreted by breast cancer cells. *Mol Cancer Res*. 2009; 7: 1033-44

Eisenhardt A, Frey U, Tack M, et al. Expression analysis and potential functional role of the CXCR4 chemokine receptor in bladder cancer. *Eur Urol* 2005; 47: 111-7

Elgavish A, Prince C, Chang PL et al. Osteopontin stimulates a subpopulation of quiescent human prostate epithelial cells with high proliferative potential to divide in vitro. *Prostate*. 1998; 35: 83-94

Elgert KD, Alleva DG, Mullins DW. Tumor-induced immune dysfunction: the macrophage connection. *J Leukoc Biol* 1998; 64: 275-90

Ellerhorst J, Nguyen T, Cooper DN, et al. Differential expression of endogenous galectin-1 and galectin-3 in human prostate cancer cell lines and effects of overexpressing galectin-1 on cell phenotype. *Int J Oncol.* 1999; 14: 217-24

Engl T, Relja B, Marian D, et al. CXCR4 chemokine receptor mediates prostate tumor cell adhesion through alpha5 and beta3 integrins. *Neoplasia.* 2006; 8: 290-301

Entschladen F, Drell TL, Lang K, et al. Tumour cell migration, invasion, and metastasis: navigation by neurotransmitters, *Lancet Oncol.* 2004; 5: 254-8

Entschladen F, Gunzer M, Scheuffele CM, et al. T lymphocytes and neutrophil granulocytes differ in regulatory signaling and migratory dynamics with regard to spontaneous locomotion and chemotaxis. *Cell Immunol.* 2000; 199: 104-14

Ewing J. Neoplastic diseases. "A treatise on tumors". Philadelphia: 1928. WB Saunders Company

Farzan M, Babcock GJ, Vasilieva N, et al. The role of post-translational modifications of the CXCR4 amino terminus in stromal-derived factor 1 alpha association and HIV-1 entry. *J Biol Chem.* 2002; 277: 29484-89

Farzan M, Mirzabekov T, Kolchinsky P, et al. Tyrosine sulfonation of the amino terminus of CCR5 facilitates HIV-1 entry. *Cell* 1999; 96: 667-76

Feldman ED, Weinreich DM, Carroll NM, et al. Interferon gamma-inducible protein 10 selectively inhibits proliferation and induces apoptosis in endothelial cells. *Ann Surg Oncol.* 2006; 13: 125-33

Feng Y, Broder CC, Kennedy PE, et al. HIV-1 entry cofactor: functional cDNA cloning of a seven-transmembrane, G protein-coupled receptor. *Science.* 1996; 272: 872-77

Ferrer FA, Miller LJ, Andrawis RI, et al. Angiogenesis and prostate cancer: in vivo and in vitro expression of angiogenesis factors by prostate cancer cells. *Urology.* 1998; 51: 161-7

Ferrer FA, Patschenko AG, Miller LJ, et al. Angiogenesis and neuroblastomas: interleukin-8 and interleukin-8 receptor expression in human neuroblastoma. *J Urol.* 2000; 164: 1016-20

Festuccia C, Angelucci A, Gravina GL, et al. Epidermal growth factor modulates prostate cancer cell invasiveness regulating urokinase-type plasminogen activator activity. EGF-receptor inhibition may prevent tumor cell dissemination. *Thromb Haemost.* 2005; 93: 964-75

Festuccia C, Bologna M, Gravina GL, et al. Osteoblast conditioned media contain TGFbeta1 and modulate the migration of prostate tumor cells and their interactions with extracellular matrix components. *Int J Cancer*. 1999; 81: 395–403

Fidler IJ. The organ microenvironment and cancer metastasis. *Differentiation*. 2002; 70: 498–505

Fidler IJ. The pathogenesis of cancer metastasis: The ‘seed and soil’ hypothesis revisited. *Nat Rev Cancer*. 2003; 3: 453-58

Folkins C, Shaked Y, Man S, et al. Glioma tumor stem-like cells promote tumor angiogenesis and vasculogenesis via vascular endothelial growth factor and stromal-derived factor 1. *Cancer Res*. 2009; 69: 7243-51

Folkman J. Angiogenesis in cancer, vascular, rheumatoid and other disease. *Nature Med*. 1995; 1: 27-31

Forssmann U, Ugucioni M, Loetscher P, et al. Eotaxin-2, a novel CC chemokine that is selective for the chemokine receptor CCR3, and acts like eotaxin on human eosinophil and basophil leukocytes. *J Exp Med*. 1997; 185: 2171-6

Foulds L. The experimental study of tumor progression. *Cancer Res* 1964;14: 327–39

Franco OE, Shaw AK, Strand DW, et al. Cancer associated fibroblasts in cancer pathogenesis. *Semin Cell Dev Biol*. 2010; 21: 33-9

Frederick MJ, Henderson Y, Xu X, et al. In vivo expression of the novel CXC chemokine BRAK in normal and cancerous human tissue. *Am J Pathol*. 2000; 156: 1937-50

Frigo DE, Sherk AB, Wittmann BM, et al. Induction of Kruppel-like factor 5 expression by androgens results in increased CXCR4-dependent migration of prostate cancer cells in vitro. *Mol Endocrinol*. 2009; 23: 1385-96

Fuchs E, Tumber T, Guasch G. Socializing with the neighbors: stem cells and their niche. *Cell*. 2004; 116: 769-78

Fujisawa N, Sakao Y, Hayashi S, et al. Alpha-chemokine growth factors for adenocarcinomas; a synthetic peptide inhibitor for alpha-chemokines inhibits the growth of adenocarcinoma cell lines. *J Cancer Res Clin Oncol*. 2000; 126: 19-26

Fulwyler MJ. Electronic separation of biological cells by volume. *Science* 1965; 150: 910–11

Fushimi T, O’Connor TP, Crystal RG. Adenoviral gene transfer of stromal cell derived factor-1 to murine tumors induces the accumulation of dendritic cells and suppresses tumor growth. *Cancer Res*. 2006; 66: 3513–22

Gabellini C, Trisciuglio D, Desideri M, et al. Functional activity of CXCL8 receptors, CXCR1 and CXCR2, on human malignant melanoma progression. *Eur J Cancer*. 2009; 45: 2618-27

Gale LM and McColl SR. Chemokines: extracellular messengers for all occasions? *Bioessays*. 1999; 21: 17-28

Gardner TA, Lee SJ, Lee SD, et al. Differential expression of osteocalcin during the metastatic progression of prostate cancer. *Oncol Rep*. 2009; 21: 903-8

Geiger TR, Peeper DS. Metastasis mechanisms. *Biochim Biophys Acta*. 2009 ; 1796: 293-308

Gelmini S, Mangoni M, Castiglione F, et al. The CXCR4/CXCL12 axis in endometrial cancer. *Clin Exp Metastasis*. 2009; 26: 261-8

Gelmini S, Mangoni M, Serio M, et al. The critical role of SDF-1/CXCR4 axis in cancer and cancer stem cells metastasis. *J Endocrinol Invest*. 2008; 31: 809-19

Gennigens C, Menetrier-Caux C, Droz JP. Insulin-Like Growth Factor (IGF) family and prostate cancer. *Crit Rev Oncol Hematol*. 2006; 58: 124-45

Gerber BO, Zanni MP, Uguccioni M, et al. Functional expression of the eotaxin receptor CCR3 in T lymphocytes co-localizing with eosinophils. *Curr Biol*. 1997; 7: 836-43

Germano G, Allavena P, Mantovani A. Cytokines as a key component of cancer-related inflammation. *Cytokine*. 2008; 43: 374-9

Gilbert DC, Chandler I, McIntyre A, et al. Clinical and biological significance of CXCL12 and CXCR4 expression in adult testes and germ cell tumours of adults and adolescents. *J Pathol*. 2009; 217: 94-102

Gimbrone M, Cotran R, Folkman J. Tumor growth and neovascularization: an experimental model using rabbit cornea. *J Natl Cancer Inst*. 1974; 52: 413-27

Givan AL. Flow cytometry: an introduction. *Methods Mol Biol*. 2004; 263: 1-32

Glaves D, Huben RP, Weiss L. Haematogenous dissemination of cells from human renal adenocarcinomas. *Br J Cancer*. 1988; 57: 32-35

Glinsky VV, Glinsky GV, Glinskii OV, et al. Intravascular metastatic cancer cell homotypic aggregation at the sites of primary attachment to the endothelium. *Cancer Res*. 2003; 63: 3805-11

Glinsky VV, Glinsky GV, Rittenhouse-Olson K, et al. The role of Thomsen–Friedenreich antigen in adhesion of human breast and prostate cancer cells to the endothelium. *Cancer Res.* 2001; 61: 4851–7

Gmyrek GA, Walburg M, Webb CP, et al. Normal and malignant prostate epithelial cells differ in their response to hepatocyte growth factor/ scatter factor. *Am J Pathol.* 2001; 159: 579-90

Goldsmith ZG, Dhanasekaran DN. G protein regulation of MAPK networks. *Oncogene* 2007; 26: 3122–42

Gómez-Curet I, Robinson KG, Funanage VL, et al. Robust quantification of the SMN gene copy number by real-time TaqMan PCR. *Neurogenetics.* 2007; 8: 271-8

Gong X, Gong W, Kuhns DB, et al. Monocyte chemotactic protein-2 (MCP-2) uses CCR1 and CCR2B as its functional receptors. *J Biol Chem.* 1997; 272: 11682-5

Gubina NE, Merekina OS, Ushakova TE. Mitochondrial DNA transcription in mouse liver, skeletal muscle, and brain following lethal x-ray irradiation. *Biochemistry (Mosc).* 2010; 75: 777-83

Guisse TA, Yin JJ, Taylor SD, et al. Evidence for a causal role of parathyroid hormone-related protein in the pathogenesis of human breast cancer-mediated osteolysis. *J Clin Invest* 1996; 98: 1544–9

Gupta SK, Lysko PG, Pillarisetti K, et al. Chemokine receptors in human endothelial cells. Functional expression of CXCR4 and its transcriptional regulation by inflammatory cytokines. *J Biol Chem.* 1998; 273: 4282-7

Gupta SK, Pillarisetti K. Cutting edge: CXCR4-Lo: molecular cloning and functional expression of a novel human CXCR4 splice variant. *J Immunol.* 1999; 163: 2368-72

Gut M, Leutenegger CM, Huder JB, Pedersen NC, Lutz H. One-tube fluorogenic reverse transcription polymerase chain reaction for the quantitation of feline coronaviruses. *J Virol. Methods.* 1999; 77: 37–46

Hackstein H, Morelli AE, Thomson AW. Designer dendritic cells for tolerance induction: guided not misguided missiles. *Trends Immunol.* 2001; 22: 437-42

Hagedorn M, Zilberberg L, Wilting J, et al. Domain swapping in a COOH-terminal fragment of platelet factor 4 generates potent angiogenesis inhibitors. *Cancer Res.* 2002; 62: 6884-90

Hanna J, Wald O, Goldman-Wohl D, et al. CXCL12 expression by invasive trophoblasts induces the specific migration of CD16 negative human natural killer cells. *Blood.* 2003; 102: 1569-77

Harbeck N, Nimmrich I, Hartmann A, et al. Multicenter study using paraffin-embedded tumor tissue testing PITX2 DNA methylation as a marker for outcome prediction in tamoxifen-treated, node-negative breast cancer patients. *J Clin Oncol*. 2008; 26: 5036-42

Hartmann TN, Burger JA, Glodek A, et al. CXCR4 chemokine receptor and integrin signaling co-operate in mediating adhesion and chemoresistance in small cell lung cancer (SCLC) cells. *Oncogene*. 2005; 24: 4462-71

Hassan S, Buchanan M, Jahan K, et al. CXCR4 peptide antagonist inhibits primary breast tumor growth, metastasis and enhances the efficacy of anti-VEGF treatment or docetaxel in a transgenic mouse model. *Int J Cancer*. 2011; 129: 225-32

Hatse S, Balzarini J, Liekens S. Stromal cell-derived factor 1 (CXCL12) binds to endothelial cells and signals through a receptor different from CXCR4. *Biochem Biophys Res Commun*. 2006; 348: 192-9

Heid CA, Stevens J, Livak KJ, et al. Real time quantitative PCR. *Genome Res*. 1996; 6: 986-94

Heidenreich A, Varga Z, Von Knobloch R. Extended pelvic lymphadenectomy in patients undergoing radical prostatectomy: High incidence of lymph node metastasis. *J Urol*. 2002; 167: 1681-86

Hellawell GO, Turner GD, Davies DR, et al. Expression of the type 1 insulin-like growth factor receptor is up-regulated in primary prostate cancer and commonly persists in metastatic disease. *Cancer Res*. 2002; 62: 2942-50

Herman JG, Stadelman HL, Roselli CE. Curcumin blocks CCL2-induced adhesion, motility and invasion, in part, through down-regulation of CCL2 expression and proteolytic activity. *Int J Oncol*. 2009; 34: 1319-27

Higuchi R, Fockler C, Dollinger G, et al. Kinetic PCR analysis: real-time monitoring of DNA amplification reactions. *Biotechnology*. 1993; 11:1026-30

Hippe A, Homey B, Mueller-Homey A. Chemokines. *Recent Results Cancer Res*. 2010; 180: 35-50

Hoffmann AC, Danenberg KD, Taubert H, et al. A three-gene signature for outcome in soft tissue sarcoma. *Clin Cancer Res*. 2009; 15: 5191-8

Holland PM, Abramson RD, Watson R, et al. Detection of specific polymerase chain reaction product by utilizing the 5'-3' exonuclease activity of *Thermus aquaticus* DNA polymerase. *Proc Natl Acad Sci USA*. 1991; 88: 7276-80

Holmes WE, Lee J, Kuang WJ, et al. Structure and functional expression of a human interleukin-8 receptor. *Science*. 1991; 253: 1278-80

Homey B, Wang W, Soto H, et al. Cutting edge: the orphan chemokine receptor G protein-coupled receptor-2 (GPR-2, CCR10) binds the skin-associated chemokine CCL27 (CTACK/ALP/ILC). *J Immunol*. 2000;164: 3465-70

Hong TM, Teng LJ, Shun CT, et al. Induced interleukin-8 expression in gliomas by tumor-associated macrophages. *J Neurooncol*. 2009; 93: 289-301

Hong X, Jiang F, Kalkanis SN, et al. SDF-1 and CXCR4 are up-regulated by VEGF and contribute to glioma cell invasion. *Cancer Lett*. 2006; 236: 39-45

Honn KV, Tang DG. Adhesion molecules and tumor cell interaction with endothelium and subendothelial matrix. *Cancer Metastasis Rev*. 1992; 11: 353-75

Horoszewicz JS, Leong SS, Chu TM, et al. The LNCaP cell line--a new model for studies on human prostatic carcinoma. *Prog Clin Biol Res*. 1980; 37: 115-32

Horoszewicz JS, Leong SS, Kawinski E, et al. LNCaP model of human prostatic carcinoma. *Cancer Res*. 1983; 43: 1809-18

Horuk R. The interleukin-8-receptor family: From chemokines to malaria. *Immunol Today*. 1994; 15: 169-74

Horuk R, Hesselgesser J, Zhou Y, et al. The CC chemokine I-309 inhibits CCR8-dependent infection by diverse HIV-1 strains. *J Biol Chem*. 1998; 273: 386-91

Howard OM, Dong HF, Shirakawa AK, et al. LEC induces chemotaxis and adhesion by interacting with CCR1 and CCR8. *Blood*. 2000; 96: 840-5

Hu W, Zhen X, Xiong B, et al. CXCR6 is expressed in human prostate cancer in vivo and is involved in the in vitro invasion of PC3 and LNCap cells. *Cancer Sci*. 2008; 99: 1362-9

Huang CY, Lee CY, Chen MY, et al. Stromal cell-derived factor-1/CXCR4 enhanced motility of human osteosarcoma cells involves MEK1/2, ERK and NF-kappaB-dependent pathways. *J Cell Physiol*. 2009; 221: 204-12

Huang EH, Singh B, Cristofanilli M, et al. A CXCR4 antagonist CTCE-9908 inhibits primary tumor growth and metastasis of breast cancer. *J Surg Res*. 2009; 155: 231-6

Hussain F, Wang J, Ahmed R, et al. The expression of IL-8 and IL-8 receptors in pancreatic adenocarcinomas and pancreatic neuroendocrine tumours. *Cytokine*. 2010; 49: 134-40

Ibrahim SF, van den Engh G. High-speed chromosome sorting. *Chromosome Res*. 2004; 12: 5-14

Ibrahim SF, van den Engh G. Flow cytometry and cell sorting. *Adv Biochem Eng Biotechnol.* 2007; 106: 19-39

Imai K, Kobayashi M, Wang J, et al. Selective secretion of chemoattractants for haemopoietic progenitor cells by bone marrow endothelial cells: a possible role in homing of haemopoietic progenitor cells to bone marrow. *Br J Haematol.* 1999; 106: 905-11

Imai T, Baba M, Nishimura M, et al. The T cell-directed CC chemokine TARC is a highly specific biological ligand for CC chemokine receptor 4. *J Biol Chem.* 1997; 272: 15036-42

Imai T, Chantry D, Raport CJ, et al. Macrophage-derived chemokine is a functional ligand for the CC chemokine receptor 4. *J Biol Chem.* 1998; 273: 1764-8

Imbriaco M, Larson SM, Yeung HW, et al. A new parameter for measuring metastatic bone involvement by prostate cancer: The Bone Scan Index. *Clin Cancer Res.* 1998; 4: 1765-72

Inoue K, Slaton JW, Eve BY, et al. Interleukin-8 expression regulates tumorigenicity and metastases in androgen-independent prostate cancer. *Clin Cancer Res.* 2000a; 6: 2104-19

Inoue K, Slaton JW, Kim S, et al. Interleukin 8 expression regulates tumorigenicity and metastasis in human bladder cancer. *Cancer Res.* 2000b; 60: 2290-99

Irimia D, Toner M. Spontaneous migration of cancer cells under conditions of mechanical confinement. *Integr Biol (Camb).* 2009; 1: 506-12

Ishida K, Iwahashi M, Nakamori M, et al. High CCR7 mRNA expression of cancer cells is associated with lymph node involvement in patients with esophageal squamous cell carcinoma. *Int J Oncol.* 2009; 34: 915-22

Ishida T, Utsunomiya A, Iida S et al. Clinical significance of CCR4 expression in adult T-cell leukemia/lymphoma: its close association with skin involvement and unfavorable outcome. *Clin Cancer Res.* 2003; 9: 3625-34

Ivarsson K, Ekerydh A, Fyhr IM, et al. Upregulation of interleukin-8 and polarized epithelial expression of interleukin-8 receptor A in ovarian carcinomas. *Acta Obstet Gynecol Scand.* 2000; 79: 777-84

Jacob K, Webber M, Benayahu D, et al. Osteonectin promotes prostate cancer cell migration and invasion: a possible mechanism for metastasis to bone. *Cancer Res.* 1999; 59: 4453-7

Jacobson O, Weiss ID, Szajek LP, et al. PET imaging of CXCR4 using copper-64 labeled peptide antagonist. *Theranostics*. 2011; 1: 251-62

Jahnichen S, Blanchetot C, Maussang D, et al. CXCR4 nanobodies (VHH-based single variable domains) potently inhibit chemotaxis and HIV-1 replication and mobilise stem cells. 2010; 107: 20565-70

Jarrard DF, Blitz BF, Smith RC, et al. Effect of epidermal growth factor on prostate cancer cell line PC3 growth and invasion. *Prostate*. 1994; 24: 46-53

Josson S, Matsuoka Y, Chung LW, et al. Tumor-stroma co-evolution in prostate cancer progression and metastasis. *Semin Cell Dev Biol*. 2010; 21: 26-32

Jung K, Lein M, Stephan C, et al. Comparison of 10 serum bone turnover markers in prostate carcinoma patients with bone metastatic spread: diagnostic and prognostic implications. *Int J Cancer* 2004; 111: 783–91

Junnila S, Kokkola A, Mizuguchi T, et al. Gene expression analysis identifies over-expression of CXCL1, SPARC, SPP1, and SULF1 in gastric cancer. *Genes Chromosomes Cancer*. 2010; 49: 28-39

Jurado J, Prieto-Alamo MJ, Madrid-Risquez J, et al. Absolute gene expression patterns of thioredoxin and glutaredoxin redox systems in mouse. *J Biol Chem*. 2003; 278: 45546-54

Kaifi JT, Yekebas EF, Schurr P, et al. Tumor-cell homing to lymph nodes and bone marrow and CXCR4 expression in esophageal cancer. *J Natl Cancer Inst* 2005; 97:1840-7

Kaighn ME, Narayan KS, Ohnuki Y, et al. Establishment and characterization of a human prostatic carcinoma cell line(PC-3). *Invest Urol*. 1979; 17: 16-23

Kamentsky LA, Melamed MR, Derman H. Spectrophotometer: New instrument for ultrarapid cell analysis. *Science* 1965; 150: 630–1

Kamohara H, Takahashi M, Ishiko T, et al. Induction of interleukin-8 (CXCL-8) by tumor necrosis factor-alpha and leukemia inhibitory factor in pancreatic carcinoma cells: Impact of CXCL-8 as an autocrine growth factor. *Int J Oncol*. 2007; 31: 627-32

Kang H, Mansel RE, Jiang WG. Genetic manipulation of stromal cell-derived factor-1 attests the pivotal role of the autocrine SDF-1-CXCR4 pathway in the aggressiveness of breast cancer cells. : *Int J Oncol*. 2005; 26: 1429-34

Karge WH 3rd, Schaefer EJ, Ordovas JM. Quantification of mRNA by polymerase chain reaction (PCR) using an internal standard and a nonradioactive detection method. *Methods Mol Biol*. 1998; 110: 43-61

Kavsak PA, Henderson M, Moretto P, et al. Biochip arrays for the discovery of a biomarker surrogate in a phase I/II study assessing a novel anti-metastasis agent. *Clin Biochem.* 2009; 42: 1162-5

Kawanishi H, Matsui Y, Ito M, et al. Secreted CXCL1 is a potential mediator and marker of the tumor invasion of bladder cancer. *Clin Cancer Res.* 2008; 14: 2579-87

Kelner GS, Kennedy J, Bacon KB et al. Lymphotactin: a cytokine that represents a new class of chemokine. *Science.* 1994; 5: 1395-99

Kennedy J, Kelner GS, Kleyensteuber S et al. Molecular cloning and functional characterization of human lymphotactin. *J Immunol.* 1995; 5: 203-9

Kiefer J, Alexander A, Farach-Carson MC. Type 1 collagen-mediated changes in gene expression and function of prostate cancer cells. *Cancer Treat Res.* 2004; 118: 101-24

Kierszenbaum AL, Rivkin E, Chang PL, et al. Galactosyl receptor, a cell surface C-type lectin of normal and tumoral prostate epithelial cells with binding affinity to endothelial cells. *Prostate.* 2000; 43: 175-83

Kim CH, Kunkel EJ, Boisvert J, et al. Bonzo/CXCR6 expression defines type 1-polarized T-cell subsets with extralymphoid tissue homing potential. *J Clin Investig.* 2001; 107: 595-601

Kitadai Y, Haruma K, Mukaida N, et al. Regulation of disease-progression genes in human gastric carcinoma cells by interleukin 8. *Clin Cancer Res.* 2000; 6: 2735-40

Kitaura M, Nakajima T, Imai T, et al. Molecular cloning of human eotaxin, an eosinophil-selective CC chemokine, and identification of a specific eosinophil eotaxin receptor, CC chemokine receptor 3. *J Biol Chem.* 1996; 271: 7725-30

Kleinhans M, Tun-Kyi A, Gilliet M et al. Functional expression of the eotaxin receptor CCR3 in CD30+ cutaneous T-cell lymphoma. *Blood.* 2003; 101: 1487-93

Klemke RL, Leng J, Molander R, et al. CAS/Crk coupling serves as a "molecular switch" for induction of cell migration. *J Cell Biol.* 1998; 140: 961-72

Knaut H, Werz C, Geisler R, et al. A zebrafish homologue of the chemokine receptor Cxcr4 is a germ-cell guidance receptor. *Nature.* 2003; 421: 279-82

Koch AE, Polverini PJ, Kunkel SL, et al. Interleukin-8 as a macrophage-derived mediator of angiogenesis. *Science.* 1992; 258: 1798-801

Kochetkova M, Kumar S, McColl SR. Chemokine receptors CXCR4 and CCR7 promote metastasis by preventing anoikis in cancer cells. *Cell Death Differ.* 2009; 16: 664-73

Koeneman KS, Yeung F, Chung LW. Osteomimetic properties of prostate cancer cells: a hypothesis supporting the predilection of prostate cancer metastasis and growth in the bone environment. *Prostate*. 1999; 39: 246-61

Kondo T, Ito F, Nakazawa H, et al. High expression of chemokine gene as a favorable prognostic factor in renal cell carcinoma. *J Urol*. 2004; 17: 2171-5

Krishnan VV, Khan IH, Luciw PA. Multiplexed microbead immunoassays by flow cytometry for molecular profiling: Basic concepts and proteomics applications. *Crit Rev Biotechnol*. 2009; 29: 29-43

Kryczek I, Lange A, Mottram P, et al. CXCL12 and vascular endothelial growth factor synergistically induce neoangiogenesis in human ovarian cancers. *Cancer Res*. 2005; 65: 465-72

Kubista M, Andrade JM, Bengtsson M, et al. The real-time polymerase chain reaction. *Mol Aspects Med*. 2006; 27: 95-125

Kucia M, Jankowski K, Reza R, et al. CXCR4–SDF-1 signalling, locomotion, chemotaxis and adhesion. *J Mol Hist*. 2004; 35: 233-45

Kucia M, Reza R, Miekus K, et al. Trafficking of normal stem cells and metastasis of cancer stem cells involve similar mechanisms: pivotal role of the SDF-1-CXCR4 axis. *Stem Cells*. 2005; 23: 879-94

Kukreja P, Abdel-Mageed AB, Mondal D, et al. Up-regulation of CXCR4 expression in PC-3 cells by stromal-derived factor-1alpha (CXCL12) increases endothelial adhesion and transendothelial migration: role of MEK/ERK signaling pathway-dependent NF-kappaB activation. *Cancer Res*. 2005; 65: 9891-8

Kung AL, Zabudoff SD, France DS et al. Small molecule blockade of transcriptional coactivation of the hypoxia-inducible factor pathway. *Cancer Cell*. 2004; 6: 33–43

Kuwada Y, Sasaki T, Morinaka K, et al. Potential involvement of IL-8 and its receptors in the invasiveness of pancreatic cancer cells. *Int J Oncol*. 2003; 22: 765-71

Lai TH, Fong YC, Fu WM, et al. Stromal cell-derived factor-1 increase alphavbeta3 integrin expression and invasion in human chondrosarcoma cells. *J Cell Physiol*. 2009; 218: 334-42

Lapham CK, Ouyang J, Chandrasekhar B, et al. Evidence for cell-surface association between fusin and the CD4-gp120 complex in human cell lines. *Science*. 1996; 274:602-5

Lasagni L, Francalanci M, Annunziato F et al. An alternatively spliced variant of CXCR3 mediates the inhibition of endothelial cell growth induced by IP-10, Mig, and I-TAC, and acts as functional receptor for platelet factor 4. *J Exp Med*. 2003; 197: 1537-49

Lee J, Horuk R, Rice GC, et al. Characterization of two high-affinity human interleukin-8 receptors. *J Biol Chem.* 1992; 267: 16283-7

Lee JH, Cho YS, Lee JY, et al. The chemokine receptor CCR4 is expressed and associated with a poor prognosis in patients with gastric cancer. *Ann Surg.* 2009; 249: 933-41

Lee LF, Louie MC, Desai SJ, et al. Interleukin-8 confers androgen-independent growth and migration of LNCaP: differential effects of tyrosine kinases Src and FAK. *Oncogene.* 2004; 23: 2197-205

Lee LG, Connell CR, Bloch W. Allelic discrimination by nick-translation PCR with fluorogenic probes. *Nucleic Acids Res.* 1993; 21: 3761-6

Lee Y, Kim SJ, Park HD, et al. PAUF functions in the metastasis of human pancreatic cancer cells and upregulates CXCR4 expression. *Oncogene.* 2010; 29: 56-67

Legler DF, Loetscher M, Roos RS, et al. B cell-attracting chemokine 1, a human CXC chemokine expressed in lymphoid tissues, selectively attracts B lymphocytes via BLR1/CXCR5. *J Exp Med.* 1998; 187: 655-60

Lehr JE, Pienta KJ. Preferential adhesion of prostate cancer cells to a human bone marrow endothelial cell line. *J Natl Cancer Inst.* 1998; 90: 118-23

Lehrer S, Diamond EJ, Mamkin B, et al. Serum interleukin-8 is elevated in men with prostate cancer and bone metastases. *Technol Cancer Res Treat.* 2004; 3: 411

Lespagnard L, Gancberg D, Rouas G, et al. Tumor-infiltrating dendritic cells in neoplasms with a correlation to usual prognostic factors and to clinical outcome. *Int J Cancer.* 1999; 84: 309-14

Li A, Dubey S, Varney ML, et al. IL-8 directly enhanced endothelial cell survival, proliferation, and matrix metalloproteinases production and regulated angiogenesis. *J Immunol.* 2003; 170: 3369-76

Li A, Varney ML, Singh RK. Expression of interleukin 8 and its receptors in human colon carcinoma cells with different metastatic potentials. *Clin Cancer Res.* 2001; 7: 3298-304

Li A, Varney ML, Singh RK. Constitutive expression of growth regulated oncogene (gro) in human colon carcinoma cells with different metastatic potential and its role in regulating their metastatic phenotype. *Clin Exp Metastasis.* 2004; 21:571-9

Liao F, Rabin RL, Smith CS, et al. CC-chemokine receptor 6 is expressed on diverse memory subsets of T cells and determines responsiveness to macrophage inflammatory protein 3 alpha. *J Immunol.* 1999; 162: 186-94

Libura J, Drukala J, Majka M, et al. CXCR4–SDF-1 signaling is active in rhabdomyosarcoma cells and regulates locomotion, chemotaxis, and adhesion. *Blood* 2002; 100: 2597–606

Lin B, White JT, Lu W, et al. Evidence for the presence of disease-perturbed networks in prostate cancer cells by genomic and proteomic analyses: a systems approach to disease. *Cancer Res.* 2005; 65: 3081-309

Liu Y, Ji R, Li J, et al. Correlation effect of EGFR and CXCR4 and CCR7 chemokine receptors in predicting breast cancer metastasis and prognosis. *J Exp Clin Cancer Res.* 2010; 29: 16

Lo BK, Yu M, Zloty D, et al. CXCR3/ligands are significantly involved in the tumorigenesis of basal cell carcinomas. *Am J Pathol.* 2010; 176: 2435-46

Lodowski DT, Palczewski K. Chemokine receptors and other G protein-coupled receptors. *Curr Opin HIV AIDS.* 2009; 4: 88-95

Loetscher M, Geiser T, O'Reilly T, et al. Cloning of a human seven-transmembrane domain receptor, LESTR, that is highly expressed in leukocytes. *J Biol Chem.* 1994; 269: 232-7

Loetscher M, Gerber B, Loetscher P, et al. Chemokine receptor specific for IP10 and MIG: structure, function, and expression in activated T-lymphocytes. *J Exp Med.* 1996; 184: 963-9

Loetscher P, Seitz M, Baggiolini M, et al. Interleukin-2 regulates CC chemokine receptor expression and chemotactic responsiveness in T lymphocytes. *J Exp Med.* 1996; 184: 569-77

Longo MC, Berninger MS, Hartley JL. Use of uracil DNA glycosylase to control carry-over contamination in polymerase chain reactions. *Gene.* 1990; 93: 125-8

Loukinova E, Dong G, Enamorado-Ayalya I, et al. Growth regulated oncogene-alpha expression by murine squamous cell carcinoma promotes tumor growth, metastasis, leukocyte infiltration and angiogenesis by a host CXC receptor-2 dependent mechanism. *Oncogene.* 2000; 19: 3477-86

Lu X, Kang Y. Epidermal growth factor signalling and bone metastasis. *Br J Cancer.* 2010; 102: 457-61

Lu Y, Cai Z, Galson DL, et al. Monocyte chemotactic protein-1 (MCP-1) acts as a paracrine and autocrine factor for prostate cancer growth and invasion. *Prostate*. 2006; 66: 1311-8

Luan J, Shattuck-Brandt R, Haghnegahdar H, et al. Mechanism and biological significance of constitutive expression of MGSA/GRO chemokines in malignant melanoma tumor progression. *J Leukoc Biol*. 1997; 62: 588-97

Luca M, Huang S, Gershenwald JE, et al. Expression of interleukin-8 by human melanoma cells up-regulates MMP-2 activity and increases tumor growth and metastasis. *Am J Pathol*. 1997; 151: 1105-13

Luppi F, Longo AM, de Boer WI, et al. Interleukin-8 stimulates cell proliferation in non-small cell lung cancer through epidermal growth factor receptor transactivation. *Lung Cancer*. 2007; 56: 25-33

Luzzi KJ, MacDonald IC, Schmidt EE, et al. Multistep nature of metastatic inefficiency: dormancy of solitary cells after successful extravasation and limited survival of early micrometastases. *Am J Pathol*. 1998; 153: 865-73

Ma Q, Jones D, Borghesani PR, et al. Impaired B-lymphopoiesis, myelopoiesis, and derailed cerebellar neuron migration in CXCR4- and SDF-1-deficient mice. *Proc Natl Acad Sci U S A*. 1998; 95: 9448-53

MacDonald IC, Groom AC, Chambers AF. Cancer spread and micrometastasis development: Quantitative approaches for in vivo models. *Bioessays*. 2002; 24: 885-93

Maione TE, Gray GS, Petro J, et al. Inhibition of angiogenesis by recombinant human platelet factor-4 and related peptides. *Science*. 1990; 247: 77-9

Mantovani A. Chemokines: introduction and overview. *Chem Immunol*. 1999; 72: 1-6

Mantovani A, Bottazzi B, Colotta F, et al. The origin and function of tumor-associated macrophages. *Immunol. Today*. 1992; 13: 265-70

Marchese A, Docherty JM, Nguyen T, et al. Cloning of human genes encoding novel G protein-coupled receptors. *Genomics*. 1994; 23: 609-18

Marchesi F, Monti P, Leone BE, et al. Increased survival, proliferation, and migration in metastatic human pancreatic tumor cells expressing functional CXCR4. *Cancer Res*. 2004; 64: 8420-7

Marelli MM, Moretti RM, Procacci P, et al. Insulin-like growth factor-I promotes migration in human androgen-independent prostate cancer cells via the α v β 3 integrin and PI3-K/Akt signaling. *Int J Oncol*. 2006; 28: 723-30

Martensson S, Bigler SA, Brown M, et al. Sialyl LewisX and related carbohydrate antigens in the prostate. *Hum Pathol.* 1995; 26: 735–39

Mashino K, Sadanaga N, Yamaguchi H et al. Expression of chemokine receptor CCR7 is associated with lymph node metastasis of gastric carcinoma. *Cancer Res.* 2002; 62: 2937–41

Masood R, Cai J, Tulpule A, et al. Interleukin 8 is an autocrine growth factor and a surrogate marker for Kaposi's sarcoma. *Clin Cancer Res.* 2001; 7: 2693-702

Masters JR. Human cancer cell lines: fact and fantasy. *Nat Rev Mol Cell Biol.* 2000; 1:233-36

Masters JR, Thomson JA, Daly-Burns B, et al. Short tandem repeat profiling provides an international reference standard for human cell lines. *Proc Natl Acad Sci USA.* 2001; 98: 8012-7.

Matloubian M, David A, Engel S, et al. A transmembrane CXC chemokine is a ligand for HIV-coreceptor Bonzo. *Nat Immunol.* 2000; 1: 298-304

Matsuo Y, Raimondo M, Woodward TA, et al. CXC-chemokine/CXCR2 biological axis promotes angiogenesis in vitro and in vivo in pancreatic cancer. *Int J Cancer.* 2009; 125: 1027-37

Matsusue R, Kubo H, Hisamori S, et al. Hepatic stellate cells promote liver metastasis of colon cancer cells by the action of SDF-1/CXCR4 axis. *Ann Surg Oncol.* 2009; 16: 2645-53

Mazzucchelli L, Blaser A, Kappeler A, et al. BCA-1 is highly expressed in *Helicobacter pylori*-induced mucosa-associated lymphoid tissue and gastric lymphoma. *J Clin Invest* 1999; 104: 49–54

Melia J. Part 1: The burden of prostate cancer, its natural history, information on the outcome of screening and estimates of ad hoc screening with particular reference to England and Wales. *BJU Int.* 2005; 95: 4-15 (Suppl. 3)

Mellado M, Rodriguez-Frade JM, Manes S, et al. Chemokine signaling and functional responses: the role of receptor dimerization and TK pathway activation. *Annu Rev Immunol* 2001; 19: 397–421

Mestas J, Burdick MD, Reckamp K, et al. The role of CXCR2/CXCR2 ligand biological axis in renal cell carcinoma. *J Immunol.* 2005; 175: 5351-7

Metzner B, Hofmann C, Heinemann C, et al. Overexpression of CXCchemokines and CXC-chemokine receptor type II constitute an autocrine growth mechanism in the epidermoid carcinoma cells KB and A431. *Oncol Rep.* 1999; 6: 1405-10

Miki J, Furusato B, Li H, et al. Identification of putative stem cell markers, CD133 and CXCR4, in hTERT-immortalized primary nonmalignant and malignant tumor-derived human prostate epithelial cell lines and in prostate cancer specimens. *Cancer Res.* 2007; 67: 3153-61

Miles FL, Pruitt FL, van Golen KL, et al. Stepping out of the flow: capillary extravasation in cancer metastasis. *Clin Exp Metastasis.* 2008; 25: 305-24

Mirisola V, Zuccarino A, Bachmeier BE, et al. CXCL12/SDF1 expression by breast cancers is an independent prognostic marker of disease-free and overall survival. *Eur J Cancer.* 2009; 45: 2579-87

Mishra P, Banerjee D, Ben-Baruch A. Chemokines at the crossroads of tumor-fibroblast interactions that promote malignancy. *J Leukoc Biol.* 2010 Jul 13 [Epub ahead of print]

Miwa S, Mizokami A, Keller ET, et al. The bisphosphonate YM529 inhibits osteolytic and osteoblastic changes and CXCR-4-induced invasion in prostate cancer. *Cancer Res.* 2005; 65: 8818-25

Miyamoto M, Shimizu Y, Okada K, et al. Effect of interleukin-8 on production of tumor-associated substances and autocrine growth of human liver and pancreatic cancer cells. *Cancer Immunol Immunother* 1998; 47:47-57

Mizutani K, Sud S, McGregor NA, et al. The chemokine CCL2 increases prostate tumor growth and bone metastasis through macrophage and osteoclast recruitment. *Neoplasia.* 2009; 11: 1235-42

Mochizuki H, Matsubara A, Teishima J, et al. Interaction of ligand-receptor system between stromal-cell-derived factor-1 and CXC chemokine receptor 4 in human prostate cancer: a possible predictor of metastasis. *Biochem Biophys Res Commun.* 2004; 320: 656-63

Moldovan A. Photo-electric technique for the counting of microscopical cells. *Science* 1934; 80: 188-189

Molino M, Woolkalis MJ, Prevost N, et al. CXCR4 on human endothelial cells can serve as both a mediator of biological responses and as a receptor for HIV-2. *Biochim Biophys Acta.* 2000; 1500: 227-40

Monti P, Leone BE, Marchesi F et al. The CC chemokine MCP-1/CCL2 in pancreatic cancer progression: regulation of expression and potential mechanisms of antimalignant activity. *Cancer Res.* 2003; 63: 7451-61

Moore BB, Arenberg DA, Stoy K, et al. Distinct CXC chemokines mediate tumorigenicity of prostate cancer cells. *Am J Pathol.* 1999; 154: 1503-12

Moore BB, Keane MP, Addison CL, et al. CXC chemokine modulation of angiogenesis: the importance of balance between angiogenic and angiostatic members of the family. *J Investig Med.* 1998; 46: 113-20

Moore MA. The role of chemoattraction in cancer metastases. *Bioessays.* 2001; 23: 674-6

Morrissey C, Vessella RL. The role of tumor microenvironment in prostate cancer bone metastasis. *J Cell Biochem.* 2007; 101: 873-86

Moser B, Schumacher C, von Tschanner V, et al. Neutrophil-activating peptide 2 and gro/melanoma growth-stimulatory activity interact with neutrophil-activating peptide 1/interleukin 8 receptors on human neutrophils. *J Biol Chem.* 1991; 266: 10666-71

Muller A, Homey B, Soto H, et al. Involvement of chemokine receptors in breast cancer metastasis. *Nature* 2001; 410: 50-6

Mundy GR. Metastasis to bone: causes, consequences and therapeutic opportunities. *Nat Rev Cancer.* 2002; 2: 584-93

Murakami T, Maki W, Cardones AR, et al. Expression of CXC chemokine receptor-4 enhances the pulmonary metastatic potential of murine B16 melanoma cells. *Cancer Res.* 2002; 62: 7328-34

Murata H, Nii R, Ito M, et al. Quantitative detection of HCMV-DNA in saliva from infants and breast milk on real-time polymerase chain reaction. *Pediatr Int.* 2009; 51: 530-4

Murdoch C, Monk PN, Finn A. Functional expression of chemokine receptor CXCR4 on human epithelial cells. *Immunology* 1999; 98: 36-41

Murphy C, McGurk M, Pettigrew J, et al. Nonapical and cytoplasmic expression of interleukin-8, CXCR1, and CXCR2 correlates with cell proliferation and microvessel density in prostate cancer. *Clin Cancer Res.* 2005; 11: 4117-27

Murphy PM. International Union of Pharmacology. XXX. Update on chemokine receptor nomenclature. *Pharmacol Rev.* 2002; 54: 227-9

Murphy PM, Baggiolini M, Charo IF, et al. International union of pharmacology. XXII. Nomenclature for chemokine receptors. *Pharmacol Rev.* 2000; 52: 145-176

Murphy PM, Tiffany HL. Cloning of complementary DNA encoding a functional human interleukin-8 receptor. *Science.* 1991; 253: 1280-3

Nagasawa T, Hirota S, Tachibana K, et al. Defects of B-cell lymphopoiesis and bone-marrow myelopoiesis in mice lacking the CXC chemokine PBSF/SDF-1. *Nature*. 1996; 382: 635-8

Najy AJ, Day KC, Day ML. ADAM15 supports prostate cancer metastasis by modulating tumor cell-endothelial cell interaction. *Cancer Res*. 2008; 68: 1092-9

Nakayama T, Hieshima K, Izawa D, et al. Profile of chemokine receptor expression on human plasma cells accounts for their efficient recruitment to target tissues. *J Immunol*. 2003;170: 1136-40

Nangia-Makker P, Hogan V, Honjo Y, et al. Inhibition of human cancer cell growth and metastasis in nude mice by oral intake of modified citrus pectin. *J Natl Cancer Inst*. 2002; 94: 1854-62

Naumann U, Cameroni E, Pruenster M, et al. CXCR7 functions as a scavenger for CXCL12 and CXCL11. *PLoS One*. 2010; 5: e9175

Naumov GN, MacDonald IC, Chambers AF, et al. Solitary cancer cells as a possible source of tumour dormancy? *Semin Cancer Biol*. 2001; 11: 271-76

Naumov GN, MacDonald IC, Weinmeister PM, et al. Persistence of solitary mammary carcinoma cells in a secondary site: a possible contributor to dormancy. *Cancer Res*. 2002; 62: 2162-68

Nelson JB, Hedican SP, George DJ, et al. Identification of endothelin-1 in the pathophysiology of metastatic adenocarcinoma of the prostate. *Nat Med* 1995; 1: 944-9

Nelson JB, Nguyen SH, Wu-Wong JR, et al. New bone formation in an osteoblastic tumor model is increased by endothelin-1 overexpression and decreased by endothelin A receptor blockade. *Urology* 1999; 53: 1063-9

Neote K, DiGregorio D, Mak JY, et al. Molecular cloning, functional expression, and signaling characteristics of a C-C chemokine receptor. *Cell*. 1993; 72: 415-25

Ngaosuwanukul N, Noisumdaeng P, Komolsiri P, et al. Influenza A viral loads in respiratory samples collected from patients infected with pandemic H1N1, seasonal H1N1 and H3N2 viruses. *Virology*. 2010; 7: 75

Niggemann B, Drell TL, Joseph J, et al. Tumour cell locomotion: differential dynamics of spontaneous and induced migration in a 3D collagen matrix. *Exp Cell Res*. 2004; 298: 178-87

Niggemann B, Maaser K, Lu H, et al. Locomotory phenotypes of human tumor cell lines and T lymphocytes in a three-dimensional collagen lattice. *Cancer Lett*. 1997; 118: 173-80

Nimmagadda S, Pullambhatla M, Stone K, et al. Molecular imaging of CXCR4 receptor expression in human cancer xenografts with [(64)Cu]AMD3100 positron emission tomography. *Cancer Res.* 2010; 70: 3935-44

Nishizawa K, Nishiyama H, Oishi S, et al. Fluorescent imaging of high-grade bladder cancer using a specific antagonist for chemokine receptor CXCR4. *Int J Cancer.* 2010; 127: 1180-7

Nitta T, Yagita H, Sato K, et al. Expression of Fc gamma receptors on astroglial cell lines and their role in the central nervous system. *Neurosurgery.* 1992;31:83-7.

Nomiyama H, Hieshima K, Nakayama T, et al. Human CC chemokine liver-expressed chemokine/CCL16 is a functional ligand for CCR1, CCR2 and CCR5, and constitutively expressed by hepatocytes. *Int Immunol.* 2001; 13: 1021-9

Nørgaard M, Jensen AØ, Jacobsen JB, et al. Skeletal related events, bone metastasis and survival of prostate cancer: a population based cohort study in denmark (1999 to 2007). *J Urol.* 2010; 184: 162-7

Oberlin E, Amara A, Bachelier F, et al. The CXC chemokine SDF-1 is the ligand for LESTR/fusin and prevents infection by T-cell-line-adapted HIV-1. *Nature.* 1996; 382: 833-5

Onuffer J, Horuck R. Chemokines, chemokine receptors and small-molecule antagonists: recent developments. *Trends Pharmacol Sci* 2002; 23: 459–67

Orsini MJ, Parent JL, Mundell SJ, et al. Trafficking of the HIV coreceptor CXCR4. Role of arrestins and identification of residues in the c-terminal tail that mediate receptor internalization. *J Biol Chem.* 1999; 274: 31076–86

Ottaiano A, Franco R, Aiello Talamanca A, et al. Overexpression of both CXC chemokine receptor 4 and vascular endothelial growth factor proteins predicts early distant relapse in stage II-III colorectal cancer patients. *Clin Cancer Res.* 2006; 12: 2795-803

Owen JD, Strieter R, Burdick M, et al. Enhanced tumour-forming capacity for immortalized melanocytes expressing melanoma growth stimulatory activity/ growth-regulated cytokine beta and gamma proteins. *Int J Cancer.* 1997; 73: 94-103

Paget S. The distribution of secondary growths in cancer of the breast. *Lancet.* 1889; 1: 571-3

Pan J, Kunkel EJ, Gossler U, et al. A novel chemokine ligand for CCR10 and CCR3 expressed by epithelial cells in mucosal tissues. *J Immunol.* 2000; 165: 2943-9

Pan J, Mestas J, Burdick MD, et al. Stromal derived factor-1 (SDF-1/CXCL12) and CXCR4 in renal cell carcinoma metastasis. *Mol Cancer*. 2006; 5: 56

Papanicolaou GN, Traut R. The diagnostic value of vaginal smears in carcinoma of the uterus. *Am J Obstet Gynecol* 1941;42: 193

Park S, Koch D, Cardenas R, et al. Cell motility and local viscoelasticity of fibroblasts. *Biophys J*. 2005; 89: 4330-42

Payne AS, Cornelius LA. The role of chemokines in melanoma tumor growth and metastasis. *J Invest Dermatol* 2002; 118: 915–22

Perera LP, Goldman CK, Waldmann TA. IL-15 induces the expression of chemokines and their receptors in T lymphocytes. *J Immunol*. 1999; 162: 2606-12

Peveri P, Walz A, Dewald B, et al. A novel neutrophil-activating factor produced by human mononuclear phagocytes. *J Exp Med*. 1988; 167: 1547-59

Phillips RJ, Burdick MD, Lutz M, et al. The stromal derived factor-1/CXCL12-CXC chemokine receptor 4 biological axis in non-small cell lung cancer metastases. *Am J Respir Crit Care Med*. 2003; 167: 1676-86

Pienta KJ, Naik H, Akhtar A, et al. Inhibition of spontaneous metastasis in a rat prostate cancer model by oral administration of modified citrus pectin. *J Natl Cancer Inst*. 1995;87: 348–53

Pinilla S, Alt E, Abdul Khalek FJ, et al. Tissue resident stem cells produce CCL5 under the influence of cancer cells and thereby promote breast cancer cell invasion. *Cancer Lett*. 2009; 284: 80-5

Ponomaryov T, Peled A, Petit I, et al. Increased production of SDF-1 following treatment with DNA damaging agents: relevance for human stem cell homing and repopulation of NOD/SCID mice. *J Clin Investig*. 2000; 106: 1331-9

Popivanova BK, Kostadinova FI, Furuichi K, et al. Blockade of a chemokine, CCL2, reduces chronic colitis-associated carcinogenesis in mice. *Cancer Res*. 2009; 69: 7884-92

Porvasnik S, Sakamoto N, Kusmartsev S, et al. Effects of CXCR4 antagonist CTCE-9908 on prostate tumor growth. *Prostate*. 2009; 69: 1460-9

Pradelli E, Karimjee-Soilihi B, Michiels JF, et al. Antagonism of chemokine receptor CXCR3 inhibits osteosarcoma metastasis to lungs. *Int J Cancer*. 2009; 125: 2586-94

Preffer F, Dombkowski D. Advances in complex multiparameter flow cytometry technology: Applications in stem cell research. *Cytometry B Clin Cytom*. 2009; 76: 295-314

Rajan R, Vanderslice R, Kapur S, et al. Epidermal growth factor (EGF) promotes the chemomigration of a human prostate cell line, and EGF immunoreactive proteins are present at sites of metastasis in the stroma of lymph nodes and medullary bone. *Prostate*. 1996; 28: 1-9

Ran M, Langer AB, Eliassi I, et al. Possibilities of interference with the immune system of tumor bearers by non-lymphoid Fc gamma RII expressing tumor cells. *Immunobiology*. 1992; 185: 415-25

Ran M, Teillaud JL, Fridman WH, et al. Increased expression of Fc gamma receptor in cancer patients and tumor bearing mice. *Mol Immunol*. 1988; 25: 1159-67

Rana A, Chisholm GD, Khan M, et al. Patterns of bone metastasis and their prognostic significance in patients with carcinoma of the prostate. *Br J Urol* 1993; 72: 933-6

Raport CJ, Gosling J, Schweickart VL, et al. Molecular cloning and functional characterization of a novel human CC chemokine receptor (CCR5) for RANTES, MIP-1beta, and MIP-1alpha. *J Biol Chem*. 1996; 271: 17161-6

Ratajczak MZ, Kucia M, Reza R, et al. Stem cell plasticity revisited: CXCR4-positive cells expressing mRNA for early muscle, liver and neural cells 'hide out' in the bone marrow. *Leukemia* 2004; 18: 29-40

Raychaudhuri B, Vogelbaum MA. IL-8 is a mediator of NF-kappaB induced invasion by gliomas. *J Neurooncol*. 2010 Jun 25 [Epub ahead of print]

Raynaud CM, Mercier O, Darteville P, et al. Expression of chemokine receptor CCR6 as a molecular determinant of adrenal metastatic relapse in patients with primary lung cancer. *Clin Lung Cancer*. 2010; 11: 187-91

Raz E, Mahabaleshwar H. Chemokine signaling in embryonic cell migration: a fisheye view. *Development*. 2009; 136: 1223-9

Rhoads RP, McManaman C, Ingvarsen KL, et al. The housekeeping genes GAPDH and cyclophilin are regulated by metabolic state in the liver of dairy cows. *J Dairy Sci*. 2003; 86: 3423-9

Richards BL, Eisma RJ, Spiro JD, et al. Coexpression of interleukin-8 receptors in head and neck squamous cell carcinoma. *Am J Surg*. 1997; 174: 507-12

Richmond A, Thomas HG. Purification of melanoma growth stimulatory activity. *J Cell Physiol*. 1986; 129: 375-84

Ritchie CK, Andrews LR, Thomas KG, et al. The effects of growth factors associated with osteoblasts on prostate carcinoma proliferation and chemotaxis: Implications for the development of metastatic disease. *Endocrinology*. 1997; 138: 1145–50

Rollins JB. Chemokines. *Blood*. 1997; 90: 909-28

Romanov VI, Goligorsky MS. RGD-recognizing integrins mediate interactions of human prostate carcinoma cells with endothelial cells in vitro. *Prostate*. 1999; 39: 108–18

Romanov VI, Whyard T, Adler HL, et al. Prostate cancer cell adhesion to bone marrow endothelium: the role of prostate-specific antigen. *Cancer Res*. 2004; 64: 2083-9

Roos RS, Loetscher M, Legler DF, et al. Identification of CCR8, the receptor for the human CC chemokine I-309. *J Biol Chem*. 1997; 272: 17251-4

Rosol TJ, Tannehill-Gregg SH, LeRoy BE, et al. Animal models of bone metastasis. *Cancer*. 2003; 97: 748–57

Rubie C, Frick VO, Ghadjar P, et al. CXC receptor-4 mRNA silencing abrogates CXCL12-induced migration of colorectal cancer cells. *J Transl Med*. 2011; 9: 22

Rucci N, Teti A. Osteomimicry: how tumor cells try to deceive the bone. *Front Biosci (Schol Ed)*. 2010; 2: 907-15

Ruffing N, Sullivan N, Sharmeen L, et al. CCR5 has an expanded ligand-binding repertoire and is the primary receptor used by MCP-2 on activated T cells. *Cell Immunol*. 1998; 189: 160-8

Salcedo R, Wasserman K, Young HA, et al. Vascular endothelial growth factor and basic fibroblast growth factor induce expression of CXCR4 on human endothelial cells: in vivo neovascularization induced by stromal-derived factor-1alpha. *Am J Pathol*. 1999; 154: 1125-35

Samson M, Labbe O, Mollereau C, et al. Molecular cloning and functional expression of a new human CC-chemokine receptor gene. *Biochemistry*. 1996; 35: 3362-7

Sanchez-Sweatman OH, Orr FW, Singh G. Human metastatic prostate PC3 cell lines degrade bone using matrix metalloproteinases. *Invasion Metastasis* 1998; 18: 297-305

Sanger F, Nicklen S, Coulson AR. DNA sequencing with chain-terminating inhibitors. *Proc Natl Acad Sci USA*. 1977; 74: 5463–7

Satyamoorthy K, Li G, Gerrero MR, et al. Constitutive mitogen-activated protein kinase activation in melanoma is mediated by both BRAF mutations and autocrine growth factor stimulation. *Cancer Res*. 2003; 63: 756-9

Sauvé K, Lepage J, Sanchez M, et al. Positive feedback activation of estrogen receptors by the CXCL12-CXCR4 pathway. *Cancer Res.* 2009; 69: 5793-800

Schadendorf D, Moller A, Algermissen B, et al. IL-8 produced by human malignant melanoma cells in vitro is an essential autocrine growth factor. *J Immunol.* 1993; 151: 2267-75

Schechter AD, Berman AB, Taubman MB. Chemokine receptors in vascular smooth muscle. *Microcirculation* 2003; 10: 265–72

Schioppa T, Uranchimeg B, Saccani A, et al. Regulation of the chemokine receptor CXCR4 by hypoxia. *J Exp Med.* 2003; 198: 1391-402

Scott LJ, Clarke NW, George NJ, et al. Interactions of human prostatic epithelial cells with bone marrow endothelium: binding and invasion. *Br J Cancer.* 2001; 84: 1417–23

Scotton CJ, Wilson JL, Milliken D, et al. Epithelial cancer cell migration: a role for chemokine receptors? *Cancer Res.* 2001; 61: 4961-65

Sehgal A, Keener C, Boynton AL, et al. CXCR-4, a chemokine receptor, is overexpressed in and required for proliferation of glioblastoma tumor cells. *J Surg Oncol.* 1998; 69: 99-104

Sehgal A, Ricks S, Boynton AL, et al. Molecular characterization of CXCR-4: a potential brain tumor-associated gene. *J Surg Oncol.* 1998; 69: 239-48

Sgadari C, Angiolillo AL, Cherney BW, et al. Interferon-inducible protein-10 identified as a mediator of tumor necrosis in vivo. *Proc Natl Acad Sci USA.* 1996; 93: 13791-6

Shah RB, Mehra R, Chinnaiyan AM, et al. Androgen-independent prostate cancer is a heterogeneous group of diseases: lessons from a rapid autopsy program. *Cancer Res.* 2004; 64: 9209–16

Shao XJ, Xie FM. Influence of angiogenesis inhibitors, endostatin and PF-4, on lymphangiogenesis. *Lymphology.* 2005; 38: 1-8

Shintani S, Ishikawa T, Nonaka T, et al. Growth-regulated oncogene-1 expression is associated with angiogenesis and lymph node metastasis in human oral cancer. *Oncology.* 2004; 66: 316-22

Sica A, Saccani A, Borsatti A, et al. Bacterial lipopolysaccharide rapidly inhibits expression of C-C chemokine receptors in human monocytes. *J Exp Med.* 1997; 185: 969-74

Sikes RA, Nicholson BE, Koeneman KS et al. Cellular interactions in the tropism of prostate cancer to bone. *Int J Cancer.* 2004; 110: 497-503

Singh S, Singh R, Sharma PK, et al. Serum CXCL13 positively correlates with prostatic disease, prostate-specific antigen and mediates prostate cancer cell invasion, integrin clustering and cell adhesion. *Cancer Lett.* 2009a; 283: 29-35

Singh S, Singh UP, Grizzle WE, et al. CXCL12-CXCR4 interactions modulate prostate cancer cell migration, metalloproteinase expression and invasion. *Lab Invest.* 2004a; 84: 1666-76

Singh S, Singh UP, Stiles JK, et al. Expression and Functional Role of CCR9 in Prostate Cancer Cell Migration and Invasion. *Clin Cancer Res.* 2004b; 10: 8743-50

Singh S, Varney M, Singh RK. Host CXCR2-dependent regulation of melanoma growth, angiogenesis, and experimental lung metastasis. *Cancer Res.* 2009b; 69: 411-5

Smith MC, Luker KE, Garbow JR, et al. CXCR4 regulates growth of both primary and metastatic breast cancer. *Cancer Res.* 2004; 64: 8604-12

Somlyo AV, Bradshaw D, Ramos S, et al. Rho-kinase inhibitor retards migration and in vivo dissemination of human prostate cancer cells. *Biochem Biophys Res Commun.* 2000; 269: 652-9

Song Z, Powell WC, Kasahara N, et al. The effect of fibroblast growth factor 8, isoform b, on the biology of prostate carcinoma cells and their interaction with stromal cells. *Cancer Res.* 2000; 60: 6730-6

Sozzani S, Allavena P, Vecchi A, et al. Chemokines and dendritic cell traffic. *J Clin Immunol.* 2000; 20: 151-60

Stacey GN. Cell contamination leads to inaccurate data: we must take action now. *Nature.* 2000; 403: 356

Staller P, Sulitkova J, Lisztwan J, et al. Chemokine receptor CXCR4 downregulated by von Hippel-Lindau tumour suppressor pVHL. *Nature.* 2003; 425: 307-11

Steele BK, Meyers C, Ozbun MA. Variable expression of some "housekeeping" genes during human keratinocyte differentiation. *Anal Biochem.* 2002; 307: 341-7

Stone KR, Mickey DD, Wunderli H, et al. Isolation of a human prostate carcinoma cell line (DU145). *Int J Cancer.* 1978; 21: 274-81

Strieter RM, Belperio JA, Phillips RJ, et al. CXC chemokines in angiogenesis of cancer. *Semin Cancer Biol.* 2004; 14: 195-200

Strieter RM, Polverini PJ, Kunkel SL, et al. The functional role of the ELR motif in CXC chemokine mediated angiogenesis. *J Biol Chem.* 1995; 270: 27348-57

Struyf S, Burdick MD, Peeters E, et al. Platelet factor-4 variant chemokine CXCL4L1 inhibits melanoma and lung carcinoma growth and metastasis by preventing angiogenesis. *Cancer Res.* 2007; 67: 5940-8

Struyf S, Burdick MD, Proost P, et al. Platelets release CXCL4L1, a nonallelic variant of the chemokine platelet factor-4/CXCL4 and potent inhibitor of angiogenesis. *Circ Res.* 2004; 95: 855-7

Sun YX, Schneider A, Jung Y, et al. Skeletal localization and neutralization of the SDF-1(CXCL12)/CXCR4 axis blocks prostate cancer metastasis and growth in osseous sites in vivo. *J Bone Miner Res.* 2005; 20: 318-29

Sun YX, Wang J, Shelburne CE, et al. Expression of CXCR4 and CXCL12 (SDF-1) in human prostate cancers (PCa) in vivo. *J Cell Biochem.* 2003; 89: 462-73

Sutton A, Friand V, Brulé-Donneger S, et al. Stromal cell-derived factor-1/chemokine (C-X-C motif) ligand 12 stimulates human hepatoma cell growth, migration, and invasion. *Mol Cancer Res.* 2007; 5: 21-33

Tabata S, Kadowaki N, Kitawaki T, et al. Distribution and kinetics of SR-PSOX/CXCL16 and CXCR6 expression on human dendritic cell subsets and CD4+ T cells. *J Leukoc Biol.* 2005; 77: 777-86

Tachibana K, Hirota S, Iizasa H, et al. The chemokine receptor CXCR4 is essential for vascularization of the gastrointestinal tract. *Nature.* 1998; 393: 591-94

Taichman RS, Cooper C, Keller ET, et al. Use of stromal cell-derived factor-1/CXCR4 pathway in prostate cancer metastasis to bone. 2002; 62: 1832-7

Takamori H, Oades ZG, Hoch OC, et al. Autocrine growth effect of IL-8 and GROalpha on a human pancreatic cancer cell line, Capan-1. *Pancreas.* 2000; 21: 52-6

Takanami I. Overexpression of CCR7 mRNA in non-small cell lung cancer: correlation with lymph node metastasis. *Int J Cancer.* 2003; 105: 186-9

Takenaga M, Tamamura H, Hiramatsu K, et al. A single treatment with microcapsules containing a CXCR4 antagonist suppresses pulmonary metastasis of murine melanoma. *Biochem Biophys Res Commun.* 2004; 320: 226-32

Takuwa Y, Masaki T, Yamashita K. The effects of the endothelin family peptides on cultured osteoblastic cells from rat calvariae. *Biochem Biophys Res Commun* 1990; 170: 998–1005

Tamamura H, Fujisawa M, Hiramatsu K, et al. Identification of a CXCR4 antagonist, a T140 analog, as an anti-rheumatoid arthritis agent. *FEBS Lett.* 2004; 569: 99-104

Tan CT, Chu CY, Lu YC, et al. CXCL12/CXCR4 promotes laryngeal and hypopharyngeal squamous cell carcinoma metastasis through MMP-13-dependent invasion via the ERK1/2/AP-1 pathway. *Carcinogenesis*. 2008; 29: 1519-27

Tang CH, Yamamoto A, Lin YT, et al. Involvement of matrix metalloproteinase-3 in CCL5/CCR5 pathway of chondrosarcomas metastasis. *Biochem Pharmacol*. 2010; 79: 209-17

Tantivejkul K, Kalikin LM, Pienta KJ. Dynamic Process of Prostate Cancer Metastasis to Bone. *J Cell Biochem*. 2004; 91 :706–17

Tarasova NI, Stauber RH, Michejda CJ. Spontaneous and ligand-induced trafficking of CXC-chemokine receptor 4. *J Biol Chem*. 1998; 273:15883-6

Thalmann GN, Sikes RA, Devoll RE et al. Osteopontin: possible role in prostate cancer progression. *Clin Cancer Res*. 1999; 5: 2271-7

Thelen M. Dancing to the tune of chemokines. *Nature Immunol*. 2001; 2: 129-34

Thelen M, Peveri P, Kern P, et al. Mechanism of neutrophil activation by NAF, a novel monocyte-derived peptide agonist. *FASEB J*. 1988; 2: 2702-6

Thomas BG, Hamdy FC. Bone morphogenetic protein-6: potential mediator of osteoblastic metastases in prostate cancer. *Prostate Cancer Prostatic Dis*. 2000; 3: 283–5

Tiffany HL, Lautens LL, Gao JL, et al. Identification of CCR8: a human monocyte and thymus receptor for the CC chemokine I-309. *J Exp Med*. 1997;186: 165-70

Townson JL, Chambers AF. Dormancy of solitary metastatic cells. *Cell Cycle*. 2006; 5: 1744-50

Trent JO, Wang ZX, Murray JL, et al. Lipid bilayer simulations of CXCR4 with inverse agonists and weak partial agonists. *J Biol Chem*. 2003; 278: 47136-44

Tsingotjidou AS, Zotalis G, Jackson KR, et al. Development of an animal model for prostate cancer cell metastasis to adult human bone. *Anticancer Res*. 2001; 21: 971–8

Tsou CL, Gladue RP, Carroll LA, et al. Identification of C-C chemokine receptor 1 (CCR1) as the monocyte hemofiltrate C-C chemokine (HCC)-1 receptor. *J Exp Med*. 1998; 188: 603-8

Tsukahara H, Hori C, Hiraoka M, et al. Endothelin subtype A receptor antagonist induces osteopenia in growing rats. *Metabolism* 1998; 47: 1403–7

Uehara H, Troncoso P, Johnston D, et al. Expression of interleukin-8 gene in radical prostatectomy specimens is associated with advanced pathologic stage. *Prostate*. 2005; 64: 40–9

Uguccioni M, Mackay CR, Ochensberger B, et al. High expression of the chemokine receptor CCR3 in human blood basophils: role in activation by eotaxin, MCP-4, and other chemokines. *J Clin Invest*. 1997; 100: 1137-43

Unlü A, Leake RE. The effect of EGFR-related tyrosine kinase activity inhibition on the growth and invasion mechanisms of prostate carcinoma cell lines. *Int J Biol Markers*. 2003; 18: 139-46

Unutmaz D, Xiang W, Sunshine MJ, et al. The primate lentiviral receptor Bonzo/STRL33 is coordinately regulated with CCR5 and its expression pattern is conserved between human and mouse. *J Immunol*. 2000; 165: 3284-92

Vaday GG, Hua SB, Peehl DM, et al. CXCR4 and CXCL12 (SDF-1) in prostate cancer: inhibitory effects of human single chain Fv antibodies. *Clin Cancer Res*. 2004; 10: 5630-9

Vaday GG, Peehl DM, Kadam PA, et al. Expression of CCL5 (RANTES) and CCR5 in prostate cancer. *Prostate*. 2006; 66: 124-34

Vandercappellen J, Liekens S, Bronckaers A, et al. The COOH-terminal peptide of platelet factor-4 variant (CXCL4L1/PF-4var47-70) strongly inhibits angiogenesis and suppresses B16 melanoma growth in vivo. *Mol Cancer Res*. 2010; 8: 322-34

Vandesompele J, De Preter K, Pattyn F et al. Accurate normalization of real-time quantitative RT-PCR data by geometric averaging of multiple internal control genes. *Genome Biol*. 2002; 3: RESEARCH0034

Varney ML, Li A, Dave BJ, et al. Expression of CXCR1 and CXCR2 receptors in malignant melanoma with different metastatic potential and their role in interleukin-8 (CXCL-8)-mediated modulation of metastatic phenotype. *Clin Exp Metastasis* 2003; 20: 723–31

Veltri RW, Miller MC, Zhao G, et al. Interleukin-8 serum levels in patients with benign prostatic hyperplasia and prostate cancer. *Urology*. 1999; 53: 139-47

Vicari AP, Caux C. Chemokines in cancer. *Cytokine Growth Factor Rev* 2002; 13: 143–54

Virchow R. Ueber bewegliche thierische Zellen. *Arch Path Anal Physiol*. 1863; 28: 237–40

Visvader JE, Lindeman GJ. Cancer stem cells in solid tumours: accumulating evidence and unresolved questions. *Nat Rev Cancer*. 2008; 8: 755-68

Waghray A, Feroze F, Schober et al. Identification of androgen-regulated genes in the prostate cancer cell line LNCaP by serial analysis of gene expression and proteomic analysis. *Proteomics*. 2001; 1: 1327-38

Wagner PL, Hyjek E, Vazquez MF, et al. CXCL12 and CXCR4 in adenocarcinoma of the lung: association with metastasis and survival. *J Thorac Cardiovasc Surg*. 2009; 137: 615-21

Wagner PL, Moo TA, Arora N, et al. The chemokine receptors CXCR4 and CCR7 are associated with tumor size and pathologic indicators of tumor aggressiveness in papillary thyroid carcinoma. *Ann Surg Oncol*. 2008; 15: 2833-41

Walter DH, Haendeler J, Reinhold J, et al. Impaired CXCR4 signaling contributes to the reduced neovascularization capacity of endothelial progenitor cells from patients with coronary artery disease. *Circ Res*. 2005; 97: 1142-51

Walther HE. *Krebmetastasen*. Bens Schwabe Verlag. Basel: Switzerland. 1948

Walz A, Perveri P, Aschauer H, Baggiolini M. Purification and amino acid sequencing of NAF, a novel neutrophil-activating factor produced by monocytes. *Biochem Biophys Res Commun* 1987; 149: 755-61

Wan XS, Zhou Z, Steele V, et al. Establishment and characterization of sublines of LNCaP human prostate cancer cells. *Oncol Rep*. 2003; 10: 1569-75

Wang B, Hendricks DT, Wamunyokoli F, et al. A growth-related oncogene/CXC chemokine receptor 2 autocrine loop contributes to cellular proliferation in esophageal cancer. *Cancer Res*. 2006; 66: 3071-7

Wang D, Wang H, Brown J, et al. CXCL1 induced by prostaglandin E2 promotes angiogenesis in colorectal cancer. *J Exp Med*. 2006; 203: 941-51

Wang D, Yang W, Du J, et al. MGSA/GRO-mediated melanocyte transformation involves induction of Ras expression. *Oncogene*. 2000; 19: 4647-59

Wang J, Wang J, Sun Y, et al. Diverse signaling pathways through the SDF-1/CXCR4 chemokine axis in prostate cancer cell lines leads to altered patterns of cytokine secretion and angiogenesis. *Cell Signal*. 2005; 17: 1578-92

Wang L, Wang L, Yang B, et al. Strong expression of chemokine receptor CXCR4 by renal cell carcinoma cells correlates with metastasis. *Clin Exp Metastasis*. 2009; 26: 1049-54

Wang W, Soto H, Oldham ER, et al. Identification of a novel chemokine (CCL28), which binds CCR10 (GPR2). *J Biol Chem.* 2000; 275: 22313-23

Ward SG. T lymphocytes on the move: chemokines, PI3-kinase and beyond. *Trends Immunol* 2006; 27: 80-7

Wawroschek F, Vogt H, Weckermann D et al. Radioisotope guided pelvic lymph node dissection for prostate cancer. *J Urol.* 2001; 166: 1715-9

Werr J, Xie X, Hedqvist P, et al. Beta1 integrins are critically involved in neutrophil locomotion in extravascular tissue in vivo. *J Exp Med.* 1998; 187: 2091-6

Whiteside TL. The role of immune cells in the tumor microenvironment. *Cancer Treat Res.* 2006; 130: 103-24

Wilbanks A, Zondlo SC, Murphy K, et al. Expression cloning of the STRL33/BONZO/TYMSTR ligand reveals elements of CC, CXC and CX3C chemokines. *J Immunol.* 2001; 166: 5145-54

Wiley H, Gonzalez E, Maki W, et al. Expression of CC chemokine receptor-7 and regional lymph node metastasis of B16 murine melanoma. *J Natl Cancer Inst.* 2001; 93: 1638-43

Wood B. 9-color and 10-color flow cytometry in the clinical laboratory. *Arch Pathol Lab Med.* 2006; 130: 680-90

Wright DE, Bowman EP, Wagers AJ, et al. Hematopoietic stem cells are uniquely selective in their migratory response to chemokines. *J Exp Med.* 2002; 195: 1145-54

www.seer.cancer.gov/statfacts/ Website for "Surveillance, Epidemiology and End Results (SEER) Program". Last accessed June 2010.

www.statistics.gov.uk Website for the "Office for National Statistics". Last accessed June 2010.

Xing Y, Liu M, Du Y, et al. Tumor cell-specific blockade of CXCR4/SDF-1 interactions in prostate cancer cells by hTERT promoter induced CXCR4 knockdown: A possible metastasis preventing and minimizing approach. *Cancer Biol Ther.* 2008; 7: 1839-48

Yamagami S, Tokuda Y, Ishii K, et al. cDNA cloning and functional expression of a human monocyte chemoattractant protein 1 receptor. *Biochem Biophys Res Commun.* 1994; 202: 1156-62

Yamaguchi K, Ogawa K, Katsube T, et al. Platelet factor 4 gene transfection into tumor cells inhibits angiogenesis, tumor growth and metastasis. *Anticancer Res.* 2005; 25: 847-51

Yanagihara S, Komura E, Nagafune J, et al. EBI1/CCR7 is a new member of dendritic cell chemokine receptor that is up-regulated upon maturation. *J Immunol.* 1998; 161: 3096-102

Yang G, Rosen DG, Liu G, et al. CXCR2 Promotes Ovarian Cancer Growth through Dysregulated Cell Cycle, Diminished Apoptosis, and Enhanced Angiogenesis. *Clin Cancer Res.* 2010 May 26. [Epub ahead of print]

Yang J, Richmond A. The angiostatic activity of interferon-inducible protein-10/CXCL10 in human melanoma depends on binding to CXCR3 but not to glycosaminoglycan. *Mol Ther.* 2004; 9: 846-55

Yang L, Carbone DP. Tumor-host immune interactions and dendritic cell dysfunction. *Adv Cancer Res.* 2004; 92: 13-27

Yang TY, Chen SC, Leach MW, et al. Transgenic expression of the chemokine receptor encoded by human herpesvirus 8 induces an angioproliferative disease resembling Kaposi's sarcoma. *J Exp Med.* 2000; 191: 445-54

Yin JJ, Mohammad KS, Kakonen SM, et al. A causal role for endothelin-1 in the pathogenesis of osteoblastic bone metastases. *Proc Natl Acad Sci USA* 2003; 100: 10954-9.

Yoshida R, Imai T, Hieshima K, et al. Molecular cloning of a novel human CC chemokine EBI1-ligand chemokine that is a specific functional ligand for EBI1, CCR7. *J Biol Chem.* 1997; 272: 13803-9

Yoshimura T, Matsushima K, Openheim JJ, et al. Neutrophil chemotactic factor produced by lipopolysaccharide (LPS)-stimulated human blood mononuclear leukocytes: partial characterization and separation from interleukin-1 (IL1). *J Immunol* 1987; 139: 788-93

Youn BS, Zhang SM, Broxmeyer HE, et al. Characterization of CKbeta8 and CKbeta8-1: two alternatively spliced forms of human beta-chemokine, chemoattractants for neutrophils, monocytes, and lymphocytes, and potent agonists at CC chemokine receptor1. *Blood.* 1998; 91: 3118-26

Yperman J, De Visscher G, Holvoet P, et al. beta-actin cannot be used as a control for gene expression in ovine interstitial cells derived from heart valves. *J Heart Valve Dis.* 2004; 13: 848-53

Yu S, Duan J, Zhou Z, et al. A critical role of CCR7 in invasiveness and metastasis of SW620 colon cancer cell in vitro and in vivo. *Cancer Biol Ther.* 2008; 7: 1037-43

Yuan Y, Liu J, Liu Z, et al. Chemokine CCL3 facilitates the migration of hepatoma cells by changing the concentration intracellular Ca. *Hepatol Res.* 2010; 40: 424-31

Zaballos A, Gutierrez J, Varona R, et al. Identification of the orphan chemokine receptor GPR-9-6 as CCR9, the receptor for the chemokine TECK. *J Immunol.* 1999; 162: 5671-5

Zagzag D, Krishnamachary B, Yee H, et al. Stromal cell-derived factor-1 α and CXCR4 expression in hemangioblastoma and clear cell-renal cell carcinoma: von Hippel-Lindau loss-of-function induces expression of a ligand and its receptor. *Cancer Res.* 2005; 65: 6178-88

Zhang J, Patel L, Pienta KJ. CC chemokine ligand 2 (CCL2) promotes prostate cancer tumorigenesis and metastasis. *Cytokine Growth Factor Rev.* 2010; 21: 41-8

Zhang S, Qi L, Li M, et al. Chemokine CXCL12 and its receptor CXCR4 expression are associated with perineural invasion of prostate cancer. *J Exp Clin Cancer Res.* 2008; 27: 62

Zhang T, Somasundaram R, Berencsi K, et al. CXC chemokine ligand 12 (stromal cell-derived factor 1 alpha) and CXCR4-dependent migration of CTLs toward melanoma cells in organotypic culture. *J Immunol.* 2005; 174: 5856-63

Zhang WB, Navenot JM, Haribabu B, et al. A point mutation that confers constitutive activity to CXCR4 reveals that T140 is an inverse agonist and that AMD3100 and ALX40-4C are weak partial agonists. *J Biol Chem.* 2002; 277: 24515-21

Zhang X, Haney KM, Richardson AC, et al. Anibamine, a natural product CCR5 antagonist, as a novel lead for the development of anti-prostate cancer agents. *Bioorg Med Chem Lett.* 2010 Jun 8. [Epub ahead of print]

Zhou HE, Li CL, Chung LW. Establishment of human prostate carcinoma skeletal metastasis models. *Cancer.* 2000; 88: 2995-3001 (suppl 12)

Zheng J, Ghorpade A, Niemann D, et al. Lymphotropic virions affect chemokine receptor mediated neural signaling and apoptosis; implications for human immunodeficiency virus type 1-associated dementia. *J Virol.* 1999; 73: 8256-67

Zhu YM, Webster SJ, Flower D, et al. Interleukin-8/CXCL8 is a growth factor for human lung cancer cells. *Br J Cancer.* 2004; 91: 1970-6

Zlotnik A. New insights on the role of CXCR4 in cancer metastasis. *J Pathol.* 2008; 215: 211-3

Zlotnik A, Yoshie O. Chemokines: a new classification system and their role in immunity. *Immunity.* 2000; 12: 121-7

Zoetewij JP, Golding H, Mostowski H, et al. Cytokines regulate expression and function of the HIV coreceptor CXCR4 on human mature dendritic cells. *J Immunol.* 1998; 161: 3219–23

Zou YR, Kottmann AH, Kuroda M, et al. Function of the chemokine receptor CXCR4 in haematopoiesis and in cerebellar development. *Nature* 1998; 393: 595-9

APPENDIX: ABSTRACTS OF
ARTICLES PUBLISHED FROM
THESIS

1. Arya M et al. J Exp Ther Oncol. 2004;4:291-303.

The importance of the CXCL12-CXCR4 chemokine ligand-receptor interaction in prostate cancer metastasis

AIM: Chemokines or chemotactic cytokines are known to be important in the directional migration or chemotaxis of leucocytes in conditions of homeostasis and in inflammatory or immunological responses. However, the role of chemokines is extending beyond their involvement in mediating leucocyte trafficking with an increasing body of evidence suggesting these proteins are intimately involved in many stages of tumour development and progression. Our aim was to study the role of the CXCL12:CXCR4 chemokine ligand:receptor complex in determining the organ-specific metastasis of prostate cancer.

MATERIALS and METHODS: CXCR4 mRNA expression was determined by RT-PCR in 3 metastatic prostate cancer cell lines DU145, LNCaP and PC3, the primary prostate cancer cell line 1542 CPT3X and the normal prostate epithelial cell lines 1542 NPTX and Pre 2.8. This was followed by Taqman quantitative PCR analysis of CXCR4 mRNA in these cell lines. Flow cytometry analysis was then used to measure the expression of the CXCR4 receptor protein on the cell surface. The influence of the receptor on cell migration was studied using Transwell, Migration Assays. Finally, Taqman quantitative PCR was performed on RNA obtained from laser microdissected fresh primary prostate tumour and benign tissue samples from patients.

RESULTS: In DU145, LNCaP and PC3 CXCR4 mRNA expression was approximately 1000, 400 and 21 times respectively that of 1542 NPTX, Pre 2.8 and 1542 CPT3X. In patient primary tumour samples and patient benign tissue specimens CXCR4 mRNA expression was similar to that of the metastatic cell line DU145. Flow cytometry analysis showed that significantly higher levels of the CXCR4 receptor were present on the cell surface of the 3 metastatic cell lines. Migration studies revealed that chemotaxis of the metastatic cell lines PC3 and DU145 was enhanced by CXCL12 ligand and inhibited by antibody to CXCR4. CXCL12 did not influence the migration of the normal prostate epithelial cell line 1542 NPTX.

CONCLUSIONS: We have demonstrated that human prostate cell lines derived from metastases express functional CXCR4 receptor and that CXCL12 ligand enhances their migratory capabilities. Also, laser microdissected primary patient tumours and patient benign tissue specimens express CXCR4 mRNA at high levels (it is suggested that post-transcriptional modification of the CXCR4 receptor plays a major role in regulating protein expression). These results suggest prostate cancers may be influenced by the CXCL12:CXCR4 pathway during metastasis. This pathway would provide a novel target for therapeutic intervention.

2. Arya M et al. Tumour Biol. 2007;28:123-31.

Clinical importance and therapeutic implications of the pivotal CXCL12-CXCR4 (chemokine ligand-receptor) interaction in cancer cell migration

Chemokines are small, secreted proteins and are now the largest known cytokine family. They mediate their effects through a family of G-protein-coupled receptors and were initially recognized for their ability to act as chemo-attractants and activators of specific types of leucocytes in a variety of immune and inflammatory responses. However, during the past 5 years there has been a chemokine revolution in cancer and all scientists and clinicians in oncology-related fields are now aware of their crucial role at all stages of neoplastic transformation and progression. The most important chemokine ligand-receptor interaction is that of the CXCL12 (stromal cell-derived factor-1, SDF-1) ligand with its exclusive receptor CXCR4; this interaction has a pivotal role in the directional migration of cancer cells during the metastatic process. This has been demonstrated by in vitro and in vivo experiments in addition to retrospective clinical studies. These findings have exciting implications in the field of cancer therapeutics, with several small molecule CXCR4 antagonists having been developed, which may provide clinical benefit in the therapy of cancer metastasis. Interestingly, it is likely that the effect of the anti-HER2 antibody [trastuzumab (Herceptin)] in breast cancer involves downregulation of the CXCR4 receptor. Unfortunately, a major problem is that chemokine receptors are expressed in other cells within the body, particularly those of the immune system and it is not clear what effects long-term CXCR4 antagonism could have on innate and adaptive immunity. However, there is little doubt that the great strides made in elucidating the complex relationship between chemokines and their role in cancer will soon translate into significant survival benefits for patients.

3. Arya M et al. Expert Rev Mol Diagn. 2005;5:209-19.

Basic principles of real-time quantitative PCR

Real-time quantitative PCR allows the sensitive, specific and reproducible quantitation of nucleic acids. Since its introduction, real-time quantitative PCR has revolutionized the field of molecular diagnostics and the technique is being used in a rapidly expanding number of applications. This exciting technology has enabled the shift of molecular diagnostics toward a high-throughput, automated technology with lower turnaround times. This article reviews the basic principles of real-time PCR and describes the various chemistries available: the double-stranded DNA-intercalating agent SYBR Green 1, hydrolysis probes, dual hybridization probes, molecular beacons and scorpion probes. Quantitation methods are discussed in addition to the competing instruments available on the market. Examples of applications of this important and versatile technique are provided throughout the review.

4. Arya M et al. Curr Med Res Opin. 2003;19:557-64.

Chemokines: key players in cancer

Chemokines are a family of low molecular weight (8-10 kDa) pro-inflammatory cytokines, which bind to G-protein coupled receptors. Their primary function is chemoattraction and activation of specific leucocytes in various immuno-inflammatory responses. However, new research suggests that they are key players in cancer being involved in the neoplastic transformation of cells, promotion of aberrant angiogenesis, tumour clonal expansion and growth, passage through the extracellular matrix (ECM), intravasation into blood vessels or lymphatics and the non-random homing of tumour metastasis to specific sites. In view of the increasing significance of chemokines and their receptors in cancers of a variety of types, manipulation of this signalling pathway may be important in the development of new anticancer agents. This review provides an overview of recent research advances in this field and examines the potential therapeutic benefits future developments may bring.

5. Arya M et al. Surg Oncol. 2006;15:117-28.

The metastatic cascade in prostate cancer

Morbidity and mortality due to prostate cancer are mainly a result of prostate cancer metastases. After the initial neoplastic transformation of cells, the process of metastasis involves a series of sequential steps, which involve neoangiogenesis and lymphangiogenesis, loss of adhesion with migration away from the primary tumour and entry into the systemic vasculature or lymphatics. Metastatic growth in sites such as lymph nodes and bone marrow then involves the specific non-random homing of prostate cancer cells. An appreciation and understanding of this metastatic cascade in relation to prostate cancer is clinically important in order to stratify men with prostate cancer into prognostic groups. Moreover, it is crucial in the future development of therapies that can prevent metastases.

6. Arya M et al. Expert Rev Anticancer Ther. 2003;3:749-52.

Expanding role of chemokines and their receptors in cancer

(Editorial – no abstract available)